



ADVANCES IN GEOPHYSICS

Volume 44

SOLUS

Renata Dmowska

ADVANCES IN
G E O P H Y S I C S

VOLUME 44

This Page Intentionally Left Blank

Advances in
G E O P H Y S I C S

Edited by

RENATA DMOWSKA

*Division of Engineering and Applied Sciences
Harvard University
Cambridge, Massachusetts*

BARRY SALTZMAN

*Department of Geology and Geophysics
Yale University
New Haven, Connecticut*


VOLUME 44



ACADEMIC PRESS

A Harcourt Science and Technology Company

San Diego • San Francisco • New York • Boston
London • Sydney • Tokyo

This book is printed on acid-free paper. 

Copyright © 2001 by ACADEMIC PRESS

All Rights Reserved.

No part of this publication may be reproduced or transmitted in any form or by any means, electronic or mechanical, including photocopy, recording, or any information storage and retrieval system, without permission in writing from the Publisher.

The appearance of the code at the bottom of the first page of a chapter in this book indicates the Publisher's consent that copies of the chapter may be made for personal or internal use of specific clients. This consent is given on the condition, however, that the copier pay the stated per copy fee through the Copyright Clearance Center, Inc. (222 Rosewood Drive, Danvers, Massachusetts 01923), for copying beyond that permitted by Sections 107 or 108 of the U.S. Copyright Law. This consent does not extend to other kinds of copying, such as copying for general distribution, for advertising or promotional purposes, for creating new collective works, or for resale. Copy fees for pre-2001 chapters are as shown on the title pages. If no fee code appears on the title page, the copy fee is the same as for current chapters. 0065-2867/01 \$35.00

Explicit permission from Academic Press is not required to reproduce a maximum of two figures or tables from an Academic Press chapter in another scientific or research publication provided that the material has not been credited to another source and that full credit to the Academic Press chapter is given.

Academic Press

A Harcourt Science and Technology Company

525 B Street, Suite 1900, San Diego, California 92101-4495, USA

<http://www.academicpress.com>

Academic Press

Harcourt Place, 32 Jamestown Road, London NW1 7BY, UK

<http://www.academicpress.com>

International Standard Book Number: 0-12-018844-9

PRINTED IN THE UNITED STATES OF AMERICA

00 01 02 03 04 05 BB 9 8 7 6 5 4 3 2 1

CONTENTS

CONTRIBUTORS vii

Fault Interaction by Elastic Stress Changes: New Clues from Earthquake Sequences

G. C. P. KING AND M. COCCO

1. Introduction	1
2. Theoretical Background	3
2.1 Coulomb Failure	3
2.2 Two-Dimensional Case: Coulomb Stress on a Plane of Specified Orientation	6
2.3 Two-Dimensional Case: Change of Coulomb Stress on Optimally Oriented Faults	7
2.4 Three-Dimensional Case: Strike-Slip and Dip-Slip Conditions	9
2.5 Sensitivity to the Main Shock Focal Mechanism	10
3. Examples of Coulomb Interactions	11
3.1 Coulomb Stress Changes and Aftershocks	11
3.2 Stress Changes Associated with the Landers Earthquake	12
3.3 Coulomb Stress Changes Preceding the Landers Rupture	12
3.4 Stress Changes Following the Landers Rupture but before the Big Bear Earthquake	13
3.5 Stress Changes Caused by the Landers, Big Bear, and Joshua Tree Ruptures	13
3.6 Interactions between Large Earthquakes: Western Turkey and the Aegean	15
3.7 Close Interactions between Dip-Slip Earthquakes	16
4. Summary of Modeling Successes	18
5. Summary of Problems and Open Questions	20
5.1 The Role of Static and Dynamic Loading	22
5.2 Rate and State Dependent Friction Laws	23
5.3 Fluid Flow	26
5.4 Creep in the Crust or on Faults	27
5.5 Tectonic Loading	28
5.6 Postseismic Evolution	29
6. Social Concerns	29
7. Concluding Remarks	30
References	31

Seismicity Induced by Mining: Ten Years Later

SLAWOMIR J. GIBOWICZ, AND STANISLAW LASOCKI

1. Introduction	39
2. Seismic Monitoring	40
2.1 Seismicity in Underground Mines	41
2.2 Monitoring Systems	49
2.3 Location of Seismic Events	53
2.4 Seismic Tomography	59
2.5 Spatial and Temporal Patterns	65
3. Geology, Mining, and Seismicity	70
3.1 Mining Operations and Seismicity	71
3.2 Geological Structures and Seismicity	76
4. Source Parameters and Scaling Relations	81
4.1 Source Parameters	81
4.2 Scaling Relations	86
5. Source Mechanism	89
5.1 Seismic Moment Tensor	90
5.2 Typical Source Mechanism and Complex Rock Failures	96
5.3 Stress Release Mechanism	99
6. Source Time Function	102
7. Fractals	105
8. Assessment and Prediction of Time-Dependent Seismic Hazard: Statistical Approach	123
8.1 Recurrence Relationships: Source Models for Stationary Seismic Hazard Analysis	129
8.2 Time Variations of Energy/Magnitude Distributions	133
8.3 Parameterization of Spatial Distributions of Seismic Events	143
8.4 Rock Mass Instability Concept	150
8.5 Other Studies	153
8.6 Automatic Prediction: Extrapolation of Parameterizations of Seismicity in Mines	156
9. Seismic Discrimination	159
10. Summary	161
Acknowledgments	164
References	164
INDEX	183

CONTRIBUTORS

Numbers in parentheses indicate the pages on which the authors' contributions begin

COCCO, MASSIMO (1) Istituto Nazionale di Geofisica, Via di Vigna Murata 605, 00143 Rome, Italy

GIBOWICZ, SŁAWOMIR J. (39) Institute of Geophysics, Polish Academy of Sciences, ul. Ks. Janusza 64, 01-452 Warsaw, Poland

KING, G. C. P. (1) Institute de Physique du Globe, Tectonique Lab, 4 Pl Jussieu, Paris 75252, France

LASOCKI, STANISŁAW (39) Department of Geophysics, University of Mining and Metallurgy, al. Mickiewicza 30, 30-059 Krakow, Poland

This Page Intentionally Left Blank

FAULT INTERACTION BY ELASTIC STRESS CHANGES: NEW CLUES FROM EARTHQUAKE SEQUENCES

G. C. P. KING

Institute de Physique du Globe, Paris, France

M. COCCO

Istituto Nazionale di Geofisica, Rome, Italy

1. INTRODUCTION

This paper is concerned with recent developments in our understanding of how earthquakes interact with each other. Although this subject has attracted the attention of geophysicists for many years (Rybicki, 1973; Chinnery and Landers, 1975; Das and Scholz, 1981; Rice and Gu, 1983), it has not been studied in the detail that it deserves. For this reason there have been persistent misunderstandings, some of which have been well addressed by more recent ideas.

It has been often assumed, for instance, that aftershocks all occur on the same fault as a main shock. In general that is not correct as Fig. 1 illustrates. Similarly, it is now clear that earthquakes do not usually repeat at regular time intervals. The data concerning these problems have not been ambiguous; small events including aftershocks clearly do not always fall on major faults. Historical data also indicate that major earthquakes do not always repeat at regular intervals (Ambraseys and Melvine, 1982). However, in the absence of a satisfactory theoretical framework for understanding such data, incorrect ideas have persisted.

Some attempts to explain the observations, prior to the recent work, can be identified. Off-fault events have been explained as being related to bends or offsets of faults (see King, 1986, among others). The fragmentation needed for long-term slip to traverse such barriers requires deformation away from the main faults (King and Nabelek, 1985). The concept of regularly repeating earthquakes derives from the idea that slip deficits at plate boundary segments must sooner or later be filled by earthquake slip (Nishenko and Buland, 1987). With regular plate motions such deficits might be expected to appear and disappear at regular intervals. Both explanations can be qualitatively modified to approach the newer ideas of stress coupling (see Dmwska *et al.*, 1988, 1996; Dmwska and Lovison, 1992; Taylor *et al.*, 1996, among several others). Fault bends and offsets concentrate stresses, and the reasons that stress models predict events in such regions relate to the geometry of the larger faults. It was also realized that segments of plate boundaries could

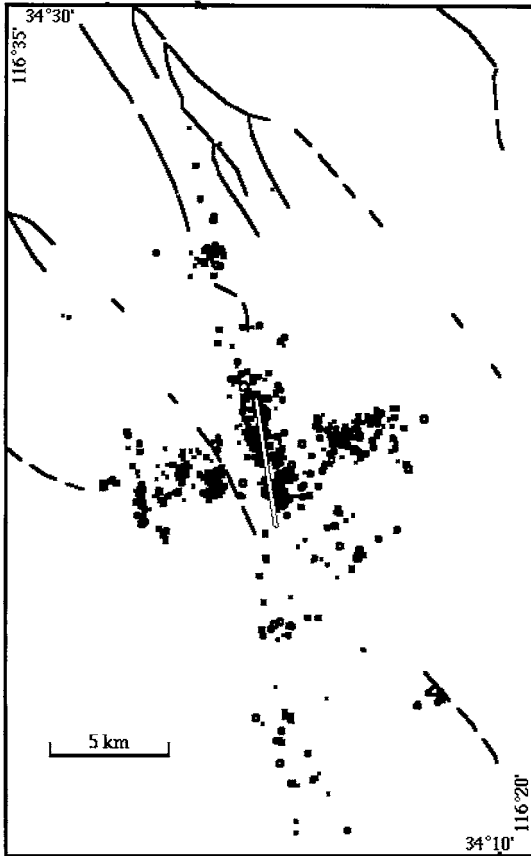


FIG. 1. Distribution of $M \geq 1$ aftershock in the 2 years after the 1979 Homestead Valley main shock. The white segment shows the earthquake fault; the dark lines are the nearby southern California faults. Location errors are better than ± 2 km.

not be expected to operate with complete independence. Slip on one segment must “load” adjacent segments and tend to promote slip. Thus earthquake cycles on adjacent segments cannot be independent. Our newer understanding does not dismiss these earlier views, but it does serve to add to and refine these earlier concepts.

The new theoretical framework is based on calculating the stress changes caused by one event and assessing where and what mechanism of earthquakes these changes may promote. For studying such stress interaction we rely on the computation of the stress field outside a rupturing fault. This is different from investigating the dynamic rupture growth which requires the reconstruction of the spatiotemporal evolution of the stress on the fault plane (Archuleta and Day, 1980; Quin,

1990; Miyatake, 1992; Mikumo and Miyatake, 1995; Bouchon, 1997, among many others).

We start by discussing the theoretical background and follow this by reviewing some of the simple examples that have allowed stress coupling concepts to be accepted. The success of simple stress modeling has caused several authors to propose modifications, adaptations, and refinements of the ideas, which are also discussed.

2. THEORETICAL BACKGROUND

To study the interaction between faults it is necessary to have a means of calculating their associated stress fields. Static displacements, strains, and stresses are usually computed by solving the elastostatic equation for a dislocation on an extended fault in an elastic, isotropic, and homogeneous half-space. This solution yields the Volterra (1907) equation

$$u_m(x_i) = \frac{1}{F} \iint_{\Sigma} \Delta u_k(\xi_i) T_{kl}^m(\xi_i, x_i) n_l(\xi_i) d\Sigma(\xi_i),$$

where F is the magnitude of a volume point force applied at $\vec{\xi}$ in the direction m . The direction cosine of the normal to the surface element $d\Sigma$ is n_k . The static displacement $u_m(x_i)$ is computed as a function of the dislocation $\Delta u_k(\xi_i)$ and the static traction $T_{kl}^m(\xi_i, x_i)$ on the fault plane Σ . According to Steketee (1958a,b), Maruyama (1964), and Aki and Richards (1980) the previous equation becomes

$$u_m(x_i) = \frac{1}{F} \iint_{\Sigma} \Delta u_k \left[\lambda \delta_{kl} \frac{\partial U_m^n}{\partial \xi_n} + \left(\frac{\partial U_m^k}{\partial \xi_l} + \frac{\partial U_m^l}{\partial \xi_k} \right) \right] n_l d\Sigma,$$

where the summation convention applies. The computation of the static displacement requires knowledge of the fault geometry, the slip distribution, and the strain nuclei (Mindlin, 1936) $U_m^k(\xi_i, x_i)$ (i.e., the static Green's functions). Using these solutions and Hooke's law, Chinnery (1961, 1963), Rybicki (1973), and Okada (1985, 1992) have derived analytical expressions for the static displacement, strain, and stress fields caused by a finite rectangular fault either at the Earth surface or at depth.

2.1. Coulomb Failure

A number of criteria can be used to characterize failure in rocks. None are entirely satisfactory and the significance of different criteria for earthquake interactions is

discussed at greater length below. However, most successes in modeling earthquake interactions are based on the widely used Coulomb failure criterion (Jaeger and Cook, 1969; Scholz, 1990). We therefore start by discussing simple Coulomb assumptions which require that both the shear and the normal stress on a preexisting or an incipient fault plane satisfy conditions analogous to those of friction on a preexisting surface.

Failure initiates and spreads on the plane when the Coulomb stress C_f sometimes referred to as the Coulomb Failure Function (CFF) exceeds a specific value

$$C_f = \tau_\beta + \mu(\sigma_\beta + p), \quad (1)$$

where τ_β is the shear stress on the failure plane, σ_β is the normal stress (positive for extension), p is the pore fluid pressure, and μ the coefficient of friction. The value of τ_β must always be positive in this expression. However, the processes of resolving shear stress onto an assigned plane may give positive or negative values. The difference in sign of τ_β indicates whether the potential for slip on the plane is right- or left-lateral.

If the failure plane is orientated at β to the σ_1 axis (see Fig. 2) we can express, under plane-stress conditions, the normal stress applied to the plane in terms of the principal stresses

$$\sigma_\beta = \frac{1}{2}(\sigma_1 + \sigma_3) - \frac{1}{2}(\sigma_1 - \sigma_3) \cos 2\beta. \quad (2)$$

Two expressions are required for shear stress, the one giving positive values being chosen. One is for left-lateral and the other for right-lateral shear

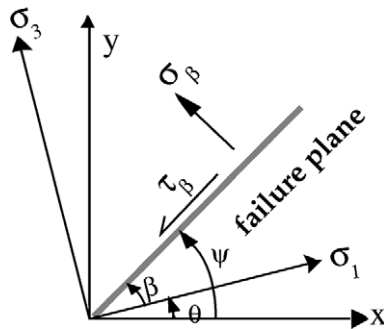


Fig. 2. The coordinate system used for calculations of Coulomb stresses. Extension and left-lateral motion on the failure plane are assumed to be positive. The total shear stress τ is reversed for calculations of right-lateral Coulomb failure on specified planes. In the calculations σ_j refers to the stress tensor components.

stress

$$\begin{aligned}\tau_{\beta}^L &= \frac{1}{2}(\sigma_1 - \sigma_3) \sin 2\beta \\ \tau_{\beta}^R &= -\frac{1}{2}(\sigma_1 - \sigma_3) \sin 2\beta,\end{aligned}\quad (3)$$

where σ_1 is the greatest principal stress and σ_3 is the least principal stress. For left- and right-lateral Coulomb stresses, respectively, Eq. (1) then becomes

$$C_f = \frac{1}{2}(\sigma_1 - \sigma_3)(\sin 2\beta - \mu \cos 2\beta) - \frac{1}{2}\mu(\sigma_1 + \sigma_3) + \mu p. \quad (4)$$

By differentiating Eq. (4) as a function of β , one finds that the maximum Coulomb stress C_f^{\max} occurs for two angles when

$$\tan 2\beta = -\mu. \quad (5)$$

Pore fluid pressure modifies the effective normal stress across the failure plane as shown in Eq. (1). When rock stress is changed more rapidly than fluid pressure can change through flow (undrained conditions, Rice and Cleary, 1976), p can be related to confining stress in the rock by Skempton's coefficient B ($p = -B\sigma_{kk}/3$), where B varies between 0 and 1. Equation (1) and subsequent expressions (such as (4)) can therefore be rewritten on the assumption that σ_{β} represents the confining stress as well as the normal stress on the plane ($p = -B\sigma_{\beta}$), [e.g., Simpson and Reasenberg (1994)]

$$C_f = \tau_{\beta} + \mu' \sigma_{\beta}, \quad (6)$$

where the effective coefficient of friction is defined by $\mu' = \mu(1 - B)$. Although useful, it must be remembered that the expression is an approximation since the normal stress across a plane need not be so simply related to confining stress (see Harris, 1998, and references therein; Beeler *et al.*, 1998; Cocco and Rice, 1999). The problems associated with fluid flow and the approximation involved in using Skempton's coefficient are discussed later.

The failure condition is inherently two-dimensional with the intermediate stress σ_2 playing no part. Thus the underlying physics can be illustrated in two dimensions. To generalize the mathematics to three dimensions it is only necessary to determine the orientation of the plane of greatest and least principal stresses in the appropriate coordinate system and to apply the failure conditions in that plane. While this is the correct mathematical formulation, in practice computer algorithms that search directly for optimum planes produce identical results and can be easier to implement (Nostro *et al.*, 1997).

2.2. Two-Dimensional Case: Coulomb Stress on a Plane of Specified Orientation

In a system where the x - and y -axes and fault displacements are horizontal, and fault planes are vertical (containing the z direction), stress on a plane at an angle ψ from the x -axis (see Fig. 2) resulting from a general stress field of any origin is given by

$$\begin{aligned}\sigma_{11} &= \sigma_{xx} \cos^2 \psi + 2\sigma_{xy} \sin \psi \cos \psi + \sigma_{yy} \sin^2 \psi \\ \sigma_{33} &= \sigma_{xx} \sin^2 \psi - 2\sigma_{xy} \sin \psi \cos \psi + \sigma_{yy} \cos^2 \psi \\ \tau_{13} &= \frac{1}{2}(\sigma_{yy} - \sigma_{xx}) \sin 2\psi + \tau_{xy} \cos 2\psi,\end{aligned}\quad (7)$$

where these relations hold for a left-lateral mechanism ($\tau_{13} = \tau_{13}^L$) and similar expressions can be derived for a right-lateral mechanism (as stated in Eq. (3)). The Coulomb stress for left-lateral C_f^L and right-lateral C_f^R motion on planes orientated at ψ with respect to the x -axis can now be written

$$C_f^L = \tau_{13}^L + \mu' \sigma_{33} \quad (8a)$$

$$C_f^R = \tau_{13}^R + \mu' \sigma_{33}. \quad (8b)$$

Equation (8b) is illustrated in Fig. 3a using a dislocation (earthquake fault) source. An elliptical slip distribution is imposed on the (master) fault in a uniform, stress-free, elastic medium. The contributions of the shear and normal components to the failure condition, and the resulting Coulomb stresses, for infinitesimal faults parallel to the master fault are shown in separate panels. Such a calculation represents the Coulomb stress on these planes resulting only from slip on the master fault (i.e., the figure shows a map of stress changes) and is independent of any knowledge of the prevailing regional stresses or any preexisting stress fields from other events. The signs in the calculation are chosen such that a positive Coulomb stress indicates a tendency for slip in the same right-lateral sense as the fault of interest. Negative Coulomb stresses indicate a reduction of this tendency. It is important to appreciate that because τ_{13} changes sign between Eqs. (8a) and (8b), a negative Coulomb stress for right-lateral fault motion is not the same as a tendency for left-lateral slip.

The distribution of increases and decreases of Coulomb stress show features common to all subsequent figures. Lobes of increased shear stress appear at the fault ends, corresponding to the stress concentrations that tend to extend the fault. Off-fault lobes also appear, separated from the fault by a region where the Coulomb stresses have not been increased. If the master fault were infinitesimal in length, and thus behaving as a point source, the off-fault lobes would be equal in amplitude to the fault-end lobes at all distances. For a finite length fault they are absent near

the fault and only become similar in amplitude at great distances compared to the fault length (King *et al.*, 1994). The normal stress field is similar to the more familiar dilatational field with maxima and minima distributed antisymmetrically across the fault, but we consider only the component of tension normal to the fault. The influence of the normal stress on the Coulomb stress distribution is to reduce the symmetry of the final distribution and to increase the tendency for off-fault failure (Stein *et al.*, 1992; King *et al.*, 1994).

2.3. Two-Dimensional Case: Change of Coulomb Stress on Optimally Orientated Faults

The calculation in the previous section is general and need not be due to an earthquake. If a stress or stress change is known, then the Coulomb stress or stress change can be calculated on any plane. We now consider a more general case where a change of stress, such as that due to an earthquake, is imposed on a preexisting stress field. The failure planes are not specified *a priori*, but they are computed accounting for the interaction between the two fields.

In the formulation that we present, “optimal” planes are regarded as those simultaneously favored by tectonic loading and the stress induced by the motion on the master fault. These are the planes on which aftershocks might be expected to occur (Rybicki, 1973; Das and Scholz, 1981; Stein *et al.*, 1992; King *et al.*, 1994; Nostro *et al.*, 1997; see Harris, 1998, for further references). Here we define such planes in terms of uniformly varying stress fields. The widely varying focal mechanisms associated with the aftershock sequences of Irpinia (Deschamps and King, 1984; Nostro *et al.*, 1997; Troise *et al.*, 1998) and Loma Prieta (Michael *et al.*, 1990; Beroza and Zoback, 1993; Amelung, 1996), however, suggests such a definition is not complete. The implications are discussed later.

In terms of simple stress fields, the optimum directions are determined by the stress change due to that earthquake $\sigma_{ij}^q (= \Delta\sigma_{ij})$ and by preexisting regional stresses σ_{ij}^r which give a total stress σ_{ij}^t

$$\sigma_{ij}^t = \sigma_{ij}^r + \sigma_{ij}^q. \quad (9)$$

The orientation of the principal axes resulting from the total stress are therefore derived using

$$\theta = \frac{1}{2} \tan^{-1} \left(\frac{2\sigma_{xy}^t}{\sigma_{xx}^t - \sigma_{yy}^t} \right), \quad (10)$$

where θ is the orientation of one principal axis to the x -axis as shown in Fig. 2 and the other is at $\theta \pm 90^\circ$. From these two directions, the angle of greatest compression θ_1 must be chosen. The optimum failure angle ψ_o is then given by $\theta_1 \pm \beta$ where one plane is left-lateral and the other right-lateral with the sign of shear stress being

chosen appropriately. Whereas the optimum planes are determined from σ_{ij}^t the normal and shear stress changes on these planes are determined only by the earthquake stress changes σ_{ij}^q . Thus the changes in stress on the optimum planes become

$$\begin{aligned}\sigma_{33} &= \sigma_{xx}^q \sin^2 \psi_o - 2\sigma_{xy}^q \sin \psi_o \cos \psi_o + \sigma_{yy}^q \cos^2 \psi_o \\ \tau_{13} &= \frac{1}{2}(\sigma_{yy}^q - \sigma_{xx}^q) \sin 2\psi_o + \tau_{xy}^q \cos 2\psi_o\end{aligned}\quad (11)$$

and the Coulomb stress changes

$$C_f^{\text{opt}} = \tau_{13} + \mu' \sigma_{33}.\quad (12)$$

The two optimum planes correspond to left-lateral and right-lateral shear. The Coulomb stress change is the same on both so that the Coulomb stress is the same whether calculated for left- or right-lateral planes in expression (12). It is important to emphasize that we calculate the change of Coulomb stress on planes that are optimum after the earthquake, with the optimum orientations being calculated from the earthquake stress field plus the regional stress field. The Coulomb stress changes caused by the earthquake stress changes are then resolved onto these planes. Where earthquake stresses are large they can rotate the principal axes.

The results of a calculation to find optimum orientations and magnitudes of Coulomb stress changes are shown in Fig. 3b. The slip on the master fault is the same as in Fig. 3a. A uniform 100-bar compressional stress is introduced with the orientation shown. White lines indicate optimum left-lateral orientations and black lines, right-lateral orientations. The shear and normal stress contributions to the Coulomb stress change are again shown in separate panels.

It can be seen from expression (9) that only the deviatoric part of the regional stress determines the orientation of principal axes, and hence the optimum stress orientations. Thus it is sufficient to apply the regional stress as a simple uniaxial compression or extension. This assumes, however, that the intermediate principal stress is vertical, and thus a two-dimensional description is complete. In general this is not true since the relative magnitudes of the principal stresses control the focal mechanisms which need not be strike-slip.

The relative amplitude of the regional stress to the earthquake stress drop ($\Delta\tau$) might be expected to have an effect. This is explored for the strike-slip case in Fig. 4, which shows the Coulomb stress change C_f^{opt} on optimally orientated right-lateral planes in which the regional field is equal to the stress drop $\Delta\tau$ (*left panel*) and 10 times $\Delta\tau$ (*right panel*). These examples span likely conditions. It is evident that, except close to the master fault, the orientations of the optimal planes and Coulomb stress changes on these planes are little altered. The optimal orientations are essentially fixed by the regional stress except very close to the fault where the stress change caused by slip on the master fault is comparable to the regional stress.

For stress drops similar in amplitude to the regional stress, Coulomb stress changes close to the fault are positive as a consequence of rotation of the target fault planes. If the regional stress were zero, then the Coulomb stress change on optimally orientated planes would be positive everywhere since shear stress must increase for some planes. Only for very high regional stress would the Coulomb stress change at the fault plane be negative. Although these effects are real, they are difficult to model. To do so requires knowledge of the main fault geometry, slip distribution, and inhomogeneities of the regional stress. Failure to model aftershocks for events such as Loma Prieta is consequently not a strong negative test of Coulomb interaction methods.

The effects of varying the orientation of regional stresses and changing the coefficient of friction μ' are shown in Fig. 5. Possible changes of regional stress orientation are limited since the main fault must move as a result of the regional stress; the 30° range covers the likely range. Similarly, values of friction between 0.0 and 0.75 span the range of plausible values. All of the panels show the same general features, fault-end and off-fault Coulomb stress lobes. Thus modeling is most sensitive to the regional stress direction, almost insensitive to the regional stress amplitude, and modestly sensitive to the coefficient of effective friction. In other words, while the relative magnitude of the regional stress with respect to the earthquake stress drop controls the changes in the orientations of the optimal planes close to the master fault (as shown in Fig. 4), the orientation of the regional stress is the most important factor controlling the orientations of the optimal planes for failure far away from the master fault (as shown in Fig. 5).

2.4. Three-Dimensional Case: Strike-Slip and Dip-Slip Conditions

The application to vertical strike-slip faults is easier because it is possible to solve a two-dimensional problem (plane stress configuration), where the vertical components of the regional stress tensor can be neglected (King *et al.*, 1994). However, the application to dip-slip faults (as well as to a general oblique faulting) requires the solution of a 3D problem where the ratio between vertical and horizontal components of regional stress tensor must be known. This means that, while in the foregoing discussion we have assumed that only strike-slip vertical faults are present and thus stress components σ_{zz} , σ_{xz} , σ_{yz} could be neglected, in a more general configuration these stress components cannot be ignored.

If the regional stress components are known, the total stress can be computed through Eq. (9), which is used to find the orientation and magnitude of the principal stresses. We can therefore calculate the orientation of the plane containing σ_1 and σ_3 and hence the optimum orientations of slip planes where the change of Coulomb failure stress will be found. The calculation is straightforward and an example is shown in Fig. 6. If we take horizontal stresses similar in amplitude to those previously employed, we can examine the change of mechanism as the vertical

stress is changed. The horizontal stresses are chosen to be 200 bars (EW) and 400 bars (NS). For Fig. 6a the vertical stress is 100 bars; in Fig. 6b the vertical stress is 300 bars; and in Fig. 6c the vertical stress is 500 bars. The predominant mechanisms are reverse faulting in Fig. 6a, strike-slip faulting in Fig. 6b, and normal faulting in Fig. 6c. If the vertical stresses are attributed to overburden pressure, then the figures correspond to depths of 300 meters, 900 meters, and 1500 meters respectively. This is clearly incorrect. Events do not occur at such shallow depths nor are systematic changes of focal mechanism with depth observed. It would seem that a confining pressure that increases with depth must be added to the horizontal stress such that the differential stresses remain similar. It is clear however, that the mechanisms are sensitive to small variations in the stresses chosen; thus to correctly predict mechanisms from stresses the stress regime must be known with precision. Direct measurements of stress throughout the seismogenic zone are never available, thus predicting mechanisms from stress must be indirect. In practice the most useful information comes from the focal mechanisms that are observed. Therefore, the calculation of stress changes on faults of predetermined directions (resulting from focal mechanisms) could be preferred to the determination of fault directions from regional stresses and stress changes. Alternatively, the stress regime can be chosen such that the observed mechanisms are produced. While in theory the two approaches are different, in practice the results are similar. However, it must always be appreciated that the stress fields used in Coulomb calculations need have little relation to the real stresses in the Earth and should not be regarded as demonstrating that such stress fields really exist. In other words, the regional stress field is only an input parameter for Coulomb stress interaction.

2.5. Sensitivity to the Main Shock Focal Mechanism

The last section showed that the Coulomb distribution can be sensitive to incorrect assumptions about regional stress, since this can cause incorrect prediction of target fault focal mechanisms. While nearby events are clearly sensitive to all of the details of the rupture process, this is not the case at some distance from the fault. This is particularly important for studying fault interaction between large magnitude earthquakes. Completely incorrect focal mechanisms clearly result in incorrect results. Errors in dip (within an acceptable range) are much less serious. Figure 7a shows the distribution for a 45° dipping normal fault and Fig. 7b shows the distribution for a vertical dike with the same opening displacement as the horizontal slip vector of the dip-slip fault. Except at distances comparable to the source dimensions, the two distributions are identical. This illustrates that, except close to a dip-slip fault, the fault dip is not important. In general, except in the near field (or at distances of a few fault lengths) a double couple point source with the appropriate seismic moment is all that is needed.

While large errors in the strike of the focal planes are serious, small errors only result in (an approximately) commensurate rotation of the Coulomb stress distribution. This is shown in Fig. 7c. It is much harder to evaluate the fault parameters close to dip-slip or oblique slip faults (such as Loma Prieta), making aftershock studies of such events harder than for strike-slip events (such as Landers). We therefore choose to illustrate aftershock studies for strike-slip events and large event interactions for mainly dip-slip events.

3. EXAMPLES OF COULOMB INTERACTIONS

3.1. Coulomb Stress Changes and Aftershocks

The methods outlined above can be applied to the aftershock distributions. Figure 8 shows the 1979 Homestead Valley sequence, the event discussed by Das and Scholz (1981) and shown in Fig. 1. The event produced no surface rupture, but seismic and geodetic observations provide evidence for the geometry of fault slip. The calculations are carried out in a half-space with the values of Coulomb stress plotted in the figures being calculated at half the depth to which the faults extend.

Figure 8 shows the four characteristic lobes of increased Coulomb stress rise and four lobes of Coulomb stress drop. The lobes at the ends of the fault extend into the fault zone while the off-fault lobes are separated from the fault over most of its length by a zone where the Coulomb stress is reduced. The distributions of aftershocks are consistent with these patterns. Many events are associated with increases of Coulomb stress of less than 1 bar, while reductions of the same amount apparently suppress them. Relatively few events fall in the regions of lowered Coulomb stress, and the clusters of off-fault aftershocks are separated from the fault itself by a region of diminished activity. The distributions of Coulomb stresses can be modified as described earlier by adjusting the regional stress direction and changing μ' . However, any improvements in the correlation between stress changes and aftershock occurrence are modest. Consequently we have chosen to show examples with an average μ' of 0.4. Whatever values we adopt, we find that the best correlations of Coulomb stress change to aftershock distribution are at distances greater than a few kilometers from the fault. Closer to the fault, unknown details of fault geometry and slip distribution influence the stress changes. Correlation between aftershock distribution and Coulomb stress changes on a vertical cross section can also be observed and are discussed by King *et al.* (1994) who also discuss the 1992 Joshua Tree (California) earthquake.

In many cases, individual aftershock mechanisms are not known, and when known one of the conjugate planes must be chosen. There is consequently an implicit assumption by some authors that they really have the mechanisms that would be predicted by the induced stress field due to the main shock. Some

authors have attempted to verify that the mainshock induced stress changes closely agree with the observed aftershock faulting mechanisms (Michael, 1991; Beroza and Zoback, 1993; Amelung, 1996). However, we emphasize that the correlation between aftershock distribution and Coulomb stress changes should be confirmed in a statistical way to be considered as supporting evidence for Coulomb stress interaction. We will discuss this topic in a later section.

3.2. Stress Changes Associated with the Landers Earthquake

Although stress interactions had been previously observed for other events, the clear correlations associated with the Landers earthquake suggested to the scientific community that Coulomb calculations might indeed prove an effective method of relating large events with each other and relating large events to their aftershock sequences. The Landers earthquake and associated events remains the best example for illustrating the techniques and we reproduce here the modeling processes following King *et al.* (1994). Since the main events were strike-slip (except for North Palm Springs), the calculations are essentially two-dimensional and an “effective” regional stress is easy to establish since only the deviatoric part in the horizontal plane is needed. We take the regional stress to be a simple compression of 100 bars, orientated at N7°E for the reasons discussed by King *et al.* (1994).

3.3. Coulomb Stress Changes Preceding the Landers Rupture

In Fig. 9 the Coulomb stress changes caused by the four $M > 5$ earthquakes within 50 km of the epicenter that preceded the Landers earthquake are shown. The Coulomb stresses are due to the 1975 $M_L = 5.2$ Galway Lake, 1979 $M_L = 5.2$ Homestead Valley, 1986 $M_L = 6.0$ North Palm Springs, and 1992 $M_L = 6.1$ Joshua Tree earthquakes. These progressively increased Coulomb stresses by about 1 bar at the future Landers epicenter. Together they also produced a narrow zone of Coulomb stress increase of 0.7–1.0 bars, which the future 70-km-long Landers rupture followed for 70% of its length. The Landers fault is also nearly optimally oriented for most of its length. It is noteworthy that the three largest events are roughly equidistant from the future Landers epicenter: the right-lateral Homestead Valley and Joshua Tree events enhanced stress as a result of the lobes beyond the ends of their ruptures, whereas the North Palm Springs event enhanced rupture as a result of an off-fault lobe. Increasing the effective friction μ' from 0.4 (Fig. 9) to 0.75 slightly enhances the effects, and dropping the friction to zero reduces them.

3.4. Stress Changes Following the Landers Rupture but before the Big Bear Earthquake

Unlike the earthquake sources modeled so far, which we approximated by simple (elliptical) slip on a single plane, there is more information about the $M = 7.4$ Landers source. Various authors have adopted different slip distributions (see Wald and Heaton, 1994, and Cohee and Beroza, 1994). Here we reproduce the results of King *et al.* (1994) who model the rupture of 13 fault segments to produce a slip distribution that is consistent with surface fault mapping, geodetic data, radar data, and the modeling of seismic data.

The stress changes caused by the Landers event are shown in Fig. 10. The largest lobe of increased Coulomb stress is centered on the epicenter of the future $M_L = 6.5$ Big Bear event, where stresses were raised 2–3 bars (Stein *et al.*, 1992; King *et al.*, 1994). The Big Bear earthquake was apparently initiated by this stress rise 3 hr 26 min after the Landers main shock. The Coulomb stress change at the epicenter is greatest for high effective friction but remains more than 1.5 bars for $\mu = 0$. There is no surface rupture or Quaternary fault trace associated with the Big Bear earthquake. Judging from its epicenter and focal mechanism (Hauksson *et al.*, 1993), the plane that apparently ruptured was optimally aligned for left-lateral failure, with the rupture apparently propagating northeast and terminating where the Landers stress change became negative.

In addition to calculating the stress changes caused by the Landers rupture, we estimate that the slip on the Big Bear fault needed to relieve the shear stress imposed by the Landers rupture. This is achieved by introducing a freely slipping boundary element along the future Big Bear rupture. The potential slip along the Big Bear fault is 60 mm (left-lateral), about 5–10% of the estimated slip that occurred several hours later. These calculations suggest that the Big Bear slip needed to relieve the stress imposed by Landers was a significant fraction of the total slip that later occurred. Thus from consideration of the stress changes and the kinematic response to those changes, it is reasonable to propose that stresses from the Landers event played a major role in triggering the Big Bear shock, although the Coulomb criterion cannot explain the time delay (3 hr and 26 min) of the Big Bear failure episode.

3.5. Stress Changes Caused by the Landers, Big Bear, and Joshua Tree Ruptures

The Big Bear earthquake was the largest of more than 20,000 aftershocks located after the Landers earthquake, large enough to result in significant stress redistribution at the southwestern part of the Landers rupture zone. Consequently

the distribution of later events cannot be examined without considering its effect. A similar argument can be applied to the smaller Joshua Tree event, whose aftershock sequence was not complete at the time of the Landers rupture. In Fig. 11 the combined Coulomb stress changes for the Joshua Tree, Landers, and Big Bear earthquakes is plotted. This distribution is shown together with all well-located $M_L \geq 1$ events that occurred during the following 25 days.

Most $M_L > 1$ aftershocks occur in regions where the failure stress is calculated to have increased by ≥ 0.1 bar, and few events are found where the stress is predicted to have dropped (see Fig. 11; Gross and Kisslinger, 1997; Hardebeck *et al.*, 1998). Even when all seismicity within 5 km of the Landers, Big Bear, and Joshua Tree faults is excluded, more than 75% of the aftershocks occur where the stress is predicted to have risen by >0.3 bar. In contrast, less than 25% of the aftershocks occur where the stress dropped by >0.3 bar.

Few aftershocks are seen near Indio in the Coachella Valley although the region was loaded by the Landers events. Further south the Imperial Valley was also loaded and again there are few events. King *et al.* (1994) speculate on the reasons for the absence of events. In general however, while areas of increased Coulomb stress usually exhibit an increase in activity, exceptions do occur.

The stress redistribution caused by the 1992 Landers earthquake also affected the seismicity within about 100 km of the epicenter for several years. The seismicity rate increased during the 7 years after the mainshock in the volumes where Coulomb stress changes favored faulting and it decreased in the stress shadow (Wyss *et al.*, 1999). On October 16, 1999, a M_w 7.1 earthquake (Hector Mine) occurred northeast of the 1992 Landers epicenter in a region of increased Coulomb stress (see the open star in Fig. 11). The Hector Mine earthquake had rupture geometry similar to the Landers event (Hauksson *et al.*, 1999; Ponti *et al.*, 1999) and produced a surface rupture approximately 45 km long with right-lateral motion. After the 1992 Landers earthquake a sharp increase of seismicity occurred in the region surrounding the future hypocenter (Wyss *et al.*, 1999). Preliminary results indicate that the greatest slip for the Hector Mine fault is located in the stress shadow of the 1992 Landers earthquake (Hauksson *et al.*, 1999; Parsons and Dreger, 2000). At the epicenter the shear stress component of the Coulomb stress change has been reported to be small and negative, but the normal stress change is larger than 1 bar giving a net increase of 0.5 bars, according to Parsons and Dreger (2000). It is worth remarking that rupture into regions of Coulomb stress shadow has been observed for other events (e.g., Nalbant *et al.*, 1998, Perfettini *et al.*, 1999) with the Izmit 1999 earthquake being the best constrained (Hubert-Ferrari, 2000). A problem with the Landers–Hector Mine region is a lack of information about either the loading processes or the seismic history of the region. Therefore the pre-earthquake stresses are poorly constrained.

3.6. Interactions between Large Earthquakes: Western Turkey and the Aegean

The Landers earthquake sequence suggests that a series of smaller events that preceded the Landers earthquake prepared a region of slightly elevated stress along much of the fault that the main event then followed. It is also clear that the stresses created by the main event largely controlled the aftershock distribution, including the location of the large Big Bear aftershock. A number of studies have shown that large events appear to interact over large areas (Reasenber and Simpson, 1992; Harris and Simpson, 1992; Jaumé and Sykes, 1996; Nostro *et al.*, 1997; Stein *et al.*, 1997; Nalbant *et al.*, 1996, 1998; see Harris, 1998, for a more detailed reference list). Here we illustrate the effect taking an example from Turkey and the western Aegean. Since 1912, 29 events ($M_s \geq 6.0$) have occurred in the region shown in Fig. 12. The area is of particular interest because the events do not lie along a single fault and the mechanisms vary. They are predominantly strike-slip and normal faulting, but some reverse faulting occurs. The later events have reliable focal mechanisms and seismic moments controlled by waveform modelling. Earlier events do not, but a combination of geological information to identify the faults involved plus damage information closely controls the possible mechanisms. Details of the mechanism information can be found in Nalbant *et al.* (1998) from which the examples presented here are abstracted. That paper splits the time period into nine intervals such that all interactions can be seen. Here we only show three example time windows. They are 1912 to 1944 (Fig. 13a), 1912 to 1967 (Fig. 13b), and 1912 to 1996 (Fig. 13c). These are insufficient to allow us to demonstrate all the interactions which require the original figures to be examined, but allow the reader to gain an impression of the size of the events and the distances between them. The results however, can be summarized. Out of 29 events, 16 (1935, 1939, 1944.1, 1953, 1957, 1964, 1967.2, 1968, 1969, 1970, 1975, 1978, 1981.1, 1981.2, 1982, 1983) occurred in regions where stress was increased by more than 0.1 bars.

The time interval between the Coulomb stress change and the subsequent events varied from 8 days to 63 years with a mean of 18 years. The 10 events after 1967 are all located in areas of Coulomb stress increase. This suggests that earlier events might be located in regions where Coulomb stress had been increased by yet earlier earthquakes. It is possible that the 1912, 1943, 1944.3, and 1963 events could be related to events in 1873, 1859, 1809 in the Gulf of Saros, to the 1889 earthquake in the Edremit Gulf, and to the 1894 earthquake in the Izmit Bay, respectively. This is discussed in greater detail by Nalbant *et al.* (1998). There are no obvious historical earthquakes to explain the events in 1919, 1924, 1928, 1932, 1944.2, 1956, 1965, and 1967.1, but they may be found in the future. The 1928 and 1944.2 events occurred in areas with a positive static stress increase induced by the 1924 event, and the 1967.1 event occurred in a region where stress was increased by

the 1965 event. The increases are lower than the 0.1 bars that we have taken as a threshold, but may nonetheless be significant.

We can therefore conclude that 16 events were clearly in regions of Coulomb stress increase. These occur in the later part of the time interval as would be expected. If less certain information about earlier events is used and smaller stress increases are presumed to be significant, then 23 of the 29 events appear to have responded to Coulomb stress interactions. Stein *et al.* (1997) examined interactions between 10 events extending to the east of the region shown in Figs. 12 and 13. Of these, all but one (8 out of 10) occurred in regions of substantially enhanced Coulomb stress. Taken together with the Nalbant *et al.* (1998) work, 24 out of 39 events since 1912 along the North Anatolian Fault, Aegean system show clear Coulomb interactions. If less certain information is included this rises to 31 out of 39. Of equal significance, no events occurred in regions where Coulomb stress was reduced. This is commonly described as the stress shadow effect (Harris and Simpson, 1993, 1996, 1998; Harris, 1998).

Stein *et al.* (1997) and Nalbant *et al.* (1998) identified a substantial increase of Coulomb stress in the Izmit area southeast of Istanbul, where active faults are present and historical events have occurred (Barka, 1996). This zone was struck by a large magnitude (M_s 7.8) event on August 17, 1999, which ruptured one of the segments previously mapped (see Fig. 12). This event occurred within the area of highest change in Coulomb stress (see Fig. 13c; Stein *et al.*, 1997; Nalbant *et al.*, 1998), suggesting that it was promoted by the sequence of previous earthquakes.

The 1999 Izmit earthquake has loaded faults in the eastern Marmara Sea between 1 and 5 bars (King *et al.*, 1999) as well as to the east of the Izmit rupture zone. On November 12, 1999, a second M 7.2 earthquake occurred at the eastern edge of the faults that ruptured during the Izmit event (see Fig. 12). It is important to point out that, while the Izmit fault was loaded by the previous ruptures, the Duzce fault was in the stress shadow (see Fig. 13c) caused by the events that occurred before 1999. The August 17, 1999, Izmit earthquake increased the stress in the Duzce area by more than 1 bar (Parsons *et al.*, 1999b; Hubert-Ferrari *et al.*, 2000), suggesting that this second shock was promoted by the previous event. These results represent a key example of the interaction between large magnitude earthquakes. The sequence of seismic events in North Anatolia points out the social implications of fault interaction studies and the significance for seismic hazard assessment (see Stein *et al.*, 1997; King *et al.*, 1999). We will discuss these topics in the following sections.

3.7. Close Interactions between Dip-Slip Earthquakes

The studies reproduced so far have all shown earthquake interactions in map view (horizontal sections), which is optimal for vertical strike-slip faults since both

minimum and maximum principal stresses lie in this plane. Various authors have examined Coulomb interactions in cross-section which is more important for dip-slip faults (Stein *et al.*, 1994; Hodgkinson *et al.*, 1996; Hubert *et al.*, 1996; Nostro *et al.*, 1997; Caskey and Wesnousky, 1997; Troise *et al.*, 1998; Crider and Pollard, 1998) where the minimum and maximum principal stresses lie in a vertical plane. Here we reproduce an example from the Nostro *et al.* (1997) paper.

Figure 14 shows in cross section an example of Coulomb stress changes caused by a vertical right-lateral strike-slip fault (a) and a 70° dipping normal fault (b). It is important to observe that the lobes of Coulomb stress changes are more pronounced in cross section for the normal fault (Fig. 14b) and in map view for the strike-slip faults (e.g., Fig. 3a). The greatest variation of Coulomb stress always occurs in the plane containing both minimum and maximum principal stresses.

The 1980 Irpinia earthquake also provides an interesting example of Coulomb stress changes caused by normal faults (four fault segments ruptured during this event forming a graben structure) which correlate well with the aftershock distribution. Figure 15 shows the Coulomb failure stress changes caused by the Irpinia earthquake both in map view at a depth of 10 km (where most of the aftershocks were located) and for a vertical cross section perpendicular to the fault strike direction. These computations were performed by Nostro *et al.* (1997) who considered an extensional regional stress field with a horizontal σ_3 oriented $N216^\circ$, and a nearly vertical σ_1 (Hippolyte *et al.*, 1994; Amato *et al.*, 1995). The correlation with the aftershock distribution is clear. Because the computed Coulomb stress changes depend on the assumed regional stress magnitude (King *et al.*, 1994), the authors have tested the sensitivity of the Coulomb stress changes to the different values of the regional stress magnitude. They found that the areas of Coulomb stress increase correlate better with the aftershock distribution for regional stress magnitudes ranging between 20 and 40 bars (which corresponds to a ratio between regional stress and coseismic stress drop ranging between 1 and 2). For larger values of the regional stress magnitude the correlation with aftershock distribution degrades. This example further confirms that when the earthquake releases all the regional stress (i.e., the coseismic stress drop is comparable to the regional stress magnitude) the optimum slip planes near the fault rotate. In general, it is observed that, if the regional deviatoric stress is much larger than the earthquake stress drop ($|\sigma_1| \approx 10\Delta\sigma$), the orientations of the optimum slip planes are less variable, and the regions of increased Coulomb stress diminish in size and become more isolated from the master fault.

The distribution of aftershocks at depth is very well correlated with the areas of Coulomb stress increase. Figure 15 shows that most of the Irpinia aftershocks are found where the predicted Coulomb stress changes are positive, suggesting that the redistribution of static stress after the Irpinia earthquake is responsible for the off-fault aftershocks. In particular, we emphasize that when normal faulting

earthquakes occur along the antithetic faults of a graben the volume between the faults is highly loaded (see also Crider and Pollard, 1998) and aftershocks occur mostly within this volume. Figure 15 also suggests evident deviations of the optimally oriented planes for normal faulting (white line segment) from the Apennine direction in areas of large Coulomb stress increase.

Nostro *et al.* (1997) have also investigated Coulomb interactions among fault segments belonging to the southern Apennine seismogenic belt by computing the stress redistribution of large earthquakes ($M > 6$) that have occurred in the past four centuries. Their calculations show that, out of 11 earthquakes, 10 occurred in areas of Coulomb stress increase. Figure 16 shows an example of interaction among normal faulting earthquakes in the Apennines: the two events in 1702 and 1732 occurred mostly inside the area of Coulomb stress increase caused by the previous 1688 and 1694 shocks (Fig. 16a). These four earthquakes also increased the Coulomb stress at the location of two subsequent events in 1805 and 1857. The Coulomb stress changes caused by the 7 largest earthquakes are shown in Fig. 16b. The orientation of the extensional stress field is well constrained by different data (Amato *et al.*, 1995; Montone *et al.*, 1999); a regional stress field with a horizontal least principal stress perpendicular to the Apennines and a nearly vertical greatest principal stress has been considered in these calculations. Nostro *et al.* (1997) found for the Apennines a correlation similar to that presented for the Aegean and Turkey (Nalbant *et al.*, 1998, Stein *et al.*, 1997). It is important to emphasize that, in regions characterized by low stressing rates, static stress perturbations of a few bars caused by large earthquakes play an important role in determining the state of stress of seismogenic faults.

4. SUMMARY OF MODELING SUCCESSES

The Coulomb interaction technique described so far is very simple. The theory is used to create colored distributions indicating regions of enhanced and reduced Coulomb stress, which are compared with the locations of earthquakes. This visual method of presentation shows that smaller earthquakes influence the location of larger ones, as in the build-up prior to the 1992 Landers earthquake. Big events influence the location of smaller ones: events of moderate size such as the Big Bear aftershock of the Landers earthquake or the smaller aftershocks that followed. Big earthquakes also apparently influence the location of other large events over substantial areas and substantial periods of time. The most dramatic examples come from Turkey, the Aegean, and Italy. Among these, the recent Izmit and the Duzce earthquakes (occurring in August and November 1999, respectively) in the western section of the North Anatolian Fault provide a striking validation of such interaction (Stein *et al.*, 1997; Nalbant *et al.*, 1998; King *et al.*, 1999; Hubert-Ferrari *et al.*, 2000).

Although most of the aftershock studies rely on the visual correlation between aftershock distribution and Coulomb stress changes, an increasing number of investigations have statistically tested the correlation between modeled static stress changes and both locations and mechanisms of triggered seismicity (Harris and Simpson, 1992, 1996; Beroza and Zoback, 1993; Bodin and Gomberg, 1994; Harris *et al.*, 1995; Gross and Kisslinger, 1997; Kilb *et al.*, 1997; Hardebeck *et al.*, 1998; Toda *et al.*, 1998; Anderson and Johnson, 1999; Seeber and Armbruster, 1999). Several investigators have developed quantitative methods for determining the importance of mainshock induced stress changes. However, they have reached different conclusions. Even if clear correlations are found for many aftershock sequences (as for the 1992; Landers or the 1995 Kobe earthquakes, see Hardebeck *et al.*, 1998; Toda *et al.*, 1998), there exist others (Loma Prieta, 1989 or Northridge, 1994) which are not as easily explained in terms of mainshock induced elastic stress changes (Beroza and Zoback, 1993; Kilb *et al.*, 1997; Hardebeck *et al.*, 1998). However, as pointed out earlier it is much harder to model nearby events for such dip-slip faults.

Convincing evidence is found for the correlation between Coulomb stress changes and seismicity rate variations for different earthquakes over a time period of several years (Reasenbergh and Simpson, 1992; Deng and Sykes, 1997a,b; Gross and Burgmann, 1998; Harris and Simpson, 1998; Toda *et al.*, 1998; Stein, 1999). We emphasize that the analysis of the correlation between Coulomb stress and seismicity rate changes is a stronger test for stress interaction than the comparison between Coulomb stress increase and aftershock distribution. In fact, seismicity may have been abundant in those zones also before the main shock (Stein, 1999). For the 1994 Northridge, California, earthquake, for instance, 65% of the observed seismicity rate changes is well correlated with the calculated stress changes (Stein, 1999, and references therein). For the 1989 Loma Prieta, California event Parsons *et al.* (1999a) found that the major right-lateral faults (slip rates larger than 7 mm/yr) appear to exhibit a different response to the stress change than do minor oblique faults. For minor oblique-slip faults (having negligible cumulative slip or lower slip rates), seismicity increased where faults were unclamped by the 1989 mainshock. In contrast, the seismicity rate change is correlated with the calculated shear stress changes for major faults (see Parsons *et al.*, 1999a, for the possible implications of such results).

There is now a sufficient number of clear examples that, although aspects of individual studies may be criticized, Coulomb stress interactions clearly do occur and exert significant control over the evolution of seismicity (see the complete reference list in Harris, 1998, Sect. 2). It is worth remarking that the successful studies appear to involve situations that are not very parameter sensitive and where limitations of the physical assumptions adopted are less likely to be important. Aftershock distributions are only really modeled well some distance from the main fault. Similarly, interactions between large events are only clear when the

distance between events is large with respect to the fault dimensions. In general, stress distributions are also insensitive to substantial changes in effective friction. In those cases where fault plane solutions are available, the regional stress need not be known well. In practice it is only used to control the predominant style of faulting in a region. For this purpose it is only necessary to establish whether the vertical principal stress is the maximum, intermediate, or minimum. Provided this is established, a wide range of values will produce the same Coulomb stress field except close to the main fault.

There are several studies which deal with the computation of the static stress changes in the near field (Caskey and Wesnousky, 1997; Nostro *et al.*, 1997; Crider and Pollard, 1998). Nostro *et al.* (1997) examined the static stress changes and the fault interaction between the subevents of the 1980 Irpinia earthquake. Nostro *et al.* (1998) also tested the interaction between southern Apennine earthquakes and historical eruptions at the Vesuvio volcano. Although they found a statistically reliable coupling, and provide a physical mechanism for such correlation, it cannot be proved that the interaction is always tenable. Moreover, there are several studies which explain the spatial and temporal variations of fault growth in terms of stress interactions and slip accumulations in self-organized processes (see Cowie, 1998, and references therein). These investigations represent a stimulating approach to considering the long-term stress effect on fault growth.

Like many successful theories, the idea that small changes of Coulomb stress as a result of one earthquake can exert a major influence on the location of future events suggests new questions and poses new problems. These are considered in the remaining sections.

5. SUMMARY OF PROBLEMS AND OPEN QUESTIONS

The foregoing examples appear to show that changes of Coulomb stress ranging between 0.1 and 1 bar (sometimes even smaller ≈ 0.01 bar) can influence the occurrence of future earthquakes. This seems very surprising. Earthquake stress drops are commonly much larger, from several bars to several hundred bars, so that such changes might seem too small to have any effect on crustal faults. Other effects such as tectonic loading, creep in the crust, tides, or atmospheric loading should swamp small changes (see Vidale *et al.*, 1998, for instance). Thus although the theory outlined above appears to work, it is appropriate to ask whether it correctly describes the physical processes that occur during faulting episodes.

Authors have addressed several aspects of this problem. No consensus has been reached and opinions can be contradictory. We will therefore first review different approaches without entering into the details of the explanations. One approach is to suggest that faults behave as a self-organized critical system (Bak and Tang, 1989; Scholz, 1991; Cowie *et al.*, 1995; Sornette and Sammis, 1995; Saleur *et al.*,

1996; Bowman *et al.*, 1998, among several others). Under these circumstances the Coulomb calculations may correctly predict the directions in which stress is enhanced, but long-range interactions mean that their strengths are not correctly estimated by the stress amplitudes. Because the fault is in a critical state, even a small stress perturbation can produce or enhance an instability (i.e., an earthquake). A second approach is to suggest that since dynamic stresses can be much larger than Coulomb static stress changes (Harris and Day, 1993; Cotton and Coutant, 1997; Belardinelli *et al.*, 1999), then the effect may be dynamic and not static. Certainly if failure occurs at peak stress then dynamic stresses should nearly always be more important than static stresses. However, peak stresses cannot be the only factor. Many events occur after a time delay of minutes to many years. It is difficult to attribute such coupling to dynamic stresses whose total duration is seconds or tens of seconds.

What can cause these time delays? There are a number of candidates. Postseismic relaxation in the crust, whether on faults or distributed through a volume, can redistribute stresses with time such that faults that were only moderately loaded after the mainshock reach threshold later (Pollitz and Sacks, 1997; Freed and Lin, 1998, among several others). Delayed failure can also result from progressive tectonic loading adding to the postearthquake stresses (Savage, 1983; Jaumé and Sykes, 1992; Simpson and Reasenber, 1994; Deng and Sykes, 1997a,b; Stein *et al.*, 1997). Another view is that failure does not result from a simple stress threshold being reached. The short-term strength of a rock is higher than the long-term strength. Gradual failure (tertiary creep) can start at stresses below that of short-term failure stress and lead to failure after a time interval. This behavior occurs in the new failure of rock, but analogous behavior is associated with frictional sliding. Faults have frictional properties that control their response to stress change and that are usually expressed by constitutive laws (Dieterich, 1972, 1979a,b, 1992, 1994; Ruina, 1983; Gu *et al.*, 1984; Rice and Gu, 1983; Rice and Tse, 1986; Tse and Rice, 1986; Scholz, 1990, 1998; Ohnaka, 1992; Rice, 1993; Roy and Marone, 1996; Boatwright and Cocco, 1996, among many others). This so-called “rate-state friction” has received considerable attention in recent years—the parameters involved are well established empirically at a laboratory scale—and thus quantitative models can be constructed (Dieterich, 1979a,b; Okubo, 1989; Blanpied *et al.*, 1991, Marone, 1998). It appears to offer at least some insight into physical processes not well described by models that treat friction as a time independent constant. Other processes, however, can modify friction with time. Fluid pressure that is perturbed by an earthquake will reequilibrate with time (Nur and Booker, 1972; Hudnut *et al.*, 1989; Roeloffs, 1988, 1996; Miller *et al.*, 1996, 1999; Noir *et al.*, 1997; Muir-Wood and King, 1993). The effective friction coefficient is not a constant. Not much work has been carried out on this effect, but there is no doubt that many authors consider that crustal fluid flow and inhomogeneities of fluid pressure must play a major role in controlling mechanics of faulting.

Finally, Coulomb calculations may have a social importance. Information is being provided about seismic hazard (Dieterich and Kilgore, 1996; Toda *et al.*, 1998). But how reliable is that information and how should it be conveyed to the public or agencies concerned with public safety? Some of the published work is driven by a desire to address such concerns, but perhaps finds it difficult to balance the desire to understand the physics and the need to address problems of hazard mitigation.

The foregoing topics overlap, but for clarity we divide our discussion into distinct topics in order to review the state of knowledge and to point out the open questions.

5.1. The Role of Static and Dynamic Loading

The Coulomb stress modeling performed for the 1992 Landers earthquake and presented above provides an excellent example of the effects of static stress changes and evidence for the correlation between aftershock distribution and mainshock-induced static stress changes (Stein *et al.*, 1992; King *et al.*, 1994). However, this earthquake also allowed short-range fault interactions to be studied (Stein *et al.*, 1992; Harris and Simpson, 1992; Cotton and Coutant, 1997), as well as long-range interactions and remotely triggered seismicity (Hill *et al.*, 1993). The 1992 Landers earthquake, after having nucleated on one fault, successively triggered rupture on four further faults within a time duration of nearly 24 seconds (Wald and Heaton, 1994; Cohee and Beroza, 1994; Cotton and Campillo, 1995). This subevent triggering was caused by the near field dynamic stress changes (Harris and Day, 1993, 1999; Cotton and Coutant, 1997; Olsen *et al.*, 1997).

Belardinelli *et al.* (1999) have studied the redistribution of dynamic stress during the 1980 Irpinia (Southern Italy) earthquake. This seismic event provides an interesting example of fault interaction due to spatiotemporal stress changes, because it ruptured several normal faults during three subevents with nearly 20 s between them. The authors have computed the dynamic stress time histories caused by an extended shear rupture using the discrete wave-number and reflectivity method proposed by Cotton and Coutant (1997), which consists of assigning the distribution of slip on a rupturing fault discretized by a set of point sources. The source time function and the rupture velocity are specified and the six components of the stress tensor $\sigma_{ik}(\vec{y}, t)$ and the Coulomb Failure Function $CFF(\vec{y}, t, \phi_r, \delta_r, \lambda_r)$ are calculated for a set of receiver points \vec{y} located outside the master fault that can be distributed on a secondary plane whose rake λ_r , strike ϕ , and dip δ angles are assigned.

Figure 17 shows an example of shear, normal, and Coulomb stress time history computed by Belardinelli *et al.* (1999) at a point located outside the rupturing fault and at a depth of 8.2 km. This figure shows that both normal and shear stress reaches, for this observer, the static level after several tens of seconds and

that the normal stress variations are much smaller than those for the shear stress. This is not general and it is possible to find other examples for which the normal stress changes can be equally important. According to Belardinelli *et al.* (1999) the dynamic stress peak (shown in Fig. 17) is reached when the rupture on the main fault is already arrested. A similar conclusion has also been obtained by Harris and Day (1993). Because of the use of smooth source time functions and low frequency Green's functions, the amplitude of dynamic stress peaks are underestimated and should be considered to be lower bounds. This implies that the dynamic Coulomb stress peak can be much larger than the static level. So why does dynamic stress not always trigger earthquakes?

In Fig. 18 we show the dynamic stress build up on the fault plane of the second subevent of the 1980 Irpinia earthquake (the fault geometry is illustrated in Fig. 15 and 17) caused by the rupture of the first subevent (see Belardinelli *et al.*, 1999). The origin time is taken at the rupture initiation on the first subevent's fault (also named master 0's event). We remark that both the fault planes of the two subevents of the Irpinia mainshock are favorably oriented with respect to the regional stress field (Nostro *et al.*, 1997). After nearly 8 s the dynamic stress reached the maximum value at the NW edge of the fault plane (the closest to the rupturing 0's subevent). After 13 s the dynamic stress reached the static configuration, as described in detail by Belardinelli *et al.* (1999). The peak dynamic stress computed up to a maximum frequency of 4.3 Hz is larger than 15 bars. This figure illustrates the temporal evolution of the induced stress field caused by coseismic ruptures.

The Coulomb stress time history shown in Fig. 17 is composed of a transient high-frequency signal superimposed on a step function. The static level associated with the step function corresponds to the static Coulomb stress (the dashed straight line in Fig. 17) resulting from the solution of Volterra's equation (Okada, 1985, 1992, and references therein). The transient phase on the stress time history corresponds to the dynamic stress changes. At close distances from the causative fault plane these two stresses act together (as shown in Fig. 18), so how can the most important one be determined? (See Gomberg *et al.*, 1998, and references therein.) Scholz (1998) concluded that fault rupture is such that failure is not sensitive to just stress amplitude, but also to the time over which loading persists. The relation between these parameters has to be sought in some sort of constitutive law of failure.

5.2. Rate and State Dependent Friction Laws

We have presented applications, observational tests, and interpretations of fault interactions and triggered seismicity caused by stress changes. It has been pointed out that, even if we can compute the induced stress perturbation, the constitutive properties of the fault control the frictional response and therefore the triggering

phenomena. It is also important to remember that, in order to determine the time of the earthquake rupture (that is, the time of a triggered event), the absolute initial stress level (prestress) on the neighboring faults must be known. For this reason the Coulomb stress analysis based on coseismic stress changes allows us only to infer where in the surrounding volume earthquakes are favored or inhibited. This also means that the achievement of the Coulomb failure criterion does not allow us to establish when (i.e., the exact timing) earthquake triggering will occur (Harris and Day, 1993; Belardinelli *et al.*, 1999). Supposing that after a stress perturbation the Coulomb criterion is satisfied (this implies that absolute stress is known), then an estimate of the time of failure can be obtained if the frictional properties of the secondary faults are known. Gomberg *et al.* (1998) pointed out that the triggering response (the time advance) to a transient or a static shear load depends on when in the loading cycle the induced load is applied.

A clear example of the problem is provided by the M 6.6 Big Bear aftershock 3 hr and 26 min after the 1992 Landers earthquake. As previously shown, this event is located in an area of high Coulomb stress increase, which leads to the conclusion that the Landers earthquake promoted the Big Bear event. Spudich *et al.* (1995) discussed the problem, pointing out that a time delay of 3.5 hr is difficult to explain in terms of Coulomb criterion considering either dynamic or static stress changes. Fault frictional properties and rheology can explain the occurrence of delayed triggering from a few tens of seconds to several hours (see Boatwright and Cocco, 1996; Gomberg *et al.*, 1998), although other phenomena can explain long time delays, such as fluid flow or viscoelastic relaxation (see for instance Hudnut *et al.*, 1989, and Freed and Lin, 1998).

Rate and state dependent friction laws are based on laboratory experiments and they are more complex than a stress threshold criterion such as the Coulomb failure. While stick-slip motion means an unstable behavior, such constitutive laws also describe how faulting can be stable (see Scholz, 1990, and references therein). Many similar formulations of rate and state dependent friction law have been proposed (see Marone, 1998, or Scholz, 1998, and reference therein). In general, these constitutive laws can be described by two coupled equations. The first one relates the sliding resistance τ to the slip velocity V and the state variables θ_i ; it is usually named the governing equation

$$\tau = F[V, \theta_i, A, B, \mu_o, \sigma_n],$$

where A and B are two positive parameters that depend on the material properties, temperature and pressure, μ_o is a reference friction value, and σ_n is the normal stress. The second law provides the time evolution of the state variable and it is called the evolution equation; here we report this equation for a single state variable

$$\frac{\partial \theta}{\partial t} = G[V, L, \theta, B].$$

The state variable θ provides a memory for the sliding surface (Dieterich, 1978, 1979a,b; Ruina, 1980, 1983). A widely used formulation for these laws is that proposed by Dieterich (1994) which is a simplified version including only one state variable (see also Dieterich and Kilgore, 1996)

$$\tau = \mu_o \sigma_n + A \ln \frac{V}{V^*} + B \ln \frac{\theta}{\theta^*}$$

$$\frac{\partial \theta}{\partial t} = 1 - \frac{\theta}{L} V.$$

These equations have been proposed to model earthquake aftereffects (see Rice, 1983) and they have been recently used to predict aftershock rates (Dieterich, 1994; Toda *et al.*, 1998) and to study stress shadowing (Harris and Simpson, 1998) as well as stress triggering (Boatwright and Cocco, 1996; Gomberg *et al.*, 1997 and 1998). Belardinelli *et al.* (1999) have interpreted the inferred 10 s of triggering delay for the second subevent of the 1980 Irpinia earthquake in terms of this rate and state dependent frictional law. This event provides a very interesting example of a delayed triggered instability. In fact, the dynamic rupture neither instantaneously jumped from the first fault segment to the second one nor jumped at the arrival time of the maximum induced stress.

Subevent triggering can occur within a few seconds, as observed, for instance, during the 1992 Landers and the 1980 Irpinia earthquakes. During such short triggering times the remote tectonic load does not play a role (Dieterich, 1994; Belardinelli *et al.*, 1999). However, if earthquake interaction occurs over longer time scales (several years as well as tens of years), the fault response to a change in stress depends on the stress perturbation amplitude, the fault frictional properties, and the tectonic stressing rate. Harris and Simpson (1998) investigated the suppression of large earthquakes by the stress shadow (negative change of Coulomb stress, $\Delta CFF < 0$, see Harris and Simpson, 1993, 1996) generated by great earthquakes in California, such as the 1857 Fort Tejon and the 1906 San Francisco events. These authors tried to constrain the approximate time that should be taken by long-term tectonic loading to recover the negative stress change. Harris and Simpson (1998) examined stress shadows in terms of earthquake failure models using rate and state dependent friction laws (Dieterich, 1994). They also examined the likelihood that the 78 years of relative quiescence for large earthquakes in the Bay area after the 1906 event is consistent with the assumption of a rate and state dependent law.

Other processes can also account for fault interaction and earthquake triggering over different spatial and temporal scales. Kenner and Segall (1999) interpreted the time dependence of the stress shadowing effect in terms of viscoelastic relaxation of the lower crust. Although these processes can contribute to the temporal variations of the stress field, fault frictional properties certainly play the dominant role in determining the time for dynamic failure and therefore they provide a major control on the seismic cycle of large faults.

5.3. Fluid Flow

Most of the applications described above are based on Coulomb stress changes caused by an earthquake, assuming a fixed value for the effective friction coefficient μ' (Eq. (6)). Several recent papers concluded that Coulomb stress changes are modestly dependent on the assumed values of the effective friction coefficient μ' (King *et al.*, 1994; Nostro *et al.*, 1998) or they suggest small values ranging between 0.0 and 0.2 (Reasenberg and Simpson, 1992; Kagan and Jackson, 1998; Harris, 1998; Gross and Burgmann, 1998). However, some of these investigations have proposed that the effective friction coefficient can change and its variations could be related to fluid migration (Reasenberg and Simpson, 1992; Harris and Simpson, 1992; Jaumé and Sykes, 1992).

There have also been reported in recent years several observations and numerical investigations which focused on normal stress variations: normal stress changes are responsible for clamping or unclamping the fault plane, thus discouraging or encouraging fault failure (Perfettini *et al.*, 1999; Parsons *et al.*, 1999a; Cocco *et al.*, 1999). Normal as well as volumetric stress changes can exert important effects on rock permeability modulating fluid flow in the crust. They contribute to permeability anisotropy that can enhance or counteract the preexisting rock-mass permeability (see Rice, 1992; Sibson, 1994, and references therein; Cocco and Rice, 1999).

It is important to point out that from its definition the effective friction coefficient is not a material property, but it depends on the state of stress of the medium (see Harris, 1998). It has to be also remarked that the physical assumptions that justify its definition cannot be so widely applicable. In other words, the use of Eq. (1) is more general than for Eq. (6) (Beeler *et al.*, 1998). Fluid flow is related to the response of the medium to volumetric and normal stress changes. The imposition of the stress perturbation $\Delta\sigma_{kk}$ occurs over a time scale that is too short to allow the loss or gain of pore fluid by diffusive transport (Rice and Cleary, 1976). We refer to this short time scale as undrained response of the medium. Therefore, the instantaneous (or undrained) response is that for which fluids do not flow ($\Delta m = 0$) and volumetric and normal stress changes are associated with pore pressure changes

$$\Delta P = -B \frac{\Delta\sigma_{kk}}{3},$$

where B is the Skempton coefficient and $\Delta\sigma_{kk}$ are the volumetric stress changes (Rice and Cleary, 1976; Roeloffs, 1996). At longer time scales Darcy's flow occurs as the tendency to achieve the global pressure equilibrium over the entire deformed region. Although fluid flow and elastic deformation should be coupled in a poro-elastic solution, most studies face these phenomena separately. Both Eqs. (1) and (6) consider the undrained response of the medium. In the former equation the undrained response (see Rice and Cleary, 1976) is represented by a pore pressure

proportional to the mean (or volumetric) stress, while in the latter it is assumed that the pore pressure is proportional to the normal stress yielding the definition of μ' . This can be a valid assumption only in the presence of a particular rheology (Rice, 1992; Reasenberg and Simpson, 1994; Harris, 1998) or anisotropy within the fault zone (Cocco and Rice, 1999). Despite this ambiguity, Eq. (6) is widely applied in Coulomb analysis.

Jaumé and Sykes (1992) and Stein *et al.* (1992) have considered the role of pore pressure changes due to undrained deformation in calculations of the coseismic Coulomb stress changes on major faults caused by the 1992 Landers earthquake. Fluid flow triggering of seismicity has been proposed to explain aftershocks (Nur and Booker, 1972; Li *et al.*, 1987), earthquake triggering, and seismicity migration during sequences (Hudnut *et al.*, 1989; Miller *et al.*, 1996; Noir *et al.*, 1997; Cocco *et al.*, 1998). Normal stress and pore pressure change affect the frictional response of faults (Linker and Dieterich, 1992) as well as fluid flow and therefore they contribute to the variations of the stress state and the mechanical conditions of fault zones.

Muir-Wood and King (1993) and King and Muir-Wood (1994) investigated the main features of hydrological changes that follow major earthquakes, which are dependent on the style of faulting. The most significant response is found for normal faulting earthquakes that can produce increase in spring and river discharge rates. Coseismic water-level changes have been also observed near Parkfield and Landers (Roeloffs and Quilty, 1997; Roeloffs, 1996, 1998). In general, all these studies indicate that earthquakes cause a variety of hydrologic phenomena, some of which can be explained by poroelastic response to the earthquake strain field, but others require nonelastic processes which yield changes in permeability near the fault zone. Roeloffs (1996), Muir-Wood and King (1993), and King and Muir-Wood (1994) have presented observations for different seismogenic areas.

Little modeling of fluid flow has been attempted although it is potentially one of the important processes for determining time constants in failure processes. Much more work is needed in this field.

5.4. Creep in the Crust or on Faults

The Coulomb modeling discussed so far assumes that all fault motion occurs as earthquakes, but faults can also move aseismically. In a more general formulation, rate and state dependent friction laws allow us to model aseismic sliding as stable motion (see Scholz, 1990, 1998, and references therein). This process occurs at depths below the seismogenic zone (Scholz, 1990) and its modeling is the basis for tectonic loading models discussed in the next section. Shallower creep can, however, occur. The central San Andreas over a stretch of 150 km appears to creep throughout the seismogenic zone with less than 3% of slip being accommodated

seismically (Amelung and King, 1997). No other major fault has been shown to creep throughout the seismogenic zone. More local creep does occur on some faults close to the surface: the San Andreas and Superstition Hills faults in the Coachella Valley creep down to about 3 km from the surface (see Bodin *et al.*, 1994). The Hayward fault creeps to 7 km depth in the south and to 5 km along most of its length and it is locked between 5 and 12 km depth (Savage *et al.*, 1993). Afterslip has also been observed on some other California faults following large events (Marone *et al.*, 1991; Bilham, 1992).

As aseismic sliding below the seismogenic layer can load shallow faults, afterslip and creeping within this layer can provide a mechanism to release part of the stress transferred by elastic interaction. Therefore, such creeping parts of faults should be included in Coulomb models, but the data to define geometries and rates are not generally available. In particular, afterslip occurs following an earthquake and contributes in transferring the stress, both to other parts of the fault and to the surrounding medium. Lack of the required information does not allow these effects to be taken into account when computing patterns of Coulomb stress changes. Finally, together with tertiary fault creep, viscous relaxation in the lower crust and fluid flow adds to the possible time constants determining when later events are triggered.

5.5. Tectonic Loading

In a previous section we have presented and discussed evidence for interactions between large earthquakes in Italy, Turkey, and the Aegean. Similar studies have been carried out for California and elsewhere. These interaction studies, however, take no account of tectonic loading and it would seem essential that it should be included if the time period of a study is sufficiently long that loading stresses become comparable to earthquake induced stress changes. The process adopted for strike-slip environments is to consider that faults extend to depth and are freely slipping below a locking depth. The latter is assumed to be at the base of the seismogenic zone (Simpson and Reasenber, 1994; Jaumé and Sykes, 1996; Deng and Sykes, 1997a,b; Stein *et al.*, 1997). The slip on the deep fault is determined considering the long-term slip rate obtained geologically or geodetically. Motion on these faults then creates stresses in the seismogenic zone that are added to those from earthquakes.

Although the above strategy seems reasonable for strike-slip environments it is not applicable to more complex fault geometries and to different tectonic settings (such as reverse or normal faults in contractional or extensional regimes). Jaumé and Sykes (1996) adopt the concept of anti-earthquakes. They assume that the form of loading in the past has been exactly the opposite of that released by an earthquake; pure elastic rebound. An appropriate rate is attributed to the build-up of that stress. This is at best an approximation. Cumulative geological structures

appear as the result of dip-slip events indicating that the stresses relieved must be different from those applied. For California, where Jaumé and Sykes applied the concept, dip-slip faulting is a minor contributor. Thus their approach was not well tested. It seems that to correctly develop loading models in such regimes, deformation in the lower crust will have to be understood.

5.6. Postseismic Evolution

Another important contribution to the long-term loading process arises from viscoelastic relaxation of the lithosphere and asthenosphere. Most of the aforementioned studies rely on computation of the elastic stress changes in the lithosphere and they do not explicitly include long-term viscoelastic processes, which provide a time dependency to Coulomb stress maps. Although purely elastic models provide insight into the effects of stress perturbation, they do not account for time dependent phenomena. In principle, including viscoelastic effects should allow better modeling of fault interaction over different earthquake cycles.

Stein *et al.* (1992) and King *et al.* (1994) use a plane stress elastic plate model to infer the stress perturbation after relaxation of the lithosphere. Although useful to constrain the magnitude of the phenomenon, this approximation does not incorporate any time dependent process. Dmowska *et al.* (1988) and Taylor *et al.* (1998) modeled the earthquake cycle and the stress perturbations in coupled subduction zones to investigate the effects on the subsequent seismicity. Freed and Lin (1998) and Pollitz and Sacks (1997) used viscoelastic models to investigate earthquake triggering; the former applied a 2D model to the 1994 Northridge earthquake, and the latter suggested that the 1995 Kobe earthquake might have been triggered by two previous earthquakes that occurred half a century before. Kenner and Segall (1999) suggested that time dependent viscoelastic stress transfer can modify the stress shadows caused by large crustal earthquakes. It can enhance the amplitude and the extent of stress shadows on a short time scale, due to the relaxation of the lower crust, but it can also reload the entire crust over longer time scales thus contributing to the recovery of stress shadows.

In general, it is important to emphasize that viscoelastic relaxation processes, poroelastic effects (fluid flow, for instance), creep, and rate and state dependent friction all contribute to the modification of the postseismic stress distribution in ways we do not yet fully understand.

6. SOCIAL CONCERNS

In this paper we have presented many observations, theoretical modeling, and interpretations of stress perturbation caused by coseismic dislocations and have

discussed how tectonic stressing rate and changes in Coulomb stress modify the failure conditions. This results in changing the probability for future earthquake ruptures (see Harris, 1998; Toda *et al.*, 1998).

We can summarize the discussion presented above by emphasizing that the seismic cycle of a fault is determined by the remote tectonic load; it is controlled by the fault frictional properties, but it is modulated by fault interaction and stress transfer. If we accept the idea that induced stress changes promote future seismic events by altering the mechanical conditions on favorably oriented faults, we must therefore expect that the probability for the occurrence of impending events will be also modified. Although there are many open questions on the most appropriate methodology for calculating stress perturbations and the applicability of induced stress to fault mechanics, the potential benefits to the public of such investigations are quite evident.

Stein *et al.* (1997) and Toda *et al.* (1998) have converted their modeling results for static stress changes on particular faults into earthquake probability changes. The implications of such calculations for seismic hazard are straightforward. However, lack of knowledge about the frictional properties of the faults limits the applicability of these calculations for social concerns. In other words, if we accept the idea that a mature fault zone can behave in a way (in terms of constitutive properties) different from a young or recent seismogenic fault, the impact of the probability change estimates is strongly reduced. Nevertheless, this topic is a fundamental research task for the scientific community in the 21st century: the success in transferring our understanding of fault interaction into earthquake probabilities will have a big social impact. This task still belongs to debate within the scientific community and further efforts are required before our conclusions can be exported to society.

7. CONCLUDING REMARKS

In this review paper we have discussed the theoretical modeling of fault interaction through stress transfer. We have mostly focused our discussion on elastic stress redistribution and we have presented a summary of modeling success as well as remaining open questions. We have also briefly discussed other factors contributing to the coseismic and postseismic stress redistribution process. Toward the end of the 20th century, we have learned how earthquakes interact and that coseismic stress changes represent an important contribution to the definition of the seismic cycle of active faults.

Convincing evidence for elastic stress interaction is provided both by interactions between large events in regions such as Turkey and the Aegean and by aftershock distributions and seismicity rate changes. Although further tests and observational constraints are required to effectively predict aftershock distributions

by means of simple stress calculations, it has been shown that mainshock induced stress changes control the subsequent seismicity. Moreover, it has been pointed out that in areas where stress calculations can be combined with knowledge of active faults, these studies contribute to the assessment of seismic hazard. One of the most convincing example comes from the North Anatolia (Turkey) and the Aegean (Greece), which were struck by destructive earthquakes that redefined the seismic hazard in the area.

Future research has to address the question of how stress changes can be transferred into earthquake probability change, whose social impact is evident. These studies must necessarily focus on a better definition of the tectonic load and the understanding of fault frictional properties. Although we understand how an earthquake can advance, delay, or inhibit a future event, we are still not able to model the timing of failure. Assessing the time delays as well as the clock advance can provide a better knowledge of fault constitutive parameters and the tectonic stressing rate of the areas. Therefore, close interaction among all the research fields that contribute to the definition of the mechanical conditions of active faults is a key strategy for further progress in this topic.

ACKNOWLEDGMENTS

The authors have extensively benefited from discussions with Ross Stein, Jim Rice, Bob Simpson, Paul Tapponier, Concetta Nostro, Maria Elina Belardinelli, Nick Beeler, Raul Madariaga, Antonio Pier-santi, Roger Bilham, Aurelia Hubert-Ferrari, Lucilla Benedetti, Pino De Natale, and Claudia Troise. We wish to thank all of them. We also thank Ruth Harris and an anonymous referee for their suggestions and the critical review of the manuscript. This research was partly supported by the European Commission Contract ENV-4970528 FAUST and IGP contribution No. 1695.

REFERENCES

- Aki, K., and Richards, P. (1980). "Quantitative Seismology." W. H. Freeman and Co., San Francisco, CA.
- Amato, A., Montone, P., and Cesaro, M. (1995). State of stress in southern Italy from borehole breakout and focal mechanism data. *Geophys. Res. Lett.* **22**, 3119–3122.
- Amato, A., and Selvaggi, G. (1993). Aftershock location and P-velocity structure in the epicentral region of the 1980 Irpinia earthquake. *Ann. Geofis.* **36**(1), 3–15.
- Ambraseys, N. N., and Melvine, C. P. (1982). "A History of Persian earthquakes". Cambridge University Press, Cambridge.
- Amelung, F. (1996). "Kinematics of Small Earthquakes and Active Tectonic and Topography in the San Francisco Bay Region (Ph.D. thesis) I. P. G. Strasbourg, France.
- Amelung, F., and King, G. C. P. (1997). Earthquake scaling laws for creeping and non-creeping faults. *Geophys. Res. Lett.* **24**(5), 507–510.
- Anderson, G., and Johnson, H. (1999). A new statistical test for static stress triggering: Application to the 1987 Supersition Hills earthquake sequence. *J. Geophys. Res.* **104**, 20,153–20,168.

- Archuleta, R. I., and Day, S. M. (1980). Dynamic rupture in a layered medium: The 1966 Parkfield earthquake. *Bull. Seismol. Soc. Am.* **70**, 671–689.
- Bak, P., and Tang, C. (1989). Earthquakes as self-organized critical phenomena. *J. Geophys. Res.* **94**, 15,635–15,637.
- Barka, A. A. (1996). Slip distribution along the North Anatolian Fault associated with large earthquakes of the period 1939 to 1967. *Bull. Seismol. Soc. Am.* **86**, 1238–1254.
- Beeler, N. M., Simpson, R. W., and Lockner, D. A. (1998). “Loading Faults to Coulomb Failure.” 1998 Fall Meeting of the American Geophysical Union, *EOS*, Transactions, Vol. 79, No. 45, November 10 1998 (abstract) F639.
- Belardinelli, M. E., Cocco, M., Coutant, O., and Cotton, F. (1999). Redistribution of dynamic stress during coseismic ruptures: Evidence for fault interaction and earthquake triggering. *J. Geophys. Res.* **104**, 14,925–14,945.
- Beroza, G. C., and Zoback, M. D. (1993). Mechanism diversity of the Loma Prieta aftershocks and the mechanics of mainshock–aftershock interaction. *Science* **259**, 210–213.
- Bilham, R. (1992). Sinistral creep on the Xianshuihe Fault at Xialatuo in the 17 years following the 1973 Luhuo earthquake. In “Proc. PRC-US Bilateral Symposium on the Xianshuihe Fault Zone,” October 1990, Chengdu, China. Seismological Press, Beijing, pp. 226–231.
- Blanpied, M. L., Lockner, D. A., and Byerlee, J. D. (1991). Fault stability inferred from granite sliding experiments at hydrothermal conditions. *Geophys. Res. Lett.* **18**, 609–612.
- Boatwright, J., and Cocco, M. (1996). Frictional constraints on crustal faulting. *J. Geophys. Res.* **101**, 13,895–13,910.
- Bodin, P., Bilham, R., Behr, J., Gombert, J., and Hudnut, K. (1994). Slip triggered on southern California faults by the Landers earthquake sequence. *Bull. Seismol. Soc. Am.* **84**, 806–816.
- Bodin, P., and Gombert, J. (1994). Triggered seismicity and deformation between the Landers, California, and Little Skull mountain, Nevada, earthquakes. *Bull. Seismol. Soc. Am.* **84**, 835–843.
- Bouchon, M. (1997). The state of stress on some faults of the San Andreas system as inferred from near-field strong motion data. *J. Geophys. Res.* **102**, 11,731–11,744.
- Bowman, D. D., Ouillon, G., Sammis, C. G., Sornette, A., and Sornette, D. (1998). An observational test of the critical earthquake concept. *J. Geophys. Res.* **103**(10), 24,359–24,372.
- Caskey, S. J., and Wesnousky, S. G. (1997). Static stress changes and earthquake triggering during the 1954 Fairview Peak and Dixie Valley earthquakes, central Nevada. *Bull. Seismol. Soc. Am.* **87**, 521–527.
- Chinnery, M. A. (1961). The deformation of the ground around a surface fault. *Bull. Seismol. Soc. Am.* **51**, 355–372.
- Chinnery, M. A. (1963). The stress changes that accompany strike-slip faulting. *Bull. Seismol. Soc. Am.* **53**, 921–932.
- Chinnery, M. A., and Landers, T. E. (1975). Evidence for earthquake triggering stress. *Nature* **258**, 490–493.
- Cocco, M., Nostro, C., and Ekstrom, G. (2000). Static stress changes and fault interaction during the 1997 Umbria-Marche earthquake sequence. *J. Seismol.* (in press).
- Cocco, M., Nostro, C., Troise, C., and De Natale, G. (1998). “Fault Interaction and Earthquake Triggering Caused by Fluid Flow: Evidence from the 1997 Umbria-Marche (Italy) Seismic Sequence.” 1998 Fall Meeting of the American Geophysical Union, *EOS*, Transactions, Vol. 79, No. 45, November 10 1998 (abstract) F802.
- Cocco, M., and Rice, J. R. (1999). “Undrained Fault Pore Pressure in Coulomb Analysis: Determined by Normal Stress or First Invariant?” 1999 Fall Meeting of the American Geophysical Union, *EOS*, Transactions, Vol. 80, No. 46, November 16 1999 (abstract) F1006.
- Cohee, B. P., and Beroza, G. C. (1994). Slip distribution of the 1992 Landers earthquake and its implications for earthquake source mechanics. *Bull. Seismol. Soc. Am.* **84**, 692–712.
- Cotton, F., and Campillo, M. (1995). Frequency domain inversion of strong motions: Application to the 1992 Landers earthquake. *J. Geophys. Res.* **100**, 3961–3975.

- Cotton, F., and Coutant, O. (1997). Dynamic stress variations due to shear faulting in a plane-layered medium. *Geophys. J. Int.* **128**, 676–688.
- Cowie, P. A. (1998). A healing-reloading feedback control on the growth of seismogenic faults. *J. Struct. Geol.* **20**, 1075–1087.
- Cowie, P. A., Sornette, D., and Vanneste, C. (1995). Multifractal scaling properties of a growing fault population. *Geophys. J. Int.* **122**, 457–469.
- Crider, J. G., and Pollard, D. D. (1998). Fault linkage: Three-dimensional mechanical interaction between echelon normal faults. *J. Geophys. Res.* **103**(10), 24,373–24,392.
- Das, S., and Scholz, C. (1981). Off-fault aftershock clusters caused by shear stress increase? *Bull. Seismol. Soc. Am.* **71**, 1669–1675.
- Deng, J., and Sykes, L. R. (1997a). Evolution of the stress field in southern California and triggering of moderate-size earthquakes: A 200-years perspective. *J. Geophys. Res.* **102**, 9859–9886.
- Deng, J., and Sykes, L. R. (1997b). Stress evolution in southern California and triggering of moderate-, small-, and micro-size earthquakes. *J. Geophys. Res.* **102**, 24,411–24,435.
- Deschamps, A., and King, G. C. P. (1994). Aftershocks of the Campania-Lucania (Italy) earthquake of 23 November, 1980. *Bull. Seismol. Soc. Am.* **84**, 935–953.
- Dieterich, J. H. (1972). Time dependence friction as a possible mechanism for aftershocks. *J. Geophys. Res.* **77**, 3771–3781.
- Dieterich, J. H. (1978). Time dependent friction and the mechanics of stick-slip. *Pure Appl. Geophys.* **116**, 790–806.
- Dieterich, J. H. (1979a). Modeling of rock friction, 1, experimental results and constitutive equations. *J. Geophys. Res.* **84**, 2161–2168.
- Dieterich, J. H. (1979b). Modeling of rock friction, 2, simulation of pre-seismic slip. *J. Geophys. Res.* **84**, 2169–2175.
- Dieterich, J. H. (1992). Earthquake nucleation on faults with rate- and state-dependent strength. *Tectonophysics* **211**, 115–134.
- Dieterich, J. H. (1994). A constitutive law for rate of earthquake production and its application to earthquake clustering. *J. Geophys. Res.* **99**, 2601–2618.
- Dieterich, J. H., and Kilgore, B. (1996). Implications of fault constitutive properties for earthquake prediction. *Proc. Natl. Acad. Sci. USA* **93**, 3787–3794.
- Dmowska, R., and Lovison, L. C. (1992). Influence of asperities along subduction interfaces on the stressing and seismicity of adjacent areas. *Tectonophysics* **211**, 23–43.
- Dmowska, R., Rice, J. R., Lovison, L. C., and Josell, D. (1988). Stress transfer and seismic phenomena in coupled subduction zones during the earthquake cycle. *J. Geophys. Res.* **93**, 7869–7884.
- Dmowska R., Zheng, G., and Rice, J. R. (1996). Seismicity and deformation at convergent margins due to heterogeneous coupling. *J. Geophys. Res.* **101**, 3015–3029.
- Freed, A. M., and Lin, J. (1998). Time-dependent changes in failure stress following thrust earthquakes. *J. Geophys. Res.* **103**(10), 24,393–24,410.
- Gomberg, J., Beeler, N. M., Blanpied, M. L., and Bodin, P. (1998). Earthquake triggering by transient and static deformations. *J. Geophys. Res.* **103**(10), 24,411–24,426.
- Gomberg, J., Blanpied, M. L., and Beeler, N. M. (1997). Transient triggering of near and distant earthquakes. *Bull. Seismol. Soc. Am.* **87**, 294–309.
- Gross, S., and Burgmann, R. (1998). The rate and state of background stress estimated from the aftershocks of the 1989 Loma Prieta, California, earthquake. *J. Geophys. Res.* **103**, 4915–4927.
- Gross, S., and Kisslinger, C. (1997). Estimating tectonic stress rate and state with Landers aftershocks. *J. Geophys. Res.* **102**, 7603–7612.
- Gu, J. C., Rice, J. R., Ruina, A. L., and Tse, S. T. (1984). Slip motion and stability of a single degree of freedom elastic system with rate and state dependent friction. *J. Mech. Phys. Solids* **32**, 167–196.
- Hardebeck, J. L., Nazareth, J. J., and Hauksson, E. (1998). The static stress change triggering model: Constraints from two southern California aftershock sequences. *J. Geophys. Res.* **103**(10), 24,427–24,438.

- Harris, R. A. (1998). Introduction to special section: Stress triggers, stress shadows, and implications for seismic hazard. *J. Geophys. Res.* **103**(10), 24,347–24,358.
- Harris, R. A., and Day, S. M. (1993). Dynamics of fault interaction: Parallel strike-slip faults. *J. Geophys. Res.* **98**, 4461–4472.
- Harris, R. A., and Day, S. M. (1999). Dynamic 3D simulations of earthquakes on en echelon faults. *Geophys. Res. Lett.* **26**, 2089–2092.
- Harris, R. A., and Simpson, R. W. (1992). Changes in static stress on southern California faults after the 1992 Landers earthquake. *Nature* **360**, 251–254.
- Harris, R. A., and Simpson, R. W. (1993). In the shadow of 1857: An evaluation of the static stress changes generated by the M8 Ft. Tejon, California, earthquake. *EOS Trans. AGU* **74**(43), Fall Meet. Suppl., 427.
- Harris, R. A., and Simpson, R. W. (1996). In the shadow of 1857—The effect of the great Ft. Tejon earthquake on subsequent earthquakes in southern California. *Geophys. Res. Lett.* **23**, 229–232.
- Harris, R. A., and Simpson, R. W. (1998). Suppression of large earthquakes by stress shadows: A comparison of Coulomb and rate-and-state failure. *J. Geophys. Res.* **103**(10), 24,439–24,452.
- Harris, R. A., Simpson, R. W., and Reasenber, P. A. (1995). Influence of static stress changes on earthquake locations in southern California. *Nature* **375**, 221–224.
- Hauksson, E., Hafner, K., Hardebeck, J., Heaton, T., Hutton, K., Kanamori, H., Maechling, P., Busby, R., Zhu, L., Jones, L. M., Given, D., and Wald, D. (1999). Overview of the 10-16-1999 Mw 7.1 Hector Mine, California, earthquake sequence. 1999 Fall Meeting of the American Geophysical Union, *EOS*, Transactions, Vol. 80, No. 46, November 16 1999 (abstract) 15.
- Hauksson, E., Jones, L. M., Hutton, K., and Eberhart-Phillips, D. (1993). The 1992 Landers earthquake sequence: Seismological observations. *J. Geophys. Res.* **98**, 19835–19858.
- Hill, D. P., Reasenber, P. A., Michael, A., Arabaz, W. J., Beroza, G., Brumbaugh, D., Brune, J. N., Castro, R., Davis, S., dePolo, D., Ellsworth, W. L., Gomberg, J., Harmsen, S., House, L., Jackson, S. M., Johnston, M. J. S., Jones, L., Keller, R., Malone, S., Munguia, L., Nava, S., Pechmann, J. C., Sanford, A., Simpson, R. W., Smith, R. B., Stark, M., Stickney, M., Vidal, A., Walter, A., Wong, V., and Zollweg, J. (1993). Seismicity remotely triggered by the Magnitude 7.3 Landers, California, earthquake. *Science* **260**, 1617–1623.
- Hippolyte, J. C., Angelier, J., and Roue, F. (1994). A major geodynamic change revealed by Quaternary stress pattern in the southern Appenines (Italy). *Tectonophysics* **230**, 199–210.
- Hodgkinson, K. M., Stein, R. S., and King, G. C. P. (1996). The 1954 Rainbow Mountain-Fairview Peak-Dixie Valley earthquakes: A triggered normal faulting sequence. *J. Geophys. Res.* **101**, 25,459–25,471.
- Hubert, A., King, G. C. P., Armijo, R., Meyer, B., and Papanastasiou, D. (1996). Fault re-activation, stress interaction, and rupture propagation of the 1981 Corinth earthquake sequence. *Earth Planet. Sci. Lett.* **142**, 573–585.
- Hubert-Ferrari, A., Barka, A., Nalbant, S., Meyer, B., Armijo, R., Tapponier, P., and King, G. C. P. (2000). Seismic hazard in the Marmara Sea following the 17 August 1999 Izmit earthquake. *Nature* **16**.
- Hudnut, K. W., Seeber, L., and Pacheco, J. (1989). Cross-fault triggering in the November 1987 Superstition Hills earthquake Sequence, southern California. *Geophys. Res. Lett.* **16**, 199–202.
- Jaeger, J. C., and Cook, N. G. W. (1979). "Fundamentals of Rock Mechanics," 3rd ed. Chapman and Hall, London.
- Jaumé, S. C., and Sykes, L. R. (1992). Change in the state of stress on the southern San Andreas fault resulting from the California earthquake sequence of April to June 1992. *Science* **258**, 1325–1328.
- Jaumé, S. C., and Sykes, L. R. (1996). Evolution of moderate seismicity in the San Francisco Bay region, 1850 to 1993: Seismicity changes related to the occurrence of large and great earthquakes. *J. Geophys. Res.* **101**, 765–789.

- Kagan, Y. Y., and Jackson, D. D. (1998). Spatial aftershock distribution: effect of normal stress. *J. Geophys. Res.* **103**(10), 24453–24468.
- Kenner, S., and Segall, P. (1999). Time dependence of the stress shadowing effect and its relation to the structure of the lower crust. *Geology* **27**(2), 119–122.
- Kilb, D., Ellis, M., Gombert, J., and Davis, S. (1997). On the origin of diverse aftershock mechanisms following the 1989 Loma Prieta earthquake. *Geophys. J. Int.* **128**, 557–570.
- King, G. C. P. (1986). Speculations on the geometry of the initiation and termination processes of earthquake rupture and its relation to morphology and geological structure. *Pure Appl. Geophys.* **124**(3), 565–585.
- King, G. C. P., Hubert-Ferrari, A. D., Barka, A., Jacques, E., Nalbant, S., Meyer, B., Armijo, R., and Tapponier, P. (1999). Seismic hazard in the sea of Marmara following the Izmit earthquake. 1999 Fall Meeting of the American Geophysical Union, *EOS*, Transactions, Vol. 80, No. 46, November 16 1999 (abstract) F664.
- King, G. C. P., and Muir-Wood, R. (1994). The impact of earthquakes on fluids in the crust. *Ann. Geofis.* **37**(6), 1453–1460.
- King, G. C. P., and Nabelek, J. (1985). The role of bends in faults in the initiation and termination of earthquake rupture: Implications for earthquake prediction. *Science* **228**, 986–987.
- King, G. C. P., Stein, R. S., and Lin, J. (1994). Static stress changes and the triggering of earthquakes. *Bull. Seismol. Soc. Am.* **84**, 935–953.
- Li, V. C., Seale, S. H., and Cao, T. (1987). Postseismic stress and pore pressure readjustment and aftershock distributions. *Tectonophysics* **144**, 37–54.
- Linker, M. F., and Dieterich J. H. (1992). Effects of variable normal stress on rock friction: observations and constitutive equations. *J. Geophys. Res.* **97**(4), 4923–4940.
- Marone, C. (1998). Laboratory-derived friction laws and their application to seismic faulting. *Ann. Rev. Earth Planet. Sci.* **26**, 643–696.
- Marone, C. J., Scholz, C. H., and Bilham, R. (1991). On the Mechanics of earthquake afterslip. *J. Geophys. Res.* **96**, 8441–8452.
- Maruyama, T. (1964). Static elastic deformation in an infinite and semi-infinite medium. *Bull. Earth Res. Inst.* **42**, 289–368.
- Michael, A. J. (1991). Spatial variations of stress within the 1987 Whittier Narrows, California, aftershock sequence: New techniques and results. *J. Geophys. Res.* **96**, 6303–6319.
- Michael A. J., Ellsworth, W. L., and Oppenheimer, D. H. (1990). Coseismic stress changes induced by 1989 Loma Prieta, California, earthquake. *Geophys. Res. Lett.* **17**, 1441–1444.
- Mikumo, T., and Miyatake, T. (1995). Heterogeneous distribution of dynamic stress drop and relative fault strength recovered from the results of waveform inversion: The 1984 Morgan Hill, California, earthquake. *Bull. Seismol. Soc. Am.* **85**, 178–193.
- Miller, S. A., Ben-Zion, Y., and Burg, J. P. (1999). A three-dimensional fluid-controlled earthquake model: Behavior and implications. *J. Geophys. Res.* **104**, 10621–10638.
- Miller, S. A., Nur, A., and Olgaard, D. L. (1996). Earthquakes as a coupled shear stress-high pore pressure dynamical system. *Geophys. Res. Lett.* **23**, 197–200.
- Mindlin, R. (1936). Force at a point in the interior of a semi-infinite solid. *Physics* **7**, 195–202.
- Miyatake, T. (1992). Numerical simulation of three-dimensional faulting processes with heterogeneous rate- and state-dependent friction. *Tectonophysics* **211**, 223–232.
- Montone P., Amato, A., and Pondrelli, S. (1999). Active stress map of Italy. *J. Geophys. Res.* **104**, 25,595–25,610.
- Muir-Wood, R., and King, G. C. P. (1993). Hydrological signatures of earthquake strain. *J. Geophys. Res.* **98**, 22,035–22,068.
- Nalbant, S. S., Barka, A. A., and Alptekin, O. (1996). Failure stress change caused by the 1992 Erzincan earthquake ($M_s = 6.8$). *Geophys. Res. Lett.* **23**, 1561–1564.

- Nalbant, S. S., Hubert, A., and King, G. C. P. (1998). Stress coupling between earthquakes in northwest Turkey and the north Aegean Sea. *J. Geophys. Res.* **103**(10), 24,469–24,486.
- Nishenko, S. P., and Buland, R. (1987). A generic recurrence interval distribution for earthquake forecasting. *Bull. Seismol. Soc. Am.* **77**, 1382–1399.
- Noir, J., Jacques, E., Békri, S., Adler, P. M., Tapponnier, P., and King, G. C. P. (1997). Fluid flow triggered migration of events in the 1989 Dobi earthquake sequence of central Afar. *Geophys. Res. Lett.* **24**, 2335–2338.
- Nostro, C., Cocco, M., and Belardinelli, M. E. (1997). Static stress changes in extensional regimes: An application to southern Apennines (Italy). *Bull. Seismol. Soc. Am.* **87**, 234–248.
- Nostro, C., Stein, R. S., Cocco, M., Belardinelli, M. E., and Marzocchi, W. (1998). Two-way coupling between Vesuvius eruptions and southern Apennine earthquakes, Italy, by elastic stress transfer. *J. Geophys. Res.* **103**(10), 24,487–24,504.
- Nur, A., and Booker, J. R. (1972). Aftershocks caused by pore fluid flow? *Science* **175**, 885–887.
- Ohnaka, M. (1992). Earthquake source nucleation: a physical model for short-term precursors. *Tectonophysics* **211**, 149–178.
- Okada, Y. (1985). Surface deformation due to shear and tensile faults in a half-space. *Bull. Seismol. Soc. Am.* **75**, 1135–1154.
- Okada, Y. (1992). Internal deformation due to shear and tensile faults in a half-space. *Bull. Seismol. Soc. Am.* **82**, 1018–1040.
- Okubo, P. G. (1989). Dynamic rupture modeling with laboratory derived constitutive relations. *J. Geophys. Res.* **94**, 12,321–12,336.
- Olsen, K. B., Madariaga, R., and Archuleta, R. J. (1997). Three-dimensional dynamic simulation of the 1992 Landers earthquake. *Science* **278**, 834–838.
- Parsons, T., and Dreger, D. (2000). Static-stress impact of the 1992 Landers earthquake sequence on nucleation and slip at the site of the 1999 M-7.1 Hector Mine earthquake, southern California. *Geophys. Res. Lett.* (in press).
- Parsons, T., Stein, R. S., Simpson, R. W., and Reasenber, P. (1999a). Stress sensitivity of fault seismicity: A comparison between limited-offset oblique and major strike-slip faults. *J. Geophys. Res.* **104**, 20,183–20,202.
- Parsons, T., Toda, S., Stein, R., Barka, A., and Dieterich, J. H. (1999b). Seismic hazards in the Marmara sea region resulting from the August 17, 1999, Izmit earthquake, Turkey. 1999 Fall Meeting of the American Geophysical Union, *EOS*, Transactions, Vol. 80, No. 46, November 16 1999 (abstract) F664.
- Perfettini, H., Stein, R., Simpson, R., and Cocco, M. (1999). Stress transfer by the $M = 5.3$, 5.4 Lake Elsnam earthquakes to the Loma Prieta fault: Unclamping at the site of the peak 1989 slip. *J. Geophys. Res.* **104**, 20,169–20,182.
- Pollitz, F. F., and Sacks, I. S. (1997). The 1995 Kobe, Japan, earthquake: A long-delayed aftershock of the offshore 1944 Tonankai and 1946 Nankaido earthquakes. *Bull. Seismol. Soc. Am.* **87**, 1–10.
- Ponti, D., Bryant, W. A., Rockwell, T. K., and Kendrick, K. J. (1999). Surface rupture, slip distribution and other geologic observation associated with the Mw 7.1 Hector Mine earthquake of 16 October 1999. 1999 Fall Meeting of the American Geophysical Union, *EOS*, Transactions, Vol. 80, No. 46, November 16 1999 (abstract) 15.
- Quin, H. (1990). Dynamic stress drop and rupture dynamics of the October, 15, 1979 Imperial Valley, California, earthquake. *Tectonophysics* **175**, 93–118.
- Reasenber, P. A., and Simpson, R. W. (1992). Response of regional seismicity to the static stress change produced by the Loma Prieta earthquake. *Science* **255**, 1687–1690.
- Rice, J. R. (1992). Fault stress states, pore pressure distributions and the weakness of the San Andreas fault. In "Fault Mechanics and Transport Properties of Rock. A Festschrift in Honor of W. F. Brace" (B. Evans and T.-F. Wong, eds.). Academic, San Diego, pp. 475–503.

- Rice, J. R. (1993). Spatio-temporal complexity of slip on a fault. *J. Geophys. Res.* **98**, 9885–9907
- Rice, J. R., and Cleary, M. P. (1976). Some basic stress diffusion solutions for fluid-saturated elastic porous media with compressible constituents. *Rev. Geophys.* **14**, 227–241.
- Rice, J. R., and Gu, J. (1983). Earthquake aftereffects and triggered seismic phenomena, *Pure Appl. Geophys.* **121**, 187–219.
- Rice, J. R., and Tse, S. T. (1986). Dynamic motion of a single degree of freedom system following a rate and state dependent friction law. *J. Geophys. Res.* **91**, 521–530.
- Roeloffs, E. (1996). Poroelastic techniques in the study of earthquake-related hydrologic phenomena. *Adv. Geophys.* **37**, 135–195.
- Roeloffs, E. (1998). Persistent water level changes in a well near Parkfield, California, due to local and distant earthquakes. *J. Geophys. Res.* **103**, 869–889.
- Roeloffs, E., and Quilty, E. G. (1997). Water level and strain changes preceding and following the August 4, 1985, Kettleman Hills, California, earthquake. *Pure Appl. Geophys.* **149**, 21–60.
- Roeloffs, L. A. (1988). Fault stability changes induced beneath a reservoir with cyclic variations in water level. *J. Geophys. Res.* **93**, 2107–2124.
- Roy, M., and Marone, C. (1996). Earthquake nucleation on model faults with rate-and state-dependent friction: Effects of inertia. *J. Geophys. Res.* **101**, 13,919–13,932.
- Ruina, A. (1980). Friction Laws and Instabilities: A Quasi-Static Analysis of Some Dry Friction Behavior (Ph.D. thesis) Brown University, Providence, RI.
- Ruina, A. (1983). Slip instabilities and state variable friction laws. *J. Geophys. Res.* **88**, 10,359–10,370.
- Rybicki, K. (1973). Analysis of aftershocks on the basis of dislocation theory. *Phys. Earth Planet. Inter.* **7**, 409–422.
- Saleur, H., Sammis, C. G., and Sornette, D. (1996). Discrete scale invariance, complex fractal dimensions, and log-periodic fluctuations in seismicity. *J. Geophys. Res.* **101**, 17,661–17,677.
- Savage, J. C. (1983). A dislocation model of strain accumulation and release at a subduction zone. *J. Geophys. Res.* **88**, 4984–4995.
- Savage, J. C., Lisowski, M., and Svarc, J. L. (1993). Postseismic deformation following the 1989 (M 7.1) Loma Prieta, California, earthquake. 1993 Fall Meeting, *EOS Trans. AGU*, **74**(43), 182.
- Scholz, C. H. (1990). “The Mechanics of Earthquakes and Faulting.” Cambridge Univ. Press. New York.
- Scholz, C. H. (1991). Earthquakes and faulting: Self-organized critical phenomena with characteristic dimension. In “Spontaneous Formation of Space-Time Structures and Criticality” (T. Ritse and D. Sherrington, eds.). Kluwer Academic, pp. 41–56.
- Scholz, C. H. (1998). Earthquakes and friction laws. *Nature* **391**, 37–42.
- Seeber, L., and Armbruster, J. G. Earthquakes as beacons of stress changes. *Nature* (submitted).
- Sibson, R. H. (1994). Crustal stress, faulting and fluid flow. In “Geofluids: Origin, Migration and Evolution of Fluids in Sedimentary Basins” (J. Parnell, ed.). 1994 Geological Society Special Publication No. 78, pp. 69–84.
- Simpson, R. W., and Reasenber, P. A. (1994). “Earthquake-Induced Static Stress Changes on Central California Faults, in The Loma Prieta, California Earthquake of October 17, 1989—Tectonic Processes and Models” (R. W. Simpson, ed.). *U.S. Geol. Surv. Prof. Paper 1550-F*, pp. F55–F89.
- Sornette, D., and Sammis, C. G. (1995). Complex critical exponents from renormalization group theory of earthquakes: Implications for earthquake predictions. *J. Phys. Ser. 1*, **5**, 607–619.
- Spudich, P., Steck, L. K., Hellweg, M., Fletcher, J. B., and Baker, L. (1995). Transient stresses at Parkfield, California, produced by the M7.4 Landers earthquake of June 28, 1992: Observations from the UPSAR dense seismograph array. *J. Geophys. Res.* **100**, 675–690.
- Stein, R. S. (1999). Stress transfer in earthquake occurrence. *Nature* **402**, December.
- Stein, R. S., Barka, A. A., and Dieterich, J. H. (1997). Progressive failure on the North Anatolian fault since 1939 by earthquake stress triggering. *Geophys. J. Int.* **128**, 594–604.

- Stein, R. S., King, G. C. P., and Lin, J. (1992). Change in failure stress on the southern San Andreas fault system caused by the 1992 Magnitude = 7.4 Landers earthquake. *Science* **258**, 1328–1332.
- Stein, R. S., King, G. C. P., Lin, J. (1994). Stress triggering of the 1994 M = 6.7 Northridge, California, earthquake by its predecessors. *Science* **265**, 1432–1435.
- Steketee, J. A. (1958a). Some geophysical applications of the elasticity theory of dislocations. *Can. J. Phys.* **36**, 1168–1198.
- Steketee, J. A. (1958b). On Volterra's dislocations in a semi-infinite elastic medium. *Can. J. Phys.* **36**, 193–205.
- Taylor, M. A. J., Dmowska, R., and Rice, J. R. (1998). Upper plate stressing and seismicity in the subduction earthquake cycle. *J. Geophys. Res.* **103**(10), 24,523–24,542.
- Taylor, M. A. J., Zheng, G., Rice, J. R., Stuart, W. D., and Dmowska, R. (1996). Cyclic stressing and seismicity at strongly coupled subduction zones. *J. Geophys. Res.* **101**, 8363–8381.
- Toda, S., Stein, R. S., Reasenber, P. A., Dieterich, J. H., and Yoshida, A. (1998). Stress transferred by the 1995 Mw = 6.9 Kobe, Japan, shock Effect on aftershocks and future earthquake probabilities. *J. Geophys. Res.* **103**(10), 24,543–24,566.
- Troise, C., De Natale, G., Pingue, F., and Petrazzuoli, S. M. (1998). Evidence for static stress interaction among earthquakes in south-central Apennines (Italy). *Geophys. J. Int.* **134**, 809–817.
- Tse, S. T., and Rice, J. R. (1986). Crustal earthquake instability in relation to the depth variation of frictional slip properties. *J. Geophys. Res.* **91**(B9), 9452–9472.
- Vidale, J., Agnew, D., Johnston, M., and Oppenheimer, D. (1998). Absence of earthquake correlation with earth tides: An indication of high preseismic fault stress rate. *J. Geophys. Res.* **103**(10), 24,567.
- Volterra, V. (1907). Sur l'équilibre des corps élastiques multiplément connexes. *Ann. Sci. Ecole Norm. Supl. Paris* **24**, 401–517.
- Wald, D. J., and Heaton, T. H. (1994). Spatial and temporal distribution of slip for the 1992 Landers, California, earthquake. *Bull. Seismol. Soc. Am.* **84**, 668–691.
- Wyss, M., Hreinsdottir, S., and Marriot, D.A. (1999). Southern extent of the October 1999 Mw 7.1 Hector Mine earthquake limited by Coulomb stress changes due to the M7.3 Landers earthquake of 1992. 1999 Fall Meeting of the American Geophysical Union, *EOS*, Transactions, Vol. 80, No. 46, November 16 1999 (abstract) 15.

SEISMICITY INDUCED BY MINING: TEN YEARS LATER

SLAWOMIR J. GIBOWICZ

*Institute of Geophysics, Polish Academy of Sciences
ul. Ks. Janusza 64, 01-452 Warsaw, Poland*

STANISLAW LASOCKI

*Department of Geophysics, University of Mining and Metallurgy
al. Mickiewicza 30, 30-059 Krakow, Poland*

1. INTRODUCTION

In the previous review of seismicity induced by mining (Gibowicz, 1990), the general description of the problems involved and the state-of-the-art of relevant research in this field at the end of 1980s was given. During the last decade, seismic monitoring has been expanded in several mining districts, a number of new techniques have been introduced, and new significant results have been obtained in studies of seismic events induced by mining. Dr. Renata Dmowska, coeditor of *Advances in Geophysics*, invited us therefore to contribute a new review, describing in some detail the latest achievements in the field.

A distinction between the adjectives induced and triggered, often used interchangeably to describe artificially stimulated seismicity, should be made as proposed by McGarr and Simpson (1997). They consider that "... 'induced seismicity' is that for which the causative activity can account for either most of the stress change or most of the energy required in order to produce the earthquakes. In contrast, 'triggered seismicity' is used if the causative activity accounts for only small fraction of the stress change or energy associated with the earthquakes ...". In the first case, human activity and in the second case, tectonic loading play the primary roles. Thus, seismic events observed in mines are induced events, whereas seismic events associated with the impoundment of reservoirs are triggered events.

Another distinction, that between a seismic event in a mine and a rockburst, should be clarified as well. Earthquake seismologists tend to describe as rockbursts any seismic events which occur in a given mine. For mining engineers, however, rockbursts are violent failures of rock that result in visible damage to excavations. This distinction was also emphasized in the previous review (Gibowicz, 1990) as it is highly important in mining practice.

The first two International Symposia on Rockbursts and Seismicity in Mines, held in Johannesburg, South Africa, in 1982 and in Minneapolis, Minnesota, in

1988, were followed in the 1990s by the 3rd Symposium held in Kingston, Ontario, in 1993 and by the 4th Symposium held in Krakow, Poland, in 1997. The proceedings of these last two symposia (Young, 1993; Gibowicz and Lasocki, 1997) contain 12 keynote lectures and some 130 technical papers on the subject, written by experts from some 15 countries.

In the 1990s a number of books and special issues of well-known professional journals related to seismicity in mines have been published. The first ever textbook on this subject, *An Introduction to Mining Seismology*, was published in 1994 (Gibowicz and Kijko, 1994). The second book, *Seismic Monitoring in Mines*, written by Mendecki and his colleagues from the ISS International, South Africa, (Mendecki, 1997a) contains a description of a very specific methodology for assessing in real time the seismic hazard associated with mining. The other two books, *Induced Seismicity* (Knoll, 1992) and *Tectonophysics of Mining Areas* (Idziak, 1996a), contain a collection of papers related to the subjects specified by their titles. Five Special Issues of *Pure and Applied Geophysics* devoted to stimulated seismicity phenomena have been published between 1992 and 1998 and reprinted as separate books (McGarr, 1992a; Gupta and Chadha, 1995; Knoll and Kowalle, 1996; Talebi, 1997, 1998), and one Special Issue of *Tectonophysics* was published in 1998 (Trifu and Fehler, 1998).

This review is organized to some extent similarly to the previous one. New techniques in seismic monitoring in mines, geological and mining factors affecting seismicity, source parameters and their scaling relations, and shearing versus non-shearing source mechanisms are briefly described. Statistical techniques and methods, however, used extensively in recent years in studies of seismicity in mines, especially for seismic hazard assessment, have not been previously reported. They are discussed in some detail now. The other topic that has only recently become of considerable importance is the seismic discrimination between underground explosions and seismic events originating in deep mines. The problem is briefly discussed at the end of this review.

2. SEISMIC MONITORING

Seismicity induced by mining is commonly described as the occurrence of seismic events caused by rock failures. This is a result of changes in the stress field in the rock mass near mining excavations. The total state of stress around a mine excavation is the sum of the ambient stress in the rock mass and the stresses induced by mining works. The vertical component of ambient stress is due to the overburden, whereas applied tectonic forces can affect the horizontal ambient stresses. Mine tremors do not necessarily occur in all mining situations at a given depth where the lithostatic stress is of considerable value. The primary requirement for inducing seismicity appears to be human activity where the rocks are in a highly prestressed condition.

Grasso and Sornette (1998) examined the hypothesis, proposed in recent years (Bak and Tang, 1989), that the earth's crust is in a self-organized critical (SOC) state to explain and understand the phenomenon of induced seismicity. They found that both pore pressure changes and mass transfers leading to incremental deviatoric stresses smaller than 1 MPa are sufficient to trigger seismic instabilities in the uppermost part of the crust in otherwise historically aseismic areas. Once triggered, stress variations of at least one order of magnitude less are enough to sustain seismicity. They argue that these observations are in agreement with the SOC hypothesis, as they show that a significant fraction of the crust is not far from instability. Although not all stress perturbations trigger seismicity, this fact is still compatible with the SOC hypothesis, which includes the presence of large heterogeneity in the stress field.

Sykes *et al.* (1999) disputed the claim that earthquakes represent a SOC phenomenon, however, implying a system maintained under near-failure conditions at all times; this is correct on global but not on regional scales. The critical point model for regional seismicity suggests that only during the periods of long wavelength correlations in the regional stress field, emphasized by increased seismic moment/energy release in moderate earthquakes, is a region of the earth's crust truly in or near a SOC state (Jaumé and Sykes, 1999). The question of continuous versus discontinuous criticality is directly related to the question of earthquake predictions (e.g., Sammis and Smith, 1999).

McGarr *et al.* (1999) reviewed case histories of induced and triggered seismicity to illustrate a variety of causes, scales, and crustal environments. Mining-induced events are caused by increases in the shear stress or decreases in the normal stress acting on the fault planes. Pumping in mines to prevent flooding reduces the crustal pore pressure and strengthens the rock mass. In mines, therefore, seismic events are induced only in those regions where the ambient stress has been modified substantially by the mine excavations. The stress perturbations, although often quite small, frequently result in generation of seismicity because near-failure conditions are common in both active and stable tectonic environments.

Seismicity in underground mines is observed in numerous mining districts throughout the world. The most comprehensive studies are carried out in South Africa, Poland, Canada, the United States, and the Czech Republic. The literature is extensive and only the more interesting results published since 1990 in accessible journals and books are briefly reported here. References to works published before 1990 can be found elsewhere (Gibowicz, 1990; Johnston, 1992; Gibowicz and Kijko, 1994).

2.1. Seismicity in Underground Mines

Extensive studies of seismicity, mostly in deep gold mines, have been carried out for a long time in South Africa. The gold-bearing reefs of the Witwatersrand

system are mined by stoping at depths down to 3.5 km below the surface. This creates flat voids in the quartzitic strata extending horizontally up to several kilometers with an initial excavated thickness of a meter. Developments and methods used in seismicity studies have been reported in several publications in the 1990s. Seismicity associated with pillars at Western Deep Levels gold mine (Lenhardt, 1990; Leach and Lenhardt, 1990); seismic wave attenuation in deep-level gold and platinum mines (Spottiswoode, 1993); application of source parameters to detect changes in rock mass behavior in the Welkom gold mines (van Aswegen and Butler, 1993); and practical use of the instability concept of Mendecki (1997b) in the Klerksdorp mining area (Glazer, 1997), are some of the topics recently studied in South Africa. Additional topics will be discussed in the following chapters. The seismic monitoring technique has been also used to study the caving processes above a longwall in a 160-m-deep coal seam within the Highveld coalfield in the province of Mpumalanga, South Africa (Minney *et al.*, 1997).

Seismicity induced by underground mining is a well-known long-studied phenomenon in Poland, observed in the Upper Silesian Coal Basin and in the Lubin copper district in Lower Silesia. The bimodal character of seismicity in Upper Silesia has been confirmed by numerous studies. The low-energy events are associated directly with mining operations and occur around longwalls and openings. The high-energy events, often called regional events, occur as a rule in geologically disturbed areas and in their generation tectonic stresses play a significant role (e.g., Idziak, 1996b; Mutke and Stec, 1997). The spatial distribution of seismic events in the Upper Silesian Basin is not uniform. Despite mining operations throughout the Basin, the seismicity is concentrated in four distinct areas forming different geological units. The location of two major epicenter clusters and active mines there is shown in Fig. 1, reproduced from Lasocki and Idziak (1998). Nonuniform distributions of this type suggest a fractal character of seismicity in Upper Silesia (e.g., Idziak, 1996b). Similar phenomena are recognized in the Lubin copper district. A detailed study of the source mechanism and source parameters of seismic events at Polkowice copper mine has been completed by Król (1998). Their relationships with geological and mining factors are of special interest.

Seismic events and rockbursts are often observed in metalliferous, coal, and potash mines in Canada. Seismic activity in Canadian mines increased significantly during the 1980s, particularly in northern Ontario hard rock mines operating at depths down to 2 km. In response, the Canada-Ontario-Industry Rockburst Project was initiated in 1985. From 1990 to 1995 an expanded second phase of the Rockburst Project, the Canadian Rockburst Research Program, was in progress (e.g., Plouffe *et al.*, 1993). Significant improvements were made in the past decade with the installation of the Sudbury Local Telemetered Network (SLTN) around the Sudbury mining district in Ontario and seismic stations in five other mining camps of northern Ontario and northwestern Quebec (Talebi *et al.*, 1997). These improvements concerned the determination of source location and event magnitude,

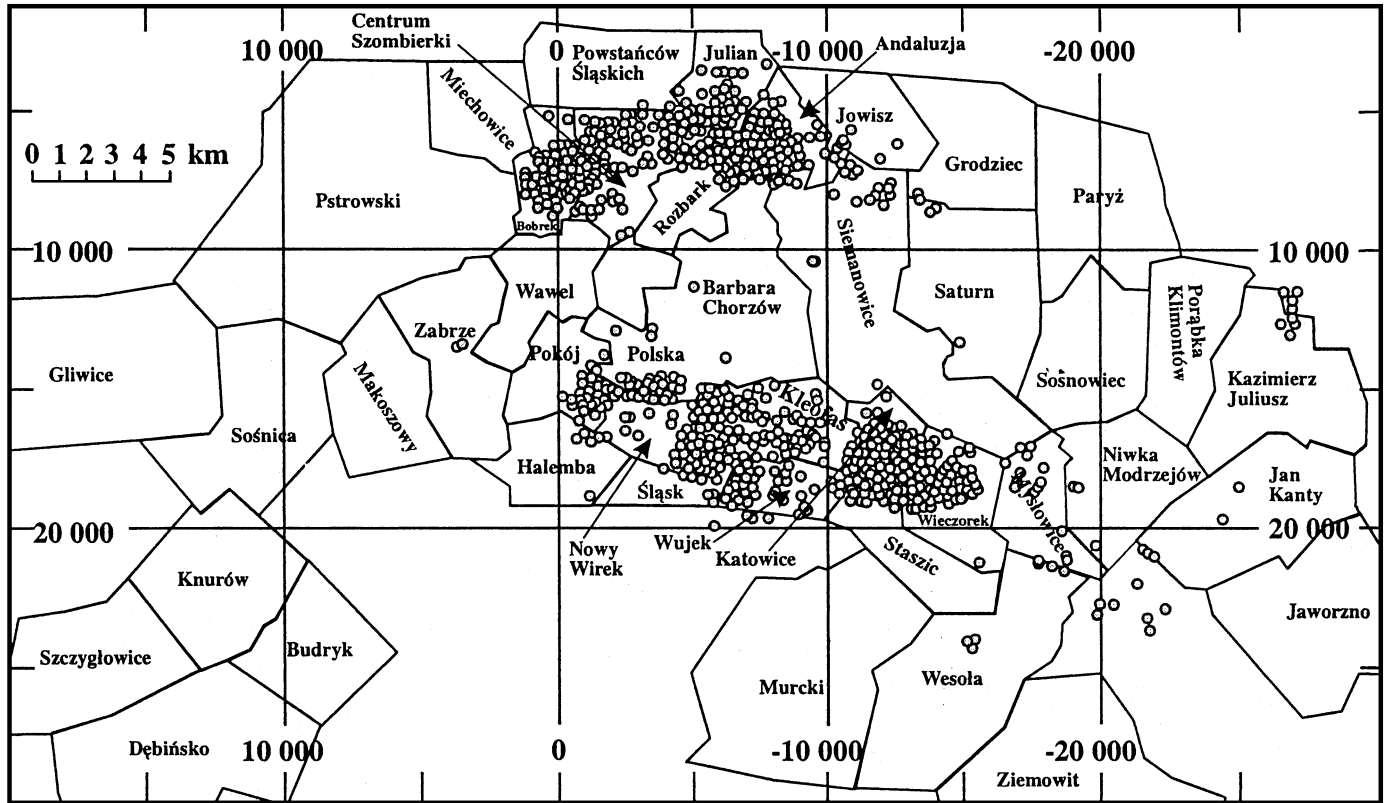


Fig. 1. Location of two major clusters of seismicity in the Upper Silesian Coal Basin, Poland, displayed on the background of active mines. [Lasocki and Idziak (1998), Fig. 2; reprinted with kind permission from Birkhäuser Verlag AG.]

detection capabilities, quality of data, and the procedure for data transfer and analysis. The waveforms of seismic events recorded in a mine in the Sudbury district were processed to study attenuation effects, source parameters, and scaling laws (Talebi *et al.*, 1994). SLTN operations were terminated in the late 1990s.

About half of the deep mines in the Sudbury Basin are monitored continuously by seismic systems. Not all deep mines in the area, however, are seismically active; several display little or no seismicity at all. There are several groups of two mines which share boundaries and which appear to have similar mining configurations and geological structures but display dramatically different levels of seismicity. A comparison of the characteristics of both seismic and aseismic mines could provide a valuable contribution to the study of mining-induced seismicity (Morrison, 1993).

Three-dimensional boundary-element modeling of stress effects, source mechanisms of seismic events, and underground observations have been used to understand mining effects at Ansil mine, located in the Noranda mining camp in the southern part of the Abitibi green-stone belt, and several conclusions have been drawn (McCreary *et al.*, 1993). Noranda's hard rock Brunswick No. 12 mine, located in Bathurst, New Brunswick, is affected by seismic activity and rockburst-related damage to underground excavations. Since 1994, the mine has employed several systems for seismic monitoring. A rockburst hazard assessment technique has been introduced, based on seismic energy, apparent stress, and seismic moment criteria, to identify those events that are relevant for assessment and decision-making processes (Alcott *et al.*, 1998).

In the U.S.A., the Wasatch Plateau and Book Cliffs coal mining districts of east-central Utah, containing more than 30 underground mines, are notable as one of two areas in the western U.S. where mining-induced seismicity is significant (Wong, 1993). Mining tremors account for about one-fourth of the seismic events annually recorded in the seismically active Utah region (Arabasz *et al.*, 1997). Total mining seismicity in the area sharply increased after 1992, posing a challenge for understanding the complex interaction between geology, mining, and observed seismicity. The largest mining-induced event in the region occurred in the Gentry Mountain area on May 14, 1981 and had an estimated local magnitude of 3.8 (Arabasz *et al.*, 1997). The Coeur d'Alene mining district, located within a zone of minor natural seismicity in northern Idaho, is one of the few metal-mining areas in the United States where large rockbursts occur. Rockbursts have become increasingly common during recent years. During the 1960s and 1970s, rockbursts in the district were attributed to the failure of pillars ahead of advancing mine faces. During the 1980s, seismic activity at the Lucky Friday mine at Mullan increased significantly as mining went deeper, and observations of the in-mine damage suggested that the predominant mechanism of the rockbursts changed from pillar failure to fault slip (Sprenke *et al.*, 1991). Three types of geological structures have been also identified that contribute to seismicity of this mine (Scott *et al.*, 1993).

The highest level of mining-induced seismicity in the Czech Republic is observed in the Ostrava-Karvina Coal Basin. Seismic activity and the number of rockbursts there increased significantly in recent years as a result of mining at greater depth under complex geological conditions (e.g., Konečný, 1992). Observations from local seismic networks in mines and from a regional seismic network (in operation since 1988) are used to study the spatial and temporal distributions of seismic events in several mines and their relationships to mining and geological structures (e.g., Konečný, 1992; Kalenda, 1995; Vesela, 1995; Holub, 1996a). Investigation of seismic events in the Kladno coal district continues (e.g., Rudajev, 1995).

In India, seismic events and rockbursts induced by mining have been known for a long time in the Kolar Gold Fields situated in the Karnaka State. The deepest mining operations are carried out there at depths exceeding 3.2 km and the rockburst problems are almost as old as the mining activity itself (e.g., Behera, 1990; Srinivasan and Shringarputale, 1992). An unusual and probably unique seismic phenomenon is observed in these mines, called "area rockburst" (Jha *et al.*, 1993). The area rockburst is a sequence of rockbursts that follow in quick succession with their sources concentrating in a small area of 100–200 m radius. The occurrence of a major rockburst triggers a chain of 20 to 200 rockbursts of similar or smaller size in the same area over a period of a few hours to a few days. They take place at all depth levels in both currently mined and old working areas. The spatial and temporal distributions of area rockbursts are highly irregular. They are similar to earthquake swarms and follow similar patterns with the number and magnitude of the events increasing gradually with time and then gradually decreasing.

The mining of the Khibiny Massif apatite deposits in the Kola Peninsula in Russia was started in 1929. The first seismic event with magnitude 3.1 was felt in 1948. A more intensive excavation began in the mid-1960s, and the first significant tremor occurred in 1981. At present more than 100 million tons of ore are extracted annually from three underground and three open-pit mines (Kremenetskaya and Tryapitsin, 1995). The strongest tremor with magnitude 4.1–4.3 occurred on April 16, 1989 causing extensive damage at Kirovsk mine (Syrnikov and Tryapitsin, 1990; Kremenetskaya and Tryapitsin, 1995). The maximum measured displacement was 20 cm and was traced along a fault on the surface for 1200 m and observed to a depth of at least 220 m. The main tremor was followed by several hundred aftershocks during the next 2 months. The event occurred simultaneously with a 240-ton explosion in one of the Kirovsk mines, implying that the blast triggered the tremor. Vigorous monitoring of the area is carried out, within a program developed by the Kola Complex of geodynamic measuring stations in the Khibiny and Lovozero rock masses. Monitoring includes acoustic and electromagnetic observations (Melnikov *et al.*, 1996). There are several seismic stations in the area, and a Norwegian local array operates in the vicinity of Apatity town. The ARCESS seismic array in northern Norway records all larger events from the area.

In the northern Ural bauxite mines in Russia rockbursts first occurred at the beginning of 1970s at a depth of 350 m. Seismic observations there have been carried out from 1980. The largest events have magnitude ranging from 3.0 to 3.5 (Kolesov, 1993; Lomakin and Junusov, 1993), and some of them occur at depths distinctly greater than the depth of mining (Voinov *et al.*, 1987). The largest tremors in the Tashtagol iron-ore deposits, Gornaya Shoria, have magnitudes ranging from 3.0 to 3.5 (Lomakin and Junusov, 1993).

The first recorded rockburst in China occurred in 1933 at the SL coal mine when the mining depth was about 200 m. The number of coal mines affected by seismicity increases steadily with increasing mining depth and mining intensity. At present, seismic events occur at 33 coal mines, and over 2000 rockbursts have taken place since 1949, with the largest event of magnitude 4.2 (Wu and Zhang, 1997). Rockbursts have occurred in almost all coal types, in various types of roof, and under all mining conditions. Seismic and acoustic monitoring systems are widely used, and a complex rockburst prevention system is claimed to be successfully applied. In recent years, rockbursts have also occurred in some metalliferous mines.

The Liaoning Province in northeastern China is a highly seismic region where tens of destructive tectonic earthquakes have occurred. During the last three decades, seismic events induced by mining have become quite frequent (Zhong *et al.*, 1997). The seismic activity first appeared at Taiji coal mine, Beipiao County, where in 1970 the excavation of a shaft reached a depth of 500 m, and a series of small tremors occurred. Up to 1989 over 1300 events were recorded by local seismic stations, with the largest event of magnitude 4.3, which took place in April 1977. The observed seismicity is closely related to active faults. Furthermore, a correlation is observed between the number of seismic events in mines and the number of natural earthquakes in the area (Fig. 2). This observation suggests that many seismic events at Taiji coal mine are triggered by natural earthquakes (Zhong *et al.*, 1997). Since the 1970s, a series of tremors have also occurred in other coal mines, such as Xilin, Haizhou, Wulong, and Aiyou. The Binggou coal mine, Jianchang County, has an excavation history exceeding 200 years, and there are many voids left by mining works. A number of seismic events caused by roof collapse have been observed, with the maximum magnitude of 3.9, particularly between 1976 and 1985 in which 56 large collapse events occurred (Zhong *et al.*, 1997).

The Central Queensland University Regional Seismic Network in Australia, established in 1990, records seismic events generated by the rock mass failure and roof falls in longwall coal mines in the Bowen Basin. A relatively high compressive horizontal stress is dominant there, reaching three times the vertical stress value (McKavanagh *et al.*, 1995). The concept of seismic monitoring from the surface of longwall caving characteristics was used at Capcoal's Southern Colliery, German Creek, in late 1990. Over 150 longwall related seismic events were recorded, classified into strata failure events without a subsequent fall and events associated

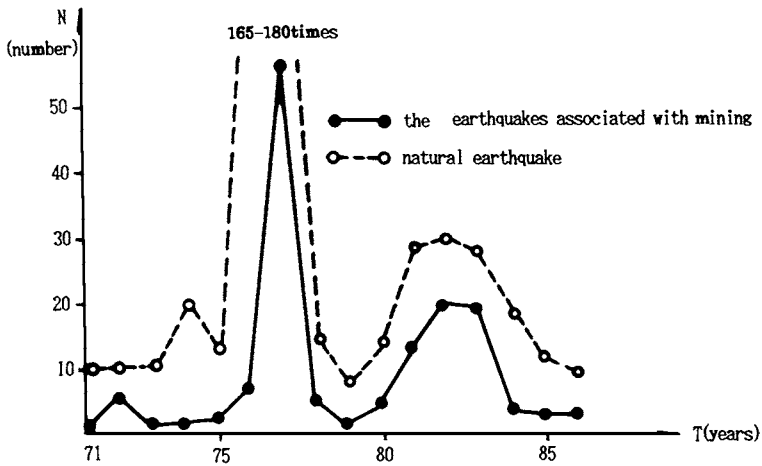


FIG. 2. Correlation between natural earthquakes in the western part of the Liaoning Province and seismic events associated with mining at Taiji coal mine, China. [Zhong *et al.* (1997), Fig. 5; reprinted with kind permission from Birkhäuser Verlag AG.]

with falls characterized by complex waveforms. The first detailed seismic monitoring study was undertaken at Gordonstone mine in Central Queensland in 1994 to investigate the extent of ground failure caused by longwall mining (Hatherly *et al.*, 1997; Hatherly and Luo, 1999). Seismic monitoring systems are in use in coal mines under the massive strata at Newstan, West Wallsend, Moonee, and Clarence to monitor the development of dangerous caving situations in longwall mining.

Two experiments were carried out in 1988 and 1991 in the English Midlands at Littleton and Coventry collieries to image fracture development around the working face by monitoring seismic activity using three component down-hole geophones (Toon and Styles, 1993). A borehole seismic monitoring permitted delineation of the spatial and temporal development of the fractures around an active longwall face. A somewhat unusual application of seismic monitoring techniques was performed by the British Geological Survey around Rosslyn Chapel in the Midlothian Coalfield to monitor seismic activity following pit closure (Redmayne and Richards, 1998). Accurate locations were obtained for 247 events that occurred between November 1987 and January 1990. A rapid decay of seismicity following pit closure was demonstrated.

El Teniente Mine is an underground copper mine located in central Chile, which is strongly affected by rockbursts and where seismic activity is of considerable intensity. A digital full waveform system was installed in January 1992 to cover the whole mine. At present, the seismic network is composed of 29 stations with 4.5-Hz triaxial geophones (Dunlop and Gaete, 1997). The El Teniente Sub6 sector

is the deepest productive sector at the mine. The ore production there began in 1989 but it was repeatedly stopped by large rockbursts between 1989 and 1992. The production was resumed in January 1994 and, following the observed relationships between mining and seismic parameters, was restricted to an area with a lower column of intact rock and controlled production rates to minimize the size of the ruptures. No rockbursts have been observed since.

In French coal mines, large seismic networks have been implemented to monitor the areas prone to rockbursts; and two of the seismic networks were used to study seismic activity in some detail (Ben Sliman and Revalor, 1992). The influence of wave propagation models and network size and geometry on the location accuracy of seismic events was assessed. At the Provence colliery, coal is mined by a longwall technique at a depth reaching 1100 m and the rate of production is steadily increased (Bigarre *et al.*, 1993). The mine experiences some 20 seismic events daily with magnitude 1.5 and greater. Most of these events are attributed to the longwall operations and several of them cause serious damage at the advancing face and along haulage gateways. In the southern part of the colliery, several major tectonic faults are present and they most probably play a major role in dynamic loading of the coal seam by fault slips induced by mining. Numerical 3D modeling of fractured rock mass has been undertaken to quantify rockburst potential of fault slip along major preexisting geological structures.

Specific studies on seismicity in underground mines are occasionally reported in other countries. The Miike coal mine is an undersea coal mine in the Kyushu province in Japan. Rockbursts have repeatedly occurred there on the longwall face in a limited area in the deepest part of the mine (Kaneko *et al.*, 1992). Seismic and acoustic emission monitoring systems, *in situ* stress measurements, *in situ* test drilling, and numerical analyses are used to clarify stress field conditions and to design destressing operations. It was confirmed that large seismic events occur in the area with a low seismic energy release background and high stress concentration.

In May 1993 more than 200 seismic events, with the largest event of magnitude 1.9, from an underground dolomite mine near Schwaz in Tyrol, Austria, were recorded by a local seismic network established in the late 1980s to monitor natural seismicity in Tyrol (Lenhardt and Pascher, 1996). Underground observations revealed a number of discontinuities along which the rock mass was able to move. Seismic records imply two different source mechanisms of events involved in the sequence. One seems to be associated with block sliding along several discontinuities and the other requires collapse as well.

It follows from studies of seismicity induced by underground mining that seismic events do not necessarily occur in all mining situations; their maximum size is different in different mining districts; and their depth is usually close to that of mining excavations.

2.2. Monitoring Systems

The first applications of seismic instruments to monitor seismicity in mines were introduced at the beginning of the twentieth century (see Gibowicz and Kijko, 1994), and routine seismic monitoring has been in use for over 30 years. Its main objective was immediate location of seismic events in mines, estimation of their strength, and prediction of large rock mass instabilities. The first two objectives were readily achieved, but the prediction of large seismic events in mines remains an open question, although the first positive results are reported from South Africa (e.g., Mendecki, 1997b,c; van Aswegen *et al.*, 1997). Furthermore, modern statistical techniques, based on seismic catalogs as principal input data, provide indications on the present and future course of seismicity generation processes in mines (see Sect. 8). The introduction of modern digital seismic systems to mines, and progress in the theory and methods of quantitative seismology, have led to the implementation of real-time monitoring as a mine management tool for estimation of rock mass response to mining.

Seismic monitoring in mines should consist of sensors, data transmission and acquisition, signal processing, and data analysis and interpretation tools, leading to quantification of rock mass seismic response to mining and possibly to estimation of the potential for rock instability (see Mendecki, 1997a). The modern digital seismic system should provide, apart from the event time and location, seismic moment and radiated seismic energy, two independent source parameters. Other source parameters (source radius, average slip, stress drop, apparent stress) can be also estimated from the recorded high quality waveforms.

The transducer is the key element of any seismic monitoring system, transforming the ground motion into an electric signal. The type of transducer to be used depends on the range of amplitudes and frequencies to be recorded which, in turn, depend on the magnitude of seismic events and their distance from the sensor. The corner frequencies, corresponding to the maximum of the ground velocity spectra, define the range of frequencies that must be recorded for meaningful interpretation of seismic sources. For correct determination of seismic moment, frequencies down to an octave below the corner frequency of the largest expected event must be recorded, and to estimate correctly the radiated seismic energy, frequencies five times above the corner frequency of the smallest event are usually needed (Mendecki, 1993). A possible range of corner frequencies of shear waves as a function of seismic moment is shown in Fig. 3 for several values of stress drop and a range of rock types, reproduced from Mendecki (1997c). Ground motion amplitudes at the sensor depend also on the distance from the event and on the rock mass characteristics, and therefore an extremely wide dynamic range in amplitude is needed. For reasons of economy, the sensors used in mine monitoring systems are usually (for example in South African mines) either miniature geophones or

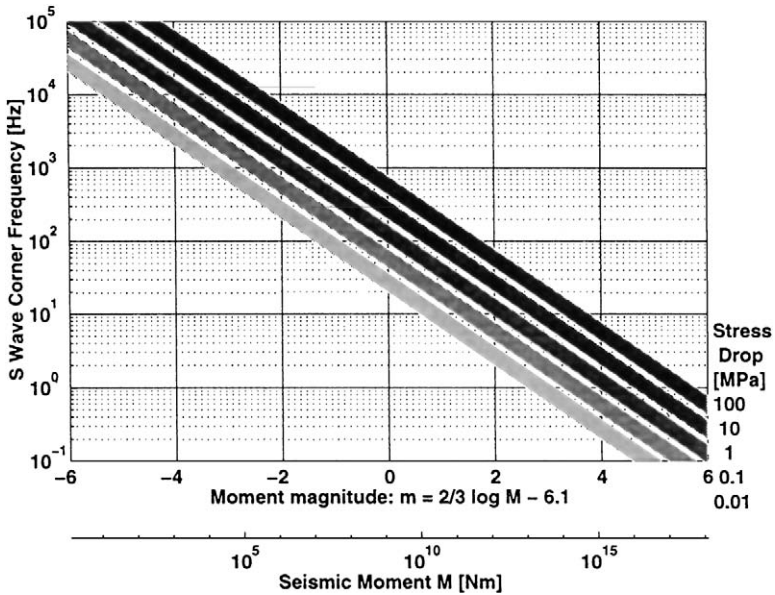


Fig. 3. Expected *S*-wave corner frequency as a function of seismic moment or moment magnitude for a range of stress drops. [Mendecki (1997c), Fig. 2, reprinted from *Rockbursts and Seismicity in Mines*, Proceedings of the 4th International Symposium, Krakow, Poland, 11–14 August 1997. 450 pp., EUR 137.50/US \$162.00/GBP97.00, A. A. Balkema, P.O. Box 1675, Rotterdam, Netherlands.]

piezo-electric accelerometers (Mendecki, 1997c). For events with corner frequencies below 4 Hz the low-cost sensors are inadequate and 0.7–1.0 Hz seismometers, used for example in Polish mines, or force-balance accelerometers are required. More details about seismic transducers are given by Mountfort and Mendecki (1997a).

The data acquisition system must record the amplitude and timing of ground motion at sensors distributed throughout the selected volume of a mine and must assemble the records at a central site for processing. The main functions of a modern monitoring system and data flow are shown in Fig. 4, reproduced from Mountfort and Mendecki (1997b). This is a good illustration of the Integrated Seismic System (ISS), the most comprehensive automatic system widely used in South African mines and elsewhere, described in detail by Mendecki (1993) and Mountfort and Mendecki (1997b). Its dynamic range is greater than 120 dB with a resolution of 12 bits, and the sampling frequency is 2000 samples per second.

Generally, the records are digitized as close to the sensor as possible to reduce transmission errors. In mines, the results of seismic analysis must be available almost immediately, and various media are used for communication such as optical fibers, copper cables, and radio. Triggering is widely used to reduce the

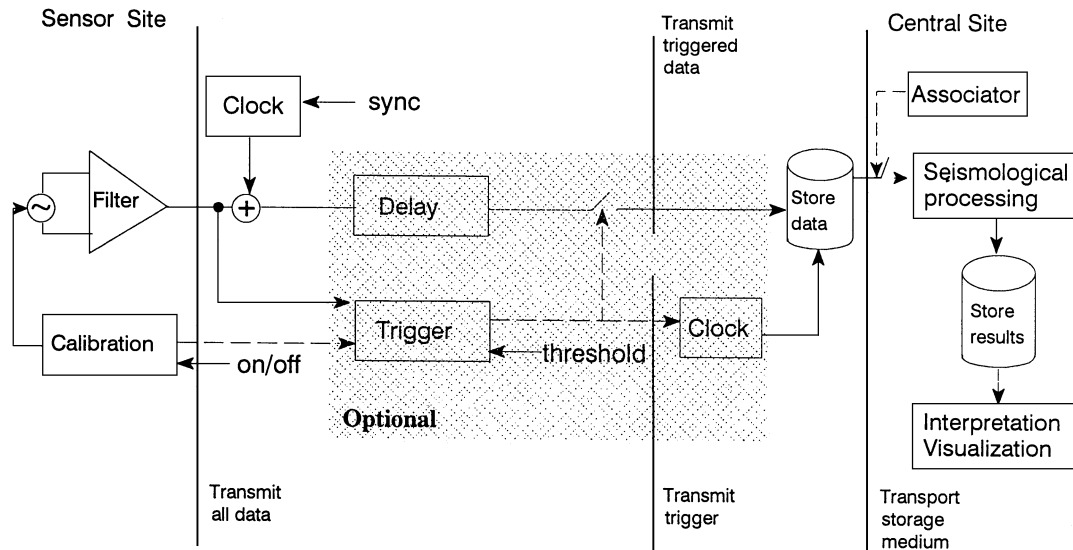


FIG. 4. Basic functions of a modern seismic monitoring system used in mines. Dashed lines represent control signals, and vertical lines represent points at which data may be transmitted from multiple sites to a central site for common processing. [Mountfort and Mendecki 1997, Fig. 2.1, reprinted for *Seismic Monitoring in Mines*, © 1997 Chapman & Hall, with kind permission from Kluwer Academic Publishers.]

amount of data at the sensor site before transmission, and then the time must be maintained locally at each sensor. Triggering, validation, and data reduction processes can be used to select and preprocess the records for storage and transmission. The central site should have adequate resources for seismic processing and interpretation and for archival storage of event and waveform data (e.g., Mendecki, 1997c).

Various seismic monitoring systems are in use in different countries. In Canada, the MP250 system designed for automatic event detection and source location was used at the beginning of the 1990s by about 20 mines across the country. The system does not record waveforms; it records first arrival times only. A computer code, an automatic data analysis and source location system was developed by CANMET for a rapid and comprehensive analysis of MP250 data (Ge and Mottahed, 1993). The analysis consists of two parts: arrival time difference and residual analyses. The system has been adopted in two major Ontario mines, the Creighton mine at Sudbury and the Kidd Creek mine at Timmins, and is in operation in some mines in Quebec as well. Similarly, an MP250-based monitoring system, which uses simple voltage threshold picking of first wave arrivals, has been used at the Lucky Friday mine in northern Idaho since 1973 to provide source locations and energy estimates of seismic events (Dodge and Sprenke, 1992). A whole-waveform seismic monitoring system based on a computer has been developed to provide more accurate source locations and information on source characteristics. Comparison of source locations produced by the MP250 system to those produced by the whole-waveform system shows that significant timing errors are common in the MP250 system (Dodge and Sprenke, 1992).

Advances in signal processing technology have led to the development of high performance, low cost, whole-waveform seismic monitoring systems, such as the Queen's Microseismic System (QMS) designed at Queen's University, Kingston, Ontario (e.g., Young *et al.*, 1992), replaced later by the Engineering Seismology Group (ESG) system from Kingston. Different versions of these systems have been installed in a number of Canadian underground mines as either an enhancement to an MP250 automatic source location system or as a stand-alone rock mass monitoring system.

A new digital seismic monitoring system was designed for Polish coal and copper mines and was tested at Wujek coal mine in Upper Silesia (Koza, 1997). The system transmits data in a continuous mode, the dynamic range is 90 dB (120 dB in a modified version), the sampling frequency is 500 Hz, and the maximum length of a communication line is 12 km. Transmission errors are automatically detected, centralized synchronization timing is available, and multiple signals can be multiplexed into a single channel. A modified version of the system was adapted for strain measurements at Rudna copper mine. The sampling frequency of 250 Hz is sufficient to separate dynamic and static strain signals.

2.3. Location of Seismic Events

Location of seismic events is the first step in studies and monitoring of seismicity in mines. Accuracy is one of the most important factors in such studies, and the requirements in this respect are demanding. In mining practice, the expected accuracy for hypocenter locations are a few tens of meters, or even a few meters in some cases. The location error might be considered to consist of two components: random location scatter and systematic bias (e.g., Gibowicz and Kijko, 1994). Random location scatter is caused by errors in arrival-time measurements, and systematic bias is generated by the differences between the rock mass structure at the source and receiver and the velocity model used in the location procedure.

The influence of systematic errors can be eliminated by a detailed analysis of travel-time anomalies, or by calibration explosions, or by the simultaneous location of a group of seismic events and velocity model determination. The values of random errors of hypocenter parameters can therefore be used as a quality criterion of the spatial distribution of seismic stations. Consequently, the problem of optimum event location is equivalent to an analysis of the spatial distribution of seismic stations ensuring the minimum values of random errors in the source location procedure (e.g., Gibowicz and Kijko, 1994; Kijko and Sciocatti, 1995a).

Although underground seismic networks are widely used in mines, surprisingly little attention is paid to the optimum design of such networks. Their performance is usually evaluated after installation and operation for a time, and the optimal configuration is predesigned and theoretically tested in a few cases only. A number of papers are available that are devoted to the subject of optimal network planning and event location techniques; see Gibowicz and Kijko (1994), Kijko and Sciocatti (1995a), and Mendecki and Sciocatti (1997) for comprehensive reviews and references. Two methods frequently used to design the optimum configuration of seismic networks in mines are based on either a statistical or a direct approach (Mendecki and Sciocatti, 1997).

With the statistical approach, the choice of one or another station configuration should depend upon the expected location error that would be found if a given configuration is used. Thus the choice should depend upon a certain value related to the given geometrical configuration, and the best network would be defined by its minimum. The value should depend upon a covariance matrix of the event unknown location parameters (Kijko and Sciocatti, 1995a). The covariance matrix can be graphically interpreted in terms of a confidence ellipsoid, where its eigenvalues form the lengths of the principal axes of the ellipsoid. Finding a configuration for which the volume of this ellipsoid is the smallest is referred to as *D*-optimum planning. The volume is proportional to the product of the eigenvalues, or equivalently, to the determinant of the covariance matrix. The *D*-optimization of the coordinates of seismic stations becomes much more complex when the travel times of seismic

waves are described by nonlinear equations and the vector containing the event coordinates is of random variable character. The location of seismic events, based on the travel times of seismic waves recorded at several stations, is of such a nature. The described approach to optimal planning of a seismic network can be used in practice only when a relatively small area of high seismicity can be defined. Otherwise, when a seismic area is large and divided into several subregions, the *D*-planning procedure must be modified (for details and applications, see Kijko and Sciocatti, 1995a).

In a direct approach to the optimal planning of seismic networks, the sensitivity of the solution of a system of nonlinear or linear equations to small changes in the data is measured by the condition number of the system. The optimal configuration of seismic stations is defined as that having the smallest condition number of the system of nonlinear equations (Mendecki and Sciocatti, 1997). This procedure is also known as *C*-optimal planning. For a small condition number, small changes in the errors of arrival times of seismic waves and velocity model should not considerably influence the location of seismic events. Otherwise, the location would be unstable and the condition number would be large. Minimization of the condition number can be taken as a deterministic criterion to design any experiment leading to solving a system of equations. The procedure is described in Mendecki and Sciocatti (1997), where examples of its practical application are also given.

Various approaches to the location of seismic events in mines are based as a rule on time residuals of seismic waves. For a given velocity model a time residual is defined as the difference between the observed and calculated arrival time of a given seismic wave. To constrain the location determination, the direction or the azimuth of the wave-front can be added; this is possible only if the straight line is a fair approximation of the ray path between the source and the station (Mendecki and Sciocatti, 1997).

Two conceptually different approaches to the location problem, based on time residuals, are used (Gibowicz and Kijko, 1994). In the first approach, no attempt is made to distinguish the time residuals caused by time reading errors and velocity model inaccuracy. Typical representatives of such an approach are the classic least-squares procedures and the Bayesian procedure. In the second approach, the time residuals are split into two components: random ones related to the reading errors of arrival times, and travel-time residuals caused by insufficient knowledge of the velocity structure.

Several location procedures are in use, depending on the assumptions made on the nature of velocity model uncertainty. The extension of the classic least-squares procedure to that with controllable variables (the velocity model parameters) subject to random errors is one of them. This approach is possible if the fluctuations of velocity model parameters, from an average model, can be expressed in statistical terms. In the mining application, knowledge of the rock mass seismic velocities and their variances is usually adequate for this technique. Another procedure

employs the concept of relative location of seismic events and is based on arrival-time differences between a reference (master) event and nearby events. The travel-time residuals caused by insufficient knowledge of the velocity model are of a systematic character and are removed implicitly. The method is commonly used in mines where large production blasts are fired during excavations. The most difficult location technique is the procedure of simultaneous inversion of velocity structure and location of a set of seismic events.

The classic way to solve a system of nonlinear equations, used in the location procedure, is to linearize the system by a Taylor expansion around a trial position and solve the resultant linear system, usually by a least-squares method. This means that the L_2 norm of the residual vector is minimized, which in turn requires an assumption that the distribution of residuals is of Gaussian nature. The time residuals do not follow the Gaussian distribution and occasionally large residuals strongly affect the location results. Then the L_1 norm is preferable: it minimizes the sum of the absolute values of time residuals and is less sensitive to outliers.

In general, the solution of nonlinear station equations can be found by an iterative approach; the Nelder–Mead simplex minimization procedure is often used. To find the global minimum, appropriately chosen starting points for the iterative procedure are needed. The weighting factors are also necessary, especially when automatic processing is performed, to quantify the measure of reliability of the arrival times. Centering and scaling techniques, standard methods used in statistical applications, lead to the simplification of inverse problems and to the improvement of numerical stability. For the location of seismic events in mines, the L_1 norm and centering were introduced by Prugger and Gendzwill (1988) and used at Saskatchewan potash mines, Canada; they were also implemented in the location procedures used in South African gold mines (Mendecki, 1993). Other nonlinear techniques which can be used to solve the location problems include genetic algorithms and simulated annealing (e.g., Sambridge and Gallagher, 1993).

Several field experiments have been conducted, each using four source location methods, to estimate the coordinates of a compact explosive source in an underground mine in Australia (Blair, 1993). The four location methods were (1) a least-squares solution, (2) an iterative improvement to the least-squares solution, and (3) a 5-point and (4) an 8-point simplex optimization scheme. The results showed that there was little difference between methods (2) and (4), and method (1) was inferior to all other methods. Synthetic models provided results consistent with the experimental data, provided that a small amount of travel-time scatter was assumed. When the scatter was increased, however, method (1) was found to be the most robust, implying that in real mining environments this method might well be the superior one for the location of seismic events under specific mining conditions.

In some cases, the location procedure can be significantly simplified. This can be achieved if a single velocity model is acceptable. After simple algebraic

transformations, the location parameters are least-square solutions of the set of linear equations. Linear methods used for event locations are very attractive. They are fast and free from all the problems related to iterative procedures. An obvious limitation to these simple methods follows from the fact that they ignore complex velocity structures and their applications may often lead to unreasonable solutions. At present, the linear methods are usually used for determination of a starting point for further iterative computation.

A constant isotropic velocity model was accepted for the location of seismic events at hard rock Galena mine at Wallace in northern Idaho (Swanson *et al.*, 1992). Dense clusters of accelerometers are used there to achieve a high level of event detection. Various sources of error in the location process were examined, and the errors were used to investigate the accuracy of event locations for both analog and digital monitoring systems in the mine. Similarly, an isotropic velocity model was adopted for the event location in a mine in the Lorraine coal basin, France, where the rock mass structure is highly complex and could not be approximated by simple models (Ben Sliman and Revalor, 1992). The arrival time of shear waves was additionally included into the location procedure and the optimum velocity ratio of P to S waves was estimated. In another coal mine in the Arc basin, Provence, a four-layer non-horizontal model was used for the location of seismic events. The influence of the number and type of seismic waves used in the location procedure on the location accuracy was considered by Dębski (1995). The best results are provided by a combination of direct and reflected waves, which are often observed in underground mines. An automatic complex procedure for searching arrival times of seismic events and the optimal location of seismic events was described by Růžek (1995). The procedure is based on the Hilbert transform of input records (energy flux envelopes) and on the Simplex location algorithm.

One of the problems involved in the event location procedures is whether norm L_1 or L_2 is the best to handle arbitrarily erratic data. Finding an optimal value of p for the norm L_p , where p is not necessarily equal to 1 or 2, might lead to better results. Kijko (1994) introduced the concept and the application of the adaptive L_p norm to the location of seismic events in mines. This concept allows selection of the most appropriate value of p and provides more robust solutions than L_1 or L_2 procedures when outliers occur in the input data.

The performance of the three norms in the presence of one outlying time residual is shown in Fig. 5, adapted from Kijko (1994) by Mendecki and Sciocatti (1997). For each value of the outlying time residual present at one station, 1000 seismic events were generated. For each event, P -wave arrival times recorded by the other 11 stations were perturbed by normally distributed random numbers with a standard deviation equal to 5 ms. Figure 5 shows the average error of the hypocenter location calculated by the three norm procedures for outlying residuals in the range of 5 to 100 ms. The results indicate that up to a certain value of an outlier the use

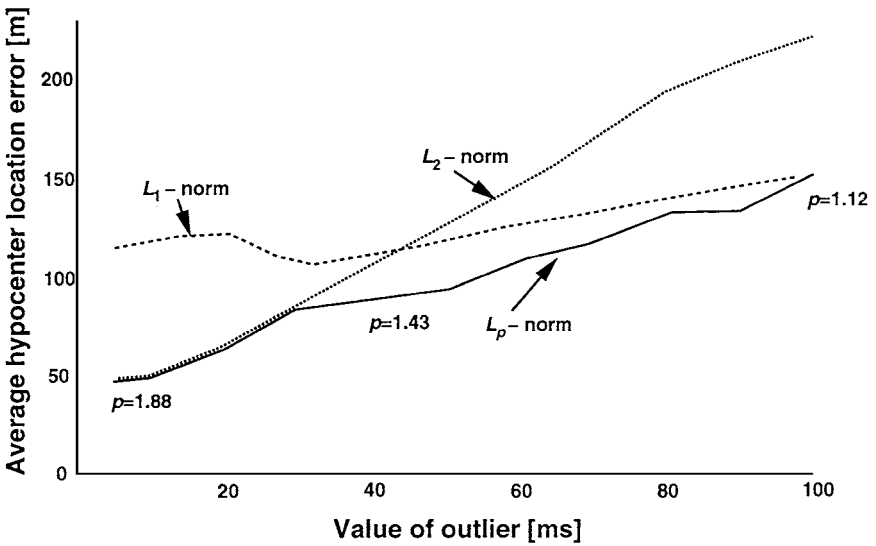


FIG. 5. Comparison of seismic event location procedures based on the L_1 , L_2 , and adaptive L_p norms in the presence of one outlying arrival time in the range from 5 to 100 ms. [Mendecki and Sciocatti, 1997, reprinted from *Seismic Monitoring in Mines*, Fig. 5.2, © 1997 Chapman & Hall, with kind permission from Kluwer Academic Publishers.]

of the adaptive norm provides a substantial improvement over the L_1 norm; for larger outliers both norms provide similar results. When the outliers are small, the least-squares technique and the adaptive norm are essentially the same.

In classic location algorithms the only input data are the arrival times of seismic waves recorded by a given network, and no additional, a priori, information is used. The areas of the most probable locations of seismic events in mines, on the other hand, are usually known. Seismic activity usually concentrates in the vicinity of mining works, and even a short practice at any seismic network in a mine is sufficient to find from visual inspection of seismic records that the event occurred in a particular area of the mine. This a priori information can be included into an algorithm based on the Bayesian estimation theory, and it has been formulated for the location of seismic events in mines (Gibowicz and Kijko, 1994). The algorithm permits the combination of a priori information with that contained in the arrival times of seismic waves. Several numerical simulations of its application in different situations typical for mining conditions have demonstrated the effectiveness of the Bayesian approach and its superiority over the conventional location procedure. The Bayesian procedure is used in several coal and copper mines in Poland, and some experiments have also been performed in gold mines in South Africa and at the Men-Tou-Gou coal mine near Beijing in China.

When the velocity model is not known adequately, the location of seismic events can be improved by the arrival time difference (ATD) method, also known as “master event” location or relative location (see Gibowicz and Kijko, 1994, or Mendecki and Sciocatti, 1997). This is an old and highly popular method in which the travel time anomalies resulting from velocity model uncertainties are removed implicitly during the formation of equations. The procedure requires an accurately located master event (e.g., blast) in the proximity of the event to be located, that has reliable arrival times at stations used in the location calculations; all locations performed are related to the master event. Thus it is inherently assumed that the velocities of seismic waves from the master event to the stations and those from the target event are the same. The location accuracy, therefore, is heavily dependent on the distance between the master and target events as well as the difference in average wave velocity along the respective ray paths. To demonstrate the efficiency of the ATD location procedure, comprehensive tests were performed at copper mines in the Lubin mining district (Król and Kijko, 1991). Over 350 blasts from eight mining sectors were located twice, by the ATD and conventional methods. The average errors of epicenter locations by the two procedures are shown in Fig. 6. The ATD approach provides evidently better results. This technique has been routinely used at potash mines in Germany and at coal and copper mines in Poland.

Spottiswoode and Milev (1998) proposed a novel approach to the location procedure of seismic events in mines. They assembled seismic events with similar waveforms (doublets) into multiplets, relocated them simultaneously using arrival-time differences based on cross-correlation between all event pairs, and identified the orientation of the most likely plane on which the events are located. In contrast to the conventional master event method, no single master event was used. Each

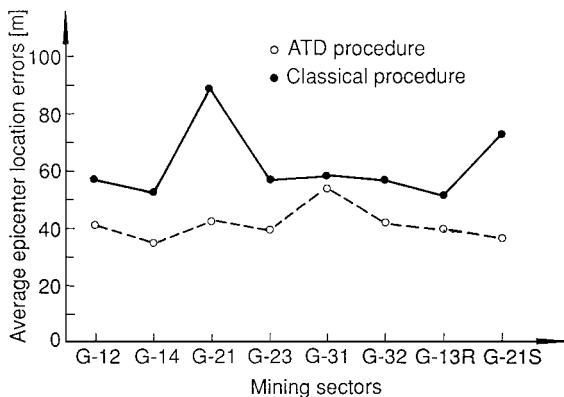


Fig. 6. Comparison of the average errors of epicenter locations of 354 dynamite blasts fired at Polkowice and Rudna copper mines, Poland, determined by the ATD and classic procedures. [Reprinted from Król and Kijko (1991), Fig. 4.]

event was a master event for the other event. The method was tested on seismic data recorded at a site in Blyvooruitzicht gold mine, South Africa, where a stabilizing pillar has been mined with the aid of precondition blasting. Some 40% of events that were previously located in a diffuse cloud within the pillar were found to form three distinct multiplets.

Simultaneous location of a group of seismic events and determination of a velocity model are founded on the same assumptions as the ATD approach: the travel time anomalies from a set of close seismic events tend to be strongly correlated and have nearly constant values at the same stations. In contrast to the ATD approach, in which the hypocenter of only one event is located, in this procedure a set of hypocenters and velocity model parameters are jointly determined. The procedure is known as the simultaneous structure and hypocenter (SSH) determination method (e.g., Gibowicz and Kijko, 1994) or as the joint hypocenter and velocity determination (JHVD) method (e.g., Mendecki and Sciocatti, 1997). The method is effective when applied to the location of seismic events that are spatially clustered, which is often the case in mining. It is assumed that the average velocity of a seismic wave from one event in the cluster to a given station is the same for all the other events in the cluster. If two events in the cluster, therefore, are far apart the assumption that the wave travels through the same rock mass would be no longer valid, and conversely, if the cluster is too small, increased numerical instability may appear since the arrival time equations would become very similar. The procedure does not require velocity calibration blasts and is fast. Its application in an area of high seismicity for a specific period of time makes it also possible to detect spatial and temporal variations of the velocity model parameters caused by stress migration.

The JHVD procedure was applied by Mendecki (1987) to study seismicity associated with a pillar in a gold mine in the Klerksdorp district and by Mendecki and Sciocatti (1997) to improve the location accuracy of seismic events occurring in different clusters at the Elansrand gold mine in South Africa. An example of the distribution of seismic events located by the JHVD method and those located using fixed velocities of seismic waves at a Zambian copper mine is shown in Fig. 7, reproduced from Mendecki and Sciocatti (1997). Events located by the JHVD procedure are on the average 50 m closer to the mined ore body than the same events located using fixed velocities. In the case where seismic events are not spatially clustered, more complex techniques for velocity inversion are required.

2.4. Seismic Tomography

Seismic tomographic imaging is used to map the spatial variation of seismic parameters in rocks. Periodic repetition of tomographic imaging in a given area would provide monitoring of rapidly changing conditions in mines. Several seismic

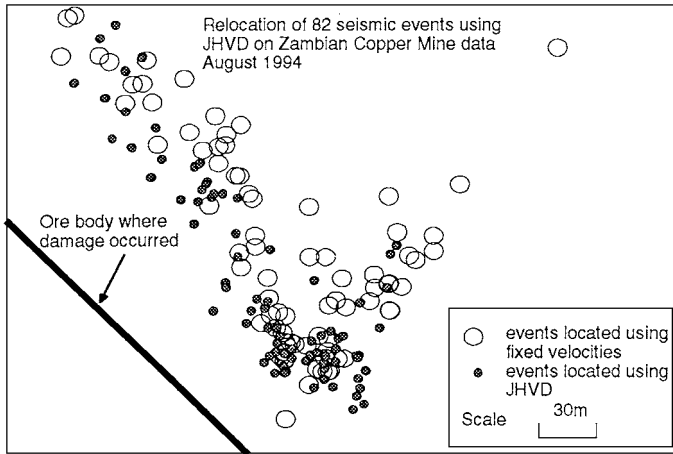


Fig. 7. An example of the distribution of seismic events located by the JHVD method and those located using fixed seismic wave velocities at a Zambian copper mine. [Mendecki and Sciocatti, 1997, reprinted from *Seismic Monitoring in Mines*, Fig. 5.6, © 1997 Chapman & Hall, with kind permission from Kluwer Academic Publishers.]

quantities may be imaged, such as wave velocity or attenuation. The most common are *P*-wave velocity images because of the relative simplicity and accuracy of the measurement. Velocity imaging has been shown to be particularly useful for seismicity studies in mines (e.g., Young and Maxwell, 1992; Maxwell and Young, 1996). Velocity images can be calculated by using either controlled explosive sources or passively monitored seismicity. Passive source velocity images can be computed from seismicity data by a simultaneous inversion procedure for source location and velocity structure. The results show very good correlation with a velocity image calculated using data from active explosive sources (Young *et al.*, 1992; Maxwell and Young, 1993a, 1997a).

Detailed velocity structures will obviously improve the accuracy of hypocenter location. This was shown by an experiment carried out at Strathcona mine in the Sudbury Basin, Ontario, where the controlled source blasts were used as simulated passively monitored sources to image the velocity structure by application of joint hypocenter location-velocity inversion techniques (Maxwell and Young, 1993a). Blast monitoring data provide an opportunity to compare passive and active source inversion results. Source location errors were determined by calculating hypocenter location of blasts and comparing them with true blast locations. Using the controlled source-imaged velocity structure, the average source location error was found to be 5.5 m, as shown in Fig. 8, reproduced from Maxwell and Young (1993a). For the simplified model of a constant velocity, the average source location error was determined to be 10.5 m.

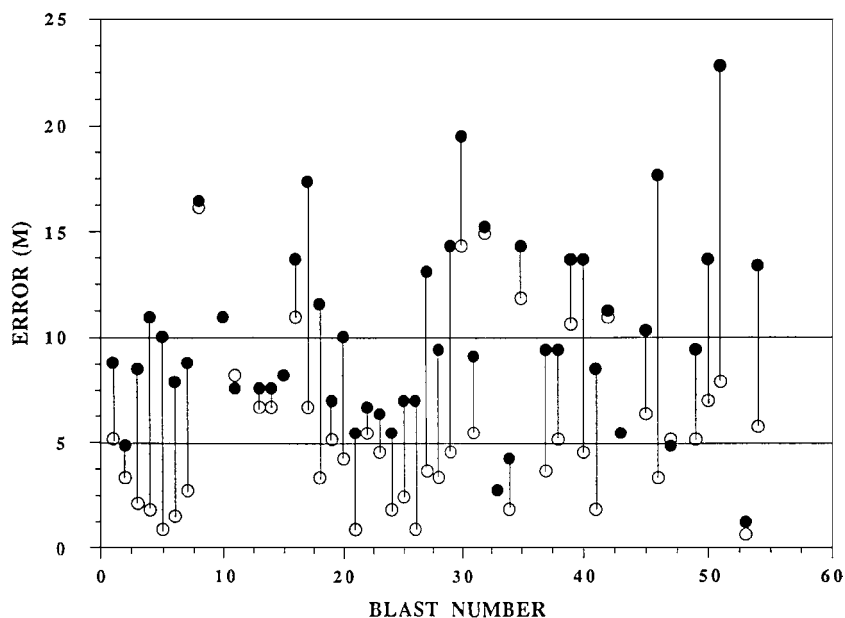


FIG. 8. Source location errors measured from actual blast locations at Strathcona mine, Ontario, for both constant average velocity model (closed circles, average error of 10.5 m) and controlled source-imaged velocity structure (open circles, average error of 5.5 m). [Reprinted from Maxwell and Young (1993a), Fig. 5, © 1993 Seismological Society of America.]

Comparisons between velocity images and seismicity in Canadian mines (Young and Maxwell, 1992; Young *et al.*, 1992) and in South African mines (Maxwell and Young, 1996, 1997a) have shown that the largest events are associated with regions of high velocity, whereas low velocity areas are generally not seismic. An example of such a pattern in an active stope at Strathcona mine is shown in Fig. 9, reproduced from Young *et al.* (1992). In this figure the results of a passive source *P*-wave velocity image are plotted on a vertical cutting plane, and the location of a large seismic event and associated seismicity are shown as well.

Controlled studies around an underground opening in homogeneous unfractured granite at the Underground Research Laboratory (URL), Manitoba, where a 3.5-m-diameter circular tunnel was excavated at a depth of 420 m, have shown a strong correlation between velocity and stress (Maxwell and Young, 1995, 1996). To determine the velocity structure at the URL and to assess the accuracy of the source locations, signals generated by a series of controlled seismic sources were recorded with seismic array. The travel times were inverted to image the 3D-velocity structure around the tunnel. The resulting velocity image plotted on a cutting plane perpendicular to the tunnel axis, superimposed with the location

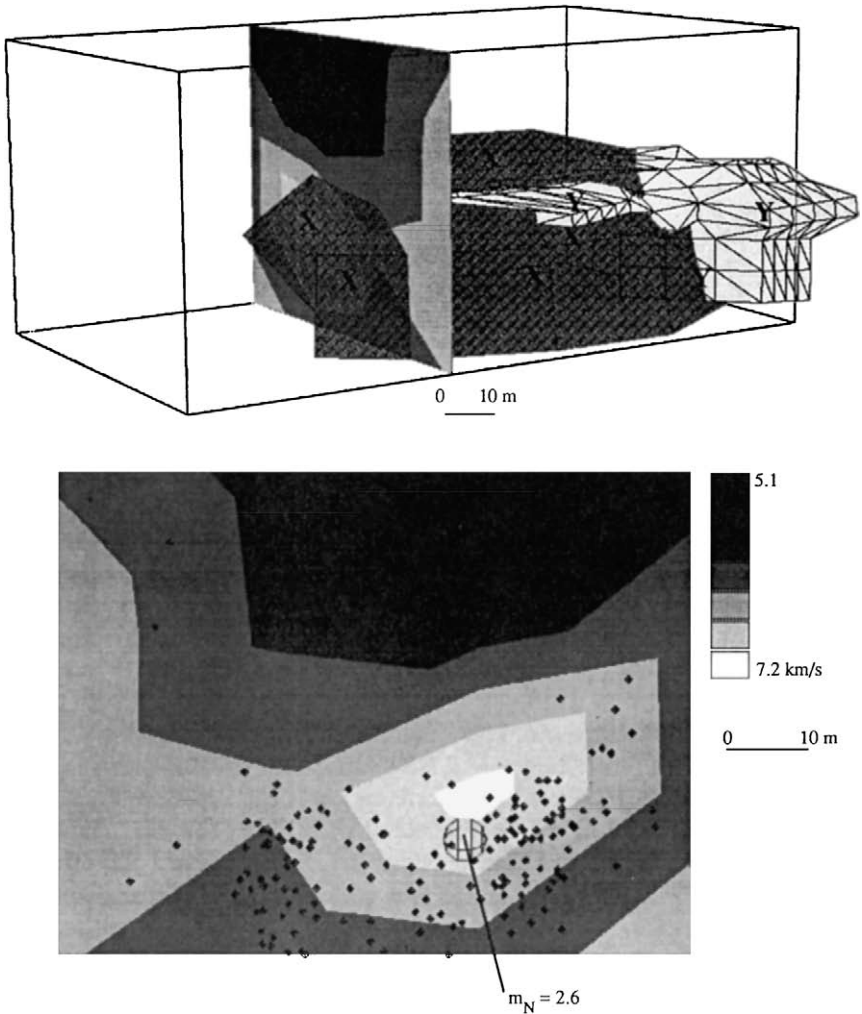


FIG. 9. Perspective view of the geometry of an active stope at Strathcona mine (labeled X) superimposed with the results of a passive source P -wave velocity image plotted on a vertical cutting plane and an isosurface of event density (labeled Y). The cutting plane is also shown with the superimposition of a magnitude 2.6 event and associated seismicity. [Young *et al.* (1992), Fig. 11, reprinted with kind permission from Birkhäuser Verlag AG.]

of seismic events located in that section of the tunnel, is shown in Fig. 10, reproduced from Maxwell and Young (1996). Velocities are plotted as relative perturbations from an initial starting model of the average velocity around the tunnel. Figure 10 also shows contours of the magnitude of the maximum compressive

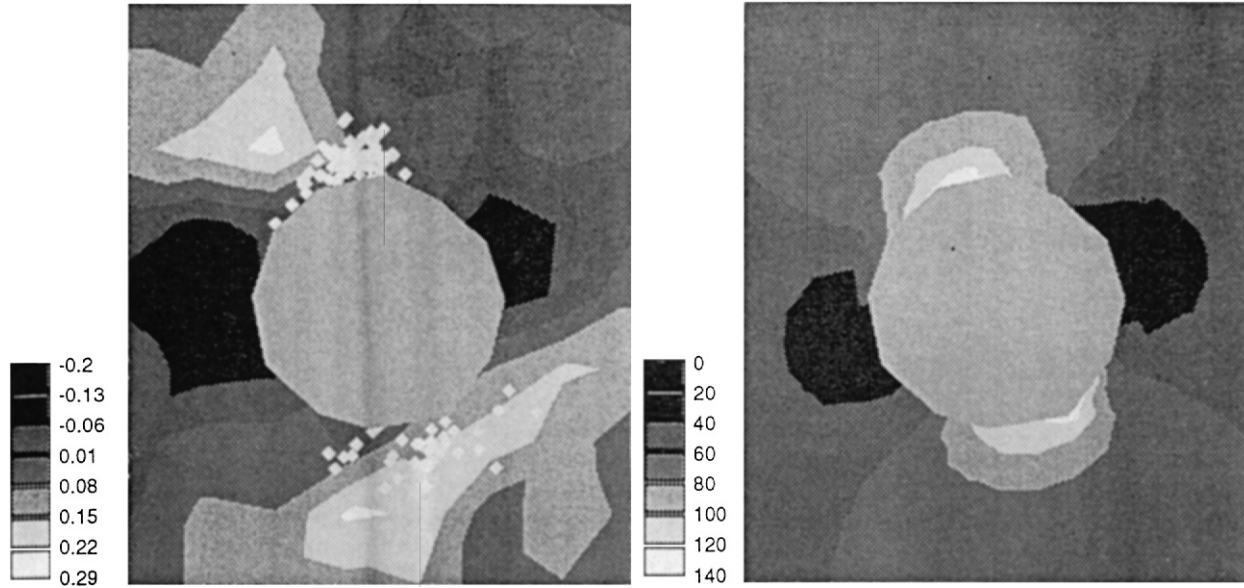


FIG. 10. Active-source image of spatial variation in P -wave velocity on a plane perpendicular to the tunnel axis in the Underground Research Laboratory, Manitoba, superimposed with the location of microseismic events in that section of the tunnel. Maximum compressive stress contours, computed by a boundary element method, are also shown. [Maxwell and Young, 1996; reprinted from *International Journal of Rock Mechanics and Mining Sciences*, © 1996 Elsevier Science Ltd, with permission from Elsevier Science.]

stress, computed using a boundary element program designed to calculate elastic stress changes around underground openings. *In situ* stress gauges and extensometers generally validated stress changes around the tunnel. The seismicity appears to be generated in a region of velocity gradient, corresponding to the area separating the plastically deformed or failed zone from the elastically stressed zone.

Thus, the relationship between velocity and seismicity can be interpreted by frictional stability; the largest events occur in regions of high normal stress where the rock mass is able to store significant strain energy. A holistic interpretation of velocity images and seismicity can therefore be used to understand the seismic response of the rock mass to mining induced stress changes (e.g., Maxwell and Young, 1997a). Sequential images of temporal velocity variations can be used to isolate stress changes, based, for example, on repeated explosions at the same location or from seismicity data using a doublet technique. Several practical applications of these techniques to alleviate rockburst hazard in Canadian and South African mines have been discussed (Maxwell and Young, 1992, 1993b,c, 1995, 1996, 1997b, 1998).

Watanabe and Sassa (1996) developed two methods of seismic attenuation tomography. One is amplitude attenuation tomography, based on the first arrivals of *P* waves. The effects of velocity structure on wave amplitude were removed, and the decrease of wave frequency during propagation was estimated in order to obtain directly the values of quality factor. The other method is pulse broadening tomography, based on broadening of rise time or pulse width of the first arrivals. In this method, attenuation information is obtained from time data only. Watanabe and Sassa (1996) integrated the seismic travel time and seismic attenuation tomography and applied it to field data at Kamioka mine in Gifu prefecture, central Japan. Faults and fractured zones were detected.

Seismic velocity tomographic techniques are widely used in Polish coal mines to assess rockburst hazard and the efficiency of prevention measures undertaken there (e.g., Dubiński, 1997). Tomographic high frequency measurements at the Merkers potash mine in Thuringen, Germany, were carried out to assess the zones of high permeability in a salt rock formation, associated with open microcracks leading to dilatancy and acoustic emission (Manthei, 1997). Both velocity and frequency-dependent attenuation, corresponding to travel time and amplitude tomography imaging, were obtained for *P* and *S* waves, indicating the areas of lower velocity and higher attenuation. The image reconstruction accuracy of active amplitude tomography was discussed by Dębski (1997) who considered the dispersion of amplitudes of seismic waves radiated by various explosive sources.

Large systems of equations generated by seismic tomography can be solved by a number of methods. One-row-action techniques, such as algebraic reconstruction technique (ART) and simultaneous iterative reconstruction technique (SIRT) are commonly used in seismic tomography. The conjugate gradient technique has also been widely used in recent years; details can be found in Gibowicz and

Kijko (1994) and Maxwell and Young (1997a). Practical problems connected with velocity inversions in mines were discussed by Maxwell and Young (1993a).

2.5. Spatial and Temporal Patterns

Seismic events induced by mining are not uniformly distributed either in space or in time. Extensive studies performed on the space–time–energy distributions of seismic events in mines show that the tendency to form nests, swarms, and clusters is commonly observed (e.g., Talebi *et al.*, 1994; Čiž and Růžek, 1997; Dunlop and Gaete, 1997; Gibowicz, 1997a). This tendency is apparent not only on a regional scale (see, e.g., Fig. 1) but on a highly local scale as well. Figure 11, reproduced from Trifu *et al.* (1993), shows, for example, the spatial distribution of seismic activity in a 1-km³ volume within Strathcona mine, Ontario, below 600 m depth, observed between the middle of February and April 1991. Another example is presented in Fig. 12, reproduced from Lasocki *et al.* (1997), where the distribution of seismicity is shown on a whole mine scale at Wujek coal mine, Poland, observed between 1988 and 1993.

A variety of techniques have been applied to quantify the spatial and temporal properties of natural earthquakes. Similar methods have also been applied to study

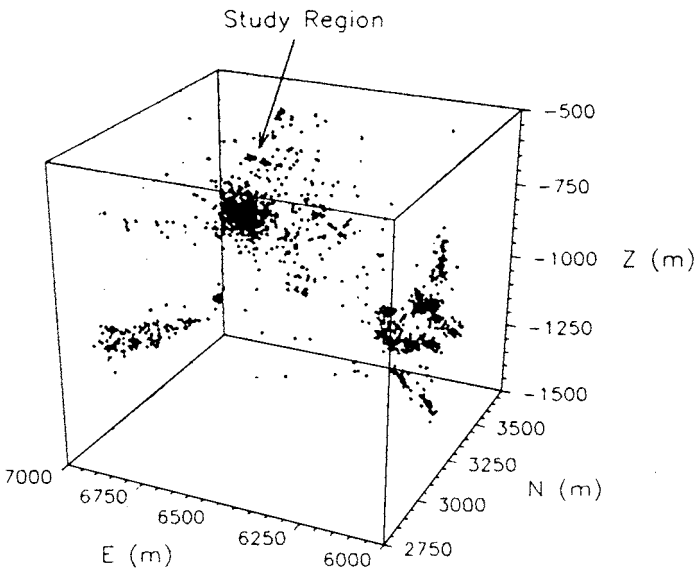


FIG. 11. Spatial distribution of seismic events recorded during the monitoring period in 1991 from a small area below a depth of 600 m at Strathcona mine, Ontario, Canada. [Reprinted from Trifu *et al.* (1993), Fig. 3.]

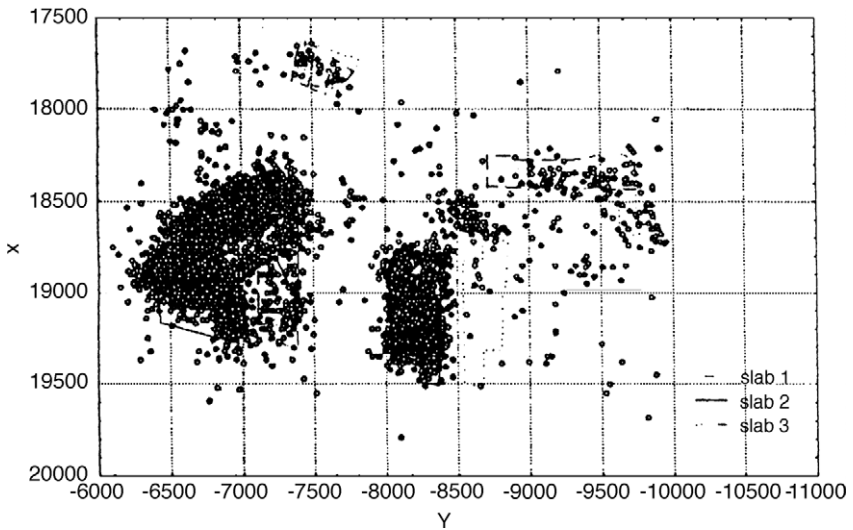


Fig. 12. Seismicity of level 501 at Wujek coal mine, Poland, recorded from 1988 to 1993. [Lasocki *et al.* (1997), Fig. 1, reprinted from *Rockbursts and Seismicity in Mines*, Proceedings of the 4th International Symposium, Krakow, Poland, 11–14 August 1997. 450 pp., EUR 137.50/US \$162.00/GBP97, A. A. Balkema, P.O. Box 1675, Rotterdam, Netherlands.]

anomalous patterns and clustering in mining-induced seismicity. In many respects, mining seismicity and tectonic seismicity are quite similar and the process involved in the generation of seismicity patterns should be scale invariant (e.g., Gibowicz and Kijko, 1994). Preliminary results from cluster analyses of seismicity in a deep South African gold mine were presented by Kijko and Funk (1996). In total over 20,000 seismic events were analyzed, covering the time period of 1 year. The ability of the space–time clustering analysis applied to detect anomalous clusters of seismicity is demonstrated in Fig. 13, reproduced from Kijko and Funk (1996), where the location of four out of seven identified clusters is shown. Furthermore, the results of the analysis support the notion that seismicity at given active faces is affected by seismicity at other mining faces, and that the degree of interaction is a function of distance between the faces. Mining engineers have suspected this for some time.

Xie and Pariseau (1993) studied the seismicity associated with a rockburst-prone pillar in a metalliferous ore vein in the Galena mine, Idaho, and found that the distributions of seismic events have a fractal clustering structure. The degree of clustering increased with an upcoming major event, corresponding to a decreasing fractal dimension. The fractal dimension is positively correlated with the coefficient b in the frequency-magnitude/energy relations (Guo and Ogata, 1995). Holub (1996a) reported that lower b values correspond to a higher level of

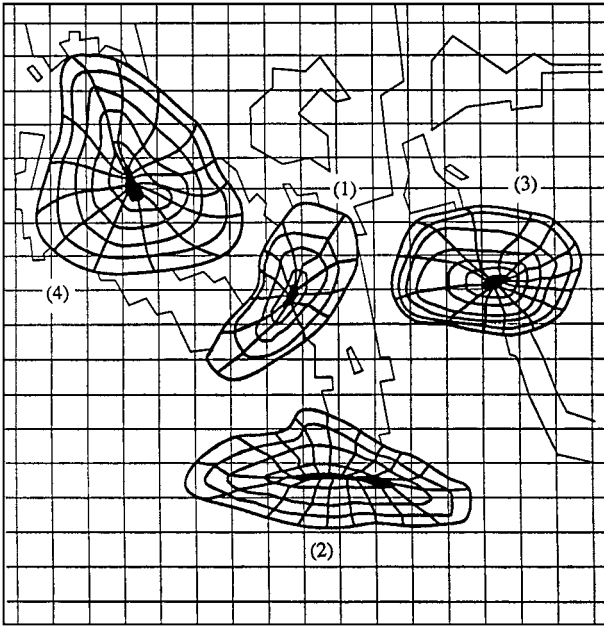


FIG. 13. Four clusters of seismic events at a gold mine in South Africa identified by a space-time clustering analysis algorithm. [Reprinted from Kijko and Funk (1996), Fig. 1, with kind permission from Birkhäuser Verlag AG.]

seismicity; and the inverse holds true for a number of coal mines and for different time intervals in the Ostrava-Karvina Mining District, Czech Republic.

Seismicity patterns in space and time, based on a number of seismic parameters, were extensively studied in South Africa (e.g., van Aswegen and Butler, 1993; Mendecki, 1997b,c; van Aswegen *et al.*, 1997). To monitor rock mass response to mining, Mendecki (1997b,c) assumed that rock could be analyzed as a fluid that tends to flow into the voids created by mining. A seismic event is considered to be the result of instability in the flow of rock. He proposed to describe seismicity quantitatively by at least four largely independent parameters: average time and distance between consecutive seismic events, including source size, sum of seismic moments, and sum of energy.

From these parameters, for a given volume of rock mass and time interval, several new quantities can be calculated, describing seismic flow of rock. These are the apparent volume, the seismic viscosity, the seismic relaxation time, the Deborah number, the seismic diffusivity, the Schmidt number, and numerous others, all based largely on various combinations of seismic moment and energy. Additionally, the energy index of a given event within a large suite of events is often calculated. The index is the difference between the seismic energy of the event and

that of the regression line between the seismic moment and the energy, on a logarithmic scale, fitted to the data from the selected set of events (e.g., van Aswegen and Butler, 1993). Mendecki (1997b,c) and his colleagues (van Aswegen *et al.*, 1997) believe that plotting various combinations of these parameters as a function of time can provide indications of impending instabilities, corresponding to major seismic events.

A new efficient method to study the nonrandom character of the spatial distribution of seismic series in mines was proposed by Lasocki *et al.* (1997). The method is based on the deflection of straight lines connecting epicenters of every two consecutive events, measured from the NS direction. The deflection series are analyzed by a nonparametric kernel estimation of their probability density function. The method was applied to three sets of events from Wujek coal mine, Poland, which occurred between 1988 and 1993 in different areas of the mine. The dominant directions of the distribution were significantly different for the three selected data sets. Furthermore, the dominant trends in the same set of events became different when various energy thresholds were considered. This suggests that the generation of events is controlled by various factors and that mining-induced seismicity is a multimodal phenomenon. Some of these trends could be associated with known geological, tectonic, and mining features, and the others were not. The analysis of deflection was also used to study the directional patterns of seismic events of energy equal to or greater than 10^6 J from two major event clusters (see Fig. 1) in the Upper Silesian Coal Basin, Poland (Lasocki and Idziak, 1998). The clusters are neither confined to particular mines nor cover evenly the whole area of mining works. Four dominant directions of epicenter migration were found. Two trends are connected with the events that belong to the same cluster and are related to its shape. The other two are linked with the subseries of events that alternate between the clusters, indicating that mutual positions of events in such series are not randomly distributed. The dominant directions identified from the in-cluster series support recent hypotheses about possible tectonic instability of the region (e.g., Zuberek *et al.*, 1996).

Seismic anisotropy is a field undergoing rapid expansion. A new understanding of the behavior of fluid-saturated microcracked rock allows noncatastrophic deformation to be monitored by seismic shear waves. The evolution of such rock under changing conditions can be calculated and future behavior predicted by an anisotropic poroelasticity (APE) model, developed by Zatsepin and Crampin (1997) and Crampin and Zatsepin (1997), where the parameters controlling microscale deformation also control shear-wave splitting. Shear-wave splitting occurs when shear waves propagate through solids that are effectively anisotropic, such as rocks containing aligned cracks or ellipsoidal inclusions. The behavior of shear waves crossing an anisotropic region is illustrated schematically in Fig. 14, reproduced from Crampin (1997). The splitting writes characteristic signatures into three-component seismograms, which can readily be interpreted in terms of geophysical parameters. Such distributions of stress-aligned microcracks are known

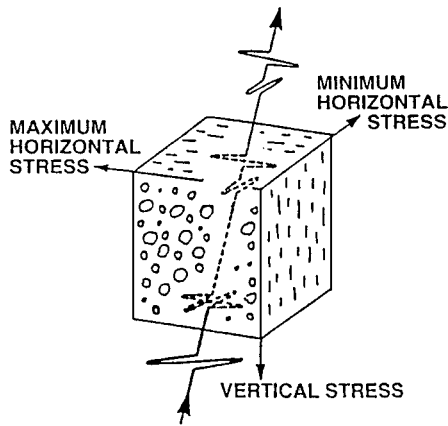


FIG. 14. Schematic illustration of shear-wave splitting below about 1 km depth in the Earth's crust, for the waves propagating through distributions of stress-aligned fluid-filled intergranular microcracks (EDA-cracks). These near-parallel crack orientations are below the depth where the increasing vertical stress is greater than the minimum horizontal stress. [Crampin (1997), Fig. 1, reprinted from *Rockbursts and Seismicity in Mines*, Proceedings of the 4th International Symposium, Krakow, Poland, 11–14 August 1997. 450 pp., EUR 137.50/US \$162.00/GBP97.00, A. A. Balkema, P.O. Box 1675, Rotterdam, Netherlands.]

as extensive-dilatancy anisotropy (EDA) and the individual inclusions are known as EDA-cracks (Crampin *et al.*, 1984). Stress-aligned shear-wave splitting is now widely observed in almost all rocks in the uppermost half of the crust (Crampin, 1994). The importance of APE for investigation of seismic events in mines is that there is now an underlying mathematical basis for monitoring, modeling, and predicting the behavior of stress and seismic events and rockbursts as mining progresses (Crampin, 1997). It should be noted, however, that the stress-based interpretation of shear-wave splitting is controversial; preferred mineral orientation is an alternative interpretation.

This new technique for monitoring and modeling of rock mass deformation has not been widely used as yet in studies of seismicity in mines. Graham *et al.* (1991) reported the results of their analysis of ground acceleration and velocity seismograms recorded during 1987 by a GEOS (General Earthquake Observation System) station situated on the surface above an active mining face at Western Deep Levels gold mine in South Africa. The polarizations of shear waves have a nearly uniform alignment, consistent with shear waves propagating through the effective anisotropy of parallel vertical microcracks throughout the rock mass. The observed anisotropy appeared to be caused by the regional stress regime rather than local stress disturbances generated by mining operations. The only mine-by experiment known to us was undertaken in the Underground Research Laboratory, Manitoba, to investigate the excavation damage around a 3.5-m-diameter tunnel at 420 m depth in the Lac du Bonnet granite batholith (Holmes *et al.*, 1993;

Crampin, 1997). Four differently polarized shear-wave signals were generated by nylon rods, which were pulsed with a Schmidt hammer. These sources produced very consistent shear-wave signals with the four different radiated signals splitting in the expected polarizations for stress-oriented nearly horizontal EDA-cracks.

3. GEOLOGY, MINING, AND SEISMICITY

Recent studies of seismicity in mines, undertaken in various mining districts of the world, have confirmed that at least two broad types of seismic events are observed universally—those directly connected with mining operations and those associated with movement on major geological discontinuities. Obviously, seismicity in mines is strongly affected by local geology and tectonics, and interaction between mining and lithostatic and tectonic stresses on a local and regional scale (e.g., Gibowicz and Kijko, 1994). *In situ* stress measurements collected at the Underground Research Laboratory in Manitoba indicate that major geological discontinuities can act as boundaries for stress domains, and that the magnitude and direction of the stress field can change rapidly when these discontinuities are traversed (Martin, 1990).

Johnston (1992) published a worldwide survey of various parameters connected with mining-associated seismicity. Seismic events from the Republic of South Africa, Sweden, Poland, Czechoslovakia, Canada, and the United States were sorted according to type of geological conditions and preexisting regional stress field. The seismicity was found to be bimodal and was divided into two broad types: seismicity directly associated with mining activity and geometry, and seismicity occurring on preexisting faults and discontinuities in or near the mining district. Locations of the first-type events are determined consistently by the location of the mine face and by local geological structure. Their epicenters are located at a specific distance ahead and behind the active face and their depths usually correspond to geological and mechanical zones of weakness. The maximum magnitude of these events depends mostly on the strength properties of the rock mass, and the overall level of seismicity is believed to be a function of the extent of the excavation. The characteristics of the second-type events are much less clear. Their locations depend on the location of preexisting discontinuities in the area, but controlling factors of their maximum magnitude are not well understood.

Both types of seismicity were extensively studied in the mines of the Ostrava-Karvina Coal Basin, Czech Republic (Głowacka *et al.*, 1992; Holub, 1996b, 1997). The energy–frequency relation for seismic events at Doubrava coal mine from this district is shown, as an example, in Fig. 15, reproduced from Głowacka *et al.* (1992). The observed values are approximated by a bimodal and Gutenberg–Richter truncated distributions. The bimodal distribution fits the data rather well. It was found that the events with energy greater than 10^6 J were the result of stress accumulation in an area greater than that corresponding directly to mining excavations.

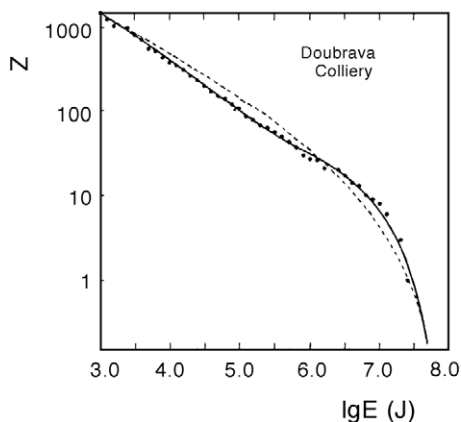


FIG. 15. Energy-frequency distribution of seismic events from a longwall at Doubrava coal mine, Czech Republic, approximated by a bimodal (continuous curve) and truncated Gutenberg-Richter (dashed curve) distribution models. [Głowacka *et al.* (1992), Fig. 1, reprinted from *Induced Seismicity*, 1992. 480 pp., EUR 126.50/US \$149.00/GBP89.00, A. A. Balkema, P.O. Box 1675, Rotterdam, Netherlands.]

Similarly, Sprende *et al.* (1991) believe that low-level seismicity in the immediate vicinity of the Lucky Friday mine in the Coeur d'Alene mining district, Idaho, is driven in the short term by mining rate. The district is situated within a minor zone of seismicity and in the longer term, cycles of tectonic stress build-up and release may be important.

3.1. Mining Operations and Seismicity

Seismic events of the first type are of low magnitude, and their number is generally a function of mining activity. The events usually occur within 100 m of the mining face or on some preexisting discontinuities and zones of weakness near the face. Intact rocks can be ruptured as well. The spatial distribution of seismic events of the first type is well illustrated in Figs. 12 and 16. Figure 16, reproduced from Hatherly *et al.* (1997), shows horizontal locations of 629 events recorded in 1994 at Gordonstone coal mine in Central Queensland, Australia. Several triaxial geophones were deployed there in three vertical boreholes and over a 6-week period more than 1200 events were recorded. The events were well located, with an accuracy of a few meters. The seismicity correlated with periods of longwall production and occurred mainly within the mining panel 250 m wide. The zone of activity extended from behind the face at the sides of the panel and up to 70 m ahead of the face in the middle. The zone extended to a height of about 120 m above the seam, and there was lesser activity to a depth of about 30 m into the floor. Hatherly and Luo (1999) proposed a model for longwall caving which involves

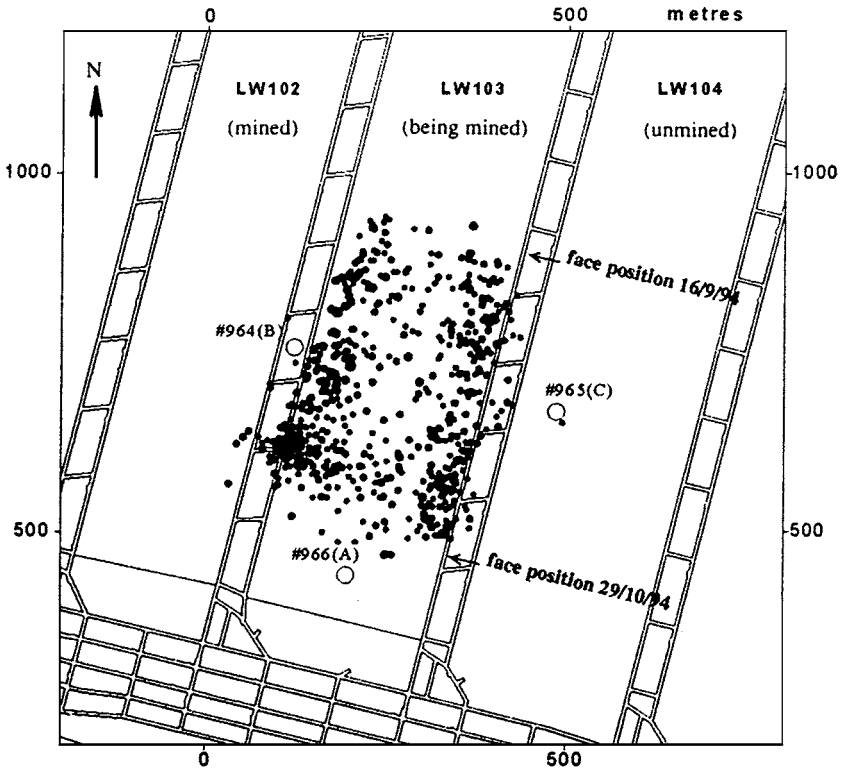


Fig. 16. Horizontal locations of 629 seismic events recorded in 1994 at Gordonstone coal mine in Central Queensland, Australia. The triaxial geophone arrays were located in holes numbered 964, 965 and 966. [Hatherly *et al.* (1997), Fig. 1, reprinted from *Rockbursts and Seismicity in Mines*, Proceedings of the 4th International Symposium, Krakow, Poland, 11–14 August 1997. 450 pp., EUR 137.50/US \$162.00/GBP97.00, A. A. Balkema, P.O. Box 1675, Rotterdam, Netherlands.]

two stages of failure. The first is the failure ahead of the longwall face and in the rock mass above and below the coal seam; seismicity with dominant shear failure is observed. When the longwall face mines through the damaged rock mass, the second stage commences. The seismic events can originate behind the face; tensile failure is postulated.

Senfaute *et al.* (1997) performed a detailed study of the space distribution of seismic events at a longwall working face at the Provence coal mine, France. The longwall was 720 m long and 200 m wide, and during its extraction over 2200 seismic events were recorded. Their distribution depends on the configuration of mining works (see Fig. 17). When the working face ran along the old mined out areas, the events were more numerous ahead of the face (Fig. 17a). But when the working face ran along a pillar, the events were more numerous behind the face (Fig. 17b).

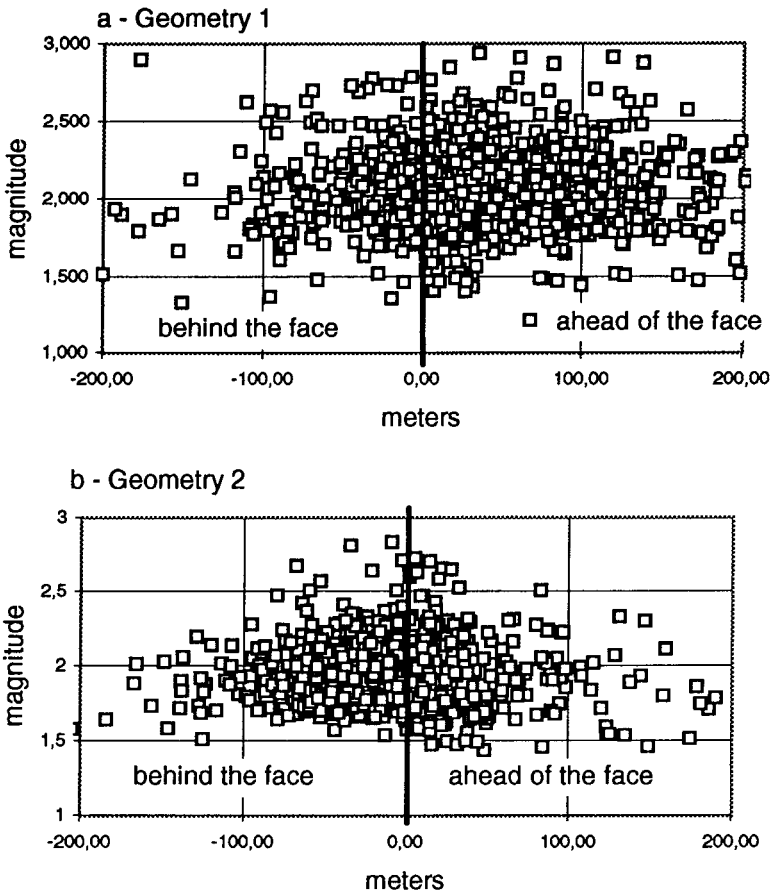


FIG. 17. Locations of seismic events with respect to a longwall working face at the Provence coal mine, France, (a) for the working face running along the old mined out areas, and (b) for the face running along a pillar. [Senfaute *et al.* (1997), Fig. 4; reprinted with kind permission from Birkhäuser Verlag AG.]

Seismic monitoring of a test tunnel, at a depth of 420 m in the Underground Research Laboratory, provided interesting results (Talebi and Young, 1992; Martin and Young, 1993). During excavation of the tunnel, spalling in the roof and floor resulted in typical well-bore breakout geometry. The location of seismic events associated with the excavation generally fell within one radius of the tunnel wall and appeared as random events. Within the well-bore breakout geometry, however, the seismic events were clustered implying crack damage and coalescence. Laboratory experiments suggest that a small amount of crack damage can reduce intact rock strength by 50% or more.

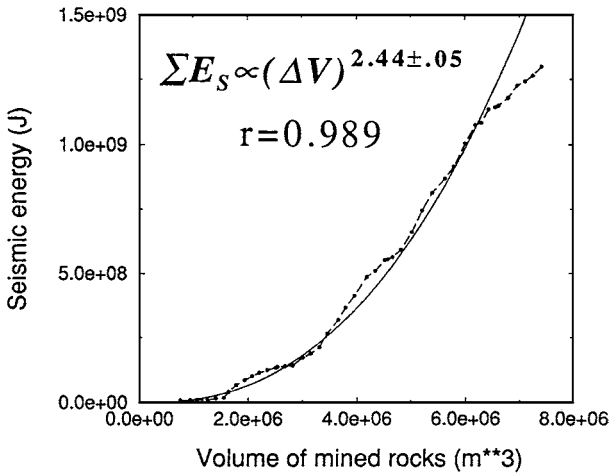


FIG. 18. Cumulative seismic energy release versus volume of coal mined from mine B in the Wasatch Plateau and Book Cliffs mining district, Utah, in monthly intervals from July 1992 to March 1996. Smooth curve is a power-law fit to the data. [Arabasz *et al.* (1997), Fig. 6, reprinted from *Rockbursts and Seismicity in Mines*, Proceedings of the 4th International Symposium, Krakow, Poland, 11–14 August 1997, 450 pp., EUR 137.50/US \$162.00/GBP97.00, A. A. Balkema, P.O. Box 1675, Rotterdam, Netherlands.]

The correlation between seismic activity and extracted deposit volume has long been known from observations. Such dependence is well illustrated in Fig. 18, reproduced from Arabasz *et al.* (1997), where cumulative seismic energy is shown as a function of the volume of coal mined from mine B in the Wasatch Plateau and Book Cliffs mining districts of east-central Utah. The sum of released seismic energy follows a power law with respect to the volume of mined rocks, and a power-law exponent of 2 to 3 provides the relation that fits the data quite well. Kremenetskaya and Tryapitsin (1995) obtained results to some extent similar for the cumulative seismic energy release and the amount of extracted ore in the mines of the Khibiny Massif, Kola Peninsula, Russia, between 1948 and 1991.

Stope convergence measurements are often used to study seismic processes in mines. Boler and Swanson (1992) investigated stope convergence behavior at Galena mine, Idaho. The mine experienced seismicity during extraction of near-vertical silver veins to a depth of 2 km. Three gauges for monitoring the convergence of a burst-prone stope were installed in June 1990 and monitored for several months. The stope was also monitored by an array of accelerometers, and seismic events with magnitude -5 and above were recorded with an automatic monitoring system. Coseismic convergence steps were observed for seismic events of magnitude -2 and greater. Figure 19 shows the cumulative convergence versus the cumulative number of seismic events for the study period. The tracking of event

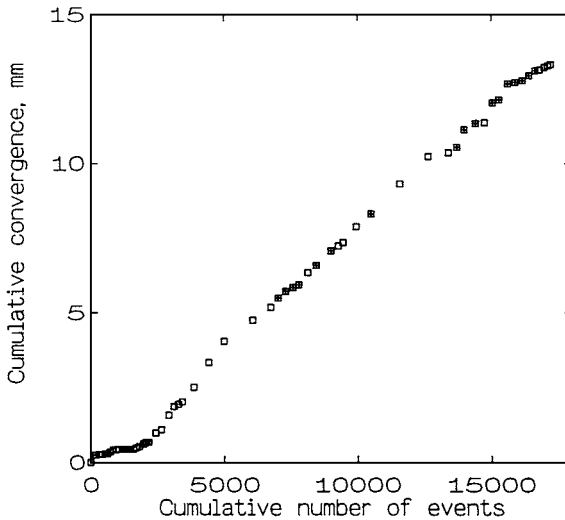


FIG. 19. Cumulative convergence versus cumulative number of seismic events recorded in 1990 at Galena mine in the Coeur d'Alene district, Idaho. [Boler and Swanson (1992), Fig. 5, reprinted with kind permission from Birkhäuser Verlag AG.]

occurrence and stope convergence is remarkably steady, with some 1200 events recorded per millimeter of closure.

Malan and Spottiswoode (1997) found that time-dependent deformations around deep-level mines occur at rates well in excess of those expected from creep of a solid rock mass. They modeled the time-dependency by extension and mobilization of the fracture zone, using a boundary element technique. Viscoplastic behavior of existing cracks and the resulting formation of new fractures adequately described the rate of stope closure and seismicity over a time scale of hours. They introduced time-dependent weakening of the rock mass into the model, which provided a better fit to the observed stope closure during the weekly cycle of mining.

Detailed studies have shown an association between zones of high P -wave velocity and the hypocentral location of seismic events induced by mining (e.g., Maxwell and Young, 1993b). The mechanism of the association, however, is not well understood. Maxwell and Young (1995) investigated the relationship between stress, velocity, and induced seismicity around a tunnel in the Underground Research Laboratory. The rock mass around the tunnel was unfractured and essentially homogeneous. An image of the velocity structure around the tunnel indicated a distinct zone of high velocity corresponding to a zone of increased elastic stresses, where a breakout notch formed. An area of decreased velocity, perpendicular to this zone, was found to be associated with a region of tensile elastic stress. The stress changes are believed to have preferentially opened and closed preexisting

microfractures in the rock, decreasing and increasing the P -wave velocity. The seismicity induced by the excavation in the notch region was found to be located in the transition between the high-velocity/high-stress, intact rock and the low-velocity/destressed, fractured rock (Maxwell and Young, 1995, 1998). Scott *et al.* (1997) have reported similar results from investigation of a rockburst site at the Sunshine mine, Kellogg, Idaho. Seismic activity there appeared to be associated with areas where a velocity gradient was apparent, as documented by seismic tomography.

Mining operations are occasionally associated with exceptionally large seismic events as well. Irregular mine geometry, especially when "Chamber and Pillar" method is used, could lead to large magnitude events. The 1989 Volkershausen rockburst in the potash mining district along the river Werra, Germany, with magnitude 5.4 (Knoll, 1990) is a spectacular example of such an effect. The event caused the collapse of some 3200 pillars at a depth of 850–900 m within an area of about 3×3 km. Similarly, the 1995 Solvay Trona mine, Wyoming, event of magnitude 5.1 entailed the extensive collapse of pillars at a depth of 490 m over an area of about 2×1 km (Pechmann *et al.*, 1995). Waveform modeling of seismic records indicated a considerable implosive component in the seismic source, which is consistent with observations of surface subsidence.

An interesting example of direct correlation between mining and seismicity comes from a copper mine in Poland (Wiejacz, 1993). In July 1992 a miner's strike was declared for the whole Lubin Mining District, which lasted 32 days. At the Polkowice mine the labor stoppage resulted in a threefold drop in the number of observed seismic events with energy greater than 10^2 J. After the mining was resumed, the number of seismic events reached its prestrike level within some 30 days. Later on, the number of events was a little larger than before the stoppage, possibly because of greater mining activity at that time. A similar decrease of seismicity was also observed by the GERESS (German Seismic System) array in Germany, at a distance of about 320 km (Jost and Jost, 1994). During the strike, the number of GERESS automatic locations of seismic events from the Lubin area was reduced by 57%, and the number of events in the NEIC bulletin decreased by 64%.

3.2. Geological Structures and Seismicity

Although lithostatic stresses and their redistribution around mine excavations are the dominant driving forces in the generation of most seismic events in mines, tectonic stresses also play a significant role. This is especially true in the case of the largest mine tremors, with magnitude close to 4 and above. Wong (1993) has reviewed the available focal mechanisms of large events from various mining districts to evaluate the effects of tectonic stresses. He found that, in general, seismic events in mines occur in regions subjected to horizontal compressive

tectonic stresses. The larger events are often the result of reverse and sometimes strike-slip faulting. This mode of deformation probably reflects the increase in shear stress along preexisting zones of weakness. Alternatively, tectonic stresses could act as a trigger of seismic events where the main sources of strain energy are the redistributed lithostatic stresses.

The seismicity induced in deep gold mines in South Africa may be an exception. The seismicity there is mainly characterized by normal faulting, believed to be caused by stope closure, and tectonic stresses there do not appear to be significant. Dennison and van Aswegen (1993) modeled stresses on the Tanton fault at President Steyn gold mine, taking into account its geometrical and frictional properties. They also monitored fault dynamic behavior during extensive mining of a tabular ore-body at a depth of 2400 m and found that tectonic stresses were not needed to explain the fault behavior, and *in situ* stress measurements showed that these stresses were not important. Gay (1993) evaluated the relationship between rockbursts and seismicity associated with the two main mining methods used in deep South African mines, namely scattered and longwall mining. He found that the frequency of rockbursts increases when mining takes place close to geological structures. The nature of the damage, however, is such that using better support systems could readily prevent it.

In the Coeur d'Alene mining district, Idaho, compressive tectonic stresses are important. Whyatt *et al.* (1993) described an unusual concentration of rockburst activity during development of the 5300 level of the Lucky Friday mine in 1990, strongly correlated with *in situ* stress and geological anomalies. The localized nature of the measured stress field has been established by comparing overcore stress measurements, raise bore breakouts, and geological indications of stress orientations collected from the whole Lucky Friday mine and the adjacent Star mine. The mining-induced stress at the crosscut stub was estimated with a homogeneous elastic model to be only 5% of the natural stress field. Swanson (1992) examined the relationship between local geology, vein/stope layout, and the location of large seismic events and rockbursts at Galena mine. He found two structures associated with large events and rockbursts: the largest vein in the mine and a near-vertical plane striking throughout the length of the mine that is subparallel to the major faults there. He used models of stress interaction to show that mining-induced deformation was mobilized along a 1.5-km length of this plane during the occurrence of a series of large seismic events in 1990.

Creighton mine is the deepest and most seismically active mine operating in the Sudbury Basin, Ontario (Morrison *et al.*, 1993). Mining extends to a depth of 2400 m and seismicity is monitored below the 1800 m level. Morrison *et al.* (1993) have studied spatial distributions of seismic energy release in this mine, using a 2D numerical model involving a single frictional surface and a changing mining geometry. Their results imply that chaotic behavior is an intrinsic part of this simple representation of mining. The rock environment is naturally complex

but often appears to display unusual sensitivity to minor changes that point to self-organized criticality. Steacy *et al.* (1997) used a 3D self-organized critical model to simulate seismicity in Creighton mine. Almost 400 faults were included in the model, each represented by an individual 2D cellular automata. The model was loaded from point sources that simulated blasting, and was parameterized by loading it with an actual blast sequence and comparing the predicted and observed seismicity. The model successfully predicted the global statistics of seismicity observed in the mine, and the number and timing of large events as well.

Statistical analysis of spatial distribution of seismic events induced by mining in the Ostrava-Karvina Coal Basin, Czech Republic, shows that geological structures there act as concentrators of stresses generated by mining operations in their vicinity (Kaláb and Müller, 1996).

Recently, the most extensive studies on relationships between geological features and seismicity in mines have been carried out in the Upper Silesian Coal Basin, Poland (e.g., Idziak, 1996b; Idziak and Teper, 1996a; Teper, 1996; Zuberek *et al.*, 1996; Idziak *et al.*, 1997; Mutke and Stec, 1997; Wiejacz and Ługowski, 1997; Lasocki and Idziak, 1998). Figure 20, reproduced from Zuberek *et al.* (1996), shows the spatial distribution of seismic events induced by mining in the Basin on the complex tectonic background of the area. The seismic events concentrate in specific regions corresponding to different geological units. The studies indicate that tectonics plays a significant role in the generation of at least some of the largest events in the area. Some parts of the Upper Silesian Coal Basin (e.g., the zones of large latitudinal faults) are connected with large discontinuities in the deep crustal basement with active shear stresses. The spatial distribution of larger seismic events is not uniform on a mine scale either. Figure 21, reproduced from Mutke and Stec (1997), shows, as an example, the distribution of events with magnitude greater than 1.2 at Kleofas coal mine, observed from 1990 to 1995.

Nonuniform distribution of seismic events suggests the fractal character of seismicity in the Basin (Idziak and Zuberek, 1995; Idziak, 1996b), where the fault patterns also display their fractal nature (Teper and Idziak, 1995; Idziak and Teper, 1996a). The temporal variations of event coordinates indicate some kind of strange attractors, and imply involvement of dynamic processes on a regional scale in the generation of seismicity. Furthermore, migration of seismicity between its major clusters (see Fig. 1) cannot be explained on the ground of changes in mining works (Idziak, 1996b). The dominant directions of epicenter distribution within the clusters also support recent hypotheses addressing the internal structure and low tectonic instability of the deep crustal basement in Upper Silesia (Lasocki and Idziak, 1998).

Idziak *et al.* (1997) have investigated the focal mechanism of almost 400 seismic events, which occurred in the vicinity of the Klodnicki fault—the main regional dislocation in the central area of the Upper Silesian Coal Basin. For selected groups of events with similar orientations of nodal planes, local stress tensors were also

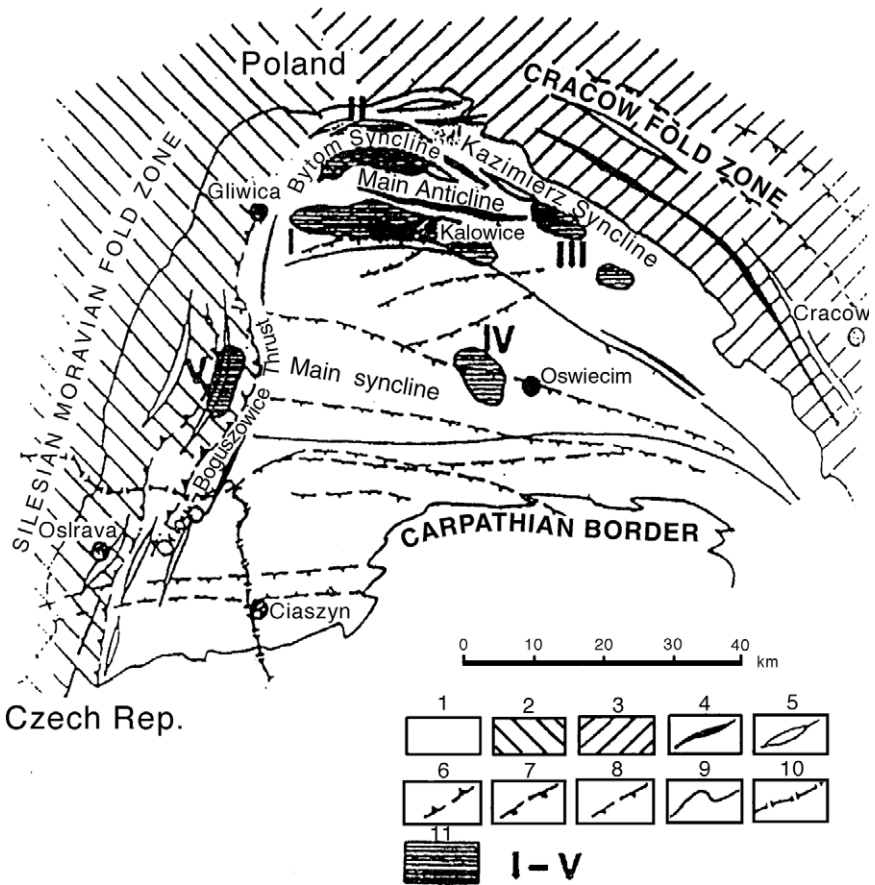


FIG. 20. Spatial distribution of seismic activity, marked by shaded zones, induced by mining in the Upper Silesian Coal Basin, Poland, displayed on the complex tectonic background of the region. [Reprinted from Zuberek *et al.* (1996), Fig. 1.]

determined. A relationship between the spatial distribution of slip vector and the pattern of neotectonic deformations of the Carboniferous rock mass was found. Wiejacz and Ługowski (1997) made another study of the effects of geological structures on the mechanism of seismic events at Wujek coal mine. Figure 22, reproduced from their work, shows focal mechanisms of events located near the Arkona fault—one of the principal faults in the mine. They found that such a fault, even if tectonically passive, could play an important role in the generation of seismicity in the mine. In the vicinity of faults the directions of excavations and longwall fronts seem to play a secondary role.



FIG. 21. Distribution of seismic events with magnitude greater than 1.2 recorded between 1990 and 1995 at Kleofas coal mine, Poland. Dashed lines mark tectonic faults. [Mutke and Stec (1997), Fig. 3, reprinted from *Rockbursts and Seismicity in Mines*, Proceedings of the 4th International Symposium, Krakow, Poland, 11–14 August 1997. 450 pp., EUR 137.50/US \$162.00/GBP97.00, A. A. Balkema, P.O. Box 1675, Rotterdam, Netherlands.]

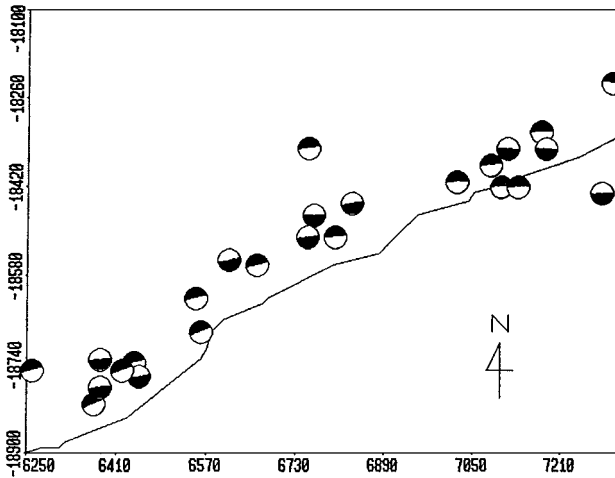


FIG. 22. Distribution of double-couple focal mechanisms of seismic events located near the Arkona fault (continuous line) at Wujek coal mine, Poland. [Wiejacz and Lugowski (1997), Fig. 4, reprinted from *Rockbursts and Seismicity in Mines*, Proceedings of the 4th International Symposium, Krakow, Poland, 11–14 August 1997. 450 pp., EUR 137.50/US \$162.00/GBP97.00, A. A. Balkema, P.O. Box 1675, Rotterdam, Netherlands.]

4. SOURCE PARAMETERS AND SCALING RELATIONS

Determination of source parameters of seismic events in mines is based mostly on spectral analysis of P and S waves. The other approach, waveform modeling in the time domain, involves rather complex techniques and is not suitable for routine applications to large sets of data usually generated by seismic monitoring in mines. The approach to determine source parameters in the time domain from the source time function appears as a possibility for investigation of seismicity in mines; it is briefly described in Chapter 6.

Spectral analysis has become a standard technique used in studies of seismic events induced by mining. Early attempts have shown that simple source models in the form of a circular dislocation (Brune, 1970, 1971; Madariaga, 1976) can be successfully used for the interpretation of seismic spectra and for the determination of source parameters of seismic events in mines. Spectral analysis usually employs the fast Fourier transform algorithm, which is computationally efficient and produces reasonable results, provided that the effect of the windowing of time series is properly taken into account. The windowing problem manifests itself as "energy leakage" into the sidelobes, obscuring other spectral features and distorting source parameters. This effect is usually suppressed by application of various tapers. The use of adaptive multitapers instead of a single taper (e.g., Hamming window) provides more stable and better results (Mendecki and Niewiadomski, 1997).

4.1. Source Parameters

Seismic moment, corner frequency, and seismic energy flux are traditionally inverted from the spectra, corrected for the instrumental, distance, and attenuation effects of each waveform, and then averaged. Occasionally, the quality factor Q is considered as an independent parameter during the inversion to improve the match between the observed and theoretical spectra (e.g., Spottiswoode, 1993; Mendecki, 1993). Mendecki and Niewiadomski (1997) proposed stacking the spectra of P , SH or SV waves over all the stations involved and determining the source parameters from the stacked spectra. This approach tends to average out incoherent site effects, source directivity, and random fluctuations of the high-frequency part of the spectrum. When Q is not known, the best average Q may be determined for all stations during the stacking procedure.

From the corner frequency, the source radius can be estimated either from the Brune (1970, 1971) source model or from the Madariaga (1976) model. Both models are used in studies of seismic events in mines. In general, Brune's model tends to overestimate the source size in comparison to the size of underground damage caused by rockbursts (see Gibowicz and Kijko, 1994). The source radii derived

from the Madariaga model, on the other hand, better fit documented evidence of underground damage (e.g., Trifu *et al.*, 1995).

Imanishi and Takeo (1998) recently proposed a new method to estimate the source dimensions of small earthquakes based on stopping phases which are radiated at the termination of rupture propagation, without assuming a rupture velocity. They detected on accelerograms two high-frequency stopping phases, being the Hilbert transforms of each other for several small earthquakes at two local stations. Assuming a circular source, it was possible to determine relative locations of nearest and farthest edges of the circular fault using the difference of arrival times between these two stopping phases. It could be expected that the application of this method to seismic events in mines would provide better estimates of their source dimensions that would be independent of a rupture velocity.

Stress release estimates, the average stress drop and apparent stress, are readily calculated from seismic moment, radiated energy, and source radius. A multitude of other parameters has been also proposed to describe the behavior of seismic sources in mines (Mendecki, 1993; Mendecki, 1997b,c; van Aswegen *et al.*, 1997); they all result from a combination of basically two independent parameters describing the seismic spectrum.

An automatic procedure for determining source parameters from spectra is needed for daily processing of large numbers of seismic events observed in mines. Many seismic networks record hundreds of events a day. A highly efficient algorithm for calculating source parameters is based on ground velocity and displacement power spectra, proposed by Andrews (1986), and is used by the ISS monitoring system (Mendecki and Niewiadomski, 1997).

Source parameters have been estimated for thousands of seismic events, in the moment magnitude range from -3.6 to over 5 , in various mining districts all over the world. Figure 23, reproduced from Kaiser and Maloney (1997a), shows the range of seismic moment and seismic energy of seismic events most often studied. The relations between S - and P -wave corner frequencies are of practical interest, since they both are used to estimate source dimensions. In general, the corner frequencies of P waves are expected to be greater than those of S waves. Abercrombie and Leary (1993), who analyzed borehole records of small earthquakes in the 2- to 250-Hz frequency range, reported that the P -wave corner frequencies are approximately equal to those of S waves, but the scatter in their data is considerable. Gibowicz (1995) studied the corner frequencies of P and S waves generated by some 650 seismic events in various mines. He found that the relation between these corner frequencies is linear on a logarithmic scale for frequencies from 5 to 4010 Hz for P waves and from 4 to 3250 Hz for S waves. The relation is shown in Fig. 24, reproduced from Gibowicz (1995). The corner frequency of P waves is higher as a rule than that of S waves by about 25%.

Source parameters have been used for various practical purposes, such as assessment of rockburst hazard and damage potential, design of support in rockburst-prone areas, and rockburst prediction.

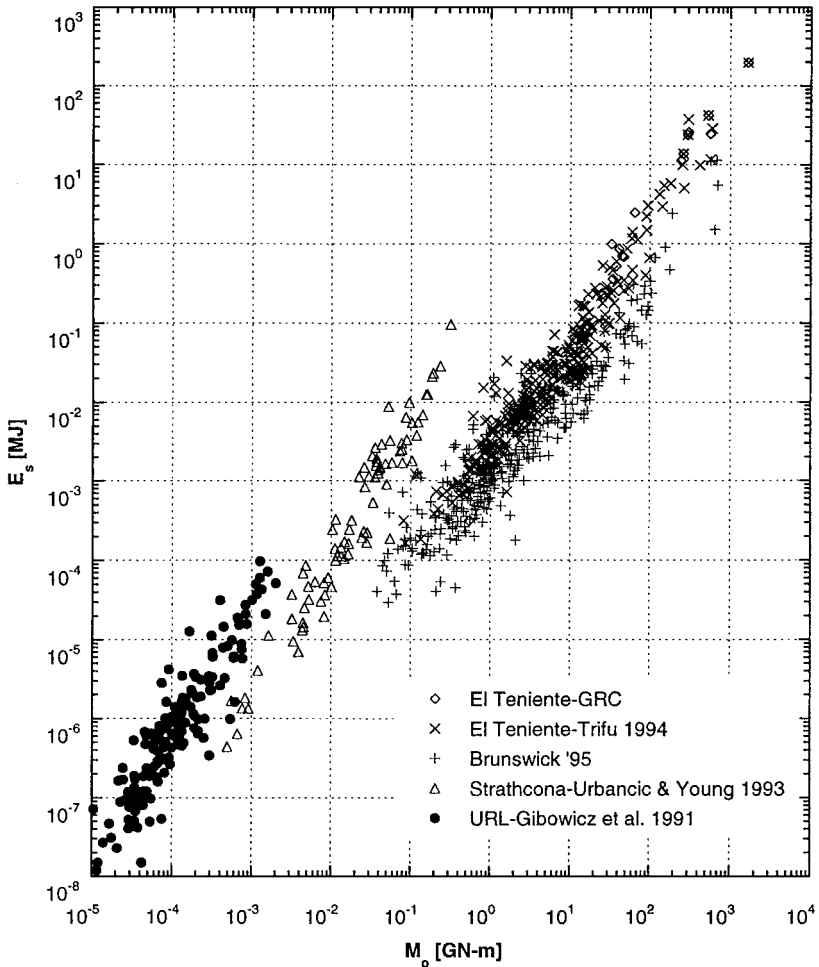


FIG. 23. Radiated seismic energy E_s versus seismic moment M_o for induced seismic events in various mining districts. [Kaiser and Maloney (1997a), Fig. 3, reprinted with kind permission from Birkhäuser Verlag AG.]

Urbancic and Young (1993) investigated space-time variations in source parameters of microseismic events, with moment magnitude less than 0, at Strathcona mine, Sudbury, Canada. The microseismicity was directly associated with excavation of ore at a depth of 710 m. Source parameters were calculated for 85 events located within the immediate excavation volume. Two-thirds of these events was characterized by low values of S over P wave energy ratio and low apparent stress, implying the existence of a non-shear component of failure. Spatially, the source parameters allowed definition of a pattern of systematic fracture behavior in the

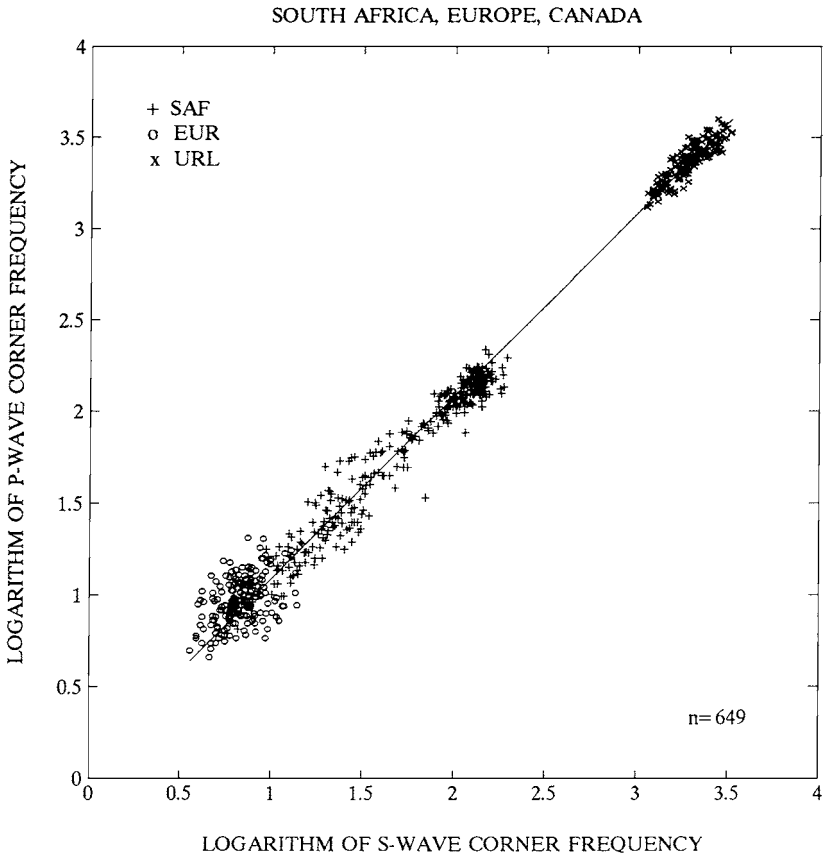


FIG. 24. *P*-wave corner frequency versus *S*-wave corner frequency for seismic events from South African (SAF) gold mines, European (EUR) coal mines, and the Underground Research Laboratory (URL) in Canada. The slope of the straight line is equal to one. [Gibowicz (1995), Fig. 3, reprinted with kind permission from Birkhäuser Verlag AG.]

rock mass, comparing favorably with mapped structure associated with ground problems. Temporally, the events were observed to locate either in close proximity to the excavation at depth or at shallower depths away from the excavation during the preexcavation and postexcavation periods. The source parameter levels generally increased from the preexcavation to the postexcavation periods, indicating that stress levels were increasing as a result of the excavation geometry and procedure. This was considered to be significant as rockbursts occurred above the area 6 months after the excavation.

Trifu *et al.* (1995) used source parameters for an evaluation of homogeneous and inhomogeneous faulting models to assess damage potential at Strathcona mine.

The analysis included an investigation of peak ground velocity and acceleration scaling relations with magnitude for near-source data. For the inhomogeneous source model, estimates of asperity radius were obtained. To validate the use of this source model for seismic hazard assessment, a comparison of its predicted ground motion level with underground geomechanical measurements was carried out. For distances close to the source, corresponding to relatively higher damage levels, a good agreement between these two kinds of measurements was found. Furthermore, a good agreement between the asperity radii and the size of the regions of the highest observed local damage provided additional support for use of the inhomogeneous source model in the assessment of seismic hazard in mines.

Alcott *et al.* (1998) discussed a methodology to assess potential rockburst hazards using seismic source parameters, which is designed to provide a simple means for including the most relevant source parameters into the daily ground control decision-making process. The ISS data and observed damage at a Brunswick mine, Canada, were used to calibrate and verify the proposed methodology. Seismic events were classified into four groups: those representing minor hazard, seismically triggered gravity-driven hazard, stress-adjustment-driven hazard, and deformation-driven hazard. Using the proposed technique, based on the variations of seismic energy, seismic moment, and apparent stress, it was possible to delineate areas of elevated rockburst hazard potential and to identify precursory and decay trends indicating progressive worsening and improving conditions in seismically active areas of the mine.

Glazer (1998) applied seismic source parameters to combat rockburst hazard in the Vaal Reefs gold mine, South Africa. He introduced the concept of apparent stress index to normalize apparent stress values for events within a wide range of seismic moment values. The index is calculated as the ratio of measured over mean values of apparent stress. Thus, values of the index above one indicate higher stress levels than the average, and values below one indicate stress levels lower than the average. It was found that large events are associated with areas of high gradients of the apparent stress index. Damage is often observed in areas characterized by high values of the index, even when a seismic event is located outside of these areas. Changes in the values of the index before large events are occasionally observed. Glazer (1998) believes that contour mapping of the apparent stress index could help to optimize the design of support.

Król (1998) investigated the focal mechanism and source parameters of 246 seismic events, which occurred in 1997 at Polkowice copper mine, Poland. He found a number of relationships between the average values of selected source parameters and the quantities describing geological structure, mining conditions, seismic activity, and rockburst hazard in the mine.

The dynamic loads imposed by rockbursts are directly related to the resultant ground motions. Thus, the first step in design of systems for the support of openings

affected by such loading is to assess the ground motion characteristics. Kaiser and Maloney (1997a,b) presented scaling laws, supported by theoretical considerations and based on world-wide data, for the design of support in rockburst-prone areas. The design scaling laws relate seismic source intensity (event magnitude, radiated energy, or a combination of seismic moment and stress drop) to the peak ground motion parameters in the design area, some distance from the source. These scaling laws reflect the most relevant critical conditions for engineering design.

Cichowicz (1991) investigated the time variation of source parameters of microseismic events before and after large seismic events in a deep gold mine in South Africa. The small-scale stope fracturing in the close vicinity of a dyke was studied. The magnitude of microseismic events ranged from -3 to -1 . An automatic monitoring system was used, consisting of triaxial accelerometers installed in a borehole 150 m ahead of the advancing face. Seismic moment, radiated energy, corner frequency, dynamic stress drop, Q -coda of S waves, and the degree of polarization of P waves were estimated. The first four parameters describe the seismic source and the last two parameters characterize the rock mass. It was found that the degree of polarization of P waves decreased between 0.5 and 2 days before each larger event with magnitude greater than 0.5. Series of foreshocks typically had higher stress drops than the average corresponding microevents, and they were associated with gradual stress concentration within the dyke, which formed an asperity of greater strength than the surrounding rock mass.

4.2. Scaling Relations

A source scaling relation describes the manner in which the source duration or the source dimension increases with increasing seismic moment. In studies of large earthquakes it has been found that stress drop is roughly independent of the seismic moment, which means that seismic moment is proportional to the third power of the rupture length. The constant stress drop model implies a self-similar rupture process regardless of the scale of the seismic events.

This scaling relation has been confirmed by innumerable studies and has become an accepted model for large and moderate earthquakes. The constant stress drop pattern has also been reported for small volcanic events and for volcanic explosion earthquakes (Nishimura and Hamaguchi, 1993). The source parameters of small earthquakes recorded at 2.5-km depth in southern California are compatible with earthquake scaling at constant stress drop down to magnitude -2 (Abercrombie and Leary, 1993). The constancy of stress drop was found long ago for some seismic events in gold mines in South Africa and in coal mines in Poland (for a review, see Gibowicz and Kijko, 1994). In contrast to these results, several studies of small earthquakes have been interpreted as evidence of a breakdown in the similarity between large and small earthquakes (e.g., Glassmoyer and Borchardt,

1990). The breakdown in scaling relations for small seismic events induced by mining has been also reported.

Feignier (1991) investigated the influence of geological structure on the scaling relations for seismic events with local magnitudes ranging from 1.0 to 4.2 from the Lacq gas field in southwestern France. He demonstrated that many factors influence source parameters and scaling relations, but the overall result for the whole data set implies a self-similar behavior. This indicates that the tectonic stress field and the depth of events are the main factors affecting the scaling relations. A detailed analysis of the seismic response of different geological layers, however, has shown that stress drop depends on the strength of the layer. In contrast to large and moderate earthquakes, this feature could be observed on small events because of their limited spatial extension; and this is the second-order factor influencing scaling relations. Furthermore, Feignier (1991) also found that self-similarity is not always verified in each geological layer. Areas with a high degree of fracturing induce low stress drops whereas a more intact area leads to higher stress drop events; and this could be a third-order factor affecting scaling relations.

Gibowicz *et al.* (1991) studied source parameters and scaling relations of seismic events at the Underground Research Laboratory in the magnitude range from -3.6 to -1.9 . They found that the scaling relation between seismic moment and source radius indicated a decrease in stress drop with decreasing seismic moment. Characteristic tremors with a fault length of about 1 m seem to be generated in the area, enforced by the excavation geometry and local microtectonics.

Urbancic *et al.* (1992a) examined excavation induced microseismic events, with moment magnitudes less than 0, at the Underground Research Laboratory and at Strathcona mine in an attempt to determine the role of geology, excavation geometry, and stress on scaling relations between seismic moment and source radius. They observed that the interaction of stresses with preexisting fractures, fracture complexity, and depth of events are the main factors influencing source parameters and scaling relations of very small events. Self-similar relations were found for events at similar depths or for weakly structured rock mass with reduced clamping stresses. Nonsimilar behavior, on the other hand, was found for events with increasing depth or for heavily fractured areas under stress confinement. Overall, depth and fracture complexities appear to favor nonsimilar generation processes of seismic events in mines.

Urbancic *et al.* (1993b) presented the results of their analysis of 68 microseismic events, with moment magnitude from -2.4 to -1.1 , associated with the excavation of ore in a highly stressed rock mass at about 620 m depth at Strathcona mine. A dependence of static and dynamic stress drops on seismic moment was found. The observed scaling dependence does not appear to be related to the source inhomogeneity, but is thought to be related to scale length effects. In contrast, Talebi *et al.* (1994) concluded that the scaling relation between seismic moment and source radius for events at Creighton mine strongly indicates a self-similar

behavior of their sources. They analyzed some 150 events in the magnitude range from 0.4 to 2.6.

Urbancic and Trifu (1996) expanded their investigation into scaling behavior by examining the role of source complexity, rupture velocity, and deviatoric stresses. They analyzed microseismic events, with moment magnitude ranging from -2.4 to -0.3 , which occurred within both highly and moderately stressed and fractured rock masses at Strathcona mine. Their results indicate a relatively strong dependence between stress release, over two orders of magnitude, and seismic moment, over three orders of magnitude.

McGarr (1994) attempted to explain the apparent dependence of stress release parameters on seismic moment in his comparison between mining-induced and laboratory seismic events. He considered apparent stress as a function of seismic moment and found that over a huge range of seismic moment the apparent stress falls in the range from about 0.01 to 10 MPa. Thus, the apparent stress globally shows no systematic dependence on seismic moment, supporting the idea that earthquakes generally are constant stress drop phenomena. For the individual sets of events, however, induced by either mining or laboratory, the apparent stress exhibits strong and systematic dependence on seismic moment. This strong dependence is understandable for the laboratory events because the fault area in this case is fixed. For each set of induced events, the fault area also appears to be approximately fixed but the slip is inhomogeneous, presumably as a result of barriers distributed over the fault plane. Thus, for individual sequences the principal difference between large and small events involves average slip and not source dimension (McGarr, 1994). The trade-off between stress drop and rupture velocity inherent in all kinematic source models, on the other hand, implies that the dependence on seismic moment can be attributed just as well to systematic variations of rupture velocity (Deichmann, 1997).

Gibowicz (1995) reached some conclusions similar to those of McGarr (1994) in his study of scaling relations for 1575 seismic events induced in South African, Canadian, Polish, and German underground mines, with moment magnitude ranging from -3.6 to 4.1 (seismic moment from $5 * 10^3$ to $2 * 10^{15}$ N · m). The constant stress drop scaling means that seismic moment is inversely proportional to the third power of corner frequency. Such behavior was confirmed for most of the considered data. The only evidence for a breakdown in the similarity between large and small events seems to be apparent for the smallest seismic events with moment magnitude below -2.5 . Figure 25, reproduced from Gibowicz (1995), shows the distribution of seismic moment versus *S*-wave corner frequency for all the investigated events. It should be noted that the average values of seismic moment that referred to the same range of corner frequency are vastly different in various mining areas. For the same corner frequency, the seismic moment of the events from hard-rock gold mines in South Africa is higher than that of the events from Polish coal mines, on the average by a factor of about 150. Even at a single mine, such as Strathcona mine, the differences in seismic moment between various data sets

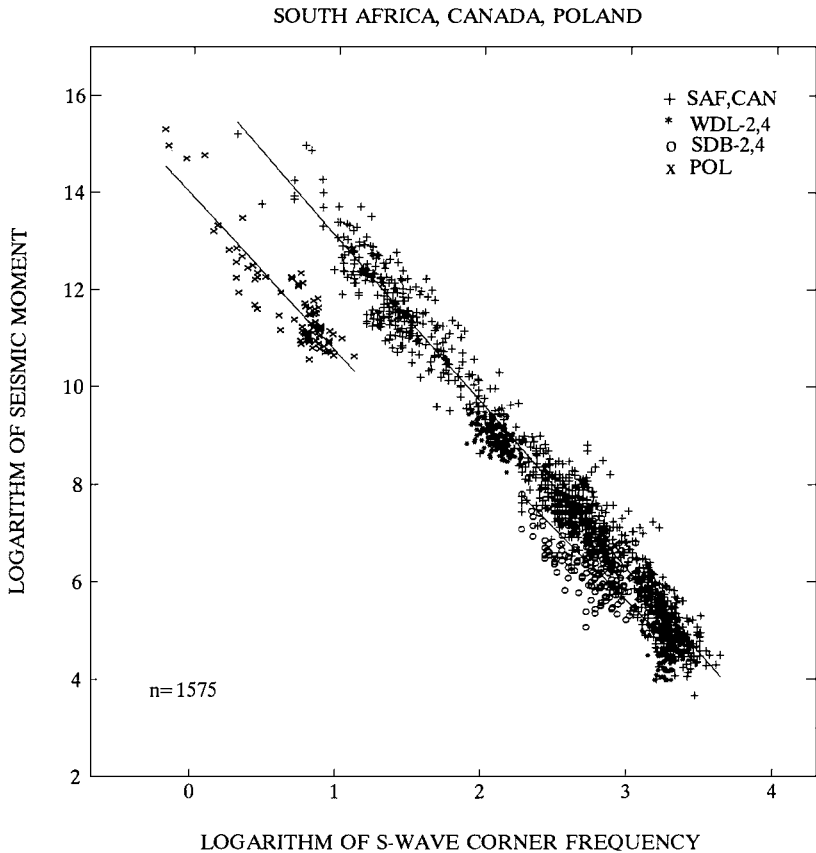


FIG. 25. Seismic moment versus *S*-wave corner frequency for 1575 seismic events from South African (SAF, WDL), Canadian (CAN, SDB), and Polish (POL) mines. [Gibowicz (1995), Fig. 12, reprinted with kind permission from Birkhäuser Verlag AG.]

are characterized by a factor as high as 7. Similar conclusions were drawn in an additional study of scaling relations for seismic events induced at Polish copper mines (Gibowicz, 1997b). A comparison of source parameters of seismic events at Polish coal and copper mines was also made by Domański (1997).

5. SOURCE MECHANISM

The most important progress made in source mechanism studies of seismic events induced by mining during the last decade is the seismic moment tensor inversion technique, used on a massive scale. Results from earthquake mechanism

studies indicate growing evidence that alternative mechanisms other than shear failure are possible (e.g., Dziewonski *et al.*, 1997). The most prominent cases of what appear to be anomalous focal mechanisms are reported from seismicity studies in mines. The moment tensor inversion technique has been used in numerous studies of seismic events in deep mines in South Africa, Poland, Canada, and Japan. A brief overview of the obtained results follows.

5.1. Seismic Moment Tensor

In general, seismic moment tensor is used to describe the source mechanism of an earthquake under the assumption that the point-source approximation is valid. This approximation is valid for the long period displacement—the fault-plane dimensions are assumed to be shorter than the wavelength of the seismic waves used in the analysis. To the first order, moment tensors describe completely the equivalent forces of general seismic point sources. The conservation of angular momentum for the equivalent forces leads to the symmetry of the moment tensor. The eigenvalues of a symmetric second-order tensor are all real and its eigenvectors are mutually orthogonal. For low frequencies the moment tensor can be treated as having the same source time function for all its components. Given a set of amplitudes at a given time, the moment tensor can be obtained by inversion of the linear system of equations containing the six components of the moment tensor, the observed amplitudes, and the transfer and excitation functions for seismic waves. A moment tensor then can be decomposed into isotropic and deviatoric parts. The isotropic part corresponds to a volume change in the source. The deviatoric part can be decomposed in turn into a Compensated Linear Vector Dipole (CLVD), corresponding to a uniaxial compression or tension, and a Double Couple (DC), describing shearing processes in the source. Such decomposition seems to be the most interesting one for source studies of seismic events induced by mining, although a multitude of different decompositions are possible (e.g., Gibowicz, 1993; Gibowicz and Kijko, 1994). During moment tensor inversions based on observations in close proximity to the source, the seismic radiation in the near field should be taken into account (Niewiadomski, 1997).

McGarr (1992b) made a detailed study of a seismic event recorded in early 1988 on the surface and at the underground GEOS stations in the Vaal Reefs gold mine in South Africa. The seismograms indicated seismic moment tensors having substantial implosive components. The moment tensor was decomposed into isotropic and deviatoric components from which both the coseismic volumetric closure and the total shear deformation could be estimated. He found that they are proportional to each other, consistent with earlier analyses of the tabular mine stope interaction with the surrounding rock mass. McGarr (1992c) in another study of 10 mine tremors recorded by GEOS surface and underground stations in the Western

Deep Levels and Vaal Reefs gold mines found that the moment tensors fall into two separate categories. Seven of the events involved substantial coseismic volumetric reduction together with normal faulting, and for the remaining three events the volumetric closure was not significantly different from zero. They were largely double-couple sources involving normal faulting.

Inversions of a standard second-order moment tensor are routinely performed by the ISS system (e.g., Mendecki, 1993), although the results are not readily available in the professional literature. Occasionally, when volumetric changes in the source area are significant, the different time dependencies of different moment tensor components need to be considered. Niewiadomski (1997) described a procedure for the time-dependent moment tensor inversion for P waves. The procedure allows evaluation of the source duration and provides insight into the source complexity by calculating the spatial distribution of pressure and tension axes in time. It seems that this procedure is available within the ISS system.

A relative moment tensor inversion method, based on the theory described by Dahm (1996), was used for the first time by Andersen (1999) to study seismic events induced by mining. The same technique was used by Jost *et al.* (1998) to study the source mechanism of injection-induced events at 9-km depth at the KTB deep drilling site in Germany. The relative inversion method can be applied to clusters of seismic events from a small source area, provided that the spacing between the events is smaller than the dominant wavelength of the waves used in the inversion. This approach is based on the concept of a common ray path between the cluster and a given receiver. Most relative methods require knowledge of the radiation pattern of at least one reference event, which is used to estimate the wave propagation for events from the same source area. Dahm (1996) extended this method by including the estimation of several sources without a reference event; the path effects described by Green's functions are eliminated analytically. Andersen (1999) applied the relative method to three clusters of seismic events recorded at a depth of about 1900 m at a site at Blyvooruitzicht Gold mine in South Africa. Her input data were the peak displacement amplitudes of the P , SH , and SV waves. A total of 58 events with magnitude from -1.4 to 0 were studied. The dominant source mechanism for most of the events was found to be of the shear type. The fault-plane solutions correlated well with the fracture mapping of the site. Some larger events, however, showed a significant deviation from the double-couple mechanism, thought to be caused by the opening of shear cracks. All events displayed a small positive isotropic component between 7 and 16% of the overall mechanism, representing volumetric expansion.

The application of moment tensor inversion to study the mode of failure of small seismic events induced by drilling a tunnel in the Underground Research Laboratory was reported by Feignier and Young (1992). They studied 33 microseismic events in the moment magnitude range from -4 to -2 . From the moment tensor inversion they obtained the ratio of isotropic to deviatoric components and found

a number of explosional and implosional sources. Furthermore, the location of events displaying extensional components corresponded to breakouts observed in the roof of the tunnel. In another study, Feignier and Young (1993) analyzed 37 microseismic events associated with the same tunnel excavation. Their hypocenters correlated with a zone of damage observed underground, which developed in the minimum principal stress direction. They found that as much as 75% of the mechanisms contained a significant negative isotropic component. These events were interpreted as closure of cracks that opened during earlier excavation stages.

Baker and Young (1997) applied a time-dependent moment tensor inversion to 20 seismic events recorded ahead of an advancing tunnel excavation at the Underground Research Laboratory. They found three characteristic types of seismic events there. The first group showed implosion/shear failure source mechanisms, associated with the observed collapse of excavation holes drilled at the side of the tunnel. The second group occurred in the region ahead of the face and showed tensile/shear failure mechanisms, interpreted in terms of crack initiation ahead of the face. The third group of events indicated predominant shear failure mechanisms throughout their rupture history, interpreted in terms of failure on preexisting crack surfaces. Šílený and Baker (1997) used data from the Underground Research Laboratory to test the performance of a method for fast estimation of focal mechanisms by inverting P and S wave amplitudes into moment tensors. The procedure provides an estimate of the confidence ellipses of the source mechanism, which show the errors in resolution of the individual moment tensor components and the errors in orientation of the deviatoric elements.

In Japan, the moment tensor inversion performed by Fujii and Sato (1990) on the observations from two small seismic events at Horonai coal mine has shown that they were non-double-couple events. The events were associated with longwall mining and were located in the vicinity of the longwall face. Fujii *et al.* (1997) proposed a new method for predicting rockbursts and seismicity in deep longwall coal mining. Fracturing intensity and its variation with respect to face advance were represented by the maximum shear seismic moment release rate, called by the authors the Seismic Moment Method. This method was successfully applied to three cases at Horonai and Miike coal mines, where mining works were carried out at depths from 900 to 1100 m and from 600 to 650 m, respectively.

The most extensive studies of the source mechanism of seismic events induced by mining, based on standard second-order moment tensor inversions, were undertaken in Poland, in both the coal and the copper mining districts. The procedure used is elaborated by Wiejacz (1991), based on the moment tensor inversion in the time domain, using as input data the first motion displacement amplitudes and signs of P waves and the amplitudes of SV waves recorded by the underground networks.

Wiejacz (1991, 1992) has studied the source mechanism of 60 small seismic events that occurred in 1990 and 1991 at Rudna copper mine in the Lubin mining

district. In general, the solutions that were well constrained by observations (good coverage of the focal sphere) had dominant shear components, although occasionally the isotropic component (showing both extension and contraction) could be as large as 25% of the overall mechanism. The CLVD component corresponded to uniaxial compression in all cases and was usually larger than the isotropic component. In another study of 77 events from Rudna and 38 events from Polkowice copper mines recorded in 1995, Wiejacz and Gibowicz (1997) confirmed that the moment tensor solutions are generally of double-couple type. The exceptions to this were 4 tensile events at Polkowice and 3 events at Polkowice and 1 event at Rudna with a pillar burst type component. These were the largest seismic events observed during the period of study. The mechanisms in a given area were seldom alike and they tended to form groups of a few similar events. This may be explained by the chamber and pillar mining technique used in Polish copper mines, which does not favor any specific direction in the absence of any important tectonic structures.

The most detailed study of the source mechanism of seismic events at Polkowice copper mine was carried out by Król (1998). He performed moment tensor inversion, based on observations from 25 seismic sensors, for 246 events with moment magnitude from 1.2 to 3.1, which occurred in 1997. To test the procedure adopted from Wiejacz (1991), Król (1998) additionally computed moment tensor of 20 calibration shots fired periodically in the mine. The solutions show in all cases significant isotropic explosive components in the range from 16 to 48% of the total mechanism and small double-couple components. Two types of seismic events are well known in the Polkowice mine: those radiating dilatational first arrivals only on all the sensors and those with both dilatational and compressional first arrivals. In consequence, the general moment tensor solutions of studied events show in some cases large non-double-couple components with a dominant CLVD component, although these solutions are often not stable. The deviatoric solutions are well constrained and are similar to double-couple solutions. These solutions in turn show a good correlation with geological and mining structures in the area. It is interesting to note that the double-couple component is the highest in the source mechanism of the events located ahead of the mining face and the lowest behind the working face. Similarly, the constrained double-couple solutions corresponding to reverse faulting are relevant to about half of the events situated ahead of mining, whereas they characterize over 80% of the events located behind the face.

The source mechanisms of 55 seismic events from Wujek and 83 events from Ziemowit coal mines in the Upper Silesian Coal Basin, Poland, were studied by Gibowicz and Wiejacz (1994). The events occurred in 1993 and had moment magnitudes from 1.1 to 2.4. The general, deviatoric, and double-couple moment tensor solutions for 20 events from Wujek mine are shown, as an example, in Fig. 26. In most cases the double-couple component was dominant, forming above 60% of the general solution. The double-couple component in the deviatoric

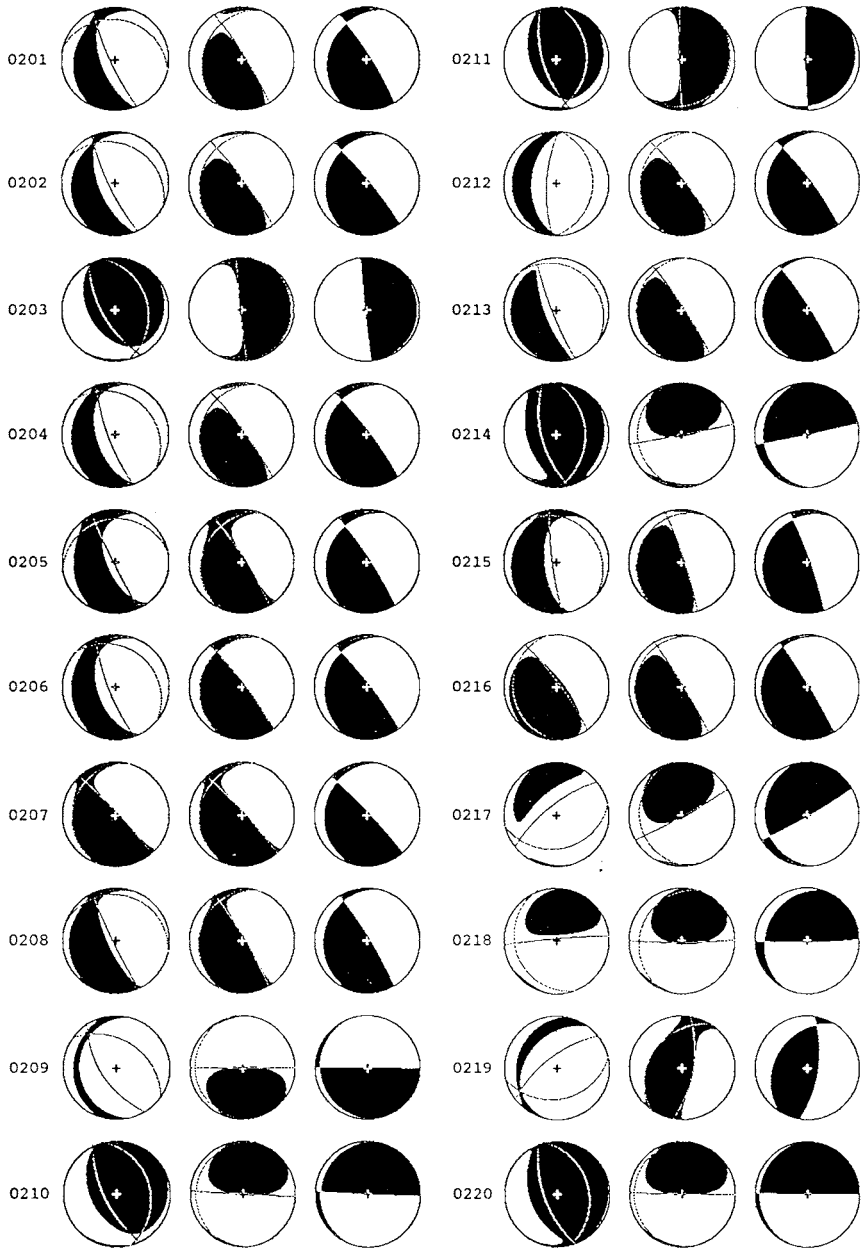


FIG. 26. General, deviatoric, and double-couple moment tensor solutions displayed on lower hemisphere equal-area projections, for 20 selected events recorded in 1993 at Wujek coal mine, Poland. The areas of compression are shaded, and the event numbers are given at the left-hand side of the tensor solutions. [Reprinted from Gibowicz and Wiejacz (1994), Fig. 3.]

solution was as large as 80% of the mechanism. Further studies of the source mechanism of seismic events at Wujek and Ziemowit mines and their relationships to geological and mining structures were undertaken by Wiejacz (1995a,b) and Wiejacz and Ługowski (1997). Wiejacz (1995b) studied 58 events from Ziemowit mine, which occurred in 1994 and were associated with a longwall. He found that the effect of mining structures on source mechanisms is not very clear. The events split into two groups of different nature, one connected with the passing of the working face underneath the transport tunnel and the other with approaching the boundary of the extracted area in another seam. The mechanism of the first group of events was almost pure double-couple dip slips on near vertical fault planes, but with various orientations. The mechanisms of the second group had a larger non-shear component, and were often similar to the cavity collapse type mechanism.

In contrast, at Wujek mine the source mechanism correlates quite well with mining and geological structures. Wiejacz and Ługowski (1997) made a comparative study of seismic events induced in three selected regions of the mine. Study of 58 events associated with a longwall in an area distant from the existing faults has shown that the mechanisms there have near vertical nodal planes parallel to the side boundaries of the longwall area. In a region of a longwall close to the major fault, where 68 events were analyzed, the mechanisms were found to reflect the fault direction. The direction of mining and longwall front seem to play a secondary role. Similarly, the study of 25 events located in the vicinity of another large fault indicates that its direction is reflected in the mechanism of these events (see Fig. 22).

Sagan *et al.* (1996) performed moment tensor inversion of some 200 events with magnitude greater than 1.2, which occurred in 1993 at Wujek coal mine. A comparison of source mechanisms with geological features was the main purpose of the study; the Wujek mine area is situated in the region of one of the main fault discontinuities in the Upper Silesian Coal Basin. Once again, the double-couple component was dominant in most events, although a set of events with a large isotropic component was also observed. The spatial orientation of the nodal planes indicates a group of seismic events that might have their origin in unstable energy release on fault surfaces forming a regional structural pattern. Thus, stresses of tectonic origin cannot be ignored as an important factor in the generation of seismic events in the Upper Silesian Coal Basin. The results of another study of the source mechanism of 372 events from the same area (Idziak *et al.*, 1997) led to similar conclusions. For selected sets of events with similar orientations of nodal planes, located in a limited area, the resultant stress tensor for composite mechanism was determined. The results of analysis point to a relationship between the spatial distribution of slip vectors in the seismic sources and the pattern of neotectonic deformation of the Carboniferous rock mass in the Upper Silesian Coal Basin.

5.2. Typical Source Mechanism and Complex Rock Failures

From numerous studies, based on moment tensor inversion, of the source mechanism of seismic events in mines it follows that often, but not always, shearing processes are dominant in the source and its mechanism can be well represented by a double couple, conventionally called the focal mechanism. Mining of a highly stressed remnant in a deep South African gold mine was accompanied by considerable seismic activity, and several shear ruptures corresponding to the larger seismic events were encountered during mining operations. Ortlepp (1992) performed a study of microcataclastic particles from underground shear ruptures and found that certain striking features revealed by a scanning microscopic study of the fresh cataclastic "rock-flour" forming part of the filling of these ruptures provide strong evidence of violent "shock-rebound" phenomena in the faulting process. He concluded that the formation of a fault by shearing through massive strong rock is a more violent and a less homogeneous process than was thought possible.

McGarr and Bicknell (1990) have demonstrated a very efficient technique for investigating the focal mechanism by matching synthetic to real seismograms, recorded by a broadband, wide-dynamic range digital system. They investigated the focal mechanisms of two tremors located in the Vaal Reefs gold mine, near Klerksdorp, South Africa, and used them to relate these events to the geological and mining conditions in the area.

First-motion analyses of seismic records and an assessment of damage provided conclusive evidence that a fault-slip source mechanism was responsible for a magnitude 2 rockburst that occurred at the Lucky Friday mine, Idaho, in 1990 (Williams *et al.*, 1992). Movement along an argillite bed was observed, and the physical evidence of a shear-slip type failure confirmed the validity of a double-couple source model for many situations in mines.

A detailed study of focal mechanisms of seismic events in relation to results from numerical stress modeling and underground observations at Ansil mine, Canada, was performed by McCreary *et al.* (1993). They found that events with a purely shear mode of failure were prevalent in the footwall along geological contacts and the backs of development drifts. The events without double-couple solutions were scattered throughout the footwall, and were not associated with geological features. Tensile activity was associated with the greatest damage observed underground.

Urbancic *et al.* (1993a) derived fault-plane solutions for microseismic events, with magnitude less than zero, at two geologically different mine sites in Canada. They made a comparison of the focal mechanisms and the results of stress inversion and principal component analysis of microseismicity with *in situ* stress measurements and structural mapping. The obtained results suggest that microseismicity generally occurs along the most significant mapped fractures at the sites; the fault-plane solutions are consistent with *in situ* measurements of stresses; and fault planes lie in close proximity to the most significant mapped features at the sites.

In another study, Trifu and Urbancic (1996) used microseismic events, recorded within a volume at depth at Strathcona mine, to evaluate failure conditions associated with a magnitude 2.9 rockburst. A good correlation was found between stress inversion and microseismic failure planes and structural mapping, and between the *in situ* principal stress orientations and those obtained by stress inversion and numerical modeling.

Dubiński and Stec (1996) calculated the regional stress tensor from fault-plane solutions of seismic events observed at Szombierki and Wujek coal mines in Upper Silesia, Poland, and found a distinct correlation of the principal stresses with local mining conditions at these mines. Similarly, Vesela (1995) calculated the double-couple focal mechanism for over 100 seismic events at Lazy mine in the Ostrava-Karvina coal mining district, Czech Republic, and found different types of the mechanism caused by changes in the stress state of rock mass, connected with coal face advances.

Although the double-couple focal mechanism seems to be dominant in underground mines, more complex rock failures associated with seismic events are also reported from various mining districts. Stickney and Sprenke (1993) studied 21 events in the Coeur d'Alene mining district of northern Idaho, where rockbursts are a major hazard to mining. Eleven of the events generated all-dilatational first motions. Seven events were found consistent with an implosional source and two others were consistent with a shear-implosional source. These results provide observational evidence that dilatational first motions are predominant in this deep metal-mining district.

The magnitude 3.5 seismic event of 1981 in the Gentry Mountain coal mining district, Utah, was studied by Taylor (1994). He modeled the event, using a simple source representation, as a tabular excavation collapse that occurred as a result of mining activity. In contrast, the magnitude 3.6 seismic event of 1993 in the Book Cliffs coal mining district, Utah, which coincided with the crushing out of 24 pillars encompassing an area of nearly 15,000 m², was found by Boler *et al.* (1997) to be of a different source mechanism. They examined six scenarios for the event mechanism for consistency with the seismic analysis and on-site damage observations, and concluded that this catastrophic rockburst was precipitated by a subsidence-related fault slip, with normal slip on a fault in close proximity to the mining works.

A controlled collapse experiment conducted at 320 m depth at the White Pine copper mine near Lake Superior, Michigan, was described by Yang *et al.* (1998). A rectangular panel with an area of about 20,000 m² and a room height of 3 m was designed for the experiment. A total of 59,000 kg of explosives were placed in the 72 supporting pillars and detonated. The pillars were destroyed and the roof collapsed almost immediately. The source characteristics were investigated by waveform forward modeling and time-dependent moment tensor inversion. The results indicate that the source mechanism of the collapse can be represented by a

horizontal opening and closing crack. Thus, a unique source characteristic of the induced collapse is that, unlike spontaneous collapses, the induced collapse was initiated as a tensile crack. The collapse magnitude was estimated to be 3.1 from coda duration and 2.8 from surface waves recorded at regional distances (Phillips *et al.*, 1999). Over 4000 aftershocks were recorded. The rate of occurrence followed the modified Omori law with an exponential of 1.3. Phillips *et al.* (1999) identified 41 shear slip, 18 implosional, and 2 tensile events, based on *P*-wave polarity patterns. They also found that stress drops for implosional events were lower than those for shear slip events.

Four mechanisms of pillar failure have been observed in strip pillars at Western Deep Levels gold mine, South Africa (Lenhardt and Hagan, 1992). Relatively narrow pillars crush in some cases, whereas the solid core of wide pillars, if sufficiently stressed, slips or punches along one or two shear planes below the up- and down-dip edges of the pillar. Occasionally, shearing occurs simultaneously on two adjacent pillars. Closure occurs in the surrounding stopes, and serious damage to footwall development close to the pillars might result.

The violent failure of a peninsular remnant at a depth of 2300 m in a mine in the Carletonville Goldfield of South Africa, which occurred in 1994, was described by Durrheim *et al.* (1998). A seismic event with magnitude of 2.1 resulted from the failure of the remnant with movement into the workings. The event could not be explained by a single shear slip. Two different rockburst damage mechanisms were identified. Firstly, the face and footwall on the eastern side of the remnant were violently ejected into the void between the original face and first line of timber packs, following failure and dilation of the remnant and its foundation. Secondly, the hangingwall on the southern side of the remnant fragmented and collapsed when subjected to intense seismic shaking.

The mechanism of a partial collapse of dolomite-mine workings near Schwaz, Austria, which occurred in May 1993, was described by Lenhardt and Pascher (1996). The collapse was associated with a sequence of more than 200 seismic events with the largest event of magnitude 1.9. Underground observations revealed a number of discontinuities along which the rock mass was able to move. Seismic records of this series indicate two types of focal mechanism involved during the collapse. Some events seem to have been associated with pure block sliding along several discontinuities and the others were collapse events. Several phases of the collapse were also recognized from seismic observations.

The interaction of plane seismic waves with underground openings was studied by Yi and Kaiser (1993), who applied the dynamics and continuum mechanics analytical approaches. They found that low-frequency waves from a seismic source hundreds of meters away could cause both rock ejection and dynamic stress concentration at both walls of an opening in underground mines. These dynamic stress concentrations, superimposed on high static stress concentrations, may lead to different types of rock failure, including secondary rockbursts.

A study of source parameters of seismic events at a coal mine in the Ruhr basin, Germany, and those induced by the excavation of a shaft in granite at the Underground Research Laboratory, provided evidence for non-shearing events (Gibowicz *et al.*, 1990, 1991). It has been found that the ratio of *S*- to *P*-wave energy is often unusually low, and the high *P*-wave energy events are thought to be the most likely candidates for non-double-couple events. A direct comparison between the isotropic, compensated linear vector dipole and double-couple parts of the moment tensor and the energy ratio, determined for over 200 seismic events from Polish coal and copper mines, has shown that these quantities are correlated (Gibowicz, 1996). Though the correlation coefficients were small in all cases, not exceeding 0.5, they were significant at the 99% confidence level.

For small microseismic events, the source size provided by shear models is often unrealistically large when compared to visual observations of rock fractures near underground openings. A depletion of *S*-wave energy for events close to the excavations, on the other hand, implies that tensile cracking might be the dominant mechanism for these events. Cai *et al.* (1998) proposed a method to estimate the fracture size from seismic measurements. The method accepts tensile cracking as the dominant fracture mechanism for brittle rocks under compressive loads and relates the fracture size to the measured seismic energy, leading to more realistic values of the size when compared to field observations.

5.3. Stress Release Mechanism

In the well-known simple fault model of Orowan (1960) with constant friction, the final stress after the earthquake rupture is equal to the dynamic frictional stress. Two other possibilities have been considered. In the first case, the final stress is greater than the frictional stress and a partial stress drop mechanism is involved (Brune, 1970, 1976). In the second case, the final stress is smaller than the frictional stress and a frictional overshoot mechanism is considered (Savage and Wood, 1971). Several arguments in favor of both cases have been proposed (e.g., Savage and Wood, 1971; Brune, 1976; Madariaga, 1976; Smith *et al.*, 1991; Zúñiga, 1993).

Gibowicz (1998) recently examined the stress drop mechanism of seismic events induced by mining. He collected the values of uniformly estimated apparent stress and stress drop of Brune (1970, 1971), taken as a measure of static stress drop, from 850 events with moment magnitude ranging from -3.6 to 3.6 , induced at the Underground Research Laboratory (URL), Western Deep Levels (WDL) gold mine in South Africa, and two coal and copper mines in Poland. The quantity ϵ , defined as the ratio of the static stress drop $\Delta\sigma$ over the sum of apparent stress σ_a and half the static stress drop, $\epsilon = \Delta\sigma/(\sigma_a + \Delta\sigma/2)$, proposed by Zúñiga (1993) as an indicator of stress-drop mechanism, was used to study the stress release mode

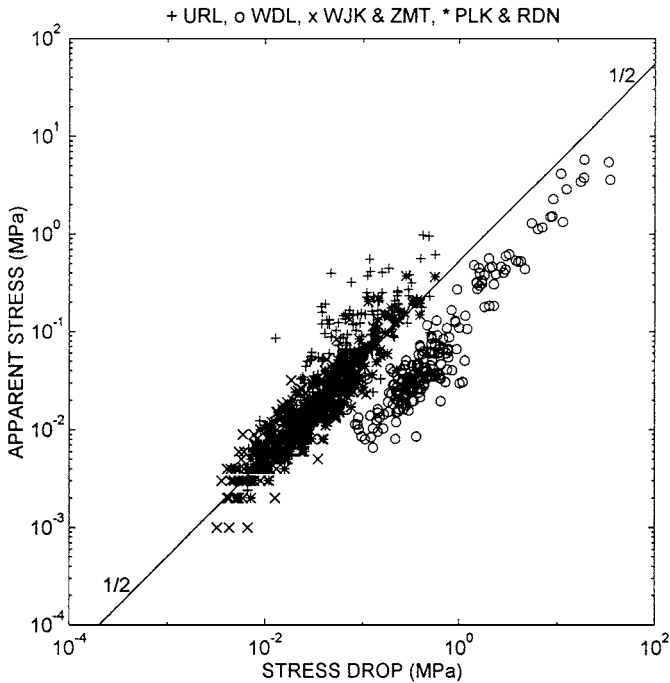


FIG. 27. Apparent stress versus Brune's stress drop for seismic events from the Underground Research Laboratory (URL) in Canada, Western Deep Levels (WDL) in South Africa, two Polish coal mines (WJK and ZMT), and two Polish copper mines (PLK and RDN). The straight line indicates the Orowan condition corresponding to apparent stress equal to half the static stress drop. [Gibowicz (1998), Fig. 1, reprinted with kind permission from Birkhäuser Verlag AG.]

in various mining environments. This ratio is bounded by the values from 0 to 2. The Orowan condition is met when $\varepsilon = 1$ or $\sigma_a = \Delta\sigma/2$, the partial stress drop mechanism corresponds to $\varepsilon < 1$, and the frictional overshoot case appears when $\varepsilon > 1$.

The values of apparent stress versus stress drop for various seismic events are presented in Fig. 27, reproduced from Gibowicz (1998). The straight line indicates Orowan's condition corresponding to apparent stress equal to half the static stress drop. From this figure it follows that all the events from the WDL clearly display a frictional overshoot mechanism; the events from the URL indicate a partial stress drop mechanism; and all the events from Polish mines fulfill Orowan's condition. The values of epsilon (Zúñiga, 1993) versus moment magnitude for seismic events from six selected mines are presented in Fig. 28 (Gibowicz, 1998), where Orowan's condition ($\varepsilon = 1$) is marked by a continuous line.

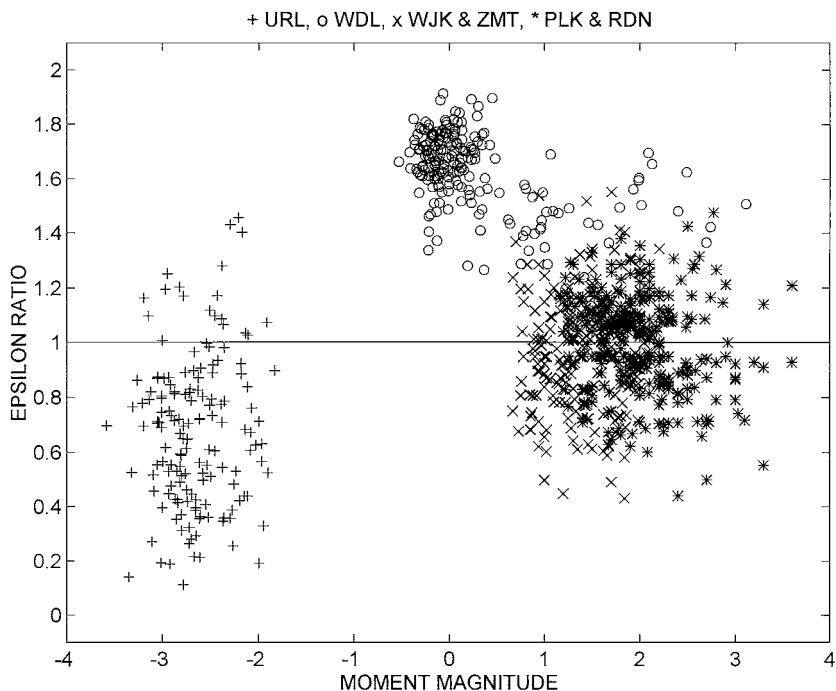


FIG. 28. Epsilon ratio, based on stress parameter estimates, versus moment magnitude for seismic events from six selected mines (see Fig. 27). [Gibowicz (1998), Fig. 2, reprinted with kind permission from Birkhäuser Verlag AG.]

The apparent stress defined as the ratio of the radiated energy over the seismic moment, multiplied by the medium rigidity, is independent of any source model assumptions. In contrast, the static stress drop determined from the seismic moment and corner frequency is heavily model dependent through the source radius–corner frequency relation. For the events from the URL, Orowan's condition would be fulfilled if the constant in the source dimension–corner frequency relation is equal to 1.82, which is the middle value between the average value of 1.32 corresponding to S waves in the source model of Madariaga (1976) and that of Brune (1970). The constant in the Madariaga model, however, depends on the rupture velocity and the azimuth of observation, and if the obtained value of 1.82 could be explained in these terms, the partial stress drop mechanism there would be irrelevant. For the events from the WDL, on the other hand, the obtained value of 3.92 of the same constant is too high for a reasonable explanation in terms of fault and observation geometry or rupture velocity, implying that the appearance of frictional overshoot mechanism there could be real (Gibowicz, 1998). It should be noted, however, that

comparisons between apparent stress and stress drop are somewhat controversial because of the stress drop dependence on the choice of source model.

The apparent stress is also defined as $\sigma_a = \eta\sigma$, where σ is the average shear stress loading the fault plane leading to slip, and η is the seismic efficiency defined as E_a/W in which E_a is the seismic energy and W is the total energy released by the earthquake (e.g., McGarr, 1999). McGarr (1994) compared apparent stresses of mining-induced seismic events in South Africa and Canada with those measured for laboratory stick-slip friction events. He found that both mining-induced and laboratory events have very low seismic efficiency; nearly all of the energy released by faulting is consumed in overcoming friction. The comparison led McGarr (1994) to the important hypothesis that the seismic efficiency $\eta = \sigma_a/\sigma \leq 0.06$.

In his most recent study McGarr (1999) tested this hypothesis against a substantially augmented data set of earthquakes for which σ can be estimated, mostly from *in situ* stress measurements. The expanded data set covered a broad range of depths, rock types, pore pressures, and tectonic settings. He found that over about 14 orders of magnitude in seismic moment, apparent stresses display distinct upper bounds determined by a maximum seismic efficiency of about 0.06, consistent with his hypothesis. The relationship between the maximum apparent stress and the average shear stress is shown on a logarithmic scale in Fig. 29, reproduced from McGarr (1999), for several laboratory stick-slip friction events as well as for induced, triggered, and natural earthquakes. McGarr (1999) also found that the behavior of σ_a and η can be expressed in terms of the ratio of the static to the dynamic coefficient of friction and the fault slip overshoot, measured for stick-slip friction events in the laboratory. Typical values of these two parameters correspond to seismic efficiencies of about 0.06. Thus upper bounds on σ_a/σ appear to be controlled by just a few fundamental aspects of frictional stick-slip behavior that are common to shallow earthquakes everywhere, and the values of apparent stress can be used to deduce the absolute level of deviatoric stress at the hypocenter (McGarr, 1994, 1999).

6. SOURCE TIME FUNCTION

The source processes of seismic events induced by mining have been extensively studied by spectral analyses of the records of seismic waves and by the moment tensor inversion technique. In spite of undertaken efforts, a number of problems remain unsolved and new approaches to study the seismic sources in mines are needed for a better understanding of their properties and their mechanism of generation. Determination of the source time function is a new approach in studies of seismicity in mines, although this approach has been in use for a long time in studies of natural earthquakes.

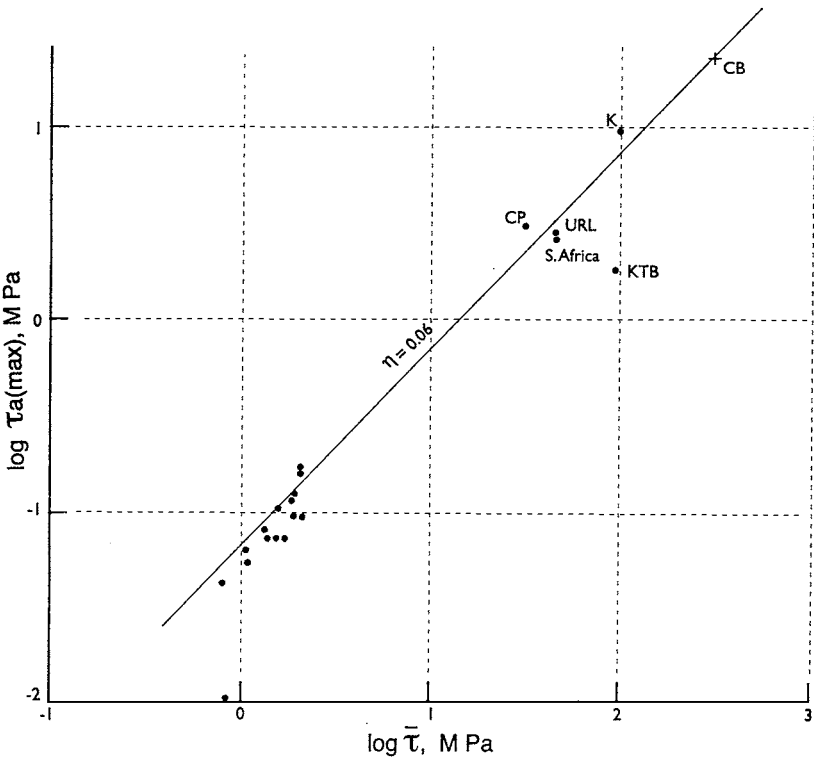


FIG. 29. The logarithm of maximum apparent stress as a function of the logarithm of average shear stress for laboratory stick-slip friction events and for induced, triggered, and natural earthquakes (for details see the original paper). The straight line indicates the seismic efficiency $\eta = 0.06$. [Reprinted from McGarr (1999), Fig. 3.]

The Source Time Function (STF) of a seismic event describes the energy release and the rupture evolution in the source. It could provide important information on rupture velocity and rupture direction when directivity effects are observed. Source parameters can be estimated in the time domain and compared with those estimated in the frequency domain. Furthermore, source tomography, based on Relative Source Time Functions (RSTF) observed at a number of stations, would provide a detailed description of the rupture processes in the source of a given event.

The extraction of STF from seismograms requires, however, separation of the source effects from those of the path, site, and instrumental response. For this, a deconvolution technique based on the Empirical Green's Function (EGF) can be used. Knowledge of the earth's crust structure, attenuation effects, and instrumental

response are then not required (e.g., Mueller, 1985; Li and Thurber, 1988; Mori and Frankel, 1990; Mori, 1993; Li *et al.*, 1995; Bour and Cara, 1997; Fletcher and Spudich, 1998; Jost *et al.*, 1998). For two seismic events of different strength, located close to each other and having similar focal mechanisms, the record of the smaller event can be considered as the EGF (Hartzell, 1978). It can be deconvolved from the record of the larger event to obtain a RSTF at a given station for the larger event (Mueller, 1985). Such deconvolution should result in a RSTF that is corrected for the path, site, and instrumental effects.

This technique is especially convenient to study seismic sources in mines, where underground seismic networks are situated in the source area and are often composed of large number of sensors. Furthermore, seismic events are located with high accuracy with standard errors not exceeding a few tens of meters. Domański and Gibowicz (1999) and Domański *et al.* (2000) described the first attempts to use the EGF technique to recover the STF of large seismic events observed at Polkowice and Rudna copper mines in Poland. They applied the classical spectral division deconvolution technique, developed by Mueller (1985), to separate the STF from the records. The observed seismogram of a given larger event can be expressed as the convolution of its STF, the impulse response of the path, recording site, and recording instrument. The seismogram of a smaller event, whose STF is assumed to be a delta function, is considered as an EGF. The deconvolution is performed by spectral division in the frequency domain. Then, after taking the inverse Fourier transform, the STF of the larger event is obtained.

The two events need careful selection. They should be closely located to each other. The difference in distance between the two events in a mine should not exceed some 100–200 m (Domański and Gibowicz, 1999). Their focal mechanisms should be similar and the difference between seismic moment tensor axes should not exceed 20 degrees. Finally, the magnitude of the main event should be considerably greater than that of the smaller event. The difference of about one magnitude unit provides reasonable results, although smaller differences are often acceptable.

The notion of the empirical Green's function deconvolution approach may be rather simple, but its practical applications are complex. There are numerical instabilities resulting from spectral division and several other problems inherent in the method. An example of the RSTF deconvolved from *P* waves records of the moment magnitude 2.7 event of October 27, 1996, from Rudna copper mine, using the records of a magnitude 1.9 event as a Green's function, is shown in Fig. 30, reproduced from Domański *et al.* (2000).

After retrieving the RSTF pulses from the records of several stations, it is possible to estimate whether they are symmetric or asymmetric, and in the latter case to consider their dependence on the station azimuth. If the pulse widths of the RSTF depend on the station azimuth, then it is an indication that the rupture propagated unilaterally. For a unilaterally propagating rupture, the source duration is narrowest in the direction of rupture propagation and widest in the opposite direction.

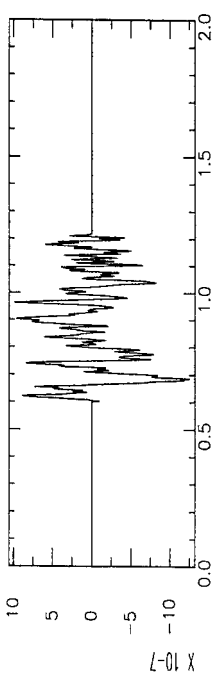
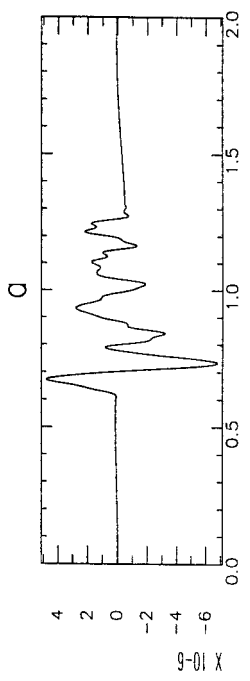
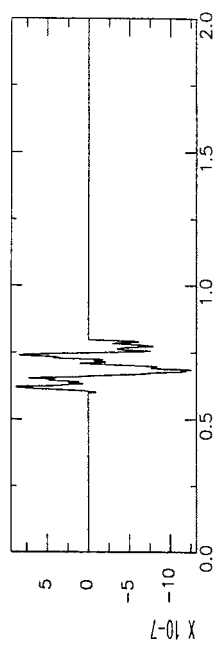
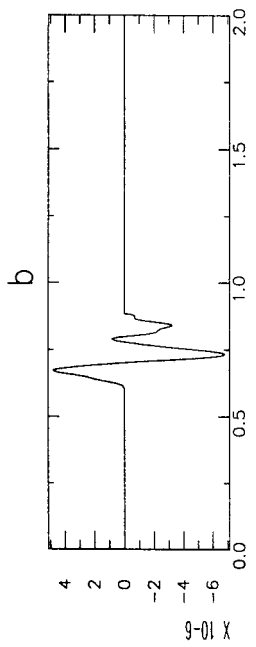
Similarly, the maximum amplitude of the source pulse would be largest in the direction of rupture propagation and smallest in the opposite direction. The spatial distribution of pulse widths of the RSTF derived at various seismic stations for the event of October 27, 1996, from the Rudna mine is shown in Fig. 31, reproduced from Domański *et al.* (2000).

The rupture direction, rupture velocity, and source size can be determined simultaneously by a least-squares method either from the distribution of the RSTF pulse widths (e.g., Li and Thurber, 1988) or from the distribution of their maximum amplitude (Li *et al.*, 1995). For a finite moving source, the relation between the pulse width and the azimuth angle measured to the propagation direction is well known (e.g., Ben-Menahem, 1962). The rupture direction is estimated by fitting the pulse duration at stations with different azimuths to a best straight line. Then the slope and intercept of this straight line are used to estimate the rupture velocity and the fault length. An example of such a procedure is shown in Fig. 32, reproduced from Domański *et al.* (2000), for the same event of October 27, 1996, from the Rudna mine. The surface of the RSTF pulse is a measure of seismic moment in the time domain. More precisely, this surface is a ratio of seismic moment of the main event over seismic moment of the smaller Green's event.

Recently, new methods for determination of source time function by the empirical Green's function approach in the time domain were proposed. They are based on the search by successive iterations for the solution of integral equations describing the observed seismograms as the convolution of the source time function with the empirical Green's function. An interesting and effective technique, in this respect, seems to be the projected Landweber method which is an iterative nonlinear technique allowing the introduction of physical constraints (positivity, causality, etc.) on the final STF (Bertero *et al.*, 1997; Piana and Bertero, 1997). A nontrivial modification of an iterative blind-deconvolution method used for image identification was also proposed as a novel technique to retrieve the STF (Bertero *et al.*, 1998). The main feature of this method, which is also based on the projected Landweber method, is the use of different constraints on the STF and the EGF. The convergence of the method is very fast and the results obtained by Bertero *et al.* (1997) for synthetic and real data were quite satisfactory.

7. FRACTALS

Fractal geometry is a mathematical tool (Mandelbrot, 1982) to characterize self-similar sets, which are essentially the same regardless of the scale on which the set is examined. A fractal approach to natural earthquakes occurrence has been widely applied in recent studies and it has been shown that seismicity exhibits approximate fractal structure with respect to space, time, and size (e.g., Barton and La Pointe, 1995).



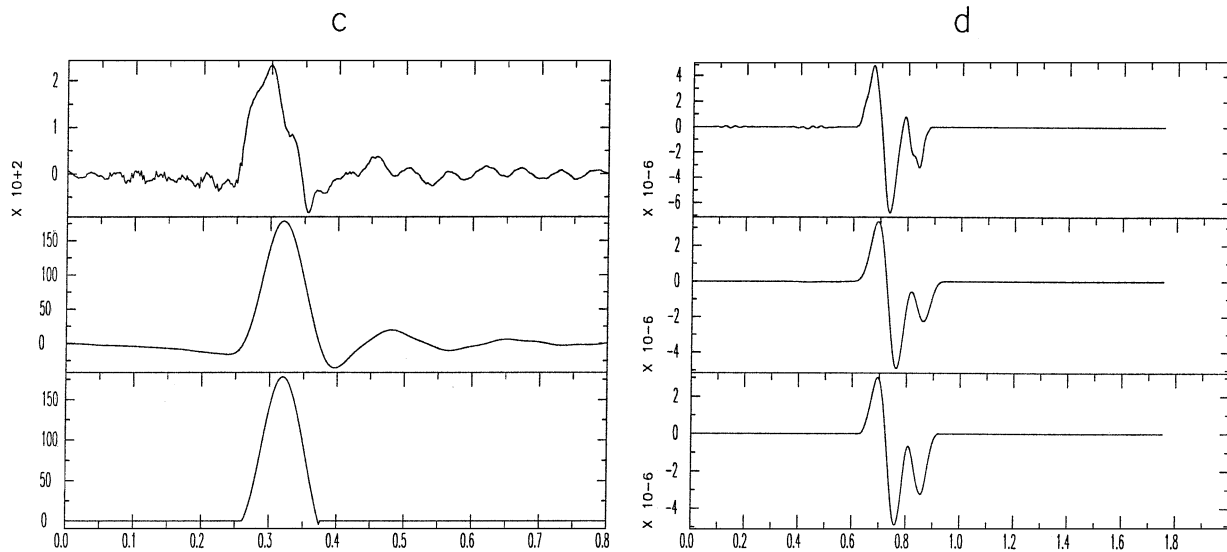


FIG. 30. Example of the relative source time function derived from P waves, recorded by the underground seismic network at Rudna copper mine, Poland, from the moment magnitude 2.7 event of October 27, 1996, using the record of a magnitude 1.9 event as a Green's function. P -wave records (a) and selected windows (b) for larger and smaller events are shown at the top. The original, smoothed, and windowed source time functions (c) and the corresponding results of the convolution of source time functions with the record of Green's event (d) are presented at the bottom of the figure. [Domański *et al.* (2000), Fig. 5, reprinted with kind permission from Birkhäuser Verlag AG.]

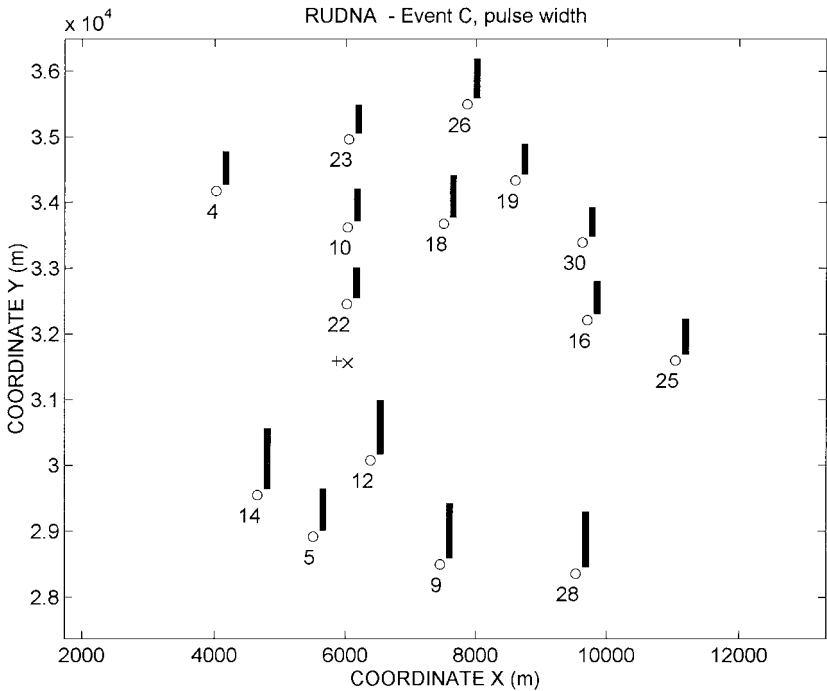


FIG. 31. Spatial distribution of pulse widths of the relative source time functions derived from the records of several seismic stations for the event of October 27, 1996, from Rudna copper mine. The locations of the main and Green's events are shown by a cross and a plus, respectively; the stations are marked by open circles and are numbered; and the pulse widths, normalized to the largest value, are shown by vertical thick bars. [Domański *et al.* (2000), Fig. 6, reprinted with kind permission from Birkhäuser Verlag AG.]

While the self-similarity of energy of seismic events in mines described by the Gutenberg-Richter relation has been known for a long time, Coughlin and Kranz (1991) showed for the first time that distributions in space and time of these events have also a fractal character. They analyzed three microseismicity data sets from Galena mine, USA, from the time periods encompassing three damaging rockbursts. The spatial and temporal fractal dimensions were estimated by the correlation integral method (Grassberger and Procaccia, 1983). For a set of N points parameterized with a variable \vec{x} , the correlation integral is given by

$$C^{(2)}(r) = \frac{1}{N(N-1)} \sum_{i=1}^N \sum_{k \neq i} \Theta(r - \|\vec{x}_i - \vec{x}_k\|), \quad (1)$$

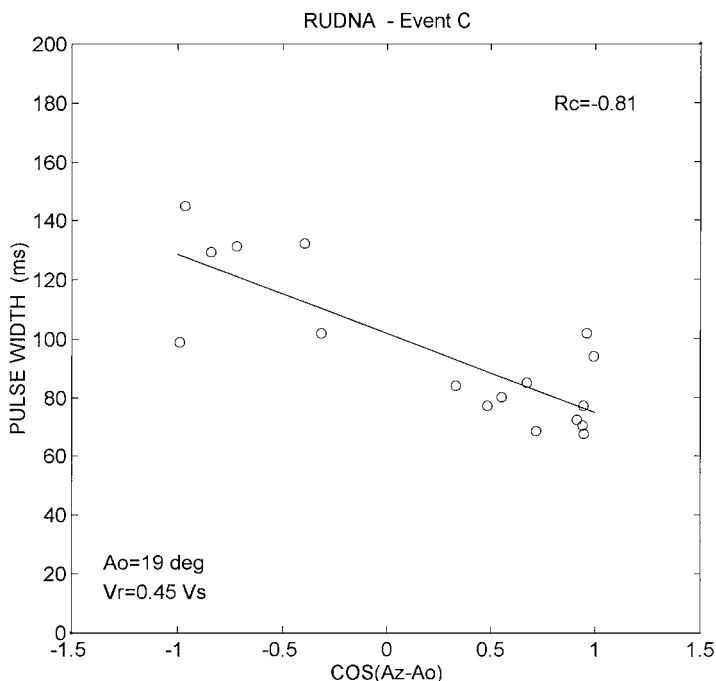


FIG. 32. Example of the best linear fit of the pulse widths of relative source time functions against the cosine of station azimuths A_z for the event of October 27, 1996, from Rudna copper mine. The equation of this straight line is used to derive the azimuth A_o of rupture propagation direction and the rupture velocity V_r . [Domański *et al.* (2000), Fig. 8, reprinted with kind permission from Birkhäuser Verlag AG.]

where $\|\vec{x}_i - \vec{x}_k\|$ is the distance between points i and k in the domain of \vec{x} , r is the reference distance, and $\Theta(\bullet)$ is the Heaviside function, which in this case counts how many pairs of points (\vec{x}_i, \vec{x}_k) fall within the interevent distance r . If the set exhibits simple invariance, then the correlation integral is proportional to the power function of r

$$C^{(2)}(r) \propto r^{D_2}. \quad (2)$$

Constant D_2 , called the correlation exponent dimension or the correlation dimension, is estimated from a linear part of $\log C^{(2)}(r)$ vs $\log r$ empirical relation.

Coughlin and Kranz (1991) considered the time of event occurrence and the location of event as separate parameterizations. In every case they found a reasonable range of r over which relation (2) approximately held. The spatial correlation dimension was significantly less than 3.0—an expected result for points uniformly

distributed in a three-dimensional space. A time-variability of spatial D_2 in some concordance with the occurrence of stronger events suggested a possible use of this parameter for monitoring of fracturing processes in mining stopes and, in particular, its late stages before an impending main failure.

Since this first study, many works explored fractal properties of seismic events from mines in space, time, and energy. The fractal dimension is a one-parameter characterization of a degree of clustering of objects building a fractal set, thus it can be used to study geometrical similarities and differences of seismically active areas as well as development of a seismogenic process in time and space. The latter possibility, in particular, gave rise to various attempts to use fractal characteristics of seismic data from mines as precursors to strong damaging events. The works concerning this subject, specific for the seismicity induced by mining, are reviewed in the next chapter together with other methods designed to evaluate the time-dependent seismic hazard.

Xie and Pariseau (1992) and Xie (1993) studied the spatial fractality of microseismic activity of a rockburst prone pillar at Galena mine. They applied the so-called number-radius or mass-radius method introduced by Xie (1993). In this method a fractal set of geometrical points (e.g., hypocenters or epicenters) should obey the law of proportionality:

$$M(r) \propto r^{D_{cl}}, \quad (3)$$

where $M(r)$ is the number of points inside the hypersphere of radius r , centered at the center of the mass of the set. The constant D_{cl} is an estimate of the fractal dimension of the set and is called the clustering dimension. Since the position of the center of mass can be significantly biased by mislocations of outlying events, and this bias will propagate to a clustering dimension estimate, it is recommended to use an average D_{cl} , obtained from several independent estimations centered at points randomly distributed around the evaluated center of mass.

A good linear correlation between $\log M(r)$ and $\log r$ obtained by Xie and Pariseau (1992) evidenced statistical self-similarity of the studied data. Xie (1993) interpreted an observed increase of the degree of clustering before a rockburst, represented by a decrease of D_{cl} , in terms of clustering of local cracks in the rock mass. During a late preparatory stage the crack density within a zone of the future main failure becomes significantly greater than the background crack density. This clustering implies the decrease of fractal dimension of spatial distribution of events. Xie (1993) concluded that it could be possible to predict the occurrence of main rockbursts by observing a decrease in D_{cl} for spatial distribution of microseismicity.

Fractal character of spatial distribution of seismic events in mines has been confirmed for practically every scale. Trifu *et al.* (1993) studied distribution of some 1500 microseismic events recorded within a selected volume at Strathcona mine in Canada. The magnitude range of the data was $[-2, 1]$. The spatial correlation

dimension, evaluated for two perpendicular directions, had an anomalous decrease before the occurrence of $M = 2.9$ rockburst and by the end of the aftershock sequence.

Mortimer and Lasocki (1996a,b) investigated local seismicity connected directly with longwall mining of single, isolated stopes. Such seismicity forms a cloud surrounding the longwall front and move together with advances of the front (Gibowicz and Kijko, 1994). For every considered seismic series the epicenters of events were related to a local moving system of coordinates centered at the center of the mining front. The series comprised all events located within the 400×400 m square around the center of the system of coordinates. In order to estimate the fractal dimension of epicenter distribution, Mortimer and Lasocki (1996a) used the box-counting method (e.g., Mandelbrot, 1982; Turcotte, 1992). In this method a volume containing studied objects (points in the case of spatial distribution of seismic sources) is covered by hypercubes (boxes) with a side length r . If the set of objects is a fractal, then the number, $N(r)$, of boxes covering the objects scales with r

$$N(r) \propto r^{-D_b}, \quad (4)$$

and a constant D_b is the box-dimension. The box-dimension, obtained for a finite sample, estimates the Kolmogorov capacity dimension of the fractal, which is the limit of D_b for $r \rightarrow 0$.

All nine analyzed series from five coal mines in Poland statistically obeyed relation (4) for the range of r starting from 20 m—the order of source location errors. The values of D_b varied from series to series between 1.0 and 1.7. An interesting observation was made that the fractal character was preserved in sub-series comprising only smaller and larger events, but the fractal dimension values were different in such subseries, and generally lower for strong events. This could suggest that, contrary to the conclusions inferred from natural seismicity (e.g., Kagan, 1994), larger events in this particular set-up of moving mining front were more strongly clustered than the smaller ones. However, due to a strong bias of the box-dimension, this result could not be considered as fully reliable. Mortimer and Lasocki (1996a) found that reliable estimates of D_b could be obtained for series comprising no less than 1500 events. It was concluded, therefore, that the box-counting method is of limited usefulness for studies of seismic series in mines.

Mortimer and Lasocki (1996b) compared the results of three methods of fractal analysis: the box-counting, the number-radius, and the correlation integral, applied to local seismicity data from one longwall at Katowice coal mine in Poland. Regardless of the method used, the spatial distribution of events exhibited fractality within the distance range from 20 to 100 m. The analysis, repeated on successive samples of a constant number of events, showed that fractal dimension estimates significantly varied in time. The exponential correlation dimension was the most stable, whereas the other two dimensions frequently exposed saw-like variations.

The authors concluded that the correlation integral method is the most useful when the number of data is limited. Furthermore, it was also shown that the distribution of event origin times is fractal.

Domański (1997) compared the fractal correlation dimension of spatial distributions of stronger events from coal and copper mines in Poland. Magnitudes of seismic events from coal mines were in the range of 0.65 to 2.2. The events from copper mines were on the average larger, with the magnitude range of 1.1 to 3.1. The correlation dimensions were different for the data sets from different kinds of mines and similar for the sets from the same kind of mines; from 1.5 to 1.75 for coal and from 2.0 to 2.3 for copper mines. The author gave no suggestion for a possible cause of the significant difference of spatial clustering of events in coal and copper mines, although a potential of fractal analysis to identify differences between seismically active zones in mines was admitted.

Gibowicz (1997a) estimated the spatial correlation dimension to describe an unusual swarm-like seismic sequence, which occurred during 12 days in April 1993 at the Western Deep Levels gold mine in South Africa. The sequence consisted of four main shock–aftershocks sequences following one another within a volume of rock of $670 \times 630 \times 390 \text{ m}^3$ size. The identified main shock–aftershocks sequences had different correlation dimensions starting from 1.75 for the first and the most clustered one up to 2.4 for the second and the least clustered. The last two sequences had nearly the same correlation dimension of about 1.9. The author explained the differences by a limited time for the development of sequences. Only the first sequence had enough time to develop fully and to reach its “natural” clustering. The developments of the second and the third were interrupted by the successive main events.

Idziak and Teper (1996b) studied a spatial distribution of epicenters of the largest events observed in the Bytom syncline, one of the main structural units forming the Upper Silesian Coal Basin in Poland. The syncline of approximate size of $16 \times 8 \text{ km}^2$ is intensively mined and is highly seismic. Most of the seismic events are directly connected with mining operations, but the largest events seem to be correlated with local geological discontinuities rather than with mine openings (Gibowicz and Kijko, 1994). The analyzed data comprised 1651 events of local magnitude above 2.2, recorded from 1977 to 1991. Using the box-counting method, Idziak and Teper (1996b) found that the distribution of epicenters of studied events was fractal within the distance range of 0.5 to 8 km. The value of the box-dimension was 1.52. The same box counting technique was applied to investigate the geometry of the fault system of the Bytom syncline. The fractal dimension in this case was estimated as 1.60. The authors suggested that the close proximity of these two values might imply the engagement of the whole fault system in the generation of large events in the area.

A one-parameter characterization of fractal properties of seismicity in mines seems to be insufficient to represent complex features of seismic event distributions.

When a fractal set is not homogeneously scale invariant, it should be described by an infinite number of dimensions rather than by one fractal dimension alone (e.g., Mandelbrot, 1989).

The most widely used method to investigate multifractal properties of natural earthquakes employs estimation of the generalized correlation integral (e.g., Hirata and Imoto, 1991; Hirabayashi *et al.*, 1992; Godano *et al.*, 1996; Wang and Lee, 1996). Given a set of N points, parametrized by \vec{x} , estimate of the generalized correlation integral is given by

$$C^{(q)}(r) = \left\{ \frac{1}{N} \sum_{i=1}^N \left[\frac{1}{N-1} \sum_{k=i}^N \Theta(r - \|\vec{x}_i - \vec{x}_k\|) \right]^{q-1} \right\}^{\frac{1}{q-1}}, \quad (5)$$

where the parameter q can take any value from $(-\infty, 1) \cup (1, +\infty)$. For complex self-similar sets the correlation integral scales with r

$$C^{(q)}(r) \propto r^{D_q}, \quad (6)$$

where D_q for various q is the multifractal spectrum of the set (e.g., Grassberger, 1983; Hentschel and Procaccia, 1983; Kurths and Herzog, 1987). In a region of low q the dimensions follow the relation $D_{q+2} = D_1 - \mu(q+1)$, which can be used to estimate D_1 (Paladin and Vulpiani, 1987). For a homogeneous fractal set all D_q are the same. For a heterogeneous fractal set, when q changes from positive to negative values, D_q characterizes clustering of the set from the most to the least intensive, respectively. The limits of a multifractal spectrum, D_∞ and $D_{-\infty}$ are finite and characteristic for the studied set. In practice D_q does not change significantly for q above 10 to 20. It is clear from relation (5) that an estimation of the fractal dimensions for $q < 1$ is unstable, which often precludes a reliable interpretation of its results.

Shivakumar *et al.* (1996) applied multifractal analysis to study the spatial distribution of three major area rockbursts at Champion reef mines in the Kolar Gold Fields in India. Three data sets consisted of 125 seismic events that occurred for 14 days after a $M = 2.48$ main event; 64 events recorded during 1 week after a $M = 2.44$ rockbursts; and 66 events for 15 days following a $M = 3.09$ main event, respectively. For q greater than 1, a linear part of the logarithm of relation (6) was easy to identify. Figure 33, reproduced from this work, shows linear fits to the actual data, leading to the evaluation of generalized correlation dimensions in the range of q from 2 to 10 for the first data set. Shivakumar *et al.* (1996) analyzed D_2 , considered D_{10} as D_∞ , and analyzed the difference between these two values, which was supposed to characterize fractal heterogeneity of the studied data sets. The differences of $D_2 - D_{10}$ were 0.52, 0.37, and 0.41 for successive data sets, respectively. The authors related these clustering features to the state of stress

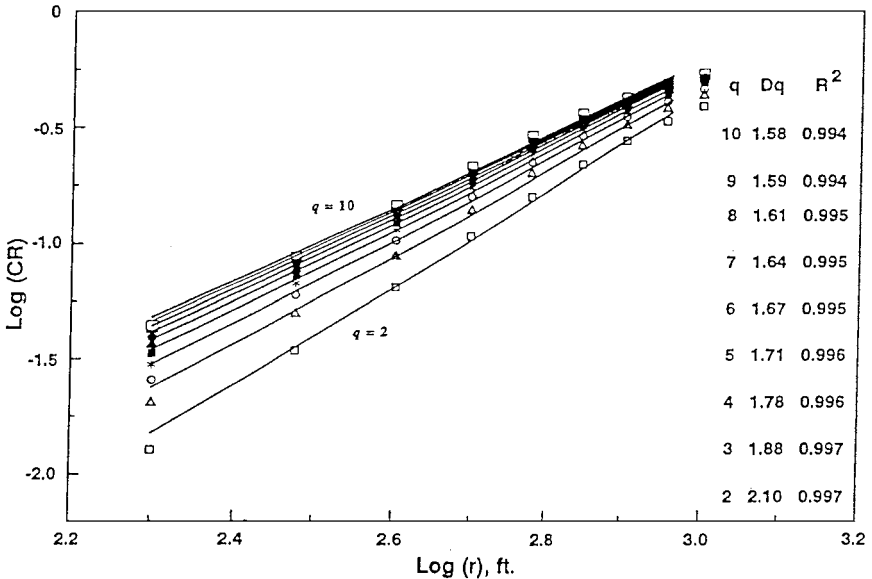
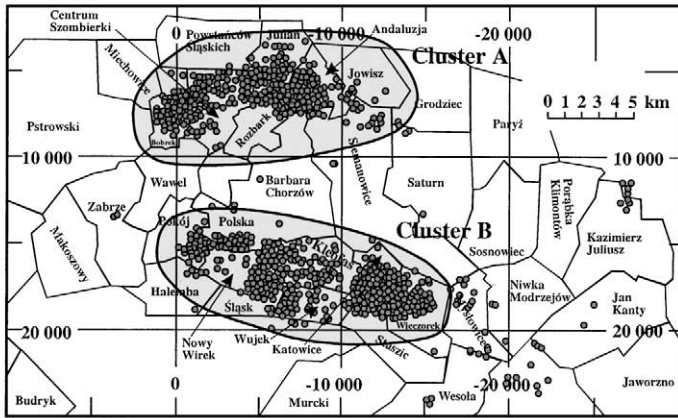


FIG. 33. Linear fits of the generalized correlation integrals of hypocenter distribution in the area rockburst-I, Kolar Gold Fields, India, for $q = 2 - 10$. CR is the generalized correlation integral and r is the reference distance (see relation (5)), and D_q is the estimate of fractal correlation dimension and R^2 is the coefficient of determination of the linear regression. [V. Shivakumar *et al.*, 1996; reprinted from *International Journal of Rock Mechanics and Mining Sciences*, ©1996 Elsevier Science Ltd, with permission from Elsevier Science.]

distribution, mining, and regional geological heterogeneity of the area, concluding that multifractal analysis can successfully distinguish individual features of factors governing the generation of induced seismicity.

The other application of multifractal analysis to seismic data from mines was presented by Mortimer *et al.* (1999) who used the generalized correlation dimension of the distribution of event energy to describe rock fracturing at different scales. The analyzed data sets comprised larger mining-induced events ($M > 2.2$), regionally distributed over the Upper Silesian Coal Basin in Poland, seismic events from a selected part of a gold mine in South Africa, local seismicity connected with mining of individual stopes in Polish coal mines, and acoustic emission of rock samples, recorded during laboratory tests. In all cases, the distribution of energy was fractal, but the multifractal spectra did not seem to be related to the spatial scale of the fracturing process. Figures 34 and 35, reproduced from Mortimer *et al.* (1999), show the spectra of regional seismic data from two active areas and of acoustic emission induced in coal samples by gas sorption and generated in a dolomite sample subjected to uniaxial compression, respectively. The multifractal

a



b

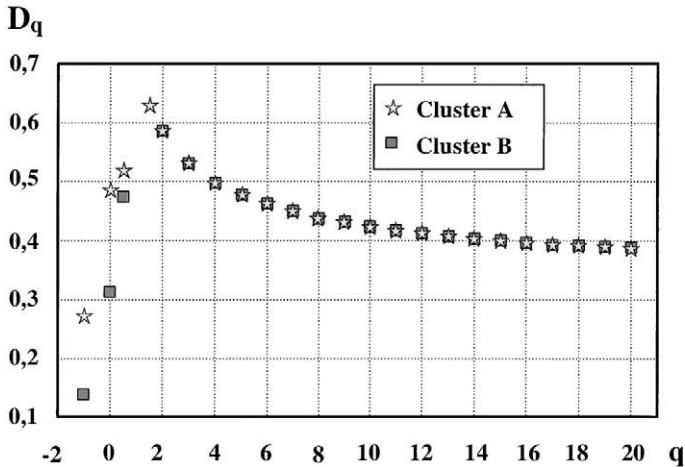


FIG. 34. Multifractal analysis of seismic energy distribution for regional seismic events from the Upper Silesian Coal Basin in Poland: (a) distribution of event epicenters, (b) multifractal spectra. [Reprinted from Mortimer *et al.* (1999), Fig. 1.]

characteristics of the acoustic emission data are highly different, whereas the spectrum of the regional seismicity nearly matches the spectrum obtained for the second coal sample. The other interesting observation is a close correspondence between the multifractal spectra of seismic energy and the spectra of epicenter distribution

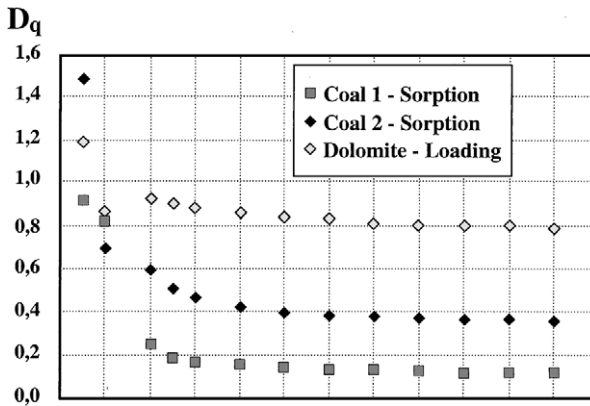


FIG. 35. Generalized fractal dimension of the energy rate of acoustic emission (AE) from rock samples during laboratory experiments. Coal 1 and Coal 2 refer to the AE generated by gas sorption in the samples of coal prone and not prone to coal and gas outbursts, respectively. Dolomite refers to the AE recorded during uniaxial compression test of a dolomite sample. [Reprinted from Mortimer *et al.* (1999), Fig. 4.]

for local seismic events connected with particular active stopes. In both cases, they are very similar in shapes and differ by about 1.0.

An increasing interest in quantitative fractal analysis of seismic data from mines raised the question of the reliability of particular estimating procedures and the certainty of their results. By estimating the fractal dimensions for Monte Carlo simulated fractals, Lasocki and De Luca (1998) tried to determine how useful the box-counting, the number-radius, and the correlation integral methods are for identifying the features of geometry of epicenter distributions. The analysis showed that the dependence of dimension estimates on the epicenter distribution is complex and variable. It is clear from relation (3) that the clustering dimension, D_{cl} , is not sensitive to the variation of azimuth distributions of the polar system of coordinates as long as the position of the center of mass of a given set remains unchanged. Thus in some cases this measure can be inappropriate to monitor the tendencies of collinear ordering of epicenters. The relation between the correlation dimension D_2 and the distribution of radial coordinates was complex. It was concluded that for the same distribution of azimuth, the direction of the change of D_2 does not determine the direction of the change of radius distribution. The box-dimension, in turn, is largely independent of the radius distribution variation only. Conversely, both the correlation and box dimensions respond monotonically to the variation of azimuth distributions. In their final conclusion, the authors stated that neither the values nor the inequalities among dimension estimates are preserved when different methods of fractal analysis are used.

An interval estimation of fractal dimensions is the next topic of importance for a quantitative fractal analysis. The fractal dimension is usually estimated by the least-squares method applied to the logarithmized form of selected relation (2), (3), (4), or (6). For the actual finite data sets, however, the logarithmic linear range of these relations is placed between the so-called depopulation and saturation regions of r . The extent of these regions depends upon the number of points in the set and the linear size of the hypercube encompassing the set (e.g., Nerenberg and Essex, 1990) and, in general, cannot be readily estimated. In practice, the range of linearity is selected visually, and the errors and biases in fractal dimension estimates are generated in most cases by the choice of this range. In consequence, the variance of the regression parameter estimator, which can be readily evaluated, does not represent a true variance of the estimator of fractal dimension and cannot be used to determine its confidence intervals (e.g., Pickering *et al.*, 1995).

Cosentino *et al.* (1997) proposed assessment of the variance of clustering dimension D_{cl} through the random split of a fractal set into subsamples, estimating the dimension for every subsample and evaluating the variance of the sample comprising these dimension estimates. The results of this procedure applied to simulated fractal sets were encouraging, although the requirement of at least 600 events in the initial data set can be difficult to satisfy by actual data. De Luca *et al.* (1999) tested the same procedure for the correlation dimension on large multicluster sets with different hierarchical levels. The tests proved that the distribution of dimension estimates for subsamples obtained by random split is approximately normal. Thus the confidence intervals of the correlation dimension could be readily evaluated. The authors also provided approximate empirical formulas for the calculation of bias in dimension estimates. In order to avoid unrealistic requirements for the size of the data, De Luca *et al.* (1999) proposed use of a resampling procedure, similar to the bootstrap (e.g., Hall, 1992; Shao and Tu, 1995) in place of the random split into nonoverlapping subsamples. This new procedure was successfully applied to natural seismicity of Sicily and to seismic data from Polish coal mines.

A comprehensive study of bias and other effects incurred on the results of fractal analysis by limitation of actual data was presented by Eneva (1996). Her actual data set consisted of 14,338 seismic events recorded for 3 months within a $400 \times 400 \times 180 \text{ m}^3$ volume at Creighton mine in Canada. As the second actual set, she considered a subset of the first one, which comprised 1654 larger events. The spatial distribution of these data looked apparently like multifractal. Eneva (1996) repeated the fractal analysis of spatial distribution for four other sets of points, randomly generated within the parallelepiped encompassing the real data. The simulations assumed a uniform distribution of points and the monofractal distribution with a preset fractal correlation dimension. In both cases of the assumed distribution, either all generated points constructed test sets (regular simulation) or only those points that fell within a location error range from the hypocenters of actual data

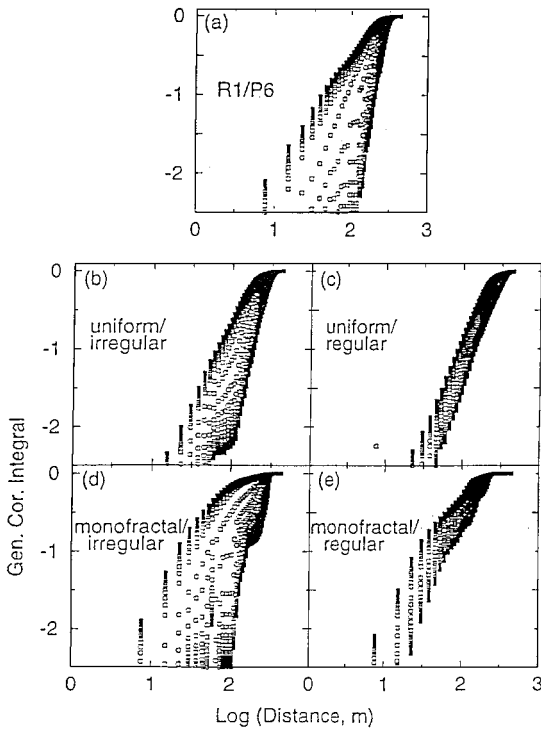


FIG. 36. Generalized correlation integrals of hypocenter distribution estimated from (a) actual seismic data from Creighton mine in Canada and (b)–(e) randomly generated point sets, for q from -25 to 25 . The simulations followed either uniform ((b), (c)) or monofractal ((d), (e)) distributions within the irregular ((b), (d)) or regular ((c), (e)) volumes outlined by the real data. [Eneva (1996), Fig. 3, reprinted with kind permission from Blackwell Science Ltd.]

(irregular simulation). Figure 36, reproduced from Eneva (1996), shows empirical $\log C^{(q)}(r)$ vs $\log r$ relations for the actual data set (Fig. 36a) and for the generated sets (Figs. 36b–e). The spatial distribution of points in every simulated set could be interpreted as multifractal. The relations obtained for monofractal irregular simulations (Fig. 36d) distinctly resemble those achieved for real data (Fig. 36a). The author concluded that strong multifractality of real data may be, in many cases, an artifact created by limitations of the data. She indicated that comparing fractal dimension estimates of data having different limitations or attributing to their values a particular physical meaning could lead to false conclusions. If data, however, come from the same environment, it is reasonable to assume that their limitations remain the same. In this connection Eneva (1996) concluded that a careful fractal analysis applied to seismic data from the same region could be used

to monitor time variations of the source distribution geometry. She also suggested the use of random simulations or bootstrap techniques in order to evaluate a bias implied by actual data limitations.

In addition to the studies to the geometry of event distributions in various domains, there is a number of works related to seismicity in mines, which try to infer a possible wider physical context of the observed fractality. It is generally accepted that earthquakes result from a nonlinear dynamic process (e.g., Kagan, 1994; Newman *et al.*, 1994). In particular, a description of natural seismicity through a self-organized criticality (SOC) of the crust (e.g., Bak and Tang, 1989; Carlson and Langer, 1989; Sornette and Sornette, 1989; Ito and Matsuzaki, 1990) is widely explored. The term SOC “refers to the spontaneous organization of a system driven from outside in a dynamical statistical stationary state, which is characterized by self-similar distributions of event size and fractal geometrical properties” (Grasso and Sornette, 1998). Thus although the fractality of distributions on its own does not imply that a system is a SOC state (Main *et al.*, 1994; Grasso and Sornette, 1998 and the references therein), self-similarity is a property strongly supporting this hypothesis and/or possible chaotic behavior of the system (e.g., Turcotte, 1989; Bak *et al.*, 1994).

The idea that seismically active rock mass of a mine might also be in a state of SOC was formulated by Grasso (1993), within a wider concept of induced SOC systems as the subsets of SOC proposed for tectonic earthquakes. He considered self-similarity in the source scaling and recurrence relations as the evidence for the SOC of seismicity in mines. Breaking of the linearity of recurrence relations was explained in terms of a finite size of local seismogenic volumes, e.g., mine pillars. A lifetime of an induced SOC system in mines was estimated from the time of activity decay after the stoppage of mining to a few tens of hours. Grasso (1993) also suggested that an observed disagreement between the spatial fractal dimension of distribution of seismic events and the fractal dimension of fault system of the active region could be attributed to the presence of aseismic instabilities. This induced SOC concept was explored later by Grasso and Sornette (1998) as evidence for a general self-organized criticality of the crust.

The state of SOC in the Sudbury Basin in Canada, encompassing 16 nickel-copper mines, was considered by Morrison *et al.* (1993) from spatial and temporal distributions of larger seismic events. They argued that a weak correlation between the origin times and locations of these events and the blasting times and locations of prominent geological structures points to chaotic behavior within a mine system.

Idziak (1999) studied fractal geometry in time and space of four spatial concentrations of larger, regional type, events from the Upper Silesian Coal Basin in Poland. He suggested, considering the observed fractality and an unexpected migration of seismic sources among active areas, that the whole region should be in a SOC state.

According to Mortimer (1997), the fractal character of temporal and spatial distributions of local seismic events, directly connected with mining of isolated longwalls, may also indicate that the mine rock mass is in a state of SOC.

Stacy *et al.* (1997) attempted to validate the idea of SOC in mines by simulating seismicity at Creighton mine in Canada by a 3D self-organized critical model. A network of 2D cellular automata distributed within the volume represented the fault structure of the mine, and the model was loaded from point sources following the actual blasting pattern. The simulated activity was then compared with the actual activity in the mine. Global characteristics of seismicity comprised a number of parameters including spatial and temporal fractal correlation dimensions. A chi-square testing procedure estimated the resemblance between these global characteristics of the actual and modeled seismicity to be about 95%.

A slightly different opinion on the mechanism of seismic event generation in mines was expressed by McGarr and Simpson (1997). They included seismic events from mines to a class of induced events, which are caused by large stress changes that result from mining or high-pressure liquid injection alone.

If a process is chaotic, due either to the SOC or other reasons, it could still be predictable, although in a limited sense. In the long term the process is not predictable but a short-term interval predictability is possible, provided the system is characterized by a low-dimensional strange attractor (e.g., Hilborn, 1994; Abarbanel, 1996). This possibility is of special interest for seismicity in mines where even short-term reliable forecasts could considerably increase the safety of miners. According to the theorem of Takens (1981), the phase-space of a dynamic system can be reconstructed from a time series of one of its observables, $s(t)$, using as a trajectory in a d -dimensional space, \mathfrak{R}^d the following vector $\vec{x}(t) = \{s(t), s(t + \tau), \dots, s(t + (d - 1)\tau)\}$, where τ is a constant time lag and d is an embedding dimension. The strangeness, i.e., the fractal dimension of an attractor, can be evaluated by using successive estimates of correlation integrals $C^{(2)}(r)$ (relation (1)) from $\vec{x}(t)$ for the increasing embedding dimension d (Grassberger and Procaccia, 1983). For every d there is a range of r where $\log C^{(2)}(r)$ scales linearly with $\log r$, and the slope $D_2(d)$ is the correlation dimension of the embedded phase-space. With the increasing embedding dimension, d , the correlation dimension $D_2(d)$ approaches a limit, D_2^l , which is the dimension of the underlying attractor. A minimal value of d , d_{\min} , from which $D_2(d)$ stabilizes, is considered as the dimension of the reconstructed phase-space. If the limit D_2^l does not exist, the series is likely to be random (e.g., Beltrami and Mareschal, 1993).

The dynamics of a d -dimensional phase space is characterized by d Lyapunov exponents, which are the average exponential rates of divergence or convergence of nearby trajectories (e.g., Wolf *et al.*, 1985). These exponents are all zero for integrable systems, at least one is positive for a chaotic system, and all are negative for periodic states. In the case of chaotic behavior, the value of the largest Lyapunov exponent λ_+ determines the predictability of the system.

Radu *et al.* (1997) used the algorithm of Grassberger and Procaccia (1983) to determine the strange attractor and the dimension of phase space of a seismic flow in mines. According to these authors, the seismic flow of rocks in a mined rock mass is complex, with turbulence that, in turn, is associated with chaotic behavior. The algorithm was applied to various parameters of seismic events from three areas in the Welkom goldfield in South Africa. These were the logarithm of seismic energy and seismic moment, the hypocenter coordinates, and the interevent distance and time of consecutive events. The time lag, τ , was chosen as the first zero of the linear autocorrelation function (Abarbanel, 1996)

$$C(m) = \frac{\sum_{k=1}^{N-m} (s_k - \bar{s})(s_{k+m} - \bar{s})}{\sum_{i=1}^N (s_i - \bar{s})^2}, \quad (7)$$

where $m = 1, 2, \dots, N$ is the number of events, s is the event parameterization and, $\bar{s} = \frac{1}{N} \sum_{i=1}^N s_i$.

Figure 37, reproduced from Radu *et al.* (1997), presents the obtained relations between the embedding dimension d and the correlation dimension of the embedded phase-space $D_2(d)$ for one of the studied seismic series. The authors concluded that all but one relation indicate that the phase-space is eight-dimensional. The dimension of the attractor was determined to be about 6.0. In one exceptional case (Fig. 37h), when the seismic series was parameterized by the interevent time, the phase-space looked four-dimensional and the dimension of the attractor was 3.3. Similar results from the seismic data from the other two areas led the authors to conclude that the process is chaotic with a low-dimensional strange attractor, and eight physical parameters are responsible for its dynamics. Furthermore, Radu *et al.* (1997) used the algorithm of Wolf *et al.* (1985) to estimate the greatest Lyapunov exponent, λ_+ , which turned out to be positive and ranged from 0.9 to 2.9. The average limits of predictability for considered cases, therefore, were estimated to be from a dozen hours to 10 days. The authors have not, however, presented the number of samples in the studied series.

Mendecki (1997c) described an application of the same procedure in studies of acceleration waveforms of two different types of seismic events. The fractal dimension of attractor was from 3.3 to 3.9 for the very small seismic event and 5.2 for the complex event associated with blasting. The largest Lyapunov exponent for the first case was 0.12–0.46, and for the second case it was 0.12. The author concluded that in both cases the propagation was chaotic and deterministic.

Cichy and Mortimer (1999) applied the algorithms for determining the dimension of strange attractor and Lyapunov exponents (Wolf *et al.*, 1985) to seismic data from the Belchatow open cast mine and from one stope at Katowice underground coal mine in Poland. They used the time series of the logarithms of event energy and times between the consecutive events. In both cases, the dimensionality of the

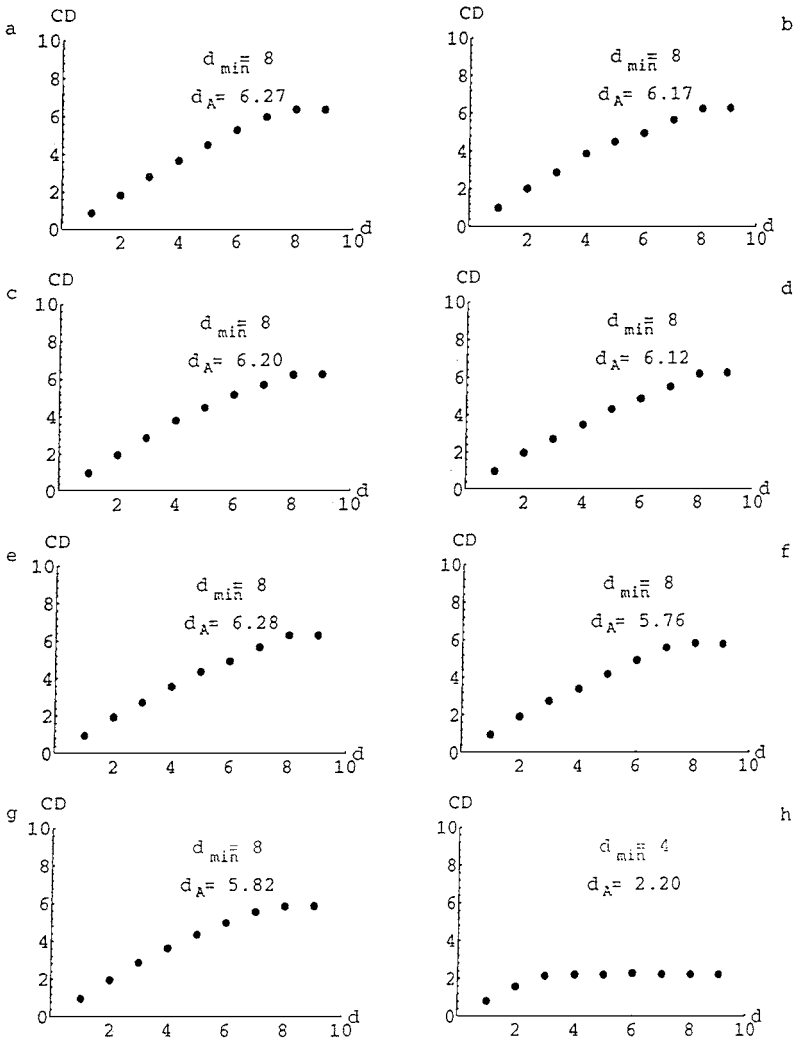


FIG. 37. Variation of the correlation dimension of embedded phase-space with embedding dimension d for a seismic series from a selected area of Welkom goldfield, South Africa, parameterized by (a) Logarithm of seismic energy, (b) logarithm of seismic moment, (c) x coordinate of hypocenter, (d) y coordinate of hypocenter, (e) z coordinate of hypocenter, (f) distance between hypocenters of the consecutive events, (g) interevent distance, including the source size, between the consecutive events and (h) interevent time between the consecutive events. d_A is the estimated fractal dimension of the attractor and d_{min} is the dimension of the reconstructed phase space. [Radu *et al.*, 1997, Fig. 9.8, reprinted from *Seismic Monitoring in Mines*, ©1997 Chapman & Hall, with kind permission from Kluwer Academic Publishers.]

phase space was determined to be between 7 and 9 (attractor dimension 3–3.5). The largest Lyapunov exponent was positive although very small.

Evidence for low-dimensional deterministic chaos governing the generation of seismic events, obtained from the algorithm of Grassberger and Procaccia (1983) of the phase space reconstruction or from the Lyapunov exponent evaluation, can be, however, strongly challenged because the size of analyzed samples is often insufficient. A conservative condition for the number of points, N , of a time series, required for a reliable estimation of the dimension of attractor D_2^I is, at least, $42D_2^I$ (Smith, 1988). More optimistic bounds proposed by Nerenberg and Essex (1990) and Eckman and Ruelle (1992) depend upon the diameter of the reconstructed attractor and other factors and range from $10^{D_2^I/2}$ to more than $10^{D_2^I}$. The number of points N needed to estimate Lyapunov exponents is about the square of that needed to estimate the dimension. Insufficient sample size could well be the reason of ambiguity of the results described above (phase space dimensionality depending on parameterization of seismic series, low Lyapunov exponents), and conclusions drawn in the described studies still need careful verification.

8. ASSESSMENT AND PREDICTION OF TIME-DEPENDENT SEISMIC HAZARD: STATISTICAL APPROACH

Here we review techniques based on seismic catalogs as principal input data, which provide indications on the present and future course of seismicity generation processes. Obviously, particular emphasis is put on estimating chances of the occurrence of seismic events that are hazardous for mining, usually strong events close to mining stopes. Recalling, however, the distinction between a rockburst and seismic event we note that such an approach narrows the problem of rockburst hazard assessment, which is a key interest of mine management, to the prediction of seismicity which can but does not necessarily have to result in rockbursts.

The term prediction, in turn, is used in a broader sense than just determination of time, location, and magnitude of a future event. Following the definition of earthquake prediction formulated by Kagan (1997a) we include into prediction or, more generally, into time-dependent seismic hazard assessment all techniques which provide time-dependent information relevant for undertaking decisions related to seismic risk. All these techniques accept in principle the variability in time of seismicity. Most of them deduce the future hazard from past-to-present time variations of a parameter or parameters estimated from seismic series.

We do not consider techniques for which seismic data are not the main input stream. Conversely, the methods, which make use of complementary, other than seismic, data are only occasionally mentioned.

The statistical sense of the time-dependent hazard assessment and prediction consists of the processing of series of seismic data. A rationale of prediction is an

expectation that such a series contains information that allows estimation of the further evolution of seismicity generation. In order to meet this condition a number of specific requirements must be met.

First of all, neither the generation of seismicity nor its parameterization can be governed by a process random in time, i.e., both stationary and memoryless. Given the seismic series parameterization ξ , the stationarity condition means that for every time moment t_i and t_j , the probability density function of ξ is $f(\xi|t_i) = f(\xi|t_j) = f(\xi)$. The process representation ξ is memoryless if its probability distribution at time t_i is independent of its values at previous times t_{i-1}, t_{i-2}, \dots . The values $\xi(t_i)$ for different t_i are then statistically independent, which implies that they are not correlated. In such a case the past does not have any influence on the present hazard which varies randomly in a way determined by the constant probability distribution.

From the practical point of view, however, we are not as much interested in the actual stochastic nature of the process as in its features reflected by the observations. The non-stationarity of the process can only be fruitful for prediction if this feature is represented in the recorded seismic series. In simple terms, this means that the data come from a time period covering significant process variations and that the average rate of event occurrence is greater than the average rate of these variations. Similarly, it is not enough that seismic signals generated by rock mass fracturing are correlated in general; this feature must also be detectable for the events from the observed magnitude range.

Seismicity in mines is under the dominant influence of mining (e.g., Gibowicz and Kijko, 1994). Mining activity itself varies in time and these variations take place during seismicity monitoring periods. Thus the non-stationarity of the event generation process can be expected, and its prints in seismic catalogs are commonly observed.

Statistical investigations of the stochastic nature of seismic series recorded close to mining stopes in underground coal mines in Poland were carried out by Lasocki (1992a) who tested the hypothesis of Poissonian structure of such series. If the event generation process were Poissonian, then it would be fully random, stationary, and memoryless, and the number of events N in a constant time interval Δt would follow the Poisson distribution

$$\Pr\{N = n; \Delta t\} = \frac{(\lambda \Delta t)^n}{n!} \exp(-\lambda \Delta t), \quad (8)$$

where λ is the constant mean rate of event occurrence. The interevent time, τ , would have an exponential distribution

$$f(\tau) = \lambda \exp(-\lambda \tau). \quad (9)$$

Four series from different mines were used to test the consistency between the sample distributions and distributions (8) and (9) implied by the Poisson process.

For long complete series, the hypothesis of consistency was rejected with very high probability. The Poissonian character of seismicity generation process, however, could not be excluded when the sampling period was shortened to 50 days. This result suggests that the recognized non-Poissonian structure of seismic series is more likely caused by time variations of the process itself rather than by a correlation between the events, which otherwise should be significant also in short samples. It was found that the series consisting of only large events tended to be Poissonian, which points to prediction of large events by the information carried by small events.

Lasocki (1992b) tested the consistency between the sample distribution of interevent time and the Weibull distribution for 14 seismic series from five Polish mines. The Weibull distribution, extensively used in survival analysis, describes the time distribution between the events in not fully random point processes. It represents a positive aging process (increasing occurrence rate process) when its shape parameter is greater than one, and a negative aging process (decreasing occurrence rate process) when the opposite is true. The Weibull distribution has occasionally been used for analysis of earthquake series (Hagiwara, 1974; Kiremidjian and Anagnos, 1984). Only the positive aging possibility was considered, which means that the longer the time has elapsed since the last event the more probable is the next event occurrence. The reason for this becomes obvious when a constant driving mechanism for earthquakes is accepted.

Surprisingly, the sample distribution of interevent time of mining events fitted the Weibull model quite well, but revealed the negative aging process. The probability of the next event occurrence seemed to decrease with the time elapsed since the last event. This result reflects a complex influence of irregular mining operations on seismic activity. In the utmost case, after stoppage or interruption of mining the negative aging is apparent: the event rate gradually decreases.

Kijko (1997) performed similar studies of interevent times from the 1-year data collected at one of deep gold mines in South Africa. The empirical cumulative distribution function of interevent time $F_{OBS}(\tau)$ was compared with the cumulative distribution function of the exponential distribution $F(\tau) = 1 - \exp(-\lambda\tau)$. A significant difference between $F_{OBS}(\tau)$ and $F(\tau)$ proved interrelations between the successive events. This time, however, the differences were mostly positive, which suggests the positive aging property. This positive aging extended to some 20 days.

Different results of these two studies are probably connected with different sources of nonrandomness in the studied samples. The mean rate of event occurrence, λ , in the series from the Polish mines was low, seldom reaching 10 events/day, and the nonrandom features found in the series from longer than 100-day periods were probably caused by time variability of the process. The South African data had $\lambda \approx 55$ events/day, and the positive interrelation was ascertained for interevent times shorter than 0.04 day. It is likely that this feature was due to the short time

correlation among the events, which cannot be found in sparse series. Thus, it seems that the nonrandomness of event occurrence in mines results predominantly from the time variation of event generation processes for long time scales and from event interrelations for short time scales. Moreover, there are intermediate-scale time periods from which the seismic series can be regarded as the outcome of Poisson process, a very important conclusion from practical point of view.

Most of the techniques for the assessment of time-dependent hazard introduce and analyze certain parameterizations of the observed series. The values of parameters, assigned to the present time, t , are usually estimated from the seismic data from a time window just preceding t . It is then implicitly assumed that the data from the considered window form a simple statistical sample, i.e., they are stationary and statistically independent. This requirement is, in general, in contradiction to the nonrandomness of seismicity. The last result from the described studies suggests, however, that there exists a window length for which such a condition is approximately fulfilled.

Fractal character of seismicity in mines in time, space, and energy/magnitude domains has been confirmed by the data from various regions (e.g., Coughlin and Kranz, 1991; Xie and Pariseau, 1992; Eneva and Young, 1993; Idziak and Zuberek, 1995; Mortimer and Lasocki, 1996a; Shivakumar *et al.*, 1996). It has been concluded, therefore, that the process of seismicity generation may be chaotic (e.g., Grasso, 1993; Mendecki, 1997c; Radu *et al.*, 1997; Grasso and Sornette, 1998). Such evidence for deterministic chaos in the generation of seismicity in mines is another argument against the randomness of this process.

The other evidence of interrelations between the time of occurrence of seismic events was given by Kijko (1997) who studied the Matsumara coefficient of randomness for the seismic catalog from a gold mine in South Africa. The coefficient, defined for interevent times, τ_i , as $C_r = [\sum_i \tau_i]^2 / \sum_i \tau_i^2$, is equal to $\pi/4$ for the Poisson occurrence, greater than $\pi/4$ for periodic events and less than $\pi/4$ for events clustered in time (Matsumara, 1984). For the studied series from mines, C_r was definitely less than $\pi/4$, although it depended on a lower cut-off of the apparent stress applied to the data. The interaction seemed to be the largest for small events.

The next important condition for a successful prediction is that the input data are more or less homogeneous, in that most of them result from the same process. Furthermore, the future seismicity that is a target of prediction must also result from the process, from which the analyzed data are collected. Regrettably, this condition is frequently violated. It is well known that seismicity induced by mining is generated by stress redistribution at different scales. Studies of the origin of seismic events in mines allows us to distinguish at least two classes of seismic events: local events directly connected with mining operations and regional events induced or triggered by mining (e.g., Gibowicz and Kijko, 1994).

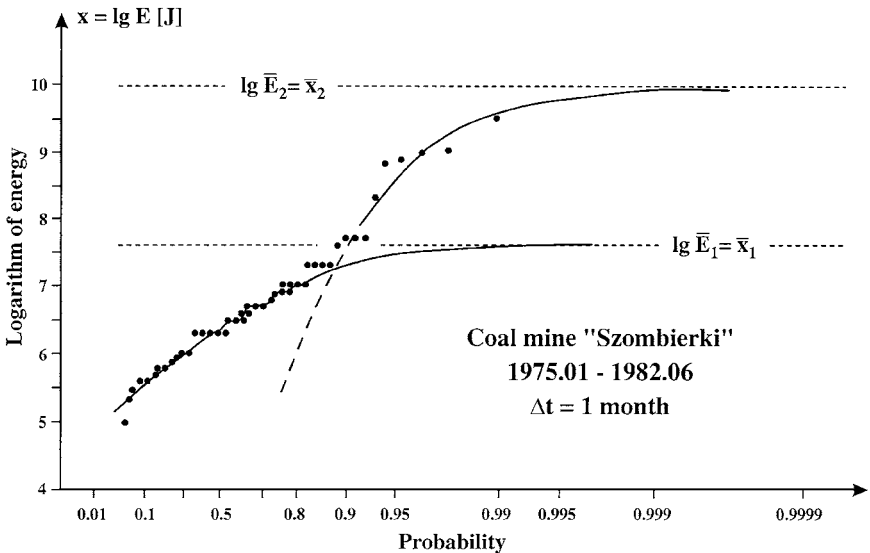


FIG. 38. Probability distribution of the monthly maximum seismic energy release at Szombierki coal mine, Poland, from January 1975 to June 1982. Continuous line indicates fits of the third Gumbel distribution. [Reprinted from Kijko *et al.* (1987), Fig. 2.]

The mixing of components from different processes in seismic series has been also confirmed by analyses of modality of magnitude, energy, or seismic moment distributions.

Kijko *et al.* (1987) studied the distribution of energy of seismic events from Polish coal mines using the extreme value theory of Gumbel (1962). If X is an outcome from a certain process (e.g., seismic energy or seismic moment release) of values $x_i, i = 1, \dots, n$, then its maximum values in equal time intervals, $y_k, k = 1, \dots, m$, form the outcome Y from the process of maximum generation. Gumbel has shown that when n tends towards infinity the distribution of Y , if it exists, can take only one form from the three possible. The first form is created by unbounded distributions like normal or exponential ones, the second by the distributions bounded from below, and the third by those bounded from above. The three Gumbel distributions are smooth and monotonic functions. In contrast, the empirical cumulative distributions of the largest seismic energies observed in mines are not smooth and distinct inflexions are observed. Figure 38, reproduced from Kijko *et al.* (1987), shows that the point of inflexion splits the empirical distribution into two branches, which can be modeled by separate curves of the third Gumbel distribution type. Such results led the authors to the conclusion that at least two seismic energy release modes, the high- and low-energy mode, are present in the studied seismic series. Similar results were obtained by Idziak *et al.*

(1991), who studied seismic series from an area of three geological units in the Upper Silesian Coal Basin in Poland.

The multimodality of magnitude distribution from seismic events in mines was also tested statistically (Lasocki and Węglarczyk, 1998). A nonparametric kernel density estimator was used to represent the sample distribution of magnitudes from a 1-month seismic series observed in a South African gold mine. It was evaluated by the critical smoothing test (Silverman, 1986) that the unimodality of the actual distribution was highly improbable.

The degree of sample homogeneity also strongly depends on the sampling constraints in terms of time, space, and event size. The problem of optimal selection of seismic data for hazard assessment is site dependent, since hazard depends on local geology, geometry of mine layouts, and characteristics of mining activity.

The events in seismic catalogs are described by a limited number of parameters, which usually are the time of occurrence, location coordinates, and at least one parameter describing the event strength: magnitude, seismic moment, or seismic energy. The series of values of these parameters form the input data for prediction. The information from these series is condensed, with some exceptions, in their parameterization and their anomalies should indicate the changes in seismic hazard. Such a "second-level" parameterization can use one parameter of the seismic event, becoming a one-parameter technique, or it can use more than one parameter, and then it is called a multiparameter technique. The prediction, on the other hand, can be based on analyses of one or more parameterizations. Then we have either univariate or a multivariate prediction. Within the multivariate approach we should distinguish between the quasi-multivariate and true multivariate methods. In the first case, the only general recommendation is to observe simultaneously more than one parameterization. In the second case, specific algorithms are needed to combine either parameterizations or their indications.

Validation is the next hot topic in statistical prediction. By the proper validation we mean any objective method which evaluates profits from a given prediction technique in comparison to the random guess. Such a method must evaluate a statistically significant number of applications of the prediction technique so that the actual probabilistic effectiveness of this technique can be estimated with high confidence.

As long as a prediction technique is not statistically validated, its effectiveness can always be questioned, no matter how strong its physical basis, how complex its algorithms, or how many so-called typical examples have been shown. This obvious statement is often overlooked and we note relatively few reports on the validation in comparison to the number of proposed prediction techniques. There are several reasons for such a situation. Most introduced techniques have adjustable parameters, for example, the length of time windows for estimating parameters, the dimensions of the volume from which seismic events are considered as input data, some weights, and others. Determination of the rules for optimal

selection of these parameters requires time-consuming studies of different seismic series. The validation can be done only after any such rules (though not necessarily optimal) are established, and it needs quite a bit of data. If access to the data is limited, then the whole procedure could become unfeasible.

The other difficulty is created by the validation procedure itself. There are no ready rules for this procedure; neither is there an agreement on the best measures of prediction efficiency. Similar problems encountered in the attempts to predict natural earthquakes have been discussed by Kagan (1997a).

We should also note a certain negative social conditioning regarding prediction of seismic hazard in mines. An understandable demand for accurate prediction and impatience of mining management often result in hastily publicizing procedures, when neither all their properties are known, nor their real efficiency has been fully tested.

8.1. Recurrence Relationships: Source Models for Stationary Seismic Hazard Analysis

Although the techniques reviewed herein do not necessarily deal with parameters used in traditional seismic hazard analyses, many of them have been developed from the well-known methodology in earthquake seismology (e.g., Cornell, 1968; Reiter, 1991). It is not strange, therefore, that the recurrence relationships describing the percentage of seismic events from a particular magnitude range in a given population are similar to those used to study natural earthquakes.

The applicability, even if approximate, of the well-known Gutenberg–Richter relation to seismic events in mines provides a handy and popular parameterization of the magnitude and energy distributions. Above a certain limiting value, M_{\min} , determined by the completeness of a seismic catalog, the logarithm of the number N of events of magnitude not smaller than M is linearly related to M : $\log N = a - bM$. A similar relationship can be written for the logarithm of seismic energy and for the logarithm of seismic moment. The constant a is determined by the event rate, λ , whereas b depends upon the ratio of large to small events. This classical relation can be readily converted into the probabilistic distribution of magnitude or energy. For magnitude it is the unbounded from above exponential distribution (Aki, 1965)

$$F(M) = \begin{cases} 0 & \text{for } M < M_{\min} \\ 1 - \exp[-\beta(M - M_{\min})] & \text{for } M \geq M_{\min} \end{cases}, \quad (10)$$

and for the seismic energy (or seismic moment) it is the Pareto distribution (e.g., Lasocki, 1989; Gibowicz and Kijko, 1994)

$$F(E) = \begin{cases} 0 & \text{for } E < E_{\min} \\ 1 - (E_{\min}/E)^{b'} & \text{for } E \geq E_{\min} \end{cases}, \quad (11)$$

where $F(\bullet)$ is the cumulative distribution function, $\beta = b \ln 10$, and b' is the slope parameter of log N vs log E relation.

To ensure a finite seismic energy release (Knopoff and Kagan, 1977), the Gutenberg–Richter relation is combined with an assumption on the existence of a physical upper limit of the magnitude range, M_{\max} , or the energy range, E_{\max} . The magnitude distribution takes the form of the bounded from above exponential distribution (Page, 1968; Cosentino *et al.*, 1977)

$$F(M) = \begin{cases} 0, & \text{for } M < M_{\min} \\ \frac{1 - \exp[-\beta(M - M_{\min})]}{1 - \exp[-\beta(M_{\max} - M_{\min})]}, & \text{for } M_{\min} \leq M \leq M_{\max}, \\ 1, & \text{for } M > M_{\max} \end{cases} \quad (12)$$

and the energy distribution is the truncated Pareto distribution (Lasocki, 1992c, 1993a)

$$F(E) = \begin{cases} 0, & \text{for } E < E_{\min} \\ \frac{1 - (E_{\min}/E)^{b'}}{1 - (E_{\min}/E_{\max})^{b'}}, & \text{for } E_{\min} \leq E \leq E_{\max}, \\ 1, & \text{for } E > E_{\max} \end{cases} \quad (13)$$

where M_{\max} and E_{\max} are characteristic for specific conditions of rock mass fracturing and must be estimated.

The shape parameter β of distributions (10)–(13) can be estimated by means of the maximum likelihood method (e.g., Aki, 1965; Utsu, 1965, 1966; Page, 1968; Kijko, 1982; Lasocki, 1989, 1992c; Gibowicz and Kijko, 1994), but the likelihood functions for relations (12) and (13) are monotonic with respect to M_{\max} and E_{\max} , and the statistical estimation of these upper bounds is not straightforward.

Kijko and Funk (1994) proposed three alternative methods of M_{\max} estimation for the seismic hazard assessment in mines. The simplest method estimates the upper bound of the magnitude distribution from the largest M_{\max}^{obs} and the second largest $M_{\max-1}^{obs}$ observed magnitudes (Robson and Whitlock, 1964)

$$\hat{M}_{\max} = 2M_{\max}^{obs} - M_{\max-1}^{obs}, \quad (14)$$

which can be considered as a rough but always available approximation of M_{\max} . The second method makes use of some properties of the end-point estimator of a uniform distribution and of the fact that any cumulative distribution function follows a uniform distribution within the interval (0,1). If it is assumed that the event magnitude follows the bounded from above exponential model (12) the

resultant estimator of M_{\max} is

$$\hat{M}_{\max} = -\frac{1}{\beta} \ln \left\{ \exp(-\beta M_{\min}) - \left[\exp(-\beta M_{\min}) - \exp(-\beta M_{\max}^{obs}) \right] \frac{n+1}{n} \right\}, \quad (15)$$

where n is the size of seismic catalog. The estimator depends upon the value of β , hence a recursive procedure must be used to obtain both β and M_{\max} simultaneously. Moreover, on some occasions the system of equations comprising Eq. (15) and the likelihood equation for β , $\partial l / \partial \beta = 0$, where l is the logarithmic likelihood function, has no solutions. The third method, used earlier in earthquake hazard studies (Kijko and Sellevoll, 1989), is based on the condition that the expected largest magnitude in the catalog is equal to the largest observed magnitude. In the case of magnitude model (12), the estimator for M_{\max} is

$$\hat{M}_{\max} = M_{\max}^{obs} + \frac{E_1(nz_2) - E_1(nz_1)}{\beta \exp(-nz_2)} + M_{\min} \exp(-n), \quad (16)$$

where $z_i = -A_i / (A_2 - A_1)$, $A_1 = \exp(-\beta M_{\min})$, $A_2 = \exp(-\beta M_{\max})$, and $E_1(\bullet)$ is the exponential integral function. This method also requires a recursive procedure to estimate the distribution parameters.

Kijko and Graham (1998) recently introduced a generic formula for the evaluation of maximum regional magnitude, which can be used for any distribution of magnitudes

$$\hat{M}_{\max} = M_{\max}^{obs} + \int_{M_{\min}}^{M_{\max}^{obs}} [F(M)]^n dm. \quad (17)$$

It was shown that when the cumulative distribution function of magnitude is given by relation (12), then estimator (16) is the approximate form of estimator (17). Kijko and Graham (1998) also considered the possibility of random variation of the Gutenberg–Richter parameter b and provided an alternative estimator to deal with such a case. A comparison of the performance of different estimators revealed better estimator efficiency, either with constant or with variable b , based on generic formula (17).

As in earthquake seismology, an increasing number of cases is reported from mines where the observed recurrence patterns differ significantly from the Gutenberg–Richter relation (e.g., Dessokey, 1984; Kijko *et al.*, 1987; Lasocki, 1987, 1993b; Subbaramu *et al.*, 1989; Johnston and Einstein, 1990; Urbancic *et al.*, 1992b; Trifu *et al.*, 1993; Finnie, 1994; Feustel, 1997; Lasocki and Węglarczyk, 1998). Evidence of the nonlinear structure of empirical log-frequency-magnitude distributions stimulated the search for nonlinear models of recurrence relationships that could better fit the observations. Lasocki (1987) tested the

goodness of fit of three theoretical models for magnitude distributions, the gamma, the Weibull, and a second-order power law derived from a parabolic form of the log-frequency-magnitude relation, to the seismic data from a selected stope of a coal mine. Out of these three models, the Weibull distribution of the cumulative distribution function

$$F(x) = \begin{cases} 0 & \text{for } x < x_0 \\ 1 - \exp[-\alpha(x - x_0)^\gamma] & \text{for } x \geq x_0 \end{cases}, \quad (18)$$

where x is either magnitude or the logarithm of seismic energy, x_0 is the lower limit of the model applicability, and α and γ are parameters, turned out to be the only good candidate for a model of magnitude or energy distributions. Unlike linear models (12) and (13), the Weibull distribution belongs to the class of so-called “soft” maximum magnitude models which do not have a rigorous upper limit of the magnitude range (e.g., Main and Burton, 1984; Kagan, 1997b). Detailed studies of this distribution, carried out on multiple well-populated seismic series from four mines, showed that the distribution can be used to model some unimodal and smooth nonlinear frequency–magnitude distributions (Lasocki, 1993b). This was also successfully used as a source model for seismic hazard analysis by Kijko *et al.* (1993) and Finnie (1994).

Regardless of their linearity or nonlinearity, all these parametric models of magnitude/energy distributions are unimodal at best. In many cases, however, the observed frequency–magnitude relations for seismic data from mines exhibit a multicomponent structure (e.g., Kijko *et al.*, 1987; Urbancic *et al.*, 1992b; Trifu *et al.*, 1993; Lasocki and Węglarczyk, 1998). In such cases the unimodal theoretical distributions may not fit the data. A recently proposed alternative to the parametric models, based on nonparametric, model-free estimators of the magnitude density, is expected to be suitable for linear as well as all kinds of nonlinear sample distributions of magnitude (Kijko *et al.*, 2000; Lasocki *et al.*, 2000). Given the sample data x_i , $i = 1, \dots, n$, the kernel estimator $\hat{f}(x)$ of an actual probability density function $f(x)$ is

$$\hat{f}(x) = \frac{1}{nh} \sum_{i=1}^n K\left(\frac{x - x_i}{h}\right), \quad (19)$$

where h is a positive smoothing factor and the kernel function $K(\bullet)$ is a probability density function symmetric around zero (e.g., Silverman, 1986). For the sample comprising event magnitudes, Kijko *et al.* (2000) used the Gaussian kernel function $K(\xi) = 1/\sqrt{2\pi} \exp(-\xi^2/2)$ and the least-squares cross-validation to estimate h (e.g., Bowman *et al.*, 1984), modified for the Gaussian kernel function. Assuming a sharp cut-off magnitude as a maximum magnitude M_{\max} , the nonparametric,

kernel estimator of the cumulative distribution function of magnitude is

$$\hat{F}(M) = \begin{cases} 0, & \text{for } M < M_{\min} \\ \frac{\sum_{i=1}^n \left[\Phi \left(\frac{M-M_i}{h} \right) - \Phi \left(\frac{M_{\min}-M_i}{h} \right) \right]}{\sum_{i=1}^n \left[\Phi \left(\frac{M_{\max}-M_i}{h} \right) - \Phi \left(\frac{M_{\min}-M_i}{h} \right) \right]}, & \text{for } M_{\min} \leq M \leq M_{\max}, \\ 1, & \text{for } M > M_{\max} \end{cases} \quad (20)$$

where $\Phi(\xi)$ denotes the standard Gaussian cumulative distribution function. From the simulation tests of efficiency, Kijko *et al.* (2000) concluded that estimator (20) provides results with tolerable and limited errors regardless of whether the sample distribution of magnitude follows the Gutenberg–Richter relation, is nonlinear unimodal, or is nonlinear multimodal.

8.2. Time Variations of Energy/Magnitude Distributions

The most popular technique for assessing the variation of seismic hazard in mines is probably the use of time variations of energy or magnitude distributions of the observed events. This approach has been used in Poland (e.g., Lasocki, 1982, 1993a), in South Africa (e.g., Kijko *et al.*, 1993; Stewart and Spottiswoode, 1993; Toper *et al.*, 1997), in the Czech Republic (e.g., Rudajev, 1993; Holub, 1995; Kalenda, 1995), and in Canada (e.g., Feustel, 1997; Trifu *et al.*, 1997).

Significant time variations of the Gutenberg–Richter b -value in mining induced seismicity and their potential for prediction were noted more than 20 years ago (e.g., Brady, 1977; Gibowicz, 1979). Since then, numerous confirmations of these variations have come from different countries. Opposite opinions, occasionally expressed, were either not substantiated empirically (e.g., Mendecki, 1997b, p. 194) or likely due to a data analysis not sufficiently precise. Urbancic *et al.* (1992b) and Young *et al.* (1992) concluded that b significantly changes in space but not in time. The studied data comprised seismic observations from a 2-month period within a specific region of Strathcona mine in Canada. Because of nonlinearity of the frequency–magnitude curve, the authors limited the magnitude range that was used to estimate the value of b . Excluding stronger events from the samples and using very narrow magnitude range (0.7 of a magnitude unit) resulted in most probably losing information on the time-variation of magnitude distribution.

The application of time changes of b for the time-dependent seismic hazard assessment in mines also has a relatively long history. In the early attempts (Lasocki, 1982), b values were estimated by the least-squares method (linear regression). Later the more robust and accurate maximum likelihood method was applied (e.g., Lasocki, 1989), although the least-squares (e.g., Stewart and Spottiswoode, 1993;

Holub, 1995; Kalenda, 1995, 1996) or weighted least-squares procedures (Trifu and Shumila, 1996; Trifu *et al.*, 1997) seem to be still in use.

The time-dependent b values provide at best a one-parameter technique for the hazard assessment, since b represents the distribution of magnitudes only. This distribution quantifies the probability that an oncoming event will be large, with no regard to the chance that the event will occur at all. The indications provided by the analysis of b value, therefore, should be integrated with information on the event rate.

In order to overcome this problem, Trifu *et al.* (1997) tried to analyze concurrent variations of a and b estimates of the classical unbounded frequency–magnitude relation. Their catalog comprised 1502 microseismic events ($M < 1$) that occurred during a 2-month period within a $200 \times 200 \times 200$ m volume at Strathcona mine in Canada. On the 28th day of the analyzed time interval a rockburst of $M = 2.9$ was recorded. The authors estimated b parameter and occurrence rates for a space–time grid. Figure 39, taken from Trifu *et al.* (1997), presents the b versus occurrence rate patterns for the intervals prior to and after the rockburst. Every b estimate is related to two occurrence rate estimates, connected with relatively smaller (filled circles) and larger (open circles) events, respectively. Trifu *et al.* (1997) interpreted the decrease in b prior to the rockburst (Fig. 39c) as due to a steady increase in the occurrence rate of the larger events, whereas the activity of the smaller events remained more or less constant.

Feustel (1997) presented similar retrospective studies of the data from an open-stope mine in eastern Canada. He analyzed time–space distributions of b and the number of events in order to identify the relations between the time-dependent hazard and the occurrence of ground falls. On all occasions, the falls were preceded by an increase in b values. It was suggested that this effect was associated with fracture development due to gravity.

An attempt to supplement the analysis of b time changes with another parameter of energy distribution was undertaken by Slavik *et al.* (1992) and Kalenda (1995). They used as the second parameter the energy value corresponding to zero of the left-hand side of the Gutenberg–Richter relation $\log N = a' - b' \log E$. This quantity, equal to $10^{(a'/b')}$, is related to a' . Thus, it can replace a' or the event rate in a 2D parameterization of the seismic energy flow, although its use as a measure of the upper limit of seismic energy results in a rather considerable over-interpretation.

A two-parameter approach, which fully integrates the time variations of the event rate and the distribution of magnitudes, was formulated by Lasocki (1993a). It was assumed that the series of seismic events connected with one mining stope results from the generalized Poisson process. The process is quasi-stationary in a time window suitable for a reliable estimation of its parameters, and the distribution of event energy is known. Thus the events are regarded as uncorrelated, which means that the probability distribution of the number of events in a constant time interval is given by the Poisson distribution (Eq. 8), but with the time-dependent λ . The

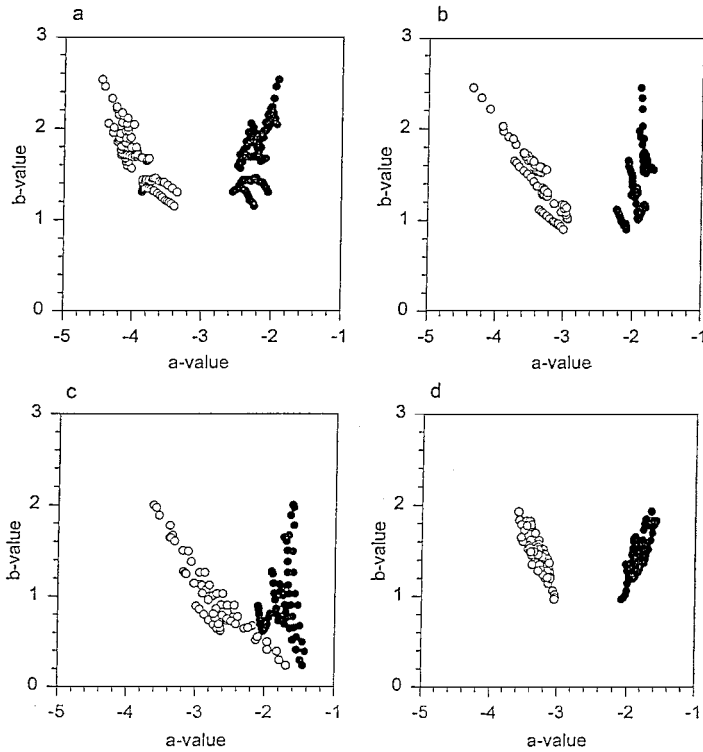


FIG. 39. Relations between the occurrence rates (a -value) of larger (open circles) and smaller (filled circles) events and b value for seismicity recorded in a 2-month period in a selected volume of Strathcona mine in Canada. (a) Days 0 to 9; (b) Days 9 to 18; (c) Days 18 to 24; (d) Days 47 to 54. A rockburst occurred on Day 28. [Trifu et al. (1997), Fig. 3, reprinted from *Rockbursts and Seismicity in Mines*, Proceedings of the 4th International Symposium, Krakow, Poland, 11–14 August 1997. 450 pp., EUR 137.50/US \$162.00/GBP97.00, A. A. Balkema, P.O. Box 1675, Rotterdam, Netherlands.]

seismic hazard is quantified by the probability that within a short time interval $[t, t + \Delta t]$ the events will occur and the first of them will exceed a prescribed value of the energy E_P

$$R(E_P, t) = \{1 - \exp[-\lambda(t)\Delta t]\}[1 - F(E_P; t)], \quad (21)$$

where $F(E; t)$ is the cumulative distribution function of energy, whose parameters vary in time. Three optional models of the distribution of energy were considered: the one-parameter Pareto distribution (Eq. 11) coming from the simple Gutenberg–Richter relation, the truncated (two-parameter) Pareto distribution (Eq. 13), and the Weibull distribution (Eq. 18).

The values of model parameters and event rate, λ , for a given time, t , are estimated from seismic data from a time window preceding t . The length of the

widow, selected according to the level of seismicity and the time variability of seismic activity, either is kept constant or is variable to maintain the same advance of mining front in every time window. Consecutive estimates of $R(E_P, t)$ for a moving time window represent variations of seismic hazard. Strong events are expected when values of R systematically increase or are high.

Lasocki (1993a) provided a comprehensive description of this technique, the maximum likelihood estimators of parameters, statistical tests of the energy distribution models, a discussion on adjustable parameter selection (e.g., time window length), and practical examples. Figure 40, reproduced from this work, presents the results of R estimation for seismicity recorded in an area of one longwall at Katowice coal mine in Poland during a 1-year period. The threshold, E_P , defining the strong event, was 10^6 J. The constant longwall advance of 30 m determined the time window, which was moved consecutively by 1 day. The time of occurrence of

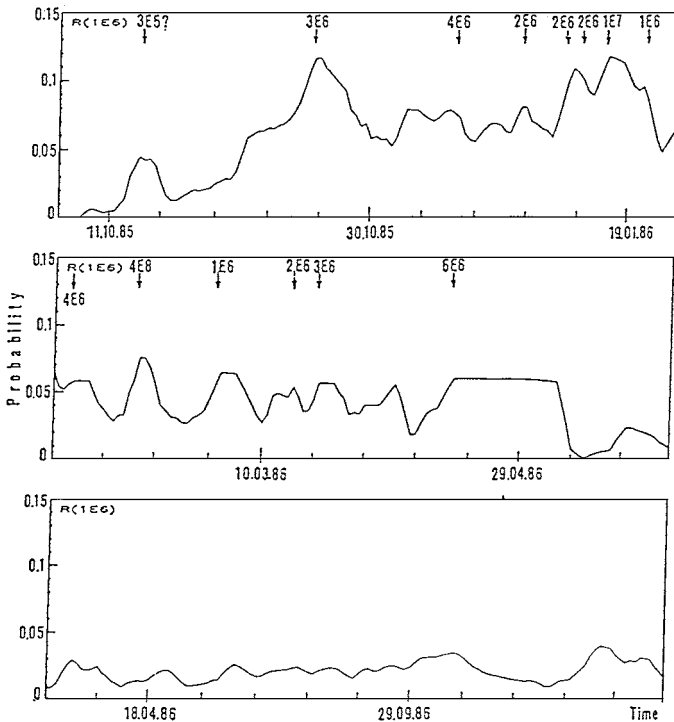


FIG. 40. Time-dependent probability of the occurrence of seismic events with energy $E \geq 10^6$ J in a longwall area at Katowice mine, Poland, shown for the sake of clarity on three separate graphs. The arrows mark the time of the occurrence of observed stronger events; their energy is also marked. [Reprinted from Lasocki (1993a), Fig. 6.]

strong events, marked by arrows, visibly correlates with local maxima of R . After numerous retrospective analyses of seismic series from various sites, the practical usefulness of this method has been confirmed and the method is used at some Polish mines for a routine day-by-day analysis of seismic hazard.

As a result of a relatively low event rate at Polish mines and consequently poorly populated time windows, the Polish applications of the described method are mostly based on a simple one-parameter Pareto model of energy distribution (Eq. 11). In some cases, however, the curvature of the frequency–magnitude relation may be significant and the classical Gutenberg–Richter relation may not be adequate. Kijko *et al.* (1993) used this method to analyze the spatially clustered seismic events from the Western Deep Levels gold mine, South Africa, recorded during a 1-year period. Seismic hazard was quantified by the probability of occurrence of a seismic event with a value of M greater than or equal to M_P

$$\Pr[M \geq M_P, t] = 1 - \exp\{\lambda(t)\Delta t[1 - F(M_P; t)]\}, \quad (22)$$

rather than by $R(M_P, t)$. A very high event rate (altogether, more than 14,300 seismic events) made it possible to apply the Weibull distribution (Eq. 18) as a model for event magnitude. In Fig. 41, taken from Kijko *et al.* (1993), a comparison is shown of the time-dependent estimates of the probability of event occurrence (Eq. 22), calculated using the classical Gutenberg–Richter exponential form (Eq. 10) and the Weibull model for magnitude. The correlation of occurrence of strong events, indicated by arrows, with local maxima of the Weibull-model-based estimates is distinctly better than of those provided by the exponential model. It was concluded that the Weibull model should be applied for small volume clusters of seismicity. The clusters of larger volumes show a more linear frequency–magnitude relation.

Finnie (1994) presented another retrospective application of this method based on the Weibull model for magnitude distribution. His catalog consisted of 5431 events that occurred in a selected area of the Far West Rand mining district in South Africa, observed during an 11-year period between 1982 and 1993. Figure 42, reproduced from Finnie (1994), shows the time-dependent probability of the occurrence of seismic events with magnitude $M_L \geq 3.8$. The analysis was done with a constant 1-year-long time window, moving every 3 months. The correlation between the actual occurrence of seismic events, indicated by bars, and the increasing branches or local maxima of the probability curve is rather good.

Lasocki (1993a) also proposed a new version of this time-dependent hazard analysis, based only on the largest energies from nonoverlapping, equal time intervals covering the time window. Assuming a Poissonian structure for seismic series in a given time window, the exact distributions of maximum energy for all three options of underlying distributions (11), (13), and (18) and the maximum likelihood estimators of their parameters were introduced. It was suggested that this version of the analysis can be used when the data due to the process under study are mixed with other seismic data, unimportant for the undertaken analysis,

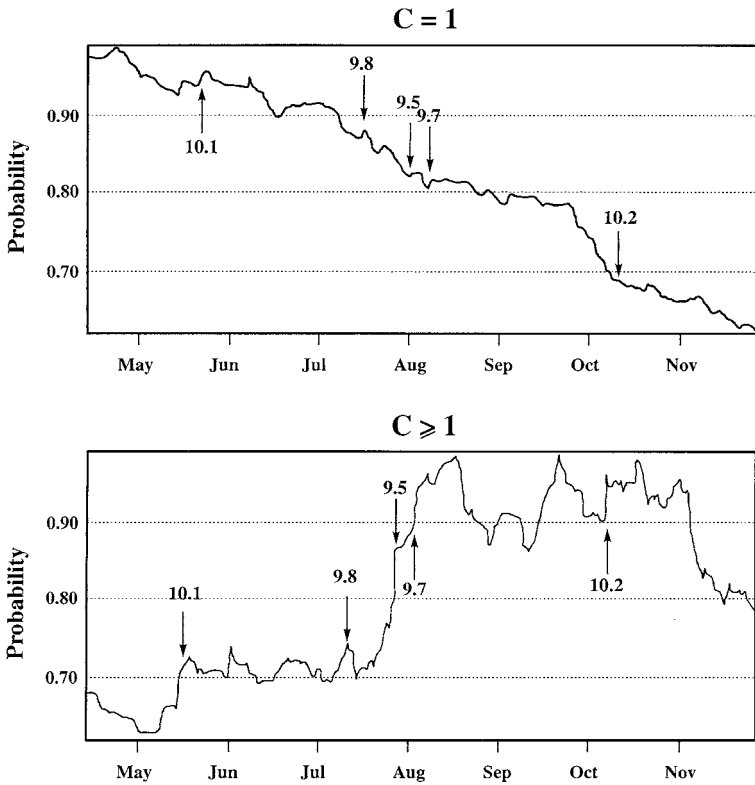


FIG. 41. Comparison of probabilities of the occurrence of larger events in a selected volume in Western Deep Levels gold mine, South Africa, estimated using the classical Gutenberg-Richter exponential form (top) and the Weibull model for magnitude distributions (bottom). The time of the occurrence of observed events is marked by arrows. [Kijko et al. (1993), Fig. 4, reprinted from *Rockbursts and Seismicity in Mines*, Proceedings of the 3rd International Symposium, Kingston, Ontario, 16–18 August 1993. 462 pp., EUR 154.00/US \$181.00/GBP108.00, A. A. Balkema, P.O. Box 1675, Rotterdam, Netherlands.]

or when the input is somehow contaminated (e.g., the level of completeness changed during the period of observation).

A three-parameter time-dependent seismic hazard assessment method, which integrates information supplied by the time of event occurrence, its seismic energy, and seismic moment, and, furthermore, accounts for a possible correlation among the events, was presented by Kijko and Sciocatti (Kijko, 1996, 1997 after Kijko and Sciocatti, 1995b). The method was fostered by the well-known fact that the events in a foreshocks–main shock–aftershocks sequence are strongly correlated and, as such, are not Poissonian. Thus, if such sequences are present in the seismic

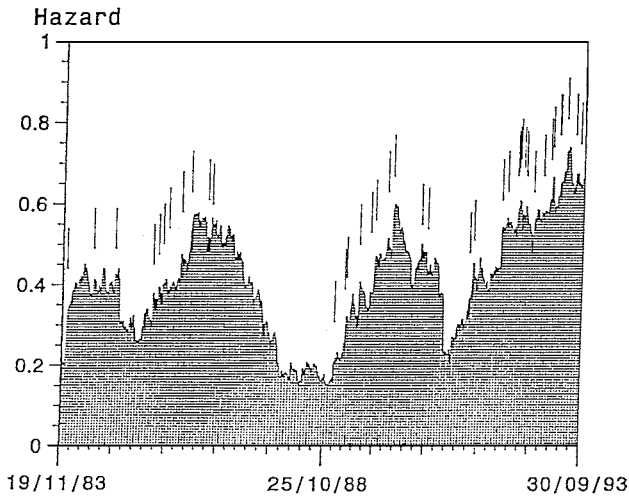


FIG. 42. Estimates of probability of the occurrence of seismic events with magnitude $M_L \geq 3.8$ for a selected area in the Far West Rand mining district in South Africa, based on the Weibull model for magnitude distributions. The time of the occurrence of observed events is indicated by vertical bars. [Reprinted from Finnie (1994), Fig. 3.]

series from a mine, the assumption about the Poissonian structure of the series in the time window may not be valid. Kijko and Sciocatti (1995b) introduced an alternative assumption that the seismic series consists of statistically independent (uncorrelated) clusters of events, but that the events within individual clusters are correlated. It was also assumed that the event size is expressed independently by seismic moment and seismic energy, whose bivariate distributions are the same for all the events, and that the cluster of events always starts from the strongest (main) event. The conditional intensity function, i.e., the probability of the occurrence of an event with energy E and seismic moment M_0

$$\Lambda(E, M_0) = \lambda \cdot f(E, M_0) + \sum_i \nu(E_i, M_{0i}) \cdot f(\tau) \cdot f(E, M_0) \quad (23)$$

comprises two terms. The first term describes the Poissonian occurrence of the main events, in which λ is the mean activity rate of the main events, and $f(E, M_0)$ is the probability density of the energy-seismic moment. The second term is responsible for the occurrence of dependent events following the main event. In this term $\nu(E_i, M_{0i})f(\tau_{ij})f(E_{ij}, M_{0ij})$ is the conditional distribution of the j -th event dependent on i -th main event, where $M_{0i} > M_{0ij}$ and $E_i > E_{ij}$, τ_{ij} is the time between the occurrence of the main and the j -th events and its probability density is $f(\tau)$.

Two models for the energy-seismic moment distribution were proposed. The

unbounded model assumes that the 2D random variable $[E, M_0]$ follows a bivariate power-law distribution

$$f(E, M_0) = \begin{cases} \frac{\beta(\beta + 1)}{E_C M_{0C}} (E/E_C + M_0/M_{0C} - 1)^{-\beta-2} & \text{if } E \geq E_{\min} \\ & \text{and } M_0 \geq M_{0\min}, \\ 0 & \text{otherwise} \end{cases} \quad (24)$$

where β , E_C , and M_{0C} are model parameters, and E_{\min} and $M_{0\min}$ are the levels of completeness of the data in energy and seismic moment domains, respectively. The assumption of finiteness of the upper boundary of both the energy and seismic moment domains modifies the density function (24) to

$$f(E, M_0) = \begin{cases} K \cdot (E/E_C + M_0/M_{0C} - 1)^{-\beta-2} & \text{if } E_{\max} \geq E \geq E_{\min} \\ & \text{and } M_{0\max} \geq M_0 \geq M_{0\min}, \\ 0 & \text{otherwise} \end{cases} \quad (25)$$

where E_{\max} and $M_{0\max}$ are the respective boundaries and

$$K = \frac{\beta(\beta + 1)}{E_C M_{0C}} \left[1 - \left(\frac{E_{\max}}{E_C} \right)^{-\beta} - \left(\frac{M_{0\max}}{M_{0C}} \right)^{-\beta} + \left(\frac{E_{\max}}{E_C} + \frac{M_{0\max}}{M_{0C}} - 1 \right)^{-\beta} \right]^{-1}.$$

The model for the event interdependency is similar to that formulated by Kagan (1991). The function $v(E_i, M_{0i})$ takes the form

$$v(E_i, M_{0i}) = k M_{0i}^{\gamma}, \quad (26)$$

where k and γ are parameters, while the time-probability density is

$$f(\tau) = \frac{\alpha \tau_0^\alpha}{\tau^{\alpha+1}}. \quad (27)$$

As in previous methods, it is assumed that time variations of the conditional intensity function (23) stem from the time variations of all the nine parameters α , β , γ , λ , k , E_C , M_{0C} , E_{\max} , and $M_{0\max}$, whose values for time t can be estimated from seismic events from the time window preceding t . The details on estimation of these parameters can be found in the work of Kijko (1996). Having determined the parameters, the probability that an event will occur within a time interval $[t + \Delta t]$ after the last event, with the energy within $[E_C, E]$ and the seismic moment within $[M_{0C}, M_0]$, is

$$\Pr(E, M_0, t) = 1 - \exp \left\{ - \int_t^{t+\Delta t} \int_{E_C}^E \int_{M_{0C}}^{M_0} \Lambda(\xi, \zeta, v) d\xi d\zeta dv \right\}. \quad (28)$$

Kijko and Sciocatti (1995b) used this approach to analyze a series of 292 events recorded for 153 days in an area of a stope at a gold mine in South Africa. They applied the time window of a constant length of 20 days, moved every 12 hours,

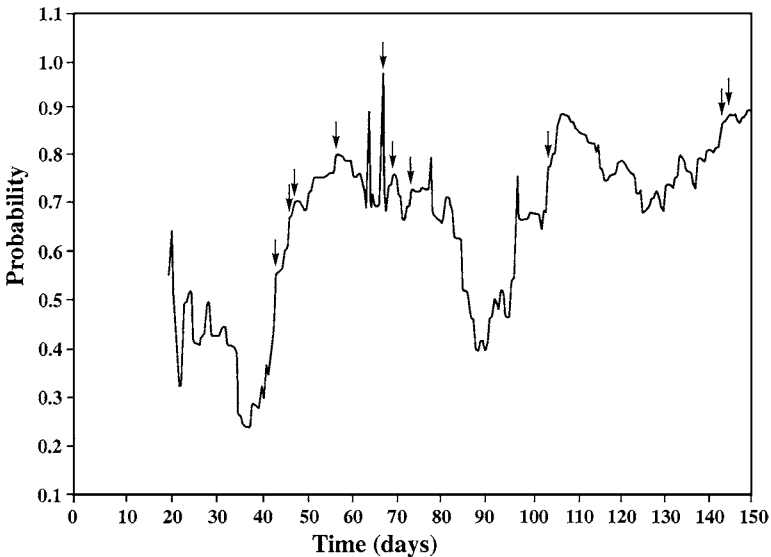


FIG. 43. Estimates of probability of the occurrence of seismic events with energy $E \geq 5.5 \times 10^5$ J in a stope area at a gold mine in South Africa, based on the three-parameter time dependent hazard assessment method. The time of the occurrence of observed events is marked by arrows. [Reprinted from Kijko (1996), Fig. 5.9.]

to estimate the probability of occurrence of an event with energy $E \geq 5.5 \times 10^6$ J in the next $\Delta t = 10$ days. It was also assumed that if the event was closer than 1 hour to the preceding event, it belonged to the same cluster. The results of the analysis are shown in Fig. 43, reproduced from Kijko (1996).

A simple model-free approach to the time variations of one-parameter representation of seismic energy distributions has gained some popularity in the Czech Republic and in Slovakia (e.g., Slavik *et al.*, 1992; Rudajev, 1993; Holub, 1995; Kalenda and Pompura, 1996). A cumulative curve of the square root of the total energy released in consecutive time windows, called the Benioff graph, represents the seismic energy flow in the rock mass. Nonlinearity of this curve, in particular a faster increase followed by a certain slow-down, is considered as a precursor to a larger event. A typical example of such a graph is shown in Fig. 44, reproduced from Kalenda and Pompura (1996). The analysis was carried out for microseismic data from an area of one chamber at Jalsava magnesite mine in Slovakia. The nonlinear features of the graph, marked by rectangles, were correlated with the occurrence of rockbursts.

Not many papers are available that are devoted to testing the efficiency of prediction techniques based on a distribution of magnitude or energy. Lasocki (1993a) studied the correlation between the seismic hazard, estimated using linear (Eq. 11) and nonlinear (Eq. 18) models of energy distribution, and the actual hazard. The

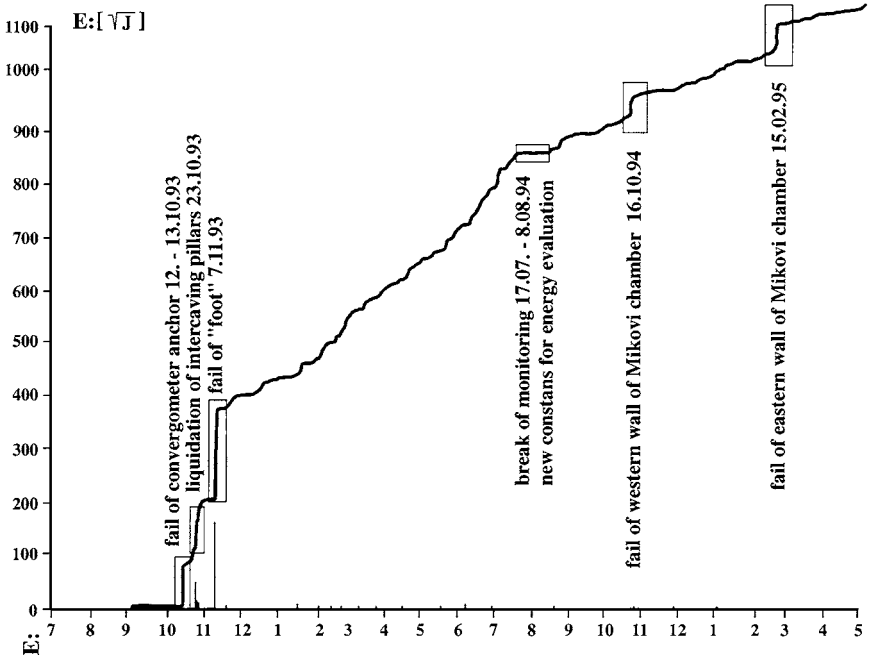


FIG. 44. Cumulative square roots of the daily energy release in one chamber at Jalsava magnesite mine in Slovakia from July 17, 1993, to May 1, 1995. S-type nonlinear features, marked by rectangles, correlate with the occurrence of rockbursts. [Kalenda and Pompura (1996), Fig. 2, reprinted with kind permission from the Institute of Rock Structure and Mechanics, the Academy of Sciences of the Czech Republic.]

study comprised five seismic series from different coal mines. The periods of observation were split into consecutive nonoverlapping time intervals. In every interval the expected number of strong events was estimated from the considered models. The significance of Spearman's rank correlation between the series of estimated numbers and the series of actual numbers of strong seismic events was then evaluated. In all five cases, one case of nonlinear model and four cases of linear model, the correlation turned out to be highly significant. The significance of the overall correlation of results from all mines studied was greater than 0.99999. It was concluded that all the models considered for the energy distribution have high potential to estimate the actual seismic hazard.

In another work (Lasocki, 1994), correlation analysis was applied to investigate the potential for prediction of the technique of time-dependent seismic hazard assessment. The studies comprised eight local seismic series. The significance of correlation between the number estimated from relation (21) and the actual number of strong events was found to range from 0.956 to 0.99993.

Among the four parameters introduced by Stewart and Spottiswoode (1993) for seismic hazard assessment, one was the estimate of the number of events corresponding to a given critical magnitude, M_p , obtained from the Gutenberg–Richter relation determined from 40 events. As a measure of the performance of every parameter the authors used the gain, which was defined as the ratio of the percentage of the total number of larger events occurring during the periods of the parameter anomaly to the percentage of the total time of the anomaly. This gain can be useful as an indicator of the prediction efficiency only if both the total time of anomaly and the number of events associated with the anomaly are considerable. Otherwise it can reach very large values by chance. The authors did not provide a global summary of the performance of the parameters but presented only some of the results. The parameter connected with the Gutenberg–Richter relation displayed a variable gain, dependent upon the definition of the anomaly, but in most cases the gain was greater than one—the level of randomness.

Kalenda (1996) considered the efficiency of prediction based on time-variations of b -value, the slope of Benioff graph, and the anomalous increase of event rate. He concluded from unequivocally defined rules of the game that 21 out of 25 strong events, identified in the studied data set as directly linked to mining, could have been predicted. The other strong events, identified as “regional,” were determined as unpredictable.

8.3. Parameterization of Spatial Distributions of Seismic Events

It is well known that seismic sources in mines are not distributed randomly in space but tend to concentrate in certain areas, forming clusters of various shapes. It is also known that this spatial distribution is not constant in time. Some of the time-dependent features of source distributions are clearly linked to the variable geometry of mining stope. The others seem to respond to internal changes during the process of rock mass fracturing.

A preparatory process leading to a rockburst may comprise different phases. At the early stage an external geometrical factor like a local geological discontinuity or mining remnants may start to affect the local stress field connected with the stope. This process may yield new stress concentration zones, which can be more seismically active. Such zones may be either isolated or connected with the zone of background activity surrounding the stope. As the preparatory process develops these zones may change both the shape and the location. In later stages of the process a certain clustering of events around a place of the future main event is expected (e.g., Ohnaka, 1992; Xie, 1993). This effect implies, in general, some ordering of the distribution of seismic sources, such as alignments, coplanar tendencies, etc.

Attempts to use the temporal changes of space distribution of mining seismicity in prediction of strong events have been undertaken for a long time. At first, they were limited to visual inspections of hypocentral maps and cross sections (e.g., Blake, 1980; Brink and O'Connor, 1984; Sato and Fuji, 1988). A more sophisticated quantitative approach was introduced during the 1990s. The reasons for growing interest in the studies of spatial distributions of seismic sources are obvious. The mechanism linking the distribution changes with increasing hazard seems to be straightforward. The expected changes also seem to be readily identifiable. Eneva and Ben-Zion (1997) even suggested that spatial distribution could be as informative as magnitude distribution. Finally, since source location is an independent parameterization of the seismic series, the analysis of its distribution could provide an independent hazard estimate, which could be eventually used, together with information coming from other parameterizations, in a multivariate prediction.

It is well documented that spatial distribution of seismic sources has a statistical fractal character. The fractal dimension quantifies a level of clustering of objects that build the fractal. The evolution of the fracturing process prior to the main event is expected to modify the geometry of source distributions. We hope, therefore, that these modifications are reflected in changes of the fractal dimension or multifractal spectrum. Since it is speculated that the distribution changes tend to increase its orderliness, then a drop in the fractal dimension may indicate an impending large event.

Coughlin and Kranz (1991) were probably the first who used fractal analysis to study temporal variations of the spatial distribution of microseismic events induced by mining. Using the data from two stopes at Galena mine, USA, from the time periods comprising damaging rockbursts they showed qualitatively that the fractal correlation dimension (relations 1 and 2) varies in time. On at least two occasions, a decrease in the dimension prior to a rockburst was noted. It was also observed that the periods of intense blasting or just following the main bursts could be associated with a decrease of fractal dimension.

Xie and Pariseau (1992) and Xie (1993) reported a significant correlation between the decrease of the fractal clustering dimension (relation 3) of spatial distribution of small events and the occurrence of significant failures of mined rock mass. Figure 45, reproduced from Xie (1993), shows the clustering dimension for five consecutive days preceding a rockburst in a pillar at Galena mine. Prior to the rockburst the spatial distribution of seismic sources reached the lowest fractal dimension. The other study of microseismicity data from a United States deep coal mine indicated a close correspondence between the low fractal dimension and the occurrence of rockbursts or bumps, whereas the dimension maintained high values in the peaceful periods of mining (Xie, 1993).

These encouraging results have evoked interest in using the spatial fractal dimension of sources as a precursor to strong events. The fractal dimension was considered as the only precursory parameter (e.g., Mortimer and Lasocki, 1996a,b;

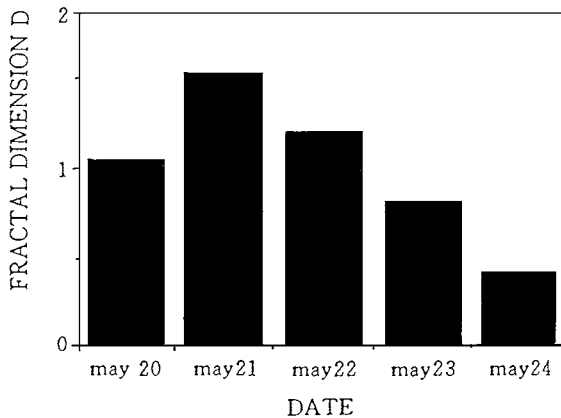


FIG. 45. Time variations of clustering dimension of spatial distribution of microseismic events for a pillar at Galena mine in USA for 5 days before the occurrence of a rockburst. [Xie (1993), Fig. 14.42, reprinted from *Fractals in Rock Mechanics*, Geomechanics Research Series I, 464 pp., EUR 93.50/US \$110.00/GBP66, A. A. Balkema, P.O. Box 1675, Rotterdam, Netherlands.]

Mortimer, 1997; Mortimer and De Luca, 1999) or as combined with other parameters describing the distribution of events (e.g., Eneva and Young, 1993; Stewart and Spottiswoode, 1993; Eneva and Villeneuve, 1997; Eneva, 1998; Lasocki and Mortimer, 1998).

Stewart and Spottiswoode (1993) introduced four parameters for seismic hazard assessment. One was related to the distribution of magnitude and another was the median seismic stress drop. The remaining two were connected with the spatial distribution of seismic sources. These are the reciprocal of the spatial fractal dimension estimate and the reciprocal of the median distance between event pairs. They were considered to represent different features of source geometry, namely the orderliness and scale of clustering of events. Daily values of these parameters were estimated from the seismic series recorded at an experimental site of a preconditioning experiment at the Blyvooruitzicht gold mine in South Africa (Adams *et al.*, 1993). Every single value was determined from 40 seismic events. All parameters exhibited considerable variations in time. Stewart and Spottiswoode (1993) used their gain over the randomness to estimate the efficiency of introduced parameters. In the examples of the results they demonstrated that if the percentage of the total time of anomaly was kept constant at 20%, the gain was 1.95 for the reciprocal of the fractal dimension and 1.65 for the reciprocal of the median distance between the events. The other two parameters were more efficient. Their respective gain was 2.55 for the parameter quantifying the distribution of magnitude and 2.8 for the median stress drop. It was concluded that the introduced parameters, including the parameters, including the parameters related to the spatial distribution of events, have certain potential to assess time-dependent hazard. Although these parameters

represent different features of rock mass fracturing, they behave in a complementary way, and they should be used therefore in combination rather than individually.

Eneva and Young (1993) studied 1654 seismic events recorded during a 2-month period in a volume of $400 \times 400 \times 180 \text{ m}^3$ at the Creighton nickel-copper mine in Canada. Six events of magnitude not smaller than 2.0 occurred within the studied volume. Two others were located within a margin of 150 m outside of this volume. The analysis comprised estimation of time changes of the degree of spatial nonrandomness and spatial fractal correlation dimension. The degree of spatial nonrandomness measures the discrepancy between the distribution of actual interevent distances and the distribution of distances between points simulated uniformly within the volume occupied by the actual events. For any N points in a volume this degree of nonrandomness for the distance range $[a, b]$ is evaluated as

$$c_{[a,b]} = \pm 100\% \sqrt{\left| \frac{\sum_{i=i_a}^{i=i_b} \Delta p_i}{P} \right|}, \quad (29)$$

where Δp_i is the excess (plus) or deficiency (minus) of event pairs with respect to the reference random distribution in the distance interval i , and $P = N(N - 1)/2$ is the total number of pairs for N events. The summation extends over all intervals from the one to which a falls (i_a) to the last one to which b falls (i_b). The authors evaluated the degree of nonrandomness over the range $[0, 76 \text{ m}]$ and the correlation dimension from overlapping groups of 100 events moved with a step of 20 events. The values obtained were considered to be associated with the times of occurrence of the last event in each group. Figures 46 and 47, reproduced from Eneva and Young (1993), present the results of the analysis, where solid lines and filled

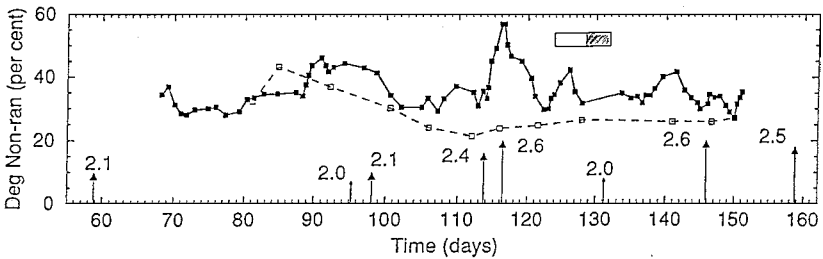


Fig. 46. Temporal variations of the degree of spatial nonrandomness of seismicity recorded for 2 months in a selected volume at Creighton nickel-copper mine in Canada. The solid and dashed lines show the results for induced events and blasts, respectively. The arrows mark larger events located within the volume (large arrowheads) and in the marginal zone outside the volume (small arrowheads); their magnitudes are also marked. [Eneva and Young (1993), Fig. 7, reprinted from *Rockbursts and Seismicity in Mines*, Proceedings of the 3rd International Symposium, Kingston, Ontario, 16–18 August 1993. 462 pp., EUR 154.00/US \$181.00/GBP108, A. A. Balkema, P.O. Box 1675, Rotterdam, Netherlands.]

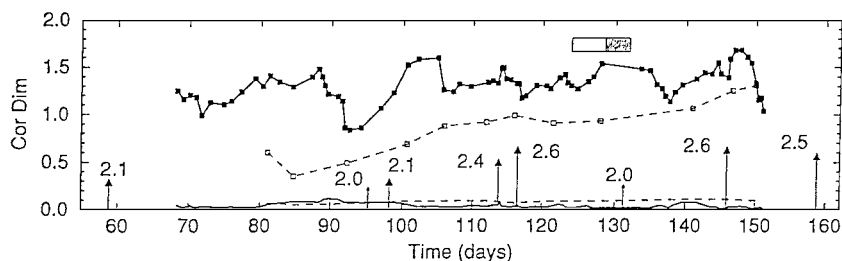


FIG. 47. Temporal variations of the correlation exponent dimension of seismicity recorded for 2 months in a selected volume at Creighton nickel–copper mine in Canada. The solid and dashed lines show the results for induced events and blasts, respectively. The arrows mark larger events located within the volume (large arrowheads) and in the marginal zone outside the volume (small arrowheads); their magnitudes are also marked. [Eneva and Young (1993), Fig. 8, reprinted from *Rockbursts and Seismicity in Mines*, Proceedings of the 3rd International Symposium, Kingston, Ontario, 16–18 August 1993, 462 pp., EUR 154.00/US \$181.00/GBP108, A. A. Balkema, P.O. Box 1675, Rotterdam, Netherlands.]

squares represent the values of the degree of spatial nonrandomness and the fractal correlation dimension, respectively. Dashed lines and open squares represent the same quantities for the events identified as blasts. The vertical arrows mark the days of occurrence of strong events, either located within the volume under the study (large arrowheads) or located in the marginal zone outside of the volume (small arrowheads). The authors concluded that an increased degree of nonrandomness preceded most of the larger events. They also identified two decreases of the fractal correlation dimension prior to larger events, two increases after the events, and one pair of larger events not associated with any change of this parameter.

Using the same technique to process data from the same volume of Creighton mine but from a different time interval, Eneva (1998) applied an original procedure to determine the prediction efficiency of the analyzed parameters. The procedure called the association in time (Eneva and Ben-Zion, 1997) compares the time of appearance of local extremes of the tested parameter with the time of occurrence of strong events. A separate count of local maxima and local minima in consecutive days preceding and following every strong event, respectively, provides the association frequency for the parameter in four categories: preceding minima, preceding maxima, following minima, and following maxima, respectively. If an extreme occurred between two events, it is considered to be associated with the event closer in time. In this way the classification of the extremes into “preceding” and “following” is equivocal.

In addition to the degree of spatial nonrandomness and spatial correlation dimension, Eneva (1998) studied the time interval of occurrence of a constant number of events, as a third candidate for the precursor to strong events. Moreover, since the results of previous studies were ambiguous with regard to the sign of anomaly

of the tested parameters, a possibility was tested of local maxima as well as local minima preceding strong events. The results were not unique and were strongly dependent on the data taken for the analysis. From 20 to 80% of the larger events were preceded by a minimum degree of spatial nonrandomness over the range [0, 75 m]. From 40 to 80% of such events were preceded by the maximum of the spatial correlation dimension, and from 60 to 80% by the maximum of the time interval. These results suggested, contrary to the earlier expectations, that the nonrandomness and orderliness of spatial distributions decrease prior to a main failure. The observed drop of event rate could support the well-known hypothesis of a preceding quiescence. Because the analysis is based, however, on only nine strong events that occurred during the period of study, these suggestions are not conclusive.

Eneva and Villeneuve (1997) analyzed extended databases from the same area, covering 3.5 years of observations. Apart from the already described parameters related to the spatial distributions and event rate, the study considers two other quantities connected with blasting. The potential for the prediction of all parameters was determined with the use of the association in time procedure. Although, in selected time intervals, the particular parameter performance was very good (e.g., precursory maxima within 6 days before 90% of the larger events), no simple and stable precursory patterns could be identified over long periods of time. It was therefore suggested using for prediction a combination set of parameters rather than relying on any single parameter. More than 70% of the larger events were found to be preceded, with 10 days lead-time, by the local extremes of at least two out of the considered six parameters.

The use of spatial and temporal fractal dimension estimates to assess the local time-dependent seismic hazard in mines was investigated by Mortimer and her colleagues (e.g., Mortimer and Lasocki, 1996a,b; Mortimer, 1997; Lasocki and Mortimer, 1998; Mortimer and De Luca, 1999). The studies were performed on seismic series recorded in the direct vicinity of mining longwalls. The source locations were related to a local system of coordinates connected with the advancing front. Three estimators of spatial fractal dimension were analyzed: the box dimension (Eq. 4), the clustering dimension (Eq. 3), and the correlation dimension (Eqs. 1 and 2). The correlation exponent dimension represented the temporal distribution of seismic events. The studies carried out on numerous seismic series from various mines showed that fractal dimensions significantly and systematically vary in time. It was also shown that the results strongly depend on sample size and the applied estimator. Figure 48, reproduced from Lasocki and Mortimer (1998), shows time variations of the box fractal dimension (D_b) and the correlation dimension (D_2) of spatial distribution of epicenters. The estimates are based on data samples comprising 100 (left-hand side graph) and 50 (right-hand side graph) consecutive events. Although they show some degree of correlation, D_b and D_2 curves are rather different. A smoothing effect imposed by the larger sample size is also visible.

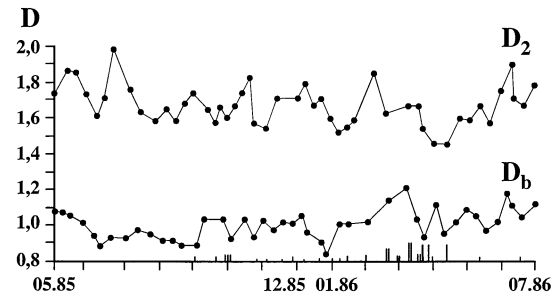
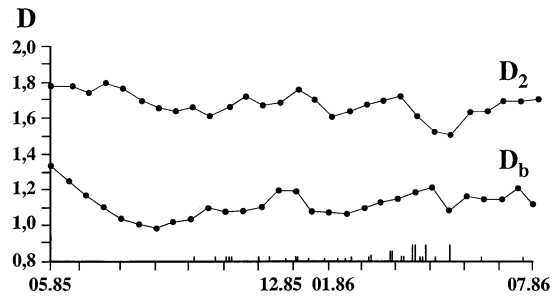


FIG. 48. Temporal variations of the correlation (D_2) and box (D_b) dimensions of the distribution of epicenters for a seismic series from a longwall area at Katowice coal mine, Poland. The estimates were obtained from 100-event (left) and 50-event (right) samples, respectively. [Lasocki and Mortimer (1998), Fig. 3, reprinted with kind permission from Trans Tech Publications.]

A correlation analysis was used to test relationship between the changes of fractal dimension and the changes of seismic activity and seismic hazard. The analysis took into account the spatial and temporal dimensions, on one hand, and the total number of events, number of strong events, total seismic energy, seismic energy released by strong events, maximum energy of one event, and the b -value, on the other. The results related to the spatial correlation dimension were ambiguous and erratic. The only significant positive correlation dimension were ambiguous and erratic. The only significant positive correlation was found, in most cases, between the fractal temporal dimension and the number of strong events and between the fractal temporal dimension and the sum of energy of strong events (Mortimer, 1997; Mortimer and De Luca, 1999).

In general, all the results strongly indicate that the variability in time of the spatial fractal dimension of seismicity is directly connected with mining. Nevertheless, it is still an open question as to what is behind these time variations and how much they are related to changes in seismic hazard. It seems that some ambiguity of described results is connected with properties still not fully recognized relating to the fractal dimension estimation procedures.

Investigation of two other simple statistical parameters of epicenter distributions was initiated by Lasocki (1996) and continued by Laskownicka (1998, 1999). These parameters are the direction of the best linear fit to a constant number of epicenters and the root-mean-square dispersion of epicenters around the fitted line. Statistical differences between the values of parameters prior to the occurrence of strong events and the values evaluated during quiet periods were tested. Altogether, 10 seismic series from different stopes at two Polish coal mines, 2 series from two Polish copper mines, and 2 series from a South African gold mine were analyzed. The significance of the differences between mean values taken from five consecutive days of the respective quiet and strong event preceding periods was tested by the Mann–Whitney and Wilcoxon tests. Of 14 examined series, the differences of the directions of a straight-line fit were significant in 12 cases and the differences of the root-mean-square dispersion were significant in 11 cases. This highly positive result points to the prediction potential of parameterizations of the spatial distributions of seismic events, although a specific working technique based on such parameterizations is a matter of further studies.

8.4. Rock Mass Instability Concept

Seismic energy and seismic moment are independent, although strongly correlated, parameters of a seismic event. Events in mines of the same seismic moment could differ in seismic energy by three orders of magnitude (e.g., Mendecki, 1993). Consequently, it has been attempted to ground the time-dependent hazard assessment on both parameters simultaneously. The technique introduced by Kijko and

Sciocatti (1995b), described in Section 8.2, which integrates the information provided by probabilistic distribution of seismic moment and energy and accounts for possible correlation among the events, represents such an approach. Mendecki and his colleagues (e.g., Mendecki, 1997b,c; van Aswegen *et al.*, 1997) developed the same initial idea into a complex quasi-multivariate methodology of seismic data analysis. A brief presentation of general concepts and applied parameterization of seismicity is given. For full details see the book edited by Mendecki (1997a).

The apparent stress

$$\sigma_A = \mu \frac{E}{M_0}, \quad (30)$$

where μ is the modulus of rigidity, is a parameter that unites the seismic energy E and seismic moment M_0 . By definition, it is sensitive to variations of the energy-to-moment ratio rather than to individual changes of these parameters. Following Gibowicz *et al.* (1990), apparent stress is used as a model independent indicator of stress release or, in general, of the stress state within the rock mass (e.g., Mendecki, 1993). Stress release estimates for low magnitude seismicity to determine the zones of an increased rockburst potential was also used by Urbancic *et al.* (1992b) and Urbancic and Young (1993).

A strong linear correlation between the $\log E$ and $\log M_0$ results in the correlation between $\log \sigma_A$ and $\log M_0$. The regression lines of $\log E$ versus $\log M_0$ and $\log \sigma_A$ versus $\log M_0$, estimated for a given seismic series, represent the expected value of seismic energy and apparent stress, respectively, given the seismic moment of an event. An anomalous apparent stress for an individual event becomes more distinct when σ_A of this event is compared with its expected value. For this, a parameter called stress index, I_s , (Glazer, 1998) or, alternatively, energy index, EI , (van Aswegen and Butler, 1993) was introduced for practical application in deep gold mines in South Africa. I_s is defined as the ratio of the apparent stress of an event to its expected value evaluated from a $\log \sigma_A$ versus $\log M_0$ regression line. EI is the ratio of seismic energy of that event to its expected value for a given seismic moment of the event. Glazer (1998) presented the examples of positive anomalies of stress index, routinely used to delineate the areas of higher than average rockburst potential.

The apparent volume, V_A , introduced by Mendecki (1993), is an other parameter expressing the relation between the energy and the moment of an individual event

$$V_A = \frac{M_0}{2\sigma_A} = \frac{M_0^2}{2\mu E}. \quad (31)$$

Apparent volume is supposed to be a measure of the rock volume with inelastic strain, associated with the seismic event.

The concept of prediction of Mendecki and his group (e.g., Mendecki, 1997b,c) relies on monitoring the process of rock mass fracturing by a set of parameters of

observed seismicity in order to recognize when the fracturing becomes unstable. Such an unstable fracturing eventually leads to a large event or a swarm of smaller events. To ascertain the instability, the following criterion is used

$$\int_{\Delta V} \dot{\sigma} \dot{\epsilon}_e dV + \int_{\Delta V} \dot{\sigma} \dot{\epsilon}_{in} dV < 0, \quad (32)$$

where $\dot{\sigma}$, $\dot{\epsilon}_e$, and $\dot{\epsilon}_{in}$ are the stress, elastic strain, and inelastic strain rates, respectively, and the integration extends over the volume of interest ΔV . Since the term with elastic strain must be positive, the fracturing becomes unstable when the second term with inelastic strain is negative and balances the positive term. It is assumed that both the stress and inelastic strain changes can be inferred from parameters related to the seismic strain rate and the seismic stress, which are defined as

$$\dot{\epsilon}_s(\Delta V, \Delta t) = \frac{\sum_{t_1}^{t_2} M_0}{2\mu \Delta V \Delta t} \quad (33)$$

and

$$\sigma_s(\Delta V, \Delta t) = \frac{\sum_{t_1}^{t_2} E}{\dot{\epsilon}_s \Delta V \Delta t} = 2\mu \frac{\sum_{t_1}^{t_2} E}{\sum_{t_1}^{t_2} M_0} \quad (34)$$

respectively, where the summation extends over all events recorded within the volume ΔV during the period $\Delta t = t_2 - t_1$. For instance, the stress rate in relation (32) is estimated from the changes in an average value of the energy index EI and the strain rate is inferred from the changes in the cumulative apparent volume $\sum V_A$. A large event is expected when the average EI drops down together with an anomalous increase of the cumulative apparent volume.

There are several other parameters proposed by Mendecki and his group, such as seismic viscosity and relaxation time, seismic softening and seismic diffusion, and seismic Schmidt and seismic Deborah numbers, to monitor the instability of the rock mass (Mendecki, 1997a). These parameters, however, are strongly redundant since they are mostly related to only two independent quantities: the sums of seismic energy and seismic moment. It seems that the authors multiplied nearly the same parameterizations of seismic series in order to provide different options for a pair of quantities, which could be used for practical monitoring of the instability criterion (Eq. 32). In most of their examples (e.g., Mendecki 1997b,c; van Aswegen *et al.*, 1997), the cumulative apparent volume is used as the one parameter in the pair while the other parameter is different in different cases. This procedure suggests that the authors ascribe a particular significance to the variations of apparent volume. The use of cumulative quantities, on the other hand, obscures fine variations of this parameter and the interpretation can be ambiguous.

This briefly described approach to prediction, based on the rockmass instability concept, is widely used in real-time applications in some South African mines

(e.g., Butler, 1997; Glazer, 1997, 1998; Minney *et al.*, 1997; van Aswegen *et al.*, 1997; Alcott *et al.*, 1998) and is considered a valuable tool in monitoring variable seismic hazard. Unfortunately, the proposed parameters have not been objectively validated so far and their actual prediction efficiency is not known.

8.5. Other Studies

The techniques described in the previous section are based to some extent on a possible precursory potential of the apparent stress. Such expectations related to stress release premonitory changes led to other studies of this and other stress release estimates. Cichowicz *et al.* (1990) investigated various parameters of microevents recorded ahead of a stope at Western Deep Levels gold mine in South Africa, including the static and dynamic stress drops. They noted that static stress drops of individual microevents were higher before than after the main event.

Stewart and Spottiswoode (1993) tried to use the seismic stress drop as an indicator of the time-dependent seismic hazard. For this purpose they introduced the parameter $TAU = (Rv)^3/E_s$, where Rv is the peak ground-velocity scaled by hypocentral distance and E_s is the seismic energy, which is proportional to the stress drop. The authors speculated that an increase of the stress drop from events located ahead of an advancing mining front could indicate fracturing of previously solid rock in which a stronger event is likely to occur. The tests performed on seismic data from the Blyvooruitzicht gold mine in South Africa, in which time variations of the median value of TAU for 40 consecutive events were analyzed, have shown in some cases reasonable correlation between the periods of high stress drop and the times of occurrence of larger events.

Gibowicz (1998) studied the stress drop mechanism of seismic events from the Underground Research Laboratory in Canada, Western Deep Levels gold mine in South Africa, and two coal and two copper mines in Poland. He used the parameter ϵ of Zúñiga (1993) defined as the ratio of the static stress drop over the sum of apparent stress and half the static stress drop. For the partial stress drop mechanism $\epsilon < 1$ while the frictional overshoot mechanism corresponds to $\epsilon > 1$. It was found that strong events occur when the partial stress drop mechanism is dominant (low values of ϵ), and then they are followed by the events for which the frictional overshoot mechanism begins to dominate (high values of ϵ).

It is well known that seismicity in mines depends strongly on mining; the dependence is complex and is not fully understood quantitatively. Several attempts, however, have been made to relate seismic parameters with some parameters describing mining operations, and then to come up with quantities sensitive to the variations of seismic hazard, which would depend upon these mining parameters. One such attempt estimates seismic hazard parameters from the total seismic energy released within a time window and the volume of rock mined out during this

time (e.g., Głowacka *et al.*, 1988, 1992; Głowacka and Kijko, 1989; Głowacka, 1993). The technique has its origin in McGarr's (1976) relation between the sum of seismic moments and the volume of convergence accompanying elastic deformation around a stope, and is based on Kijko's (1985) reformulated relation showing that

$$\sum E = C \cdot V_e^B, \quad (35)$$

where $\sum E$ is the sum of seismic energy, V_e is the volume of excavated rock, and C and B are parameters characterizing the state of the rock mass. Relation (35) is used to evaluate the anticipated value of seismic energy released within the time interval $[t - \Delta t, t]$. According to Głowacka (1993) this anticipated value is

$$\begin{aligned} \langle \sum E(t - \Delta t, t) \rangle = & \{ C[V_e(t)^B - V_e(t - \Delta t)^B] (1 - e^{-\frac{\Delta t}{\tau_r}}) \\ & + \Delta E(t - \Delta t) \} (1 - e^{-\frac{\Delta t}{\tau_r}}), \end{aligned} \quad (36)$$

where $V_e(t)$ is the volume of excavated rock up to time t , $\Delta E(t - \Delta t)$ is the energy excess, which was not released up to time $t - \Delta t$, the exponential term represents time effects of energy loading and relaxation, and τ_r is a constant. It is assumed that the actual sum of seismic energy is a random variable of either normal distribution, truncated from the left by zero (e.g., Głowacka *et al.*, 1988, 1992; Głowacka and Kijko, 1989), or lognormal distribution (e.g., Głowacka and Lasocki, 1992; Głowacka, 1993). In every case the parameter of location of the distribution is expressed by relation (36) or a similar one, and the method provides the probability, $\Pr[\sum E(t - \Delta t, t) > E_p]$, that the sum of seismic energy will exceed a specified value E_p within $[t - \Delta t, t]$. For a short time interval Δt , this probability can be understood as the probability that an event of energy greater than E_p will occur. The probability increase and an appearance of the excess of energy are supposed to precede the occurrence of a strong event. This approach was successfully tested in some coal mines in Poland (e.g., Głowacka and Kijko, 1989), in the Czech Republic (e.g., Głowacka *et al.*, 1992), and in the USA (Arabasz *et al.*, 1997).

Although it is obvious that integrating various precursory parameterizations of seismic series into a true algorithmic multivariate prediction would considerably increase the efficiency of prediction, only a few attempts in this regard have been reported. Głowacka (1992, 1993) and Głowacka and Lasocki (1992) presented one such multivariate approach. A probabilistic synthesis of precursors, proposed by Aki (1981), was used to integrate the results from the method based on the volume of excavated rock with the results from the time-dependent seismic hazard analysis based on the distribution of energy (see Sect. 8.2). Let $\Pr[\sum E(t - \Delta t, t) > E_p]$ be the probability provided by the former method and $R(E_p, t)$ be the probabilistic outcome of the time-dependent seismic hazard analysis (21). The probability of occurrence of an event with energy greater than E_p , estimated by both methods

taken together is given by

$$\Pr[E > E_p] = p_0 \frac{\Pr[\sum E(t - \Delta t, t) > E_p]}{p_0} \frac{R(E_p, t)}{p_0}, \quad (37)$$

where p_0 is the *a priori* probability of occurrence of the event, estimated by the ratio $n(E_p)/N$, where $n(E_p)$ is the number of time intervals Δt in which such an event occurred and N is the number of time intervals in the whole studied period. Relation (37) can be readily used if the component methods of hazard assessment are statistically independent and the component probabilities are low. An example of the use of this technique in assessing time-dependent seismic hazard is shown in Fig. 49, reproduced from Głowacka and Lasocki (1992). The

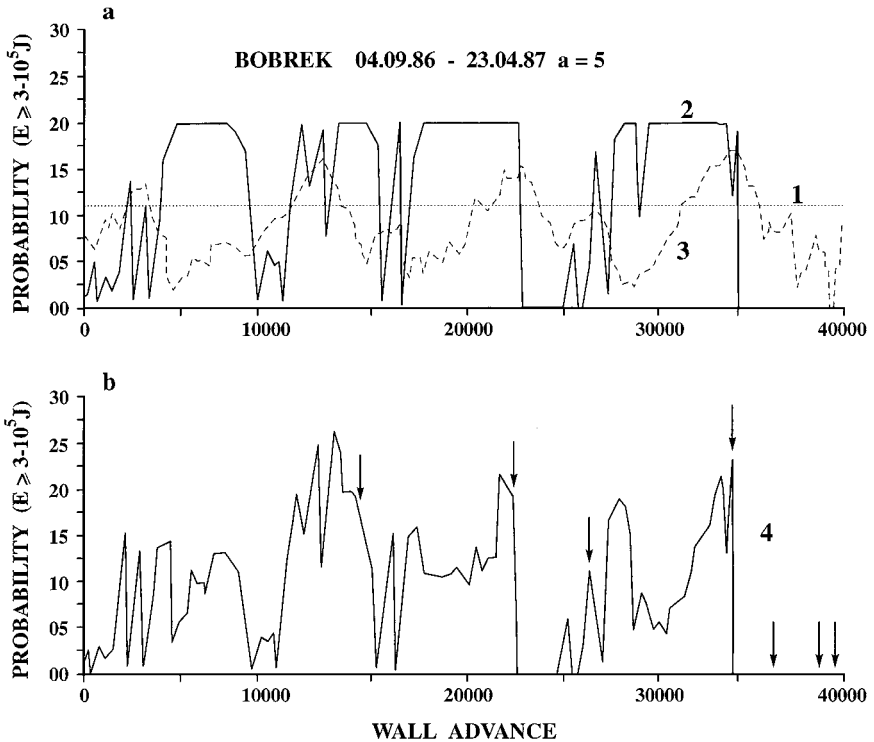


FIG. 49. Probabilistic synthesis of the results of two time dependent seismic hazard assessment methods for a longwall area at Bobrek coal mine, Poland. (a) Independent estimates of probability of the occurrence of seismic events with energy $E \geq 3 \times 10^5$ J; dotted line (1), *a priori* probability of the event occurrence, continuous line (2), probability estimates based on the volume of extracted rock, dashed line (3), estimates based on the distribution of energy. (b) Synthesized probability of the occurrence of seismic events. The time of the occurrence of observed events is indicated by arrows. [Głowacka and Lasocki (1992), Fig. 1, reprinted with kind permission from the Institute of Rock Structure and Mechanics, the Academy of Sciences of the Czech Republic.]

analyzed data were associated with a longwall at Bobrek coal mine in Poland. The estimates of $\Pr[\sum E(t - \Delta t, t) > 3 \cdot 10^5 \text{ J}]$ marked by a continuous line and of $R(3 \cdot 10^5 \text{ J}, t)$ marked by a dashed line in the upper graph of the figure can be compared with the synthesized probability $\Pr[E > 3 \cdot 10^5 \text{ J}, t]$ shown in the lower graph. The arrows mark the occurrence of events with energy $> 3 \cdot 10^5 \text{ J}$, and a horizontal dashed line in the upper graph represents the *a priori* probability p_0 . It can be seen that the synthesis caused, in some cases, a significant increase in the probability estimates.

Marcak (1993) presented another example of multivariate prediction. He applied the pattern recognition algorithm, well known in earthquake seismology (e.g., Keilis-Borok and Kossobokov, 1990; Keilis-Borok and Rotwein, 1990), to seismic data from Halemba coal mine in Poland. In his example, seven out of nine stronger events occurred during the time of increased probability, whose total duration was 10.4% of the total time of analysis.

8.6. Automatic Prediction: Extrapolation of Parameterizations of Seismicity in Mines

All the techniques discussed estimate certain parameterizations of seismic series, which are supposed to indicate the potential to generate events hazardous for mining. Past-to-present time variations of these estimates are used to evaluate the future potential. The inference is usually made by a qualitative extrapolation of the most recent trends of estimates. From the formal point of view all such methods assess the present seismic hazard and do not predict a future one, since no formal algorithms of extrapolation into the future are provided.

The problem of automatic prediction of mining seismicity has been formulated in terms of either linear (e.g., Buben and Rudajev, 1974, 1991; Rudajev and Fučík, 1982) or nonlinear (e.g., Čiž and Rudajev, 1996, 1999; Rudajev and Čiž, 1999) statistical extrapolations. The methods of such an extrapolation are usually multi-channel, i.e., they can accept more than one identically timed time series as input data. Thus such methods can conveniently integrate different parameterizations of seismic series, as well as other, nonseismological, data. The results of their application are the estimates of future values of desired parameterization(s).

A linear extrapolation requires that the input time series result from a stationary Markov process. The future values are modeled by a linear combination of the past values. Buben and Rudajev (1991) used Wiener extrapolation to various combinations of input data comprising daily number of events, daily energy release, daily values of convergence in investigated stopes, and the number of seismoacoustic pulses recorded daily in the coal seam and in the overlaying rocks. If $\vec{x}_k = [x_k^{(1)}, x_k^{(2)}, \dots, x_k^{(m)}]^T$ represents the input values for time k , where the superscript denotes the specific input time series, the predicted values \hat{x}_t for time t ,

according to the linear extrapolation, are

$$\hat{x}_t = [\vec{x}_{t-1}, \vec{x}_{t-2}, \dots, \vec{x}_{t-L}] \bullet \vec{g}, \quad (38)$$

where $\vec{g}_k = [g_1, g_2, \dots, g_L]^T$ is the vector of filter coefficients and L is its length. The filter coefficients are determined by minimization of the sum of squared errors of prediction

$$\sum_t (\vec{x}_t - \hat{x}_t)^T (\vec{x}_t - \hat{x}_t) = \min. \quad (39)$$

Buben and Rudajev (1991) attempted to predict the daily number of events and the sum of their energy using various versions of the method and filters of a length up to $L = 5$. They noted that prediction of the number of events was more accurate than prediction of energy released daily, but the overall result was not encouraging.

The main drawback of linear extrapolation rules is the stationarity condition, which in general is not fulfilled in the series generated by seismicity in mines. Nonlinear extrapolation methods make use of artificial neural networks. Formally they do not require stationarity of input time series and therefore seem to be more appropriate for the data from mines. Rudajev and Čiž (1999) applied two separate neural networks with three layers—input, hidden, and output—to predict the number of events and the sum of maximum amplitudes of their signals for consecutive 1-day periods. The latter quantity represents to some extent the daily release of seismic energy. The response $\{y_j\}$, $j = 1, \dots, M$, of neurons of the hidden layer to the input pattern $\{x_i\}$, $i = 1, \dots, N$, was modeled by a nonlinear sigmoid function $S(\bullet) = \tanh(\bullet)$

$$y_j = S \left(\sum_{i=1}^N (w_{ij} x_i - b_j) \right), \quad (40)$$

where N is the dimension of the input vector, equal to the number of input neurons, M is the number of neurons in the hidden layer, w_{ij} are weights among neurons from the input and hidden layers, and b_j are the thresholds for hidden neurons. Since Rudajev and Čiž (1999) used the networks with only one output neuron, the net response of the input pattern was

$$z = \sum_{j=1}^M (w_{j\bullet} y_j - b), \quad (41)$$

where $w_{i\bullet}$ are the weights between the hidden and output layers and b is a threshold for the output neuron. Here the input pattern denotes all values supplied simultaneously to the network, which could represent any combination of data from the same or different sources (various seismicity parameterizations, nonseismic data, etc.). The study was performed on seismic data recorded for 1100 days at Mayrau mine in the Czech Republic. The seismic input data—the daily number

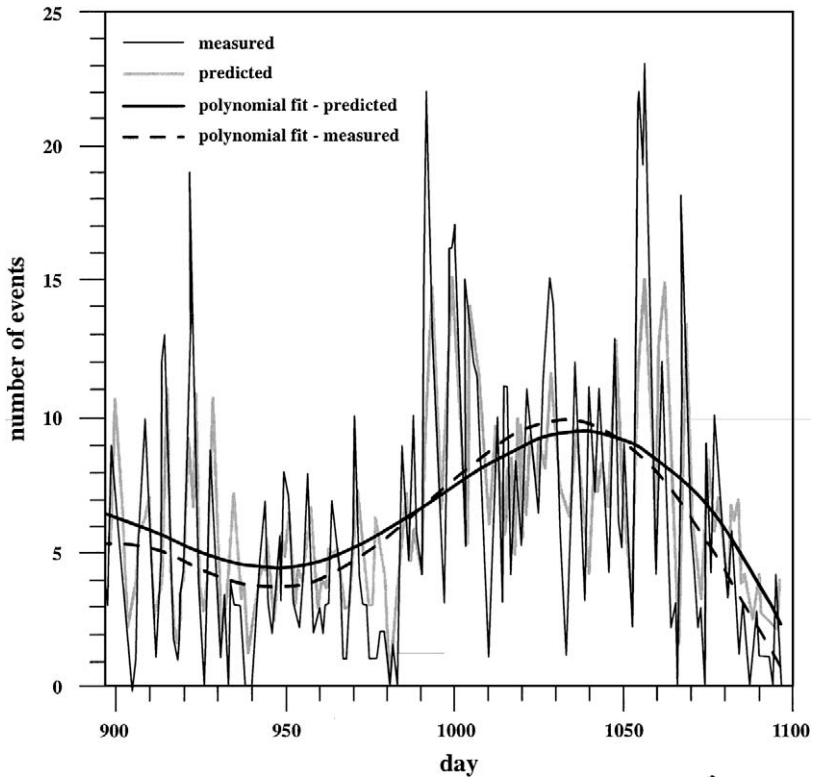


Fig. 50. Comparison of the daily number of events predicted for Mayrau mine, Czech Republic, by a neural network (thick lines) with the actual values (thin lines). The dashed lines mark smoothed values. [Rudajev and Číž (1999), Fig. 7, reprinted with kind permission from Birkhäuser Verlag AG.]

of events and the sum of maximum amplitudes—were supplemented by the total daily length of active mining. The whole data series was split into training and testing parts; a usual procedure for neural networks. The training part was used to evaluate an optimal set of weights minimizing the sum of squares of differences between the obtained and desired output from the network. The testing part was used to evaluate the effectiveness of the technique. Figure 50, reproduced from Rudajev and Číž (1999), shows a comparison between the predicted and actual numbers of events for consecutive days of the testing part. The method turned out to be robust with regard to the apparent nonstationarity of the input series. Its effectiveness was measured on the testing part by a relative mean-squared error

$$RMSE = \frac{\sum_i (PRED_i - OBS_i)^2}{\sum_i [MEAN(OBS) - OBS_i]^2}, \quad (42)$$

where *PRED* are the predicted values, *OBS* are the observed values, and *MEAN (OBS)* is the mean of all the observed values. Prediction is efficient when the *RMSE* is significantly less than one and for perfect prediction this quantity would be equal to zero. *RMSE* was about 0.55 for prediction of the number of events and 0.79 for prediction of the sum of maximum amplitudes. This difference in the accuracy of prediction has been explained by a lower accuracy of the amplitude data.

In another work, Čiž and Rudajev (1999) compared the prediction of the numbers of events per day and the daily sum of maximum amplitudes, based on a linear extrapolation and three different neural network architectures. For the tested data, the linear Wiener extrapolation and nonlinear prediction were equally efficient, although some differences in efficiency for different neural networks were noted. The statistical extrapolation of the number of events was 40–46% more efficient than the prediction by the average value and 27–42% more efficient than the prediction by the last value. The increase of efficiency in the case of the sum of maximum amplitudes was 20–26 and 33–38% respectively.

9. SEISMIC DISCRIMINATION

Large seismic events in mines are of interest to seismologists monitoring compliance with the Comprehensive Test Ban Treaty (CTBT) prohibiting nuclear explosion testing. Mining-induced events often appear explosion-like for many discrimination criteria between earthquakes and underground nuclear explosions (e.g., Bennett and McLaughlin, 1997; Bowers, 1997; Bowers and Douglas, 1997). Mine tremors occur at depths similar to underground nuclear explosions. The ratio of the body wave magnitude and surface wave magnitude from large seismic events in mines is more like that observed from an explosion than an earthquake. Short period *P* waves recorded at teleseismic distances appear simple as those observed from many underground explosions (Bowers and Douglas, 1997). Such results could lead to accusations of evasion under the CTBT (Blandford, 1996).

For CTBT research, much attention is paid to the study of chemical explosions (e.g., Denny *et al.*, 1996; Murphy, 1996). The large number of mining blasts can cause problems for any monitoring system. In addition, large mining blasts could be used to hide a simultaneous decoupled nuclear explosion (e.g., Smith, 1993; Taylor, 1994). Some mining experts believe that a rockburst could be triggered by suddenly removing a few last supports in a large excavation. This leads to the possibility of hiding a decoupled explosion in a rockburst as well (Blandford, 1996).

McGarr *et al.* (1990) investigated seismic records of three mine tremors and three explosions in deep gold mines in South Africa to test the methods of discriminating between the two types of events. All three explosions generated *S* waves that appeared to be a consequence of deviatoric stress release in the source area. The

three tremors generated P and S waves whose spectra and source parameters agree well with standard earthquake source models. For events of fixed low-frequency spectral asymptotes of P waves, the explosions typically have higher corner frequencies than natural earthquakes or mine tremors.

Taylor (1994) raised the problem of false alarms associated with mining activities. He studied, as an example, an anomalous event from the Gentry Mountain coal mining district in the eastern Wasatch Plateau, Utah. The magnitude 3.5 event occurred on May 14, 1981, and was consistently classified as an explosion based on various regional discriminants. Using a simple source representation, Taylor (1994) modeled the event as a tabular excavation collapse that occurred as a result of normal mining activities and had the signal characteristics of a vertical point force. His study raises the importance of having good catalogs of seismic data and mining information from various areas to prevent potential false alarms that may be generated from seismicity in mines.

Many spontaneously occurring shallow mine collapses have implosional source mechanisms that might provide a physical basis for discriminating them from explosions. Another kind of underground mine collapse, induced by explosively demolishing the natural pillars that support underground mine opening (Yang *et al.*, 1998), is described in Sect. 5.2.

Occasionally, large mining events are misinterpreted as natural earthquakes. Fan and Wallace (1995) studied the October 30, 1994, seismic event of body wave magnitude 5.6 and surface wave magnitude 4.7 from South Africa, when reports from the mining region were not yet available. They suggested that the event was unlikely to be a mine tremor because of its large magnitude and midcrustal depth. They determined the source mechanism and interpreted it either as representing plateau uplift or as evidence of a southward continuation of deformation related to the East African Rift system. Bennett *et al.* (1996), on the other hand, identified the 1994 event as a mining event, using observations of regional phase spectral ratios and high-frequency surface Rayleigh waves. The event in fact was caused by slip on the Stuirmanspan fault at a depth between 2 and 3 km in the President Brand mine in the Orange Free State gold mining district. Bowers (1997) has shown that surface waves from the 1994 event, recorded by broadband instruments at regional distances, are inconsistent with collapse mechanisms recently proposed for some large mining events. He found that modeling of teleseismic broadband P waves and regional distance surface waves indicates that the source depth is shallow and the observed source radiation is consistent with a normal dip-slip fault. The explosion-like ratio of body wave over surface wave magnitudes is attributable to the effect of the mechanism and the shallow depth of the source.

Bowers and Douglas (1997) used short-period and broadband P waves recorded at teleseismic distances to characterize large seismic events in different mining regions, such as South Africa, Eastern Europe, and North America. They found that mining events from South African gold and Polish copper mining districts could be

characterized by simple teleseismic P waveforms that have dilatational first motions and short duration. The dilatational first motion, observed from many mining events, is a potential criterion for discriminating between mine tremors and underground explosions, as generally only compressional first motions are observed from explosions. These waveforms can be explained by a shallow double-couple source. But there are exceptions as well. Both the March 13, 1989, Volkershausen, Germany, and the February 3, 1995, Wyoming events generated surface waves that indicated a collapse mechanism and had broadband P waveforms that provided some evidence of source complexity.

Bennett and McLaughlin (1997) investigated seismic characteristics and source mechanism of mining events for use in seismic discrimination. They used regional-distance observations from several large mine tremors in a variety of source areas, such as western and eastern USA, Poland, Germany, South Africa, and Russia. The signal analyses indicate that most mine tremors have L_g/P ratios which are not explosion-like but tend to mix with the earthquake population. They also tried to find theoretical mechanisms corresponding to the observations and have shown that cavity collapse can be represented as a closing horizontal crack. Such a mechanism is a relatively inefficient source for long-period Rayleigh waves, possibly explaining the low values of surface wave magnitude often found for mining events, and shows relatively strong short-period surface waves consistent with observations. Bennett and McLaughlin (1997) concluded that although the tension crack model seems to explain observations from mine tremors with large collapse features, it might be expected that in some mining areas the source mechanisms would be better represented by more complex combinations of the closing crack with tectonic release or faulting components.

Thus, the occurrence of large seismic events in mining areas all over the world is one of the many problems facing seismic monitoring of nuclear explosions under the Comprehensive Test Ban Treaty. Some traditional seismic discriminants may not work for many mining events, but some others, especially those based on seismic signals at regional distances, seem to provide the means for discrimination of seismic events in mines from nuclear explosions (e.g., Bennett and McLaughlin, 1997). Further studies on the source mechanism are needed to identify those mechanisms of mine tremors that could be problematic for various seismic discriminants.

10. SUMMARY

Rock failure and seismic activity are often unavoidable phenomena in extensive deep mining. If the earth's crust is in a self-organized critical state, then a significant fraction of the crust is not far from instability. Pore pressure changes and mass transfers leading to small incremental deviatoric stresses, therefore, are

sufficient to trigger seismic instabilities in the uppermost crust in otherwise historically aseismic areas (Grasso and Sornette (1998). Increases in the shear stress or decreases in the normal stress acting on the fault planes cause mining-induced events. The stress perturbations, often quite small, frequently result in generation of seismicity where near-failure conditions are present, which are believed to be common in both active and stable tectonic environments (McGarr *et al.*, 1999).

Seismic monitoring provides a powerful means for the detection and evaluation of seismic events occurring around underground openings in numerous mining districts throughout the world. The most comprehensive studies of seismicity in mines are carried out in South Africa, Canada, the United States, and Poland. Routine seismic monitoring has been in use for over 30 years. Its main objective was immediate location of seismic events in mines, estimation of their strength, and prediction of large rock mass instabilities. The first two objectives were readily achieved, but prediction of large seismic events in mines is not as yet resolved. The introduction of modern digital seismic systems to mines, however, and progress in the theory and methods of quantitative seismology have led to the implementation of real-time monitoring as a mine management tool for estimation of the rock mass response to mining.

Location of seismic events is the first step in seismic monitoring in mines. In mining practice, the expected accuracy for hypocenter locations is a few tens of meters, or even a few meters in some cases. This demanding requirement could be met with the present-day technology when the optimum design of underground seismic networks and new location methods, now available, are applied in mining practice.

Seismic tomographic imaging is used to map the spatial variations of seismic and elastic parameters in rocks. Seismic wave velocity imaging is particularly useful for seismicity studies in mines. Velocity images can be calculated using either controlled explosive sources or passively monitored seismicity. Passive source velocity images can be computed by a simultaneous inversion procedure for source location and velocity structure. Detailed velocity structures obviously improve the accuracy of hypocenter location. Comparisons between velocity images and seismicity have shown that the largest events are associated with regions of high velocity of seismic waves, whereas low velocity areas are generally not seismic. Controlled studies have shown a strong correlation between velocity and stress.

Seismic events induced by mining are not uniformly distributed in either space or time. Extensive studies performed on the space–time–energy distributions of seismic events in mines show that the tendency to form nests, swarms, and clusters is commonly observed. Obviously, seismicity in mines is strongly affected by local geology and tectonics, and by interaction between mining and crustal state of stress on a local and regional scale. This is especially true in the case of the largest mine tremors, with magnitude close to 4 and above. Extensive studies on the relationship between geological features and seismicity show that seismic events concentrate

in specific regions corresponding to different geologic units, in spite of mining works being carried out in other regions as well.

Source parameters have been estimated for thousands of seismic events, in the moment magnitude range from -3.6 to over 5 , in mining districts worldwide. They are used for various practical purposes, such as assessment of rockburst hazard and damage potential, combating rockburst hazard, design of support in rockburst-prone areas, and attempts at rockburst prediction.

Extensive studies of scaling relations of seismic events in mines, describing the manner in which the source duration or the source dimension increases with increasing seismic moment, indicate that stress drop shows globally no systematic dependence on seismic moment. The constant stress drop model implies a self-similar rupture process regardless of the strength of the seismic event. The average values of seismic moment referring to the same range of corner frequency, however, are vastly different in various mining areas.

The most important progress made in source mechanism studies of seismic events in mines during the last decade is the use on a massive scale of seismic moment tensor inversion technique. From numerous studies it follows that shearing processes are often dominant in the source and its mechanism can be well represented by a double-couple model. More complex rock failures associated with seismic events, especially with large ones, are also reported from various mining districts. Seismic events in mines are characterized by very low seismic efficiency; nearly all of the energy released by faulting is consumed in overcoming friction. The apparent stress seems to display distinct upper bounds determined by a maximum seismic efficiency of about 0.06 (McGarr, 1994, 1999).

Seismicity induced by mining exhibits a fractal structure with respect to the space, time, and event size. Fractal geometry seems to characterize distributions of various parameterizations of seismic events on every scale. Larger regional events, distributed for example over the Upper Silesian Coal Basin in Poland; all events from a given mine; seismicity accompanying mining of single isolated stopes; as well as microseismicity observed in one pillar or acoustic emission generated during laboratory experiments, are all statistical fractals in the space, time, and energy domains. Though not conclusive, such self-similarity of seismicity strongly suggests that the process of rock mass fracturing is governed by deterministic chaos. There are also indications that this process might be characterized by a low-dimensional attractor, and its short-term predictability could be feasible.

Statistical analyses of seismic series from mines provide another argument for predictability, in a sense, of rock mass response to mining. Seismicity associated with mining of individual stopes is non-Poissonian due to the time variability of generating processes in the long term and correlation among the events on the short time scale. Processing of seismic series in real time, although it cannot at present result in a precise reliable prediction, can provide useful general characteristics of the past, present, and future states of rock mass fracturing. This is accomplished

by a variety of approaches to the assessment of time-dependent hazard. Recent proposals in this respect are based on the time variability of recurrence relations, variations of spatial distribution of sources, rock mass instability criteria, changes of the apparent stress and stress drop, the probabilistic relation between the seismic energy release and the volume of extracted rock, among others. Attempts are also made to integrate particular methods in a multivariate forecasting system, including the application of neural networks for this purpose. Though this research is still in an early stage and indications provided by the present methods of hazard analysis do not comply with demands, the practical usefulness of these methods for combating rockburst hazard in mines has been widely acknowledged.

Large seismic events in mines are of interest to seismologists monitoring compliance with the Comprehensive Test Ban Treaty which prohibits nuclear explosion testing. These events often appear explosion-like for many discrimination criteria between earthquakes and underground nuclear explosions. Many mine collapses, on the other hand, have an implosional source mechanism that might provide a physical basis to discriminate them from explosions. Thus, some traditional seismic discriminants may not work for many mining events, but some others, especially those based on seismic signals recorded at regional distances, seem to provide the means for discriminating seismic events in mines from nuclear explosions.

ACKNOWLEDGMENTS

We are grateful to Art McGarr and Shahriar Talebi for their most helpful comments and suggestions, which considerably improved the original manuscript.

REFERENCES

- Abarbanel, H. D. I. (1996). "Analysis of Observed Chaotic Data." Springer Verlag, Basel.
- Abercrombie, R., and Leary, P. (1993). Source parameters of small earthquakes recorded at 2.5 km depth, Cajon Pass, southern California. *Geophys. Res. Lett.* **20**, 1511–1514.
- Adams, D. J., Gay, N. C., and Cross, M. (1993). Preconditioning—A technique for controlling rockbursts. In "Rockbursts and Seismicity in Mines" (R. P. Young, ed.). Balkema, Rotterdam, pp. 29–33.
- Aki, K. (1965). Maximum likelihood estimate of b in the formula $\log N = a - bM$ and its confidence limits. *Bull. Earthquake Res. Inst. Univ. Tokyo* **43**, 237–239.
- Aki, K. (1981). A probabilistic synthesis of precursory phenomena. In "Earthquake Prediction. An International Review" (D. W. Simpson and P. G. Richards, eds.). American Geophysical Union, Washington, pp. 566–574.
- Alcott, M., Kaiser, P. K., and Simser, B. P. (1998). Use of micro-seismic source parameters for rockburst hazard assessment. *Pure Appl. Geophys.* **153**, 41–65.
- Andersen, L. M. (1999). "A Relative Moment Tensor Inversion Technique Applied to Seismicity Induced by Mining" (M.Sc. dissertation), University of the Witwatersrand, Johannesburg.

- Andrews, D. J. (1986). Objective determination of source parameters and similarity of earthquakes of different size. In "Earthquake Source Mechanics" (S. Das, J. Boatwright, and C. H. Scholz, eds.). Am. Geophys. Union, Washington, DC. Maurice Ewing Vol. 6, pp. 259–267.
- Arabasz, W. J., Nava, S. J., and Phelps, W. T. (1997). Mining seismicity in the Wasatch Plateau and Book Cliffs coal mining districts, Utah, USA. In "Rockbursts and Seismicity in Mines" (S. J. Gibowicz and S. Lasocki, eds.). Balkema, Rotterdam, pp. 111–116.
- Bak, P., Christensen, K., and Olami, Z. (1994). Self-organized criticality: Consequences for statistics and predictability of earthquakes. In "Nonlinear Dynamics and Predictability of Geophysical Phenomena" (W. I. Newman, A. Gabriellov, and D. L. Turcotte, eds.). IUGG and AGU, Washington, pp. 69–74.
- Bak, P., and Tang, C. (1989). Earthquakes as a self-organized critical phenomenon. *J. Geophys. Res.* **94**, 15,635–15,637.
- Baker, C., and Young, R. P. (1997). Evidence for extensive crack initiation in point source time-dependent moment tensor solutions. *Bull. Seismol. Soc. Am.* **87**, 1442–1453.
- Barton, C. C., and La Pointe, P. R., Eds. (1995). "Fractals in Earth Sciences." Plenum Press, New York.
- Behra, P. K. (1990). Ultradeep mining problems in Kolar gold mines. In "Rock at Great Depth" (V. Maury and D. Fourmaintraux, eds.). Balkema, Rotterdam, pp. 687–694.
- Beltrami, H., and Mareschal, J.-C. (1993). Strange seismic attractor? *Pure Appl. Geophys.* **141**, 71–81.
- Ben-Menahem, A. (1962). Radiation of seismic body waves from a finite moving source in the earth. *J. Geophys. Res.* **67**, 345–350.
- Bennett, T. J., Marshall, M. E., Barker, B. W., and Murphy, J. R. (1996). Use of seismic signal characteristics to identify several recent rockbursts (abstract). *Seismol. Res. Lett.* **67**, 32.
- Bennett, T. J., and McLaughlin, K. L. (1997). Seismic characteristics and mechanisms of rockbursts for use in seismic discrimination. In "Rockbursts and Seismicity in Mines" (S. J. Gibowicz and S. Lasocki, eds.). Balkema, Rotterdam, pp. 61–66.
- Ben Sliman, K., and Revalor, R. (1992). Some results on the accuracy of the location of mining-induced seismic events: Experience of French coal mines. In "Induced Seismicity" (P. Knoll, ed.). Balkema, Rotterdam, pp. 3–20.
- Bertero, M., Bindi, D., Boccacci, P., Cattaneo, M., Eva, C., and Lanza, V. (1997). Application of the projected Landweber method to the estimation of the source time function in seismology. *Inverse Problems* **13**, 465–486.
- Bertero, M., Bindi, D., Boccacci, P., Cattaneo, M., Eva, C., and Lanza, V. (1998). A novel blind-deconvolution method with an application to seismology. *Inverse Problems* **14**, 815–833.
- Bigarre, P., Ben Slimane, K., and Tinucci, J. (1993). 3-Dimensional modelling of fault-slip rockbursting. In "Rockbursts and Seismicity in Mines" (R. P. Young, ed.). Balkema, Rotterdam, pp. 315–319.
- Blair, D. P. (1993). A comparative study of seismic source location methods in underground mines. In "Rockbursts and Seismicity in Mines" (R. P. Young, ed.). Balkema, Rotterdam, pp. 321–325.
- Blake, W. (1980). Evaluating data from rock burst monitoring systems using the energy of microseismic events. In "Proc. 3rd Conf. on Acoustic Emission/Microseismic Activity in Geologic Structures and Materials" (H. R. Hardy, Jr., and F. W. Leighton, eds.). Trans Tech Publications, Clausthal, pp. 109–116.
- Blandford, R. R. (1996). Regional seismic event discrimination. In "Monitoring a Comprehensive Test Ban Treaty" (E. S. Husebye and A. M. Dainty, eds.). Kluwer Academic Publishers, Dordrecht, pp. 689–719.
- Boler, F. M., Billington, S., and Zipf, R. K. (1997). Seismological and energy-balance constraints on the mechanism of a catastrophic bump in the Book Cliffs coal mining district, Utah, U. S. A. *Int. J. Rock Mech. Min. Sci.* **34**, 27–43.

- Boler, F. M., and Swanson, P. L. (1992). Observations of heterogeneous stope convergence behavior and implications for induced seismicity. *Pure Appl. Geophys.* **139**, 639–656.
- Bour, M., and Cara, M. (1997). Test of a simple empirical Green function method on moderate-sized earthquakes. *Bull. Seismol. Soc. Am.* **87**, 668–683.
- Bowers, D. (1997). The October 30, 1994, seismic disturbance in South Africa: Earthquake or large burst? *J. Geophys. Res.* **102**, 9843–9857.
- Bowers, D., and Douglas, A. (1997). Characterisation of large mine tremors using *P* observed at teleseismic distances. In “Rockbursts and Seismicity in Mines” (S. J. Gibowicz and S. Lasocki, eds.). Balkema, Rotterdam, pp. 55–60.
- Bowman, A. W., Hall, P., and Titterton, D.M. (1984). Cross-validation in nonparametric estimation of probabilities and probability densities. *Biometrika* **71**, 341–351.
- Brady, B. T., (1977). Anomalous seismicity prior to rock bursts: Implications for earthquake prediction. *Pure Appl. Geophys.* **115**, 357–374.
- Brink, A. v. Z., and O’Connor, D. (1984). Rock burst prediction research—Development of a practical early-warning system. In “Proc. 3rd Conf. on Acoustic Emission/Microseismic Activity in Geologic Structures and Materials” (H. R. Hardy, Jr., and F. W. Leighton, eds.). Trans Tech Publications, Clausthal, pp. 269–282.
- Brune, J. N. (1970). Tectonic stress and the spectra of seismic shear waves from earthquakes. *J. Geophys. Res.* **72**, 4997–5009.
- Brune, J. N. (1971). Correction. *J. Geophys. Res.* **76**, 5002.
- Brune, J. N. (1976). The physics of earthquake strong motion. In “Seismic Risk and Engineering Decisions” (C. Lomnitz and E. Rosenblueth, eds.). Elsevier, New York, pp. 141–177.
- Buben, J., and Rudajev, V. (1974). Statistical prediction of rockbursts. *Publ. Inst. Geophys. Polish Acad. Sci.* **67**, 3–32 (in Czech, English abstract).
- Buben, J., and Rudajev, V. (1991). The results of prediction of seismic events in the territory of the Bohemian massif. In “Proc. 32nd U.S. Symposium Rock Mechanics as a Multidisciplinary Science” (J. C. Roegiers, ed.). Balkema, Rotterdam, pp. 451–460.
- Butler, A. G. (1997). Space–time clustering of potentially damaging seismic events and seismic viscosity at Western Deep Levels East and West Mines. In “Rockbursts and Seismicity in Mines” (S. J. Gibowicz, and S. Lasocki, eds.). Balkema, Rotterdam, pp. 89–93.
- Cai, M., Kaiser, P. K., and Martin, C. D. (1998). A tensile model for the interpretation of microseismic events near underground openings. *Pure Appl. Geophys.* **153**, 67–92.
- Carlson, J. M., and Langer, J. S. (1989). Properties of earthquakes generated by fault dynamics. *Phys. Rev. Lett.* **62**, 2632–2635.
- Cichowicz, A. (1991). The time variation of microevents parameters occurring before and after large seismic events. Int. Conf. “Earthquake Prediction: State-of-the-Art” 15–18 October 1991, Strasbourg, Scient.-Techn. Contr., pp. 16–21.
- Cichowicz, A., Green, R. W. E., van Zyl Brink, A., Grobler, P., and Mountfort, P. I. (1990). The space and time variation of micro-event parameters occurring in front of an active stope. In “Rockbursts and Seismicity in Mines” (C. Fairhurst, ed.). Balkema, Rotterdam, pp. 171–176.
- Cichy, A., and Mortimer, Z. (1999). Chaotic dynamics of the seismicity quantified in terms of the Lyapunov exponent. “27th Czech-Polish-Slovak Conference on Mining Geophysics”, Ramzova 5-7.10.1999, *Acta Montana* (in press).
- Číž, R., and Rudajev, V. (1996). Prediction methods based on multichannel statistical extrapolation and their application on induced seismic events. *Acta Montana A.* **10**(102), 133–144.
- Číž, R., and Rudajev, V. (1999). Extrapolation of the occurrence of mining tremors by application of neural networks. *Publ. Inst. Geophys. Polish Acad. Sci.* **M-22**(310), 53–62
- Číž, R., and Růžek, B. (1997). Periodicity of mining and induced seismicity in the Mayrau mine, Czech Republic. *Studia Geophys. Geod.* **41**, 29–44.
- Cornell, C. A. (1968). Engineering seismic risk analysis. *Bull. Seismol. Soc. Am.* **58**, 1583–1606.

- Cosentino, P., De Luca, L., Lasocki, S., and Luzio, D. (1997). Evaluation of fractal dimension: Quantitative differentiation of seismicity clusters. *In* "Rockbursts and Seismicity in Mines" (S. J. Gibowicz, and S. Lasocki, eds.). Balkema, Rotterdam, pp. 45–47.
- Cosentino, P., Ficara, V., and Luzio, D. (1977). Truncated exponential frequency-magnitude relationship in the earthquake statistics. *Bull. Seismol. Soc. Am.* **67**, 1615–1623.
- Coughlin, J., and Kranz, R. (1991). New approaches to studying rock burst-associated seismicity in mines. *In* "Proc. 32nd U.S. Symposium Rock Mechanics as a Multidisciplinary Science" (J.-C. Roegiers, ed.). Balkema, Rotterdam, pp. 491–500.
- Crampin, S. (1994). The fracture criticality of crustal rocks. *Geophys. J. Int.* **118**, 428–438.
- Crampin, S. (1997). Keynote lecture: Going APE—Monitoring and modelling rock deformation with shear-wave splitting. *In* "Rockbursts and Seismicity in Mines" (S. J. Gibowicz and S. Lasocki, eds.). Balkema, Rotterdam, pp. 257–266.
- Crampin, S., Evans, R., and Atkinson, B. K. (1984). Earthquake prediction: A new physical basis. *Geophys. J. R. Astr. Soc.* **76**, 147–156.
- Crampin, S., and Zatsepin, S. V. (1997). Modelling the compliance of crustal rock—II. Response to temporal changes before earthquakes. *Geophys. J. Int.* **129**, 495–506.
- Dahm, T. (1996). Relative moment tensor inversion based on ray theory: Theory and synthetic tests. *Geophys. J. Int.* **124**, 245–257.
- Dębski, W. (1995). Selected problems of seismic event location. *Publ. Inst. Geophys. Pol. Acad. Sci.* **M-19**(281), 125–134.
- Dębski, W. (1997). Study of the image reconstruction accuracy of an active amplitude tomography. *In* "Rockbursts and Seismicity in Mines" (S. J. Gibowicz and S. Lasocki, eds.). Balkema, Rotterdam, pp. 141–144.
- Deichmann, N. (1997). Far-field pulse shapes from circular sources with variable rupture velocities. *Bull. Seismol. Soc. Am.* **87**, 1288–1296.
- De Luca, L., Lasocki, S., Luzio, D., and Vitale, M. (1999). Fractal dimension confidence interval estimation of epicentral distributions. *Ann. Geofis.* **42**, 911–925.
- Dennison, P. I. G., and van Aswegen, G. (1993). Stress modelling and seismicity on the Tanton fault: A case study in a South African gold mine. *In* "Rockbursts and Seismicity in Mines" (R. P. Young, ed.). Balkema, Rotterdam, pp. 327–335.
- Denny, M., Goldstein, P., Mayeda, K., and Walter, W. (1996). Seismic results from DOE's Non-Proliferation Experiment: A comparison of chemical and nuclear explosions. *In* "Monitoring a Comprehensive Test Ban Treaty" (E. S. Husebye and A. M. Dainty, eds.). Kluwer Academic Publishers, Dordrecht, pp. 355–364.
- Dessokey, M. M. (1984). Statistical models of the seismic hazard analysis for mining tremors and natural earthquakes. *Publ. Inst. Geophys. Pol. Acad. Sci.* **A-15**(174), 1–80.
- Dodge, D. A., and Sprende, K. F. (1992). Improvements in mining induced microseismic source locations at the Lucky Friday mine using an automated whole-waveform analysis system. *Pure Appl. Geophys.* **139**, 609–626.
- Domański, B. (1997). Comparison of source parameters of seismic events at Polish coal and copper mines. *In* "Rockbursts and Seismicity in Mines" (S. J. Gibowicz and S. Lasocki, eds.). Balkema, Rotterdam, pp. 101–105.
- Domański, B., and Gibowicz, S. J. (1999). Determination of source time function of mining-induced seismic events by the empirical Green's function approach. *Publ. Inst. Geophys. Polish Acad. Sci.* **M 22**(310), 5–14.
- Domański, B., Gibowicz, S. J., and Wiejacz, P. (2000). Source time function of seismic events at Rudna copper mine, Poland. *Pure Appl. Geophys.* (in press).
- Dubiński, J. (1997). Assessment of rockburst prevention using seismic profiling and tomography techniques in Polish coal mines. *In* "Rockbursts and Seismicity in Mines" (S. J. Gibowicz and S. Lasocki, eds.). Balkema, Rotterdam, pp. 305–309.

- Dubiński, J., and Stec, K. (1996). Variation of certain parameters of regional stress tensor under condition of rockburst hazard. *Pure Appl. Geophys.* **147**, 305–317.
- Dunlop, R., and Gaete, S. (1997). Controlling induced seismicity at El Teniente Mine: The Sub6 sector case history. In "Rockbursts and Seismicity in Mines" (S. J. Gibowicz and S. Lasocki, eds.). Balkema, Rotterdam, pp. 233–236.
- Durrheim, R. J., Haile, A., Roberts, M. K. C., Schweitzer, J. K., Spottiswoode, S. M., and Klokow, J. W. (1998). Violent failure of a remnant in a deep South African gold mine. *Tectonophysics* **289**, 105–116.
- Dziewonski, A. M., Ekstrom, G., and Nettles, M. (1997). Keynote lecture: Harvard Centroid-Moment Tensor Solutions 1976–96: Significance of the non-double couple. In "Rockbursts and Seismicity in Mines" (S. J. Gibowicz and S. Lasocki, eds.). Balkema, Rotterdam, pp. 3–16.
- Eckmann, J.-P., and Ruelle, D. (1992). Fundamental limitations for estimating dimensions and Lyapunov exponents in dynamical systems. *Physica D* **56**, 185–187.
- Eneva, M. (1996). Effect of limited data sets in evaluating the scaling properties of spatially distributed data: An example from mining-induced seismic activity. *Geophys. J. Int.* **124**, 773–786.
- Eneva, M. (1998). In search for a relationship between induced microseismicity and larger events in mines. *Tectonophysics* **289**, 91–104.
- Eneva, M., and Ben-Zion, Y. (1997). Techniques and parameters to analyze seismicity patterns associated with large earthquakes. *J. Geophys. Res.* **102**, 17,785–17,795.
- Eneva, M., and Villeneuve, T. (1997). Retrospective pattern recognition applied to mining-induced seismicity. In "Rockbursts and Seismicity in Mines" (S. J. Gibowicz and S. Lasocki, eds.). Balkema, Rotterdam, pp. 299–303.
- Eneva, M., and Young, R. P. (1993). Evaluation of spatial patterns in the distribution of seismic activity in mines: A case study of Creighton Mine, northern Ontario (Canada). In "Rockbursts and Seismicity in Mines" (R. P. Young, ed.). Balkema, Rotterdam, pp. 175–180.
- Fan, G. W., and Wallace, T. C. (1995). Focal mechanism of a recent event in South Africa: A study using a sparse very broadband network. *Seismol. Res. Lett.* **66**, 13–18.
- Feignier, B. (1991). How geology can influence scaling relations. *Tectonophysics* **197**, 41–53.
- Feignier, B., and Young, R. P. (1992). Moment tensor inversion of induced microseismic events: Evidence of non-shear failures in the $-4 < M < -2$ moment magnitude range. *Geophys. Res. Lett.* **19**, 1503–1506.
- Feigner, B., and Young, R. P. (1993). Failure mechanisms of microseismic events generated by a breakout development around an underground opening. In "Rockbursts and Seismicity in Mines" (R. P. Young, ed.). Balkema, Rotterdam, pp. 181–186.
- Feustel, A. J. (1997). Temporal-spatial b -values and observed relationships to structurally controlled ground falls in an open-stope mine. In "Rockbursts and Seismicity in Mines" (S. J. Gibowicz, and S. Lasocki, eds.). Balkema, Rotterdam, pp. 45–47.
- Finnie, G. (1994). A stationary model for time-dependent seismic hazard in mines. *Acta Geophys. Pol.* **42**, 111–118.
- Fletcher, J. B., and Spudich, P. (1998). Rupture characteristics of the three $M \sim 4.7$ (1992–1994) Parkfield earthquakes. *J. Geophys. Res.* **103**, 535–554.
- Fujii, Y., Ishijima, Y., and Deguchi, G. (1997). Prediction of coal face rockburst and micro-seismicity in deep longwall coal mining. *Int. J. Rock Mech. Min. Sci.* **34**, 85–96.
- Fujii, Y., and Sato, K. (1990). Difference in seismic moment tensors between microseismic events associated with a gas outburst and those induced by longwall mining activity. In "Rockbursts and Seismicity in Mines" (C. Fairhurst, ed.). Balkema, Rotterdam, pp. 71–75.
- Gay, N. C. (1993). Mining in the vicinity of geological structures—An analysis of mining induced seismicity and associated rockbursts in two South African mines. In "Rockbursts and Seismicity in Mines" (R. P. Young, ed.). Balkema, Rotterdam, pp. 57–62.

- Ge, M., and Mottahed, P. (1993). An automatic data analysis and source location system (ADSLS). In "Rockbursts and Seismicity in Mines" (R. P. Young, ed.). Balkema, Rotterdam, pp. 343–347.
- Gibowicz, S. J. (1979). Space and time variations of the frequency-magnitude relation for mining tremors in the Szombierki coal mine in Upper Silesia, Poland. *Acta Geophys. Pol.* **27**, 39–50.
- Gibowicz, S. J. (1990). Seismicity induced by mining. *Adv. Geophys.* **32**, 1–74.
- Gibowicz, S. J. (1993). Keynote address: Seismic moment tensor and the mechanism of seismic events in mines. In "Rockbursts and Seismicity in Mines" (R. P. Young, ed.). Balkema, Rotterdam, pp. 149–155.
- Gibowicz, S. J. (1995). Scaling relations for seismic events induced by mining. *Pure Appl. Geophys.* **144**, 191–209.
- Gibowicz, S. J. (1996). Relations between source mechanism and the ratio of *S* over *P* wave energy for seismic events induced by mining. *Acta Montana* **9**(100), 7–15.
- Gibowicz, S. J. (1997a). An anatomy of a seismic sequence in a deep gold mine. *Pure Appl. Geophys.* **150**, 393–414.
- Gibowicz, S. J. (1997b). Scaling relations for seismic events at Polish copper mines. *Acta Geophys. Pol.* **45**, 169–181.
- Gibowicz, S. J. (1998). Partial stress drop and frictional overshoot mechanism of seismic events induced by mining. *Pure Appl. Geophys.* **153**, 5–20.
- Gibowicz, S. J., Harjes, H.-P., and Schafer, M. (1990). Source parameters of seismic events at Heinrich Robert mine, Ruhr basin, Federal Republic of Germany: Evidence for nondouble-couple events. *Bull. Seismol. Soc. Am.* **80**, 88–109.
- Gibowicz, S. J., and Kijko, A. (1994). "An Introduction to Mining Seismology" Academic Press, San Diego.
- Gibowicz, S. J., and Lasocki, S., Eds. (1997). "Rockbursts and Seismicity in Mines." Balkema, Rotterdam.
- Gibowicz, S. J., and Wiejacz, P. (1994). A search for the non-shearing components of seismic events induced in Polish coal mines. *Acta Geophys. Pol.* **42**, 81–109.
- Gibowicz, S. J., Young, R. P., Talebi, S., and Rawlence, D. J. (1991). Source parameters of seismic events at the Underground Research Laboratory in Manitoba, Canada: Scaling relations for the events with moment magnitude smaller than -2. *Bull. Seismol. Soc. Am.* **81**, 1157–1182.
- Glassmoyer, G., and Borchardt, R. D. (1990). Source parameters and effects of bandwidth and local geology on high-frequency ground motion observed for aftershocks of the northeastern Ohio earthquake of 31 January 1986. *Bull. Seismol. Soc. Am.* **80**, 889–912.
- Glazer, S. N. (1997). Applied mine seismology: A Vaal Reefs perspective. In "Rockbursts and Seismicity in Mines" (S. J. Gibowicz and S. Lasocki, eds.). Balkema, Rotterdam, pp. 227–231.
- Glazer, S. N. (1998). "Practical Applications of Stress Index and Other Seismological Parameters in Combating Rockburst Hazard in Deep Gold Mine of Vaal Reefs, South Africa" (Ph.D. thesis) University of Mining and Metallurgy, Cracow.
- Głowacka, E. (1992). Application of the extracted volume as a measure of deformation for the seismic hazard evaluation in mines. *Tectonophysics* **202**, 285–290.
- Głowacka, E. (1993). Excavated volume and long-term seismic hazard evaluation in mines. In "Rockbursts and Seismicity in Mines" (R. P. Young, ed.). Balkema, Rotterdam, pp. 69–73.
- Głowacka, E., and Kijko, A. (1989). Continuous evaluation of seismic hazard induced by the deposit extraction in selected coal mines in Poland. *Pure Appl. Geophys.* **129**, 523–533.
- Głowacka, E., and Lasocki, S. (1992). Probabilistic synthesis of the seismic hazard evaluation in mines. *Acta Montana* **84**, 59–66.
- Głowacka, E., Rudajev, V., and Bucha V. (1988). An attempt of continuous evaluation of seismic hazard induced by deposit extraction for the Robert field in the Gottwald mine in Kladno, Czechoslovakia. *Publ. Inst. Geophys. Pol. Acad. Sci.* **M-10**(213), 311–319.

- Głowacka, E., Stankiewicz, T., and Holub, K. (1992). Seismic hazard estimate based on the extracted deposit volume and bimodal character of seismic activity. In "Induced Seismicity" (P. Knoll, ed.). Balkema, Rotterdam, pp. 45–53.
- Godano, C., Alonzo, M. L., and Bottari, A. (1996). Multifractal analysis of the spatial distribution of earthquakes in southern Italy. *Geophys. J. Int.* **125**, 901–911.
- Graham, G., Crampin, S., and Fernandez, L. M. (1991). Observations of shear-wave polarizations in a South African gold field: An analysis of acceleration and velocity recordings. *Geophys. J. Int.* **107**, 661–672.
- Grassberger, P. (1983). Generalized dimensions of strange attractors. *Phys. Rev. Lett. A* **97**, 227–230.
- Grassberger, P., and Procaccia, I. (1983). Characterization of strange attractors. *Phys. Rev. Lett.* **50**, 346–349.
- Grasso, J.-R. (1993). Triggering of self-organized system: Implications for the state of the uppermost crust. In "Rockbursts and Seismicity in Mines" (R. P. Young, ed.). Balkema, Rotterdam, pp. 187–194.
- Grasso, J.-R., and Sornette, D. (1998). Testing self-organized criticality by induced seismicity. *J. Geophys. Res.* **103**, 29,965–29,987.
- Gumbel, E. J. (1962). "Statistics of Extremes" Columbia University Press, New York.
- Guo, Z., and Ogata, Y. (1995). Correlation between characteristic parameters of aftershock distributions in time, space and magnitude. *Geophys. Res. Lett.* **22**, 993–996.
- Gupta, H. K., and Chadha, R. K., Eds. (1995). "Induced Seismicity." Birhauser Verlag, Basel.
- Hagiwara, Y. (1974). Probability of earthquake occurrence as obtained from a Weibull distribution analysis of crustal strain. *Tectonophysics* **23**, 313–318.
- Hall, P. (1992). "The Bootstrap and Edgeworth Expansion." Springer-Verlag, New York.
- Hartzell, S. H. (1978). Earthquake aftershocks as Green's functions. *Geophys. Res. Lett.* **5**, 1–4.
- Hatherly, P., and Luo, X. (1999). Microseismic monitoring—Implications for longwall geomechanics and its role as an operational tool. In "Proc. 2nd Int. Underground Coal Conf." (B. K. Hebblewhite, J. M. Galvin and A. J. Broome, eds.). 15–18 June 1999, Sydney, Australia.
- Hatherly, P., Luo, X., McKavanagh, B., and Dixon, R. (1997). Seismic monitoring of ground caving processes associated with longwall mining of coal. In "Rockbursts and Seismicity in Mines" (S. J. Gibowicz and S. Lasocki, eds.). Balkema, Rotterdam, pp. 121–124.
- Hentschel, H. G. E., and Procaccia, I. (1983). The infinite number of generalized dimensions of fractals and strange attractors. *Physica D* **8**, 435–444.
- Hilborn, R. C. (1994) "Chaos and Nonlinear Dynamics." Oxford University Press, Oxford.
- Hirabayashi, T., Ito, K., and Yoshii, T. (1992) Multifractal analysis of earthquakes. *Pure Appl. Geophys.* **138**, 591–610.
- Hirata, T., and Imoto, M. (1991). Multifractal analysis of spatial distribution of microearthquakes in the Kanto region. *Geophys. J. Int.* **107**, 155–162.
- Holmes, G. M., Crampin, S., and Young, P. R. (1993). Preliminary analysis of shear-wave splitting in granite at the Underground Research Laboratory, Manitoba. *Can. J. Expl. Geophys.* **29**, 140–152.
- Holub, K. (1995). Analysis of *b*-value in the frequency-energy distributions. *Publ. Inst. Geophys. Polish Acad. Sci.* **M-19**(281), 153–161.
- Holub, K. (1996a). Space-time variations of the frequency-energy relation for mining-induced seismicity in the Ostrava-Karvina Mining District. *Pure Appl. Geophys.* **146**, 265–280.
- Holub, K. (1996b). Origin and dynamics of certain induced seismicity focal regions. In "Tectonophysics of Mining Areas" (A. Idziak, ed.). University of Silesia, Katowice, pp. 110–121.
- Holub, K. (1997). Predisposition to induced seismicity in some Czech coal mines. *Pure Appl. Geophys.* **150**, 435–450.
- Idziak, A., Ed. (1996a). "Tectonophysics of Mining Areas." University of Silesia, Katowice.
- Idziak, A. (1996b). Spatial distributions of the induced seismicity in the Upper Silesian Coal Basin. In "Tectonophysics of Mining Areas" (A. Idziak, ed.). University of Silesia, Katowice, pp. 99–109.

- Idziak, A. F. (1999). A study of spatial distribution of induced seismicity in the Upper Silesian Coal Basin. *Natural Hazards* **19**, 97–105.
- Idziak, A., Sagan, G., and Zuberek, W. M. (1991). An analysis of energy distributions of shocks from the Upper Silesian Coal Basin. *Publ. Inst. Geophys. Polish Acad. Sci.* **M-15**(235), 163–182 (in Polish, English abstract).
- Idziak, A., and Teper, L. (1996a). Fractal dimension of faults network in the Upper Silesian Coal Basin (Poland): Preliminary studies. *Pure Appl. Geophys.* **147**, 239–247.
- Idziak, A., and Teper, L. (1996b). Fractality of spatial distribution of both faults and seismic events within Bytom synclina, Upper Silesia. *Acta Montana* **A9**(100), 65–72.
- Idziak, A., Teper, L., Zuberek, W. M., and Dubiel, R. (1997). Mine tremor mechanisms used to estimate the stress field near the deep-rooted fault in the Upper Silesian Coal Basin, Poland. In “Rockbursts and Seismicity in Mines” (S. J. Gibowicz and S. Lasocki, eds.). Balkema, Rotterdam, pp. 31–37.
- Idziak, A., and Zuberek, W. M. (1995). Fractal analysis of mining induced seismicity in the Upper Silesia Coal Basin. In “Mechanics of Jointed and Faulted Rocks” (H. P. Rossmanith, ed.). Balkema, Rotterdam, pp. 679–682.
- Imanishi, K., and Takeo, M. (1998). Estimates of fault dimensions for small earthquakes. *Geophys. Res. Lett.* **25**, 2897–2900.
- Ito, K., and Matsuzaki, M. (1990) Earthquakes as self-organised critical phenomena. *J. Geophys. Res.* **95**, 6853–6860.
- Jaumé, S. C., and Sykes, L. R. (1999). Evolving towards a critical point: A review of accelerating seismic moment/energy release prior to large and great earthquakes. *Pure Appl. Geophys.* **155**, 279–306.
- Jha, P. C., Srinivasan, C., and Raju, N. M. (1993). Area rockbursts in Kolar Gold Fields: The possible attribute. In “Rockbursts and Seismicity in Mines” (R. P. Young, ed.). Balkema, Rotterdam, pp. 199–203.
- Johnston, J. C. (1992). Rockbursts from a global perspective. In “Induced Seismicity” (P. Knoll, ed.). Balkema, Rotterdam, pp. 63–78.
- Johnston, J. C., and Einstein, H. H. (1990). A survey of mining associated rockbursts. In “Rockbursts and Seismicity in Mines” (C. Fairhurst, ed.). Balkema, Rotterdam, pp. 121–128.
- Jost, M. L., Busselberg, T., Jost, O., and Harjes, H.-P. (1998). Source parameters of injection-induced microearthquakes at the KTB deep drilling site, Germany. *Bull. Seismol. Soc. Am.* **88**, 815–832.
- Jost, M. L., and Jost, O. (1994). A temporary decrease of induced seismicity in the Lubin copper mining district, Poland, observed at the GERESS array, Germany. *Acta Geophys. Pol.* **42**, 177–182.
- Kagan, Y. Y. (1991). Likelihood analysis of earthquake catalogs. *Geophys. J. Int.* **106**, 135–148.
- Kagan, Y. Y. (1994). Observational evidence for earthquakes as a nonlinear dynamic process. *Physica D* **77**, 160–192.
- Kagan, Y. Y. (1997a). Are earthquakes predictable? *Geophys. J. Int.* **131**, 505–525.
- Kagan, Y. Y. (1997b) Seismic moment-frequency relation for shallow earthquakes: Regional comparison. *J. Geophys. Res.* **102**, 2835–2852.
- Kaiser, P. K., and Maloney, S. M. (1997a). Scaling laws for the design of rock support. *Pure Appl. Geophys.* **150**, 415–434.
- Kaiser, P. K., and Maloney, S. M. (1997b). Ground motion parameters for design of support in burst-prone ground. In “Rockbursts and Seismicity in Mines” (S. J. Gibowicz and S. Lasocki, eds.). Balkema, Rotterdam, pp. 337–342.
- Kaláb, Z., and Müller, K. (1996). A contribution to the seismotectonic setting of northern part of the Moravo-Silesian area. In “Tectonophysics of Mining Areas” (A. Idziak, ed.). University of Silesia, Katowice, pp. 122–131.
- Kalenda, P. (1995). Seismic monitoring and maximum event prediction at longwall No. 138704 in the Lazy coal mine, Czech republic. *Publ. Inst. Geophys. Pol. Acad. Sci.* **M-19**(281), 163–176.

- Kalenda, P. (1996). Analysis of the prediction possibility of strong mining induced seismic events in Ostrava-Karvina Coal Basin on the basis of seismological method. In "Tectonophysics in Mining Areas" (A. Idziak, ed.). University of Silesia, Katowice, pp. 145–161.
- Kalenda, P., and Pompura, I. (1996). Seismic monitoring at the Jelsava deposit. *Acta Montana A.* **9**(100), 207–215.
- Kaneko, K., Sugawara, K., and Obara, Y. (1992). Microseismic monitoring for coal burst prediction in the Miike coal mine. In "Induced Seismicity" (P. Knoll, ed.). Balkema, Rotterdam, pp. 79–92.
- Keilis-Borok, V. I., and Kossobokov, V. G. (1990). Premonitory activation of earthquake flow: Algorithm M8. *Phys. Earth Planet. Inter.* **61**, 73–83.
- Keilis-Borok, V. I., and Rotwein, I. M. (1990). Diagnosis of time of increased probability of strong earthquakes in different regions of the world: Algorithm CN. *Phys. Earth Planet. Inter.* **61**, 57–72.
- Kijko, A. (1982). A modified form of the first Gumbel distribution: Model for the occurrence of large earthquakes. Part I—Derivation of distribution. *Acta Geophys. Pol.* **30**, 333–340.
- Kijko, A. (1985). Theoretical model for a relationship between mining seismicity and excavation area. *Acta Geophys. Pol.* **33**, 231–241.
- Kijko, A. (1994). Seismological outliers: L_l or adaptive L_p norm application. *Bull. Seismol. Soc. Am.* **84**, 473–477.
- Kijko, A. (1996). "Statistical Methods in Mining Seismology." Lecture Notes. South African Geophys. Association, Pretoria.
- Kijko, A. (1997). Keynote lecture: Seismic hazard assessment in mines. In "Rockbursts and Seismicity in Mines" (S. J. Gibowicz and S. Lasocki, eds.). Balkema, Rotterdam, pp. 247–256.
- Kijko, A., Drzezla, B., and Stankiewicz, T. (1987). Bimodal character of the distribution of extreme seismic events in Polish mines. *Acta Geophys. Pol.* **35**, 157–166.
- Kijko, A., and Funk, C. W. (1994). The assessment of seismic hazards in mines. *J. South Afr. Inst. Min. Met.*, 179–185.
- Kijko, A., and Funk, C. W. (1996). Space–time interaction amongst clusters of mining induced seismicity. *Pure Appl. Geophys.* **147**, 277–288.
- Kijko, A., Funk, C. W., and Brink, A. v. Z. (1993). Identification of anomalous patterns in time-dependent mine seismicity. In "Rockbursts and Seismicity in Mines" (R. P. Young, ed.). Balkema, Rotterdam, pp. 205–210.
- Kijko, A., and Graham, G. (1998). Parametric-historic procedure for probabilistic seismic hazard analysis. Part I: Estimation of maximum regional magnitude m_{\max} . *Pure Appl. Geophys.* **152**, 413–442.
- Kijko, A., Lasocki, S., and Graham, G. (2000). Nonparametric seismic hazard analysis in mines. *Pure Appl. Geophys.* (in press).
- Kijko, A., and Sciocatti, M. (1995a). Optimal spatial distribution of seismic stations in mines. *Int. J. Rock Mech. Min. Sci.* **32**, 607–615.
- Kijko, A., and Sciocatti, M. J. (1995b). Statistical analysis of seismicity. In "Project Report: Strategies, Methodologies, and Technologies for Seismic Monitoring, Analysis and Interpretation of Rockburst Prone Mines." GAP 017—Seismology for Rockburst Prevention, Control and Prediction, Chapter 7, Dept. of Min. and Energy Affairs of South Africa, Pretoria.
- Kijko, A., and Sellevoll, M. A. (1989) Estimation of earthquake hazard parameters from incomplete data files. Part I. Utilization of extreme and complete catalogs with different threshold magnitudes. *Bull. Seismol. Soc. Am.* **79**, 645–654.
- Kiremidjian, A. S., and Anagnos, T. (1984). Stochastic slip-predictable model for earthquake occurrences. *Bull. Seismol. Soc. Am.* **74**, 739–755.
- Knoll, P. (1990). The fluid-induced tectonic rockburst of March 13, 1989, in the "Werra" potash mining district of the GDR (first results). *Gerl. Beitr. Geophys.* **99**, 239–245.
- Knoll, P., Ed. (1992). "Induced Seismicity." Balkema, Rotterdam.
- Knoll, P., and Kowalle, G., Eds. (1996). "Induced Seismic Events." Birkhauser Verlag, Basel.

- Knopoff, L., and Kagan, Y. Y. (1977). Analysis of the theory of extremes as applied to earthquake problems. *J. Geophys. Res.* **82**, 5647–5657.
- Kolesov, V. A. (1993). The state of works on the problem of rock bursts in the mines of the Sevralsboksitruuda. In “Rock Bursts in Ore and Non-ore Deposits.” Publ. House, Kola Sci. Center, Russ. Acad. Sci., Apatity, pp. 50–57.
- Konečný, P. (1992). Mining-induced seismicity (rock bursts) in the Ostrava-Karvina Coal Basin, Czechoslovakia. In “Induced Seismicity” (P. Knoll, ed.). Balkema, Rotterdam, pp. 107–129.
- Koza, J. (1997). Digital seismic system for registration of mining tremors and strain in Polish coal and copper mines. In “Rockbursts and Seismicity in Mines” (S. J. Gibowicz and S. Lasocki, eds.). Balkema, Rotterdam, pp. 145–147.
- Kremenetskaya, E. O., and Tryapitsin, V. M. (1995). Induced seismicity in the Khibiny Massif (Kola Peninsula). *Pure Appl. Geophys.* **145**, 29–37.
- Król, M. (1998). “Application of Seismic Moment Tensor and Spectral Analysis of Seismic Waves to Study Seismic Events at the Polkowice-Sieroszowice Copper Mine” (Ph.D. thesis) Institute of Geophysics, Polish Academy of Sciences, Warsaw (in Polish).
- Król, M., and Kijko, A. (1991). Relative location of mining events: Estimation of the method efficiency. *Przegląd Górniczy* **10**, 328–335 (in Polish; English abstract).
- Kurths, J., and Herzog, H. (1987). An attractor in a solar time series. *Physica D* **25**, 167–172.
- Laskownicka, A. (1998). Anomalous behaviour of selected parameters of epicentre distribution prior to strong tremors in mines. In “Proc. Mining Geophysics—Int. Conf.” VNIMI, St. Petersburg, pp. 141–146.
- Laskownicka, A. (1999). The potential forecasting abilities of selected parameters of the seismic tremors series: Examples from coal, copper and gold mines. *Publ. Inst. Geophys. Polish Acad. Sci.* **M-22**(310), 257–265 (in Polish, English abstract)
- Lasocki, S. (1982). Statistical method of estimating the probability of occurrence of strong mining shocks in the longwall region. *Publ. Inst. Geophys. Polish Acad. Sci.* **M-5**(155), 73–84 (in Polish, English abstract).
- Lasocki, S. (1987). Study of distributions of mining tremors energy. *Sci. Bull. Univ. Min. Metall., s. Mining* **129**, 177–182 (in Polish, English abstract).
- Lasocki, S. (1989). Some estimates of rockburst danger in underground coal mines from energy distribution of M.A. events. In “Proc. 4th Conf. on Acoustic Emission/Microseismic Activity in Geologic Structures and Materials” (H. R. Hardy, Jr., ed.). Trans Tech Publications, Clausthal, pp. 617–633.
- Lasocki, S. (1992a). Non-Poissonian structure of mining induced seismicity. *Acta Montana* **84**, 51–58.
- Lasocki, S. (1992b). Weibull distribution for time intervals between mining tremors. *Publ. Inst. Geophys. Polish Acad. Sci.* **M-16**(245), 241–260.
- Lasocki, S. (1992c). Truncated Pareto distribution used in the statistical analysis of rockburst hazard. *Acta Montana A* **2**(88), 121–132.
- Lasocki, S. (1993a). Statistical prediction of strong mining tremors. *Acta Geophys. Pol.* **41**, 197–234.
- Lasocki, S. (1993b). Weibull distribution as a model for sequence of seismic events induced by mining. *Acta Geophys. Pol.* **41**, 101–112.
- Lasocki, S. (1994). Parametric or nonparametric analysis of induced seismicity sequences. In “EUROCK’94-Proc. SPE/ISRM Int. Conf. Rock Mechanics in Petroleum Engineering.” Balkema, Rotterdam, pp. 639–644.
- Lasocki, S. (1996). Dispersion of foci—a possible precursor of strong tremors? *Acta Montana A.* **9**(100), 83–89.
- Lasocki, S., and De Luca, L. (1998). Monte Carlo studies of relations between fractal dimensions in monofractal data sets. *Pure Appl. Geophys.* **152**, 213–220.
- Lasocki, S., and Idziak, A. F. (1998). Dominant directions of epicenter distribution of regional mining induced seismicity series in Upper Silesian Coal Basin in Poland. *Pure Appl. Geophys.* **153**, 21–40.

- Lasocki, S., Kijko, A., and Graham, G. (2000). Model-free seismic hazard estimation. In "Proc. Int. Conf. on Seismic Hazard and Risk in the Mediterranean Region." Nicosia, N. Cyprus, October 18–22, 1999 (in press).
- Lasocki, S., and Mortimer, Z. (1998). Variations of MS source distribution geometry before a strong tremor occurrence in mines. In "Proc. 6th Conf. Acoustic Emission/Microseismic Activity in Geologic Structures and Materials" (H. R. Hardy, Jr., ed.). Trans Tech Publications, Clausthal, pp. 325–337.
- Lasocki, S., and Węglarczyk, S. (1998). Complex and variable magnitude distribution of microtremors induced by mining: An example from a gold mine, South Africa. *Unpublished presentation XXVI General Assemb. ESC* Tel Aviv August 23–28, 1998. Abstracts, 37.
- Lasocki, S., Węglarczyk, S., and Gibowicz, S. J. (1997). A new method to estimate directional character of mining-induced seismicity: Application to the data from Wujek coal mine, Poland. In "Rockbursts and Seismicity in Mines" (S. J. Gibowicz and S. Lasocki, eds.). Balkema, Rotterdam, pp. 207–211.
- Leach, A. R., and Lenhardt, W. A. (1990). Pillar associated seismicity at Western Deep Levels Mine. In "Static and Dynamic Considerations in Rock Engineering" (R. Brummer, ed.). Balkema, Rotterdam, pp. 197–205.
- Lenhardt, W. A. (1990). Seismic event characteristics in a deep level mining environment. In "Rock at Great Depth" (V. Maury and D. Fourmaintraux, eds.). Balkema, Rotterdam, pp. 727–732.
- Lenhardt, W. A., and Hagan, T. O. (1992). Observations and possible mechanisms of pillar-associated seismicity at great depth. In "Induced Seismicity" (P. Knoll, ed.). Balkema, Rotterdam, pp. 149–162.
- Lenhardt, W. A., and Pascher, C. (1996). The mechanism of mine-collapse deduced from seismic observations. *Pure Appl. Geophys.* **147**, 207–216.
- Li, Y., Doll Jr., C., and Toksoz, M. N. (1995). Source characterization and fault plane determinations for $M_{bLg} = 1.2$ to 4.4 earthquakes in the Charlevoix seismic zone, Quebec, Canada. *Bull. Seismol. Soc. Am.* **85**, 1604–1621.
- Li, Y., and Thurber, C. H. (1988). Source properties of two microearthquakes at Kilauea Volcano, Hawaii. *Bull. Seismol. Soc. Am.* **78**, 1123–1132.
- Lomakin, V. S., and Junusov, F. F. (1993). Effective seismological monitoring in mines. In "Rock Bursts in Ore and Non-ore Deposits." Publ. House, Kola Sci. Center, Russ. Acad. Sci., Apatity, pp. 73–76.
- Madariaga, R. (1976). Dynamics of an expanding circular fault. *Bull. Seismol. Soc. Am.* **66**, 639–666.
- Main, I. G., and Burton, P. W. (1984). Information theory and the earthquake frequency-magnitude distribution. *Bull. Seimol. Soc. Am.* **74**, 1409–1426.
- Main, I. G., Henderson, J. R., Meredith, P. G., and Sammonds, P. R. (1994). Self-organised criticality and fluid-rock interactions in the brittle fluid. *Pure Appl. Geophys.* **142**, 529–543.
- Malan, D. F., and Spottiswoode, S. M. (1997). Time-dependent fracture zone behaviour and seismicity surrounding deep level stoping operations. In "Rockbursts and Seismicity in Mines" (S. J. Gibowicz and S. Lasocki, eds.). Balkema, Rotterdam, pp. 173–177.
- Mandelbrot, B. B. (1982). "The Fractal Geometry of Nature." Freeman, San Francisco.
- Mandelbrot, B. B. (1989). Multifractal measures, especially for the geophysicist. *Pure Appl. Geophys.* **131**, 5–43.
- Manthéi, G. (1997). Seismic tomography on a pillar in a potash mine. In "Rockbursts and Seismicity in Mines" (S. J. Gibowicz and S. Lasocki, eds.). Balkema, Rotterdam, pp. 237–243.
- Marcak, H. (1993). The use of pattern recognition method for predicting of the rockbursts. In "Rockbursts and Seismicity in Mines" (R. P. Young, ed.). Balkema, Rotterdam, pp. 222–226.
- Martin, C. D. (1990). Failure observations and in situ stress domains at the Underground Research Laboratory. In "Rock at Great Depth" (V. Maury and D. Fourmaintraux, eds.). Balkema, Rotterdam, pp. 719–726.

- Martin, C. D., and Young, R. P. (1993). The effect of excavation-induced seismicity on the strength of Lac du Bonnet granite. In "Rockbursts and Seismicity in Mines" (R. P. Young, ed.). Balkema, Rotterdam, pp. 367–371.
- Matsumura, S. (1984). A one-parameter expression of seismicity patterns in space and time. *Bull. Seismol. Soc. Am.* **74**, 2,529–2,576.
- Maxwell, S. C., and Young, R. P. (1992). Sequential velocity imaging and microseismic monitoring of mining-induced stress change. *Pure Appl. Geophys.* **139**, 421–447.
- Maxwell, S. C., and Young, R. P. (1993a). A comparison between active source and passive source images. *Bull. Seismol. Soc. Am.* **83**, 1813–1834.
- Maxwell, S. C., and Young, R. P. (1993b). Associations between temporal velocity changes and induced seismicity. *Geophys. Res. Lett.* **20**, 2929–2932.
- Maxwell, S. C., and Young, R. P. (1993c). Stress change monitoring using induced microseismicity for sequential passive velocity. In "Rockbursts and Seismicity in Mines" (R. P. Young, ed.). Balkema, Rotterdam, pp. 373–377.
- Maxwell, S. C., and Young, R. P. (1995). A controlled *in-situ* investigation of the relationship between stress, velocity and induced seismicity. *Geophys. Res. Lett.* **22**, 1049–1052.
- Maxwell, S. C., and Young, R. P. (1996). Seismic imaging of rock mass response to excavation. *Int. J. Rock Mech. Min. Sci.* **33**, 713–724.
- Maxwell, S. C., and Young, R. P. (1997a). Seismic velocity inversion from microseismic data. In "Seismic Monitoring in Mines" (A. J. Mendecki, ed.). Chapman & Hall, London, pp. 108–118.
- Maxwell, S. C., and Young, R. P. (1997b). Assessing induced fracturing around underground excavations using velocity imaging and induced seismicity. In "Rockbursts and Seismicity in Mines" (S. J. Gibowicz and S. Lasocki, eds.). Balkema, Rotterdam, pp. 179–183.
- Maxwell, S. C., and Young, R. P. (1998). Propagation effects of an underground excavation. *Tectonophysics* **289**, 17–30.
- McCreary, R. G., Grant, D., and Falmagne, V. (1993). Source mechanisms, three-dimensional boundary-element modelling, and underground observations at Ansil Mine. In "Rockbursts and Seismicity in Mines" (R. P. Young, ed.). Balkema, Rotterdam, pp. 227–231.
- McGarr, A. (1976). Seismic moments and volume changes. *J. Geophys. Res.* **81**, 1487–1494.
- McGarr, A., Ed. (1992a). "Induced Seismicity." Birkhauser Verlag, Basel.
- McGarr, A. (1992b). An implosive component in the seismic moment tensor of a mining-induced tremor. *Geophys. Res. Lett.* **19**, 1579–1582.
- McGarr, A. (1992c). Moment tensors of ten Witwatersrand mine tremors. *Pure Appl. Geophys.* **139**, 781–800.
- McGarr, A. (1994). Some comparisons between mining-induced and laboratory earthquakes. *Pure Appl. Geophys.* **142**, 467–489.
- McGarr, A. (1999). On relating apparent stress to the stress causing earthquake fault slip. *J. Geophys. Res.* **104**, 3003–3011.
- McGarr, A., and Bicknell, J. (1990). Synthetic seismogram analysis of locally-recorded mine tremors. In "Rock at Great Depth" (V. Maury and D. Fourmaintraux, eds.). Balkema, Rotterdam, pp. 1407–1413.
- McGarr, A., Bicknell, J., Churcher, J., and Spottiswoode, S. M. (1990). Comparison of ground motion from tremors and explosions in deep gold mines. *J. Geophys. Res.* **95**, 21, 777–21, 792.
- McGarr, A., and Simpson, D. (1997). Keynote lecture: A broad look at induced and triggered seismicity. In "Rockbursts and Seismicity in Mines" (S. J. Gibowicz and S. Lasocki, eds.). Balkema, Rotterdam, pp. 385–396.
- McGarr, A., Simpson, D., and Seeber, L. (2000). Case histories of induced and triggered seismicity. In "International Handbook of Earthquake and Engineering Seismology" (P. C. Jennings, H. Kanamori, and W. H. K. Lee, eds.). Chapter 37. Academic Press (in press).

- McKavanagh, B., Boreham, B., McCue, K., Gibson, G., Hafner, J., and Klenowski, G. (1995). The CQU regional seismic network and applications to underground mining in Central Queensland, Australia. *Pure Appl. Geophys.* **145**, 39–57.
- Melnikov, N. N., Kozyrev, A. A., and Panin, V. I. (1996). Induced seismicity in large-scale mining in the Kola Peninsula and monitoring to reveal informative precursors. *Pure Appl. Geophys.* **147**, 263–276.
- Mendecki, A. J. (1987). Rock mass anisotropy modelling by inversion of mine tremor data. In “Proceedings of 6th International Congress on Rock Mechanics” (G. Herget and S. Vongpaisal, eds.). Balkema, Rotterdam, pp. 1141–1144.
- Mendecki, A. J. (1993). Keynote address: Real time quantitative seismology in mines. In “Rockbursts and Seismicity in Mines” (R. P. Young, ed.). Balkema, Rotterdam, pp. 287–295.
- Mendecki, A. J., Ed. (1997a). “Seismic Monitoring in Mines.” Chapman & Hall, London.
- Mendecki, A. J. (1997b). Quantitative seismology and rockmass stability. In “Seismic Monitoring in Mines” (A. J. Mendecki, ed.). Chapman & Hall, London, pp. 178–219.
- Mendecki, A. J. (1997c). Keynote lecture: Principles of monitoring seismic rockmass response to mining. In “Rockbursts and Seismicity in Mines” (S. J. Gibowicz and S. Lasocki, eds.). Balkema, Rotterdam, pp. 69–80.
- Mendecki, A. J., and Niewiadomski, J. (1997). Spectral analysis and seismic source parameters. In “Seismic Monitoring in Mines” (A. J. Mendecki, ed.). Chapman & Hall, London, pp. 144–158.
- Mendecki, A. J., and Sciocatti, M. (1997). Location of seismic events. In “Seismic Monitoring in Mines” (A. J. Mendecki, ed.). Chapman & Hall, London, pp. 87–107.
- Minney, D., Kotze, G., and van Aswegen, G. (1997). Seismic monitoring of the caving process above a retreating longwall at New Denmark Colliery, South Africa. In “Rockbursts and Seismicity in Mine” (S. J. Gibowicz and S. Lasocki, eds.). Balkema, Rotterdam, pp. 125–129.
- Mori, J. (1993). Fault plane determinations for three small earthquakes along the San Jacinto fault, California: Search for cross faults. *J. Geophys. Res.* **98**, 17,711–17,722.
- Mori, J., and Frankel, A. (1990). Source parameters for small events associated with the 1986 North Palm Springs, California, earthquake using empirical Green’s functions. *Bull. Seismol. Soc. Am.* **80**, 278–295.
- Morrison, D. M. (1993). Seismicity in the Sudbury Area mines. In “Rockbursts and Seismicity in Mines” (R. P. Young, ed.). Balkema, Rotterdam, pp. 379–382.
- Morrison, D. M., Swan, G., and Scholz, C. H. (1993). Chaotic behaviour and mining-induced seismicity. In “Rockbursts and Seismicity in Mines” (R. P. Young, ed.). Balkema, Rotterdam, pp. 233–237.
- Mortimer, Z. (1997). Fractal statistics for the local induced seismicity in some Polish coal mines. In “Rockbursts and Seismicity in Mines” (S. J. Gibowicz and S. Lasocki, eds.). Balkema, Rotterdam, pp. 49–54.
- Mortimer, Z., and De Luca, L. (1999). Temporal variations of the correlation dimensions of local mining seismicity with relation to the rockbursts generating process. *Acta Geophys. Pol.* **47**, 273–282.
- Mortimer, Z., and Lasocki, S. (1996a). Variation of the fractal dimension of epicentres positions in the mining induced seismicity. *Acta Montana A* **9**(100), 73–81.
- Mortimer, Z., and Lasocki, S. (1996b). Studies of fractality of epicentre distribution geometry in mining induced seismicity. *Acta Montana A.* **10**(102), 31–37.
- Mortimer, Z., Majewska, Z., and Lasocki, S. (1999). Generalized fractal dimension of induced seismicity and acoustic emission. *Publ. Inst. Geophys. Pol. Acad. Sci.* **M-22**(310), 89–94.
- Mountfort, P., and Mendecki, A. J. (1997a). Seismic transducers. In “Seismic Monitoring in Mines” (A. J. Mendecki, ed.). Chapman & Hall, London, pp. 1–20.
- Mountfort, P., and Mendecki, A. J. (1997b). Seismic monitoring systems. In “Seismic Monitoring in Mines” (A. J. Mendecki, ed.). Chapman & Hall, London, pp. 21–40.
- Mueller, C. S. (1985). Source pulse enhancement by deconvolution of an empirical Green’s function. *Geophys. Res. Lett.* **12**, 33–36.

- Murphy, J. R. (1996). Types of seismic events and their source descriptions. In "Monitoring a Comprehensive Test Ban Treaty" (E. S. Husebye and A. M. Dainty, eds.). Kluwer Academic Publishers, Dordrecht, pp. 225–245.
- Mutke, G., and Stec, K. (1997). Seismicity in the Upper Silesian Coal Basin, Poland: Strong regional seismic events. In "Rockbursts and Seismicity in Mines" (S. J. Gibowicz and S. Lasocki, eds.). Balkema, Rotterdam, pp. 213–217.
- Nerenberg, M. A. H., and Essex, C. (1990). Correlation dimension and systematic geometric effects. *Phys. Rev. A* **42**, 7065–7074.
- Newman, W. I., Gabrielov, A., and Turcotte, D. L., Eds. (1994). "Nonlinear Dynamics and Predictability of Geophysical Phenomena." IUGG and AGU, Washington.
- Niewiadomski, J. (1997). Seismic source radiation and moment tensor in the time domain. In "Seismic Monitoring in Mines" (A. J. Mendecki, ed.). Chapman & Hall, London, pp. 119–143.
- Nishimura, T., and Hamaguchi, H. (1993). Scaling law of volcanic explosion earthquakes. *Geophys. Res. Lett.* **20**, 2479–2482.
- Ohnaka, M. (1992). Earthquake source nucleation: A physical model for short term precursors. *Tectonophysics* **211**, 149–178.
- Orowan, E. (1960). Mechanism of seismic faulting in rock deformation. *Geol. Soc. Am. Mem.* **79**, 323–345.
- Ortlepp, W. D. (1992). Note on fault-slip motion inferred from a study of micro-cataclastic particles from an underground shear rupture. *Pure Appl. Geophys.* **139**, 677–695.
- Page, R. (1968). Aftershocks and microaftershocks. *Bull. Seismol. Soc. Am.* **58**, 1131–1168.
- Paladin, G., and Vulpiani, A. (1987). Anomalous scaling laws in multifractal objects. *Phys. Rep.* **156**, 147.
- Pechmann, J. C., Walter, W. R., Nava, S. J., and Arabasz, W. J. (1995). The February 3, 1995, ML 5.1 seismic event in the Trona mining district of southwestern Wyoming. *Seismol. Res. Lett.* **66**, 3–25.
- Phillips, W. S., Pearson, D. C., Yang, X., and Stump, B. W. (1999). Aftershocks of an explosively induced mine collapse at White Pine, Michigan. *Bull. Seismol. Soc. Am.* **89**, 1575–1590.
- Piana, M., and Bertero, M. (1997). Projected Landweber method and preconditioning. *Inverse Problems* **13**, 441–463.
- Pickering, G., Bull, J. M., and Sanderson, D. J. (1995). Sampling power-law distributions. *Tectonophysics* **248**, 1–20.
- Plouffe, M., Mottahed, P., Lebel, D., and Cote, M. (1993). Monitoring of large mining induced seismic events—CANMET/MRL's contribution. In "Rockbursts and Seismicity in Mines" (R. P. Young, ed.). Balkema, Rotterdam, pp. 399–403.
- Prugger, A. F., and Gendzwil, D. J. (1988). Microearthquake location: A non-linear approach that makes use of a simplex stepping procedure. *Bull. Seismol. Soc. Am.* **78**, 799–815.
- Radu, S., Sciocatti, M., and Mendecki, A. J. (1997). Nonlinear dynamics of seismic flow of rock. In "Seismic Monitoring in Mines" (A. J. Mendecki, ed.). Chapman & Hall, London, pp. 159–177.
- Redmayne, D. W., and Richards, J. A. (1998). Mining-induced earthquakes monitored during pit closure in the Midlothian Coalfield. *Q. J. Eng. Geol.* **31**, 21–36.
- Reiter, L. (1991). "Earthquake Hazard Analysis." Columbia University Press, New York.
- Robson, D. S., and Whitlock, J. H. (1964). Estimation of a truncation point. *Biometrika* **51**, 33–39.
- Rudajev, V. (1993). Keynote address: Recent Polish and Czechoslovakian rockburst research and the application of stochastic methods in mine seismology. In "Rockbursts and Seismicity in Mines" (R. P. Young, ed.). Balkema, Rotterdam, pp. 157–161.
- Rudajev, V. (1995). Investigation of induced seismic phenomena in the bituminous coal Kladno district. *Acta Montana* **A7**(96), 5–9.
- Rudajev, V., and Čiž, R. (1999). Estimation of mining tremor occurrence by using neural networks. *Pure Appl. Geophys.* **154**, 57–72.

- Rudajev, V., and Fučík, P. (1982). Application possibilities of the autoregression model for the prediction of rock bursts. *Acta Montana* **61**, 47–60 (in Czech, English abstract).
- Růžek, B. (1995). Short note on automatic location of seismic events. *Publ. Inst. Geophys., Pol. Acad. Sci.* **M-19**(281), 135–139.
- Sagan, G., Teper, L., and Zuberek, W. M. (1996). Tectonic analysis of mine tremor mechanisms from the Upper Silesian Coal Basin. *Pure Appl. Geophys.* **147**, 217–238.
- Sambridge, M., and Gallagher, K. (1993). Earthquake hypocenter location using genetic algorithms. *Bull. Seismol. Soc. Am.* **83**, 1467–1491.
- Sammis, C. G., and Smith, S. W. (1999). Seismic cycles and the evolution of stress correlation in cellular automaton models of finite fault networks. *Pure Appl. Geophys.* **155**, 307–334.
- Sato, K., and Fujii, Y. (1988). Induced seismicity associated with longwall coal mining. *Int. J. Rock Mech. Min. Sci. Geomech. Abstr.* **25**, 253–262.
- Savage, J. C., and Wood, M. D. (1971). The relation between apparent stress and stress drop. *Bull. Seismol. Soc. Am.* **61**, 1381–1388.
- Scott, D. F., Williams, T. J., and Friedel, M. J. (1997). Investigation of a rock-burst site, Sunshine Mine, Kellogg, Idaho. In “Rockbursts and Seismicity in Mines” (S. J. Gibowicz and S. Lasocki, eds.). Balkema, Rotterdam, pp. 311–315.
- Scott, D. F., Williams, T. J., and White, B. C. (1993). Host structures for slip-induced seismicity at the Lucky Friday Mine. In “Rockbursts and Seismicity in Mines” (R. P. Young, ed.). Balkema, Rotterdam, pp. 245–248.
- Senfaute, G., Chambon, C., Bigarre, P., Guise, Y., and Josien, J. P. (1997). Spatial distribution of mining tremors and the relationship to rockburst hazard. *Pure Appl. Geophys.* **150**, 451–459.
- Shao, J., and Tu, D. (1995). “The Jackknife and Bootstrap.” Springer-Verlag, New York.
- Shivakumar, K., Rao, M. V. M. S., Srinivasan, C., and Kusunose, K. (1996). Multifractal analysis of the spatial distribution of area rockbursts at Kolar Gold mines. *Int. J. Rock Mech., Min., Sci. Geomech. Abstr.* **33**, 167–172.
- Šilený, J., and Baker, C. (1997). Fast estimate of the focal mechanism of mining tremors from P and S amplitudes. In “Rockbursts and Seismicity in Mines” (S. J. Gibowicz and S. Lasocki, eds.). Balkema, Rotterdam, pp. 39–44.
- Silverman, B. W. (1986) “Density Estimation for Statistics and Data Analysis.” Chapman & Hall, London.
- Slavik, J., Kalenda, P., and Holub, K. (1992). Statistical analysis of seismic events induced by the underground mining. *Acta Montana A* **2**(88), 133–144.
- Smith, A. T. (1993). Discrimination of explosions from simultaneous mining blasts. *Bull. Seismol. Soc. Am.* **83**, 160–179.
- Smith, K. D., Brune, J. N., and Priestly, K. F. (1991). The seismic spectrum, radiated energy, and the Savage and Wood inequality for complex earthquakes. *Tectonophysics* **188**, 303–320.
- Smith, L. A. (1988). Intrinsic limits on dimension calculations. *Physics Lett. A.* **133**, 283–288.
- Sornette, A., and Sornette, D. (1989). Self organised criticality and earthquakes. *Europhys. Lett.* **9**, 197–202.
- Spottiswoode, S. M. (1993). Seismic attenuation in deep-level mines. In “Seismicity in Mines” (R. P. Young, ed.). Balkema, Rotterdam, pp. 409–414.
- Spottiswoode, S. M., and Milev, A. M. (1998). The use of waveform similarity to define planes of mining-induced seismic events. *Tectonophysics* **289**, 51–60.
- Sprenke, K. F., Stickney, M. C., Dodge, D. A., and Hammond, W. R. (1991). Seismicity and tectonic stress in the Coeur d’Alene mining district. *Bull. Seismol. Soc. Am.* **81**, 1145–1156.
- Srinivasan, C., and Shringarputale, S. B. (1992). Mine-induced seismicity in the Kolar Gold Fields. In “Induced Seismicity” (P. Knoll, ed.). Balkema, Rotterdam, pp. 173–183.
- Stacy, S. J., McCloskey, J., Bean, C. J., and Ren, J. (1997). Simulating seismicity in Creighton Mine: A 3-D self-organized critical model. In “Rockbursts and Seismicity in Mines” (S. J. Gibowicz and S. Lasocki, eds.). Balkema, Rotterdam, pp. 201–205.

- Stewart, R. D., and Spottiswoode, S. M. (1993). A technique for determining the seismic risk in deep-level mining. In "Rockbursts and Seismicity in Mines" (R. P. Young, ed.). Balkema, Rotterdam, pp. 123–128.
- Stickney, M. C., and Sprengle, K. F. (1993). Seismic events with implosional focal mechanisms in the Coeur d'Alene mining district, northern Idaho. *J. Geophys. Res.* **98**, 6523–6528.
- Subbaramu, K. R., Rao, B. S. S., Krishnamurthy, R., and Srinivasan, C. (1989). Seismic investigation of rockbursts in the Kolar Gold Fields. In "Proc. 4th Conf. Acoustic Emission/Microseismic Activity in Geologic Structures and Materials" (H. R. Hardy, Jr., ed.). Trans Tech Publications, Clausthal, pp. 265–274.
- Swanson, P. L. (1992). Mining-induced seismicity in faulted geological structures: An analysis of seismicity-induced slip potential. *Pure Appl. Geophys.* **139**, 657–676.
- Swanson, P. L., Estey, L. H., Boler, F. M., and Billington, S. (1992). Mining-induced microseismic event location: Accuracy and precision of two location systems. *Pure Appl. Geophys.* **139**, 375–404.
- Sykes, L. R., Shaw, B. E., and Scholz, C. H. (1999). Rethinking earthquake prediction. *Pure Appl. Geophys.* **155**, 207–232.
- Syrnikov, N. M., and Tryapitsin, V. M. (1990). On mechanics of an induced earthquake in the Khibiny. *Dokl. Akad. Nauk SSSR* **314**(4), 830–833.
- Takens, F. (1981). Detecting strange attractors in turbulence. In "Dynamical Systems and Turbulence, Warwick 1980" (D. Rand, and L. S. Young, eds.). Springer, Berlin, p. 366.
- Talebi, S., Ed. (1997). "Seismicity Associated with Mines, Reservoirs and Fluid Injections." Birkhauser Verlag, Basel.
- Talebi, S., Ed. (1998). "Seismicity Caused by Mines, Fluid Injections, Reservoirs, and Oil Extraction." Birkhauser Verlag, Basel.
- Talebi, S., Ge, M., Rochon, P., and Mottahed, P. (1994). Analysis of induced seismicity in a hardrock mine in the Sudbury Basin, Ontario, Canada. In "Rock Mechanics" (P. P. Nelson and S. E. Laubach, eds.). Balkema, Rotterdam, pp. 937–944.
- Talebi, S., Mottahed, P., and Pritchard, C. J. (1997). Monitoring seismicity in some mining camps of Ontario and Quebec. In "Rockbursts and Seismicity in Mines" (S. J. Gibowicz and S. Lasocki, eds.). Balkema, Rotterdam, pp. 117–120.
- Talebi, S., and Young, R. P. (1992). Microseismic monitoring in highly stressed granite: Relation between shaft-wall cracking and in situ stress. *Int. J. Rock Mech. Min. Sci.* **29**, 25–34.
- Taylor, S. R. (1994). False alarms and mine seismicity: An example from the Gentry Mountain mining region, Utah. *Bull. Seismol. Soc. Am.* **84**, 350–358.
- Teper, L. (1996). Fault dimensions and displacements in mining area: Northern part of the Upper Silesian Coal Basin. In "Tectonophysics of Mining Areas" (A. Idziak, ed.). University of Silesia, Katowice, pp. 41–56.
- Teper, L., and Idziak, A. (1995). On fractal geometry in fault systems of the Upper Silesian Coal Basin, Poland. In "Mechanics of Jointed and Faulted Rocks" (H.-P. Rossmanith, ed.). Balkema, Rotterdam, pp. 329–333.
- Toon, S. M., and Styles, P. (1993). Microseismic event location around longwall coal faces using bore-hole in-seam seismology. In "Rockbursts and Seismicity in Mines" (R. P. Young, ed.). Balkema, Rotterdam, pp. 441–444.
- Tope, A. Z., Grodner, M., Stewart, R. D., and Lightfoot, N. (1997). Preconditioning: A rockburst control technique. In "Rockbursts and Seismicity in Mines" (S. J. Gibowicz and S. Lasocki, eds.). Balkema, Rotterdam, pp. 267–272.
- Trifu, C.-I., and Fehler, M., Eds. (1998). "New Trends in Seismological Research: Studies of Seismicity Induced by Mining, Petroleum and Geothermal Activities." Special Issue, *Tectonophysics* **289**, 1–255.
- Trifu, C.-I., and Shumila, V. I. (1996). A method for multidimensional analysis of earthquake frequency-magnitude distribution with an application to the Vrancea region of Romania. *Tectonophysics* **216**, 9–22.

- Trifu, C.-I., Shumila, V., and Urbancic, T. I. (1997). Space-time analysis of microseismicity and its potential for estimating seismic hazard in mines. In "Rockbursts and Seismicity in Mines" (S. J. Gibowicz and S. Lasocki, eds.). Balkema, Rotterdam, pp. 295–298.
- Trifu, C.-I., and Urbancic, T. I. (1996). Fracture coalescence as a mechanism for earthquakes: Observations based on mining-induced microseismicity. *Tectonophysics* **216**, 193–207.
- Trifu, C.-I., Urbancic, T. I., and Young, R. P. (1993). Non-similar frequency-magnitude distribution for $M < 1$ seismicity. *Geophys. Res. Lett.* **20**, 427–430.
- Trifu, C.-I., Urbancic, T. I., and Young, R. P. (1995). Source parameters of mining-induced seismic events: An evaluation of homogeneous and inhomogeneous faulting models for assessing damage potential. *Pure Appl. Geophys.* **145**, 3–27.
- Turcotte, D. L. (1989). A fractal approach to probabilistic hazard assessment. *Tectonophysics* **167**, 171–177.
- Turcotte, D. L. (1992). "Fractals and Chaos in Geology and Geophysics." Cambridge University Press, Cambridge.
- Urbancic, T. I., Feignier, B., and Young, R. P. (1992a). Influence of source region properties on scaling relations for $M < 0$ events. *Pure Appl. Geophys.* **139**, 721–739.
- Urbancic, T. I., and Trifu, C.-I. (1996). Effects of rupture complexity and stress regime on scaling relations of induced microseismic events. *Pure Appl. Geophys.* **147**, 319–343.
- Urbancic, T. I., Trifu, C.-I., Long, J. M., and Young, R. P. (1992b). Space-time correlations of b values with stress release. *Pure Appl. Geophys.* **139**, 449–462.
- Urbancic, T. I., Trifu, C.-I., and Young, R. P. (1993a). Microseismicity derived fault-planes and their relationship to focal mechanism, stress inversion, and geologic data. *Geophys. Res. Lett.* **20**, 2475–2478.
- Urbancic, T. I., Trifu, C.-I., Young, R. P. (1993b). Stress release estimates, scaling behaviour, and source complexities of microseismic events. In "Rockbursts and Seismicity in Mines" (R. P. Young, ed.). Balkema, Rotterdam, pp. 255–260.
- Urbancic, T. I., and Young, R. P. (1993). Space-time variations in source parameters of mining-induced seismic events with $M < 0$. *Bull. Seismol. Soc. Am.* **83**, 378–397.
- Utsu, T. (1965). A method for determining the value of b on the formula $\log n = a - bM$ showing the magnitude-frequency relation for earthquakes. *Geophys. Bull. Hokkaido Univ.* **13**, 99–103 (in Japanese, English abstract).
- Utsu, T. (1966). A statistical significance test of the difference in b -value between two earthquake groups. *J. Phys. Earth* **14**, 37–40.
- van Aswegen, G., and Butler, A. (1993). Applications of quantitative seismology in South African gold mines. In "Rockbursts and Seismicity in Mines" (R. P. Young, ed.). Balkema, Rotterdam, pp. 261–266.
- van Aswegen, G., Mendecki, A. J., and Funk, C. (1997). Application of quantitative seismology in mines. In "Seismic Monitoring in Mines" (A. J. Mendecki, ed.). Chapman & Hall, London, pp. 220–245.
- Vesela, V. (1995). The investigation of rockburst focal mechanisms at Lazy coal mine, Czech Republic. *Publ. Inst. Geophys. Pol. Acad. Sci.* **M-19**(281), 47–55.
- Voinov, K. A., Krakov, A. S., Lomakin, V. S., and Khalevin, N. I. (1987). Seismological studies of rock bursts at the Northern Ural bauxite deposits. *Izv. Akad. Nauk SSSR Fiz. Zemli* **10**, 98–104 (in Russian).
- Wang, J.-H., and Lee, C.-W. (1996). Multifractal measures of earthquakes in West Taiwan. *Pure Appl. Geophys.* **146**, 131–145.
- Watanabe, T., and Sassa, K. (1996). Seismic attenuation tomography and its application to rock mass evaluation. *Int. J. Rock Mech. Min. Sci.* **33**, 467–477.
- Whyatt, J. K., Williams, T. J. and Blake, W. (1993). Concentration of rock burst activity and in situ stress at the Lucky Friday Mine. In "Rockbursts and Seismicity in Mines" (R. P. Young, ed.). Balkema, Rotterdam, pp. 135–139.

- Wiejacz, P. (1991). "Investigation of Focal Mechanisms of Mine Tremors by the Moment Tensor Inversion" (Ph.D. thesis) Institute of Geophysics, Polish Academy of Sciences, Warsaw (in Polish).
- Wiejacz, P. (1992). Calculation of seismic moment tensor for mine tremors from the Legnica-Glogow Copper Basin. *Acta Geophys. Pol.* **40**, 103–122.
- Wiejacz, P. (1993). The effect of labor strike upon induced seismicity at Polkowice copper mine, Poland. *Acta Geophys. Pol.* **41**, 351–362.
- Wiejacz, P. (1995a). Moment tensors for seismic events from Upper Silesian coal mines. In "Mechanics of Jointed and Faulted Rock" (H.-P. Rossmannith, ed.). Balkema, Rotterdam, pp. 667–672.
- Wiejacz, P. (1995b). Source mechanisms of seismic events induced at Ziemowit coal mine: Comparison with mining information. *Publ. Inst. Geophys. Pol. Acad. Sci.* **M-19**(281), 15–32.
- Wiejacz, P., and Gibowicz, S. J. (1997). Source mechanism determined by moment tensor inversion for seismic events at Rudna and Polkowice copper mines in Poland. *Acta Geophys. Pol.* **45**, 291–302.
- Wiejacz, P., and Ługowski, A. (1997). Effects of geological and mining structures upon mechanism of seismic events at Wujek coal mine, Katowice, Poland. In "Rockbursts and Seismicity in Mines" (S. J., Gibowicz and S. Lasocki, eds.). Balkema, Rotterdam, pp. 27–30.
- Williams, T. J., Wideman, C. J., and Scott, D. F. (1992). Case history of a slip-type rockburst. *Pure Appl. Geophys.* **139**, 627–637.
- Wolf, A., Swift, J. B., Swinney, H. L., and Vastano, J. A. (1985). Determining Lyapunov exponents from a time series. *Physica D* **16**, 285–317.
- Wong, I. G. (1993). Tectonic stresses in mine seismicity: Are they significant? In "Rockbursts and Seismicity in Mines" (R. P. Young, ed.). Balkema, Rotterdam, pp. 273–278.
- Wu, Y., and Zhang, W. (1997). Prevention of rockbursts in coal mines in China. In "Rockbursts and Seismicity in Mines" (S. J. Gibowicz and S. Lasocki, eds.). Balkema, Rotterdam, pp. 361–365.
- Xie, H. (1993). "Fractals in Rock Mechanics." Balkema, Rotterdam.
- Xie, H., and Pariseau, W. G. (1992). Fractal character and mechanism of rock bursts. In "Rock Mechanics as a Multidisciplinary Science: Proc. 33rd US Symposium" (J. R. Tillerson, and W. R. Wawersik, eds.). Balkema, Rotterdam, pp. 140–156.
- Xie, H., and Pariseau, W. G. (1993). Fractal character and mechanism of rock bursts. *Int. J. Rock Mech. Min. Sci.* **30**, 343–350.
- Yang, X. N., Stump, B. W., and Phillips, W. S. (1998). Source mechanism of an explosively induced mine collapse. *Bull. Seismol. Soc. Am.* **88**, 843–854.
- Yi, X., and Kaiser, P. K. (1993). Mechanisms of rockmass failure and prevention strategies in rockburst conditions. In "Rockbursts and Seismicity in Mines" (R. P. Young, ed.). Balkema, Rotterdam, pp. 141–145.
- Young, R. P., Ed. (1993). "Rockbursts and Seismicity in Mines" Balkema, Rotterdam.
- Young, R. P. and Maxwell, S. C. (1992). Seismic characterization of highly stressed rock mass using tomographic imaging and induced seismicity. *J. Geophys. Res.* **97**, 12,361–12,373.
- Young, R. P., Maxwell, S. C., Urbancic, T. I., and Feignier, B. (1992). Mining-induced microseismicity: Monitoring and applications of imaging and source mechanism techniques. *Pure Appl. Geophys.* **139**, 697–719.
- Zatsepin, S. V., and Crampin, S. (1997). Modelling the compliance of crustal rock—I. Response of shear-wave splitting to differential stress. *Geophys. J. Int.* **129**, 477–494.
- Zhong, Y. Z., Gao, C. B., and Bai, Y. (1997). Induced seismicity in Liaoning Province, China. *Pure Appl. Geophys.* **150**, 461–472.
- Zuberek, W. M., Teper, L., Idziak, A., and Sagan, G. (1996). Tectonophysical approach to the description of mining induced seismicity in the Upper Silesia. In "Tectonophysics of Mining Areas" (A. Idziak, ed.). University of Silesia, Katowice, pp. 79–97.
- Zúñiga, F. R. (1993). Frictional overshoot and partial stress drop. Which one? *Bull. Seismol. Soc. Am.* **83**, 939–944.

This Page Intentionally Left Blank

INDEX

A

- Accelerometers, in seismic monitoring system, 50
- Aegean
 - seismic hazard redefinition, 31
 - and western Turkey: interactions between earthquakes, 15–16
- Aftershocks
 - correlation with foreshocks and mainshocks, 138–139
 - Coulomb stress changes and, 11–12
 - distribution
 - Irpinia, 17–18
 - modeling, 19
 - prediction, 30–31
- Aging process, positive and negative, 125
- Algorithm
 - location of seismic events in mines, 57
 - strange attractor dimension, 121, 123
- Anisotropy, seismic, 68–70
- Apatite ore, extraction-related tremors, 45–46
- Apparent volume, cumulative, 152
- Arrival time difference method, 58–59
- Artificial neural networks, 157–158, 164
- Australia
 - field experiments using source location methods, 55
 - mining-induced seismic events, 46–47
 - seismicity correlated with longwall production, 71–72
- Austria, seismic events in dolomite mines, 48
- Automatic prediction, mining seismicity, 156–159
- Azimuth angle, relation to pulse width, 105

B

- Big Bear earthquake, as aftershock, 18, 24
- Big Bear rupture, stress changes caused by, 13–14
- Box-dimension, 111–112, 116

C

- Canada
 - Creighton mine, rock environment, 77–78
 - MP250 system for automated event detection, 52
 - seismic events in mines, 42, 44
 - Strathcona mine
 - damage potential models, 84–85
 - microseismic events, 87
 - Underground Research Laboratory, 61–64, 70, 87, 99–101
- Chaotic process, predictability, 120–121
- Chile, copper mine-related rockbursts, 47–48
- China, coal mines affected by seismicity, 46
- Clustering dimension, fractal, 144
- Collapse
 - pillar, in Wyoming, 76
 - shallow mine, 160
 - spontaneous and induced, 97–98
- Compensated Linear Vector Dipole, 90, 93
- Comprehensive Test Ban Treaty, 159, 161, 164
- Conditional intensity function, 139–140
- Controlled collapse experiment, Michigan, 97–98
- Corner frequencies
 - P and S waves, 82
 - relation to source radius, 101
 - S -wave, 88
- Correlation dimension, fractal, 117
- Correlation integral method, estimation of fractal dimensions, 108–109
- Coulomb failure, 3–5, 9, 17
- Coulomb interaction technique, 18–20
- Coulomb stress
 - on optimally oriented faults, 7–9
 - on plane of specified orientation, 6–7
- Coulomb stress changes
 - after Landers rupture, 13
 - and aftershocks, 11–12
 - caused by Joshua Tree, Landers, and Big Bear ruptures, 13–14

- preceding Landers rupture, 12
- and subsequent events: time interval, 15–16
- Crack damage, reduction of intact rock strength, 73
- Creep, in crust and in faults, 27–28
- Crustal relaxation
 - postseismic, 21
 - viscoelastic, 25
 - viscous, 28
- Czech Republic
 - mining-induced seismicity, 45
 - seismic energy distributions, 141
 - seismicity types in coal mines, 70
 - spatial distribution of seismic events, 78

D

- Data acquisition, for mine seismicity monitoring systems, 49–52
- Deconvolution, spectral division, 104
- Dip-slip faults
 - 3-D case, 9–10
 - double-couple mechanism, 95
 - and relieved stress, 29
- D-Optimum planning, 53–54
- Double-couple component, source mechanism, 93

E

- Earthquake, *see also specific earthquakes*
 - dip-slip, close interactions between, 16–18
 - large, interactions between, 15–16
 - natural, multifractal properties, 113
 - probability changes, 30
 - stress drops, 20
 - triggering, 24–25
- Elastic deformation, and fluid flow, 26–27
- Elastic strain, 152
- Empirical Green's Function, 103–104
- Energy index, 151–152
- Energy/magnitude distributions, time variations, 133–143
- Energy-seismic moment, 139–140
- England, borehole seismic monitoring, 47
- Epicenter
 - distributions, 150
 - spatial distribution, 112, 115–116

- Evolution
 - postseismic, 29
 - of seismicity, 19
- Extensive-dilatancy anisotropy, 68–70

F

- Failure plane, orientation, 4–5
- Fault plane
 - optimally oriented, Coulomb stress change on, 7–9
 - solutions, for microseismic events, 96–97
 - specified orientation: 2-D case, 6–7
 - subevents of Irpinia mainshock, 23
- Faults
 - creep in, 27–28
 - frictional properties, 21
 - interactions, 3, 10–11
 - seismic cycle, 30
 - strike-slip and dip-slip, 9–10
- Fluid flow, and elastic deformation, 26–27
- Focal mechanism
 - mainshock, Coulomb distribution sensitivity to, 10–11
 - seismic events in Polish mines, 78–79, 85
- Fractals
 - characteristics of seismicity in mines, 126
 - dimensions
 - estimation by correlation integral method, 108–109
 - spatial and temporal, 148, 150
 - and spatial distributions, 144–145
 - properties of seismic events, 110–123
 - structure, exhibited by seismicity, 105, 163
- France
 - isotropic velocity model, 56
 - seismic events
 - in coal mines, 48
 - at longwall working face, 72
 - scaling relations for, 87
- Frequency–magnitude curve, nonlinearity, 133–134
- Frictional sliding, 21
- Friction events, stick-slip, 102
- Friction laws, rate and state dependent, 23–25

G

- Geology, and mining and seismicity, 70–80
- Germany, potash mine
 - rockburst, 76
 - tomographic imaging, 64

H

- Hazard, seismic
 - and recurrence relationships, 129–133
 - time-dependent assessment and prediction, 123–159

I

- Idaho
 - compressive tectonic stresses, 77
 - double-couple source model, 96
 - rockbursts in metal-mining areas, 44, 66
 - seismicity during extraction, 74
- India
 - mining-induced seismic events, 45
 - rockburst spatial distribution, 113–114
- Instability, rock mass, 150–153
- Interevent time, sample distribution, 125–126
- Inversions, second-order moment tensor, 91–92
- Irpinia earthquake, 17–18
 - subevents, 23, 25
- Izmit earthquake, 15–16

J

- Japan
 - moment tensor inversion, 92
 - undersea coal mines: rockbursts, 48
- Joint hypocenter and velocity determination, 59
- Joshua Tree rupture, stress changes caused by, 13–14

L

- Landers earthquake
 - associated stress changes, 12
 - Big Bear aftershock, 18
 - Coulomb stress modeling, 22

Landers rupture

- Coulomb stress changes preceding, 12
- stress changes caused by, 13–14
- stress changes following, 13
- Linear extrapolation, in automatic prediction, 156–157
- Loading, static and dynamic, 22–23
- Location
 - of distribution, 154
 - seismic events: monitoring of mines, 53–59, 162
- Log-frequency-magnitude distribution, 131–132
- Loma Prieta event, seismicity, 19
- Longwall advance, 136
- Longwall calving, 71–72
- Lyapunov exponents, 120–121, 123

M

- Magnitude
 - distribution, 145–146
 - maximum regional, 131–132
- Maximum likelihood method, 130–131, 133
- Microcracks, stress-aligned, 68–69
- Microseismic events
 - Canada, Strathcona mine, 87
 - fault-plane solutions for, 96–97
 - source size, 99
 - South Africa, source parameters, 86
- Mines
 - copper
 - related rockbursts, 47–48
 - source mechanism of seismic events, 93
 - location of seismic events in, 58–59
 - open-stope, 134
 - seismicity in
 - extrapolation of parameterizations, 156–159
 - self-organized critical state of, 119–120
 - seismic networks
 - optimum configuration, 53–54
 - source time function, 104
 - seismic series, 142
 - spatial distribution of, 68
 - tremors, 40, 76
 - underground
 - scaling relations for seismic events, 88–89
 - seismicity in, 41–48

- Mining
 and geology and seismicity, 70–80
 induced seismicity
 chaotic generation, 126
 complexity of dependence, 153–154
 fractal structure, 163
 spatio-temporal patterns, 65–70
 longwall, 111
 pillar, Polish copper mines, 93
 Monitoring systems, seismicity in mines, 49–52
 MP250 system, Canada, 52
 Multifractal analysis
 real data, 118–119
 rockburst spatial distribution, 113–114
 seismic data from mines, 114–116
- N**
- Nonrandomness, spatial, 146–148
 Northridge earthquake, seismicity, 19
- O**
- Orowan's condition, 100–101
- P**
- Parametric models, alternatives to, 132–133
 Pillar failure, mechanisms, 98
 Plate boundary, slip deficits at, 1
 Poland
 copper mines: pillar mining, 93
 correlation between mining and seismicity, 76
 digital seismic monitoring system, 52
 epicenter spatial distribution, 112
 moment tensor inversions, second-order, 92
 seismic velocity tomography, 64
 Upper Silesian Basin
 geological features, 78
 seismicity in mines, 42
 source mechanism, 95
 Pore fluid pressure, 5
 Prediction
 aftershock distribution, 30–31
 automatic, seismicity in mines, 156–159
 time-dependent seismic hazard, 123–159
- Pulse width, of Relative Source Time Function, 104–105
P-wave
 corner frequency, 82
 velocity images, 60–61, 64
- R**
- Rate-state friction, 21, 23–25
 Recurrence relationships, 129–133
 Reference event, wave propagation estimated from, 91
 Relative Source Time Functions, 103–105
 Rockbursts
 in Canadian mines, 42, 44
 catastrophic, Utah, 97
 Chilean copper mines, 47–48
 degree of clustering before, 110–111
 distinction from seismic event in mine, 39
 Idaho metal-mining areas, 44, 66
 Indian mines, 45
 spatial distribution, 113–114
 potential hazards, assessment, 85–86
 preparatory process leading to, 143
 Rock failure, complex, and typical source mechanism, 96–99
 Rock mass
 deformation, monitoring, 69
 instability concept, 150–153
 response to mining, monitoring, 67
 self-organized critical state, 119
 Rock stress, 5
 Russia, mining-induced events, 45–46
- S**
- Scaling relation
 seismic events in mines, 163
 source, 86–89
 Seismic discrimination, 159–161
 Seismic events
 energy distribution, 127–128
 fractal properties, 110–123
 location: monitoring of mines, 53–59, 162
 probability of occurrence, 154–156
 scaling relations, 86–89
 self-similarity, 108
 source parameters, 81–86

- spatial distributions, parameterizations, 143–150
- Seismic hazard
 - and recurrence relationships, 129–133
 - time-dependent assessment and prediction, 123–159
- Seismicity
 - connected with longwall mining, 111
 - evolution, 19
 - generation process, 124–126
 - and geology and mining, 70–80
 - increase after Landers earthquake, 14
 - in mines
 - extrapolation of parameterizations, 156–159
 - self-organized critical state, 119–120
 - mining-induced
 - chaotic generation, 126
 - complexity of dependence, 153–154
 - fractal structure, 163
 - spatio-temporal patterns, 65–70
 - relationship to velocity, 64
 - remotely triggered, 22
 - triggered, 39
 - in underground mines, 41–48
- Seismic moment tensor, describing source mechanism, 90–95
- Seismic monitoring
 - location of seismic events, 162
 - mines, 40–70
- Seismic tomographic imaging, 59–65
- Self-organized critical state, earth's crust, 41, 119–120
- Self-similarity, seismic events, 108
- Sensitivity, Coulomb distribution to mainshock focal mechanism, 10–11
- Sensors, in mine seismicity monitoring systems, 49–52
- Shear stress, left- and right-lateral, 4–5
- Shear-wave splitting, 68–70
- Slip
 - deficits at plate boundary, 1
 - distribution on rupturing fault, 22
- Source mechanism studies
 - and complex rock failures, 96–99
 - mining events, 161
 - seismic events, 89–102
 - seismic moment tensor, 90–95
 - stress release mechanism, 99–102
- Source models, for stationary seismic hazard analysis, 129–133
- Source parameters, seismic events, 81–86
- Source time function, 102–105
- South Africa
 - failure of peninsular remnant, 98
 - microseismic events, source parameters, 86
 - rock mass response to mining, monitoring, 67
 - seismic discrimination, 159–160
 - seismicity studies in deep mines, 41–42, 77
 - seismic moment tensors, 90–91
 - underground shear ruptures, 96
 - Western Deep Levels mine, 137
 - stress release mechanism, 99–101
- Spatial correlation dimension, 109–112
- Spatial distributions, seismic events, parameterizations, 143–150
- Spatio-temporal patterns, mining-induced seismicity, 65–70
- Stopping phases, earthquake estimation based on, 82
- Strange attractor, low-dimensional, 121, 123
- Stress, *see also* Coulomb stress changes
 - apparent, 153
 - concentrated by fault bends, 1
 - Coulomb
 - on optimally oriented faults, 7–9
 - on plane of specified orientation, 6–7
 - interaction, 2
 - redistribution, caused by Landers earthquake, 14
 - static, 20–21
- Stress drop
 - amplitude, 8–9
 - earthquake, 20
 - scaling relation, 86–88
 - seismic, 153
 - static and partial, 99–102
- Stress fields, calculation, 3
- Stress release
 - estimates, 151
 - mechanism, 99–102
- Stress shadowing, 25
- Strike-slip faults
 - 3-D case, 9–10
 - and tectonic loading, 28
- Strong events
 - misinterpreted as earthquake, 160
 - time of occurrence, 147–148

Sudbury Local Telemetered Network, 42, 44

T

Tectonic loading, 7, 21, 28–29

Time-dependency

deformations around deep-level mines, 75
seismic hazard, assessment and prediction, 123–159

Time residuals

outlying, 56–57
seismic waves, 54–55

Time variations, energy/magnitude distributions, 133–143

Tomography, seismic, 59–65

Transducer, in seismic monitoring system, 49

Triggering

earthquake, 24–25
seismicity, 22, 39
subevent, 25

Tunnel excavation, seismic events recorded

ahead of, 92

Turkey, western

and Aegean: interactions between earthquakes, 15–16
seismic hazard redefinition, 31

U

Underground Research Laboratory, Manitoba, 61–64, 70, 87, 99–101

Utah

catastrophic rockburst, 97
coal mining-induced seismicity, 44
seismic energy–mined rock volume relationship, 74

V

Validation, in statistical prediction, 128–129

Velocity model

constant isotropic, 56
time residual for, 54–55

Velocity structure

around tunnel, 75–76
controlled source-imaged, 60–65
and hypocenter location, 162

W

Western Deep Levels gold mine, 42, 99–101, 137

Wyoming, pillar collapse, 76